

Stabilized isogeometric discretizations on trimmed and union geometries, and weak imposition of the boundary conditions for the Darcy flow

Présentée le 29 avril 2022

Faculté des sciences de base
Chaire de modélisation numérique et simulation
Programme doctoral en mathématiques

pour l'obtention du grade de Docteur ès Sciences

par

Riccardo PUPPI

Acceptée sur proposition du jury

Prof. F. Eisenbrand, président du jury
Prof. A. Buffa, Dr R. Vazquez Hernandez, directeurs de thèse
Prof. G. Sangalli, rapporteur
Prof. J. A. Evans, rapporteur
Prof. S. Deparis, rapporteur

A nonna Iolanda.

Acknowledgements

I cannot begin to express my thanks to my advisor Annalisa, from whom I have learned a lot scientifically and professionally. I am very grateful for her time, guidance, and for all the precious mathematical advice. I recognize that I have been given all the means to best approach my Ph.D. In particular, I even had the chance to attend a summer school in Cetraro and a workshop in Oberwolfach, both must-attend events for different reasons...

I would like to extend my deepest gratitude to Rafa, my co-advisor, who not only guided me scientifically but, above all, was a source of encouragement and motivation. Many thanks for his (almost) infinite patience and availability. This thesis would not have been definitely possible without his support.

I express my sincere thanks to Prof. Erik Burman for kindly agreeing to host me in London, despite the unfortunate circumstances of finally not allowing it. I am very grateful for his patience and help in our long email correspondence that finally allowed the publication of a paper together. I gratefully acknowledge the jury members, Professors Simone Deparis, John A. Evans and Giancarlo Sangalli, for the interesting discussion and the positive feedback during the private defense. In addition, I thank Prof. Friedrich Eisenbrand for agreeing to serve as the jury president.

I cannot leave EPFL without mentioning the fundamental help of the secretaries of the chair, Jocelyne and Pauline. They have made my life extremely easier by making me forget about any paperwork!

It goes without saying that I would never have been able to face such a challenging course without the support of friends. In this regard, I would like to thank my friend Franz with whom I have shared enormously in these years, despite the distance. Thanks to Roberta for having reconfirmed herself as a referenced point. Thanks to Jack for his friendship, my stay in Switzerland would not have been the same otherwise. My deepest thanks go to my dear friends Fabian, Eva, Giac, Edo, and Gonzo, for all the heated discussions, the bike rides, the countless beers, and all the moments together.

I would like to thank all the members of the MNS chair and all the friends and colleagues of the math institute. In particular, I am grateful to Ale Patelli, Andrea, Bernard, Émile, Felipe, Lana, Luca C., Mathieu, Ondine, Luca P., Andrea Scaglioni, and Xiadong, who made my stay at the math institute much more enjoyable.

The support of my roommates was a lifeline. No matter how bad my day was at the office, I always knew there was someone at home to help me turn it around in a positive way. I am grateful to Nico Kalb, Shery, Nico Marx, Odile, Tom, Lina, and, of course, Franky for all these years of living together and sharing.

I'm deeply grateful to Valentine for these last months together, all her support, and her positive influence.

A special thought goes out to my longtime and long-distance friends, Andrea T., Dani, Gianmi, Marco B., Marco Z., and Nico Z.

Finally, I would like to thank my parents, Mario and Valentina, my brother Lorenzo, and my grandmother Iolanda for always supporting me unconditionally and patiently welcoming me during my short visits.

Acknowledgements

My research activity was partially supported by the European Research Council through the Advanced Grant n. 694515 CHANGE - “New CHallenges for (adaptive) PDE solvers: the interplay of ANalysis and GEometry”. This support is gratefully acknowledged.

Lausanne, February 17, 2022

Riccardo Puppi

Abstract

Modern manufacturing engineering is based on a “design-through-analysis” workflow. According to this paradigm, a prototype is first designed with Computer-aided-design (CAD) software and then finalized by simulating its physical behavior, which usually involves the simulation of Partial Differential Equations (PDEs) on the designed product. The simulation of PDEs is often performed via finite element discretization techniques. A severe bottleneck in the entire process is undoubtedly the interaction between the design and analysis phases. The prototyped geometries must undergo the time-consuming and human-involved meshing and feature removal processes to become “analysis-suitable”. This dissertation aims to develop and study numerical solvers for PDEs to improve the integration between numerical simulation and geometric modeling.

The thesis is made of two parts. In the first one, we focus our attention on the analysis of isogeometric methods which are robust in geometries constructed using Boolean operations. We consider geometries obtained via trimming (or set difference) and union of multiple overlapping spline patches. As differential model problems, we consider both elliptic (the Poisson problem, in particular) and saddle point problems (the Stokes problem, in particular). As it is standard, the Nitsche method is used for the weak imposition of the essential boundary conditions and to weakly enforce the transmission conditions at the interfaces between the patches. After proving through well-constructed examples that the Nitsche method is not uniformly stable, we design a minimal stabilization technique based on a stabilized computation of normal fluxes (and on a simple modification of the pressure space in the case of the Stokes problem). The main core of this thesis is devoted to the derivation and rigorous mathematical analysis of a stabilization procedure to recover the well-posedness of the discretized problems independently of the geometric configuration in which the domain has been constructed.

In the second part of the thesis, we consider a different approach. Instead of considering the underlying spline parameterization of the geometrical object, we immerse it in a much simpler and readily meshed domain. From the mathematical point of view, this approach is closely related to the isogeometric discretizations in trimmed domains treated in the first part. In this case, we consider the Raviart-Thomas finite element discretization of the Darcy flow. First, we analyze a Nitsche and a penalty method for the weak imposition of the essential boundary conditions on a boundary fitted mesh, a problem that was not studied before, not needed for our final goal, but still interesting by itself. Then, we consider the case of a general domain immersed in an underlying mesh unfitted with the boundary. We focus on the Nitsche method presented for the boundary fitted case and study its extension to the unfitted setting. We show that the so-called ghost penalty stabilization provides an effective solution to recover the well-posedness of the formulation and the well-conditioning of the resulting linear system.

Keywords: numerical analysis, computer-aided-design, CAD, CAE, isogeometric analysis, IGA, finite element, FEM, FEA, Poisson, Stokes, Darcy, unfitted, immersed, trimming, union, coupling, Nitsche, mortar, weak imposition, boundary conditions, Raviart-Thomas, fictitious domain, CutFEM

Sommario

La moderna ingegneria manifatturiera si basa su un flusso di lavoro “progettazione-via-analisi”. Secondo questo paradigma, un prototipo viene prima disegnato con un software CAD (Computer-aided-design) e poi finalizzato simulando il suo comportamento fisico, che solitamente prevede la risoluzione numerica di equazioni alle derivate parziali (EDP) sull’oggetto disegnato. La simulazione delle EDP è spesso ottenuta tramite tecniche di discretizzazione agli elementi finiti. Un serio ostacolo all’intero processo sta senz’altro nell’interazione tra le fasi di progettazione e di analisi. Prima di diventare “adatti all’analisi”, i modelli geometrici devono essere sottoposti a costosi processi di meshing e di defeaturing, costosi in termini di tempo ed intervento umano. Questa dissertazione mira a sviluppare e studiare solutori numerici per EDP per migliorare l’integrazione tra la simulazione numerica e la modellazione geometrica.

La tesi è composta da due parti. Nella prima, concentriamo la nostra attenzione sull’analisi di metodi isogeometrici che sono robusti in geometrie costruite con operazioni booleane. Consideriamo geometrie ottenute tramite trimming (o differenza di insiemi) e unione di più patch spline sovrapposte. Come problemi differenziali modello, consideriamo sia problemi ellittici (il problema di Poisson, in particolare) che problemi di punto sella (il problema di Stokes, in particolare). Come consuetudine, il metodo di Nitsche è usato per l’imposizione debole delle condizioni al bordo di tipo essenziale e per imporre debolmente le condizioni di trasmissione alle interfacce tra le patch. Dopo aver dimostrato attraverso esempi ben congegnati che il metodo di Nitsche non è uniformemente stabile, sviluppiamo una tecnica di stabilizzazione minimale basata su un calcolo stabilizzato dei flussi normali (e su una semplice modifica dello spazio della pressione, nel caso del problema di Stokes). Il nucleo principale di questa tesi è dedicato alla derivazione e alla rigorosa analisi matematica di una procedura di stabilizzazione per ripristinare la buona posizione dei problemi discretizzati indipendentemente dalla configurazione geometrica in cui il dominio è stato costruito.

Nella seconda parte della tesi, consideriamo un approccio diverso. Invece di considerare la parametrizzazione spline sottostante all’oggetto geometrico, lo immergiamo in un dominio molto più semplice e facilmente meshabile. Dal punto di vista matematico, questo approccio è strettamente legato alle discretizzazioni isogeometriche in domini trimmati trattati nella prima parte. In questo caso, consideriamo la discretizzazione agli elementi finiti di Raviart-Thomas per il flusso Darcy. In primo luogo, analizziamo un metodo Nitsche ed un metodo di penalizzazione per l’imposizione debole delle condizioni al bordo di tipo essenziale su una mesh conforme al bordo, un problema che non è stato studiato prima, non necessario per il nostro obiettivo finale, ma comunque interessante di per sé. Ci concentriamo sul metodo di Nitsche presentato per il caso conforme al bordo e studiamo la sua estensione al caso non conforme. Mostriamo che la cosiddetta stabilizzazione “ghost-penalty” fornisce una soluzione efficace per recuperare la buona posizione della formulazione ed il buon condizionamento del sistema lineare risultante.

Parole chiave: analisi numerica, computer-aided-design, CAD, CAE, analisi isogeometrica, IGA, elementi finiti, FEM, FEA, Poisson, Stokes, Darcy, non-conforme, immerso, trimming,

Abstract (English/Italiano)

unione, accoppiamento, Nitsche, mortar, imposizione debole, condizioni al bordo, Raviart-Thomas, dominio fittizio, CutFEM

Contents

Acknowledgements	i
Abstract (English/Italiano)	iii
Notation	vi
Introduction	1
I Stabilized isogeometric discretizations on trimmed and union geometries	9
1 Preliminaries	11
1.1 Isogeometric analysis: B-splines, mesh and parametrization	11
1.1.1 The univariate case	11
1.1.2 The multivariate case	12
1.1.3 Parametrization and physical domain	13
1.2 Isogeometric discretization of the Poisson problem on untrimmed geometries . . .	14
1.3 Isogeometric discretization of the Stokes problem on untrimmed geometries . . .	15
2 Stabilized isogeometric discretization of the Poisson problem on trimmed geometries	19
2.1 Isogeometric discretization	20
2.1.1 Parametrization, mesh and approximation space in the trimmed domain .	20
2.1.2 Variational formulation using Nitsche's method	21
2.2 Lack of stability of Nitsche's method	22
2.3 The stabilized formulation and its analysis	24
2.3.1 Construction of the stabilization operator	26
2.3.2 The quasi-interpolation strategy	27
2.3.3 Stabilization operator in the parametric domain	28
2.3.4 Stabilization operator in the physical domain	31
2.3.5 <i>A priori</i> error estimates	33
2.4 Numerical examples	36
2.4.1 Some details about the implementation	36
2.4.2 Validation of stability	36
2.4.3 Validation of <i>a priori</i> error estimates	37
2.4.4 Conditioning	38
3 Stabilized isogeometric discretization of the Poisson problem on union geometries	43
3.1 Parametrization, mesh and approximation space for domains obtained via union	43
3.2 Isogeometric analysis on union geometries	47
	vii

3.2.1	Model problem and its variational formulation	47
3.2.2	Quasi-interpolation strategy	49
3.2.3	Minimal stabilization procedure	49
3.2.4	Stability analysis and <i>a priori</i> error estimates	57
3.3	Implementation aspects of the union operation	59
3.3.1	Generation of the interface quadrature mesh	60
3.3.2	Implementation of the minimal stabilization	61
3.4	Numerical examples	63
3.4.1	Convergence and conditioning under bad cuts	63
3.4.2	Influence of patch ordering	65
3.4.3	Multiple overlapped patches	66
3.4.4	A complex geometry obtained via Boolean operations	67
4	Stabilized isogeometric discretization of the Stokes problem on trimmed geometries	69
4.1	Model problem	69
4.2	Isogeometric discretization	70
4.2.1	Isogeometric spaces on trimmed geometries	70
4.3	Lack of stability of Nitsche's method	71
4.4	Stabilized Nitsche's formulations	75
4.4.1	Stabilization procedure	75
4.4.2	Interpolation and approximation properties of the discrete spaces	78
4.5	Well-posedness of the stabilized formulations	80
4.6	<i>A priori</i> error estimates	82
4.7	Numerical tests	84
4.7.1	Pentagon	84
4.7.2	Mapped pentagon	85
4.7.3	Rotating square	85
4.7.4	Square with circular trimming	89
4.7.5	Stokes flow around a cylinder	89
4.7.6	Lid-driven cavity	90
5	Stabilized isogeometric discretization of the Stokes problem on union geometries	93
5.1	Parametrization, mesh and approximation spaces for domains obtained via union operations	93
5.2	Isogeometric discretization on overlapping multipatch domains	95
5.2.1	Model Problem and its variational formulation	95
5.2.2	Stabilization procedure	97
5.2.3	Interpolation and approximation properties of the discrete spaces	100
5.2.4	Well-posedness of the stabilized formulation	101
5.2.5	<i>A priori</i> error estimates	106
5.3	Numerical example	108
	Summary of Part I	111
II	Weak imposition of the boundary conditions for the Darcy flow	113
6	The Raviart-Thomas discretization of the Darcy problem	115
7	Weak imposition of the essential boundary conditions for the Darcy flow: fitted case	119

7.1	The Darcy problem and a perturbed formulation	119
7.2	The finite element discretization	122
7.3	Stability estimates	124
7.4	<i>A priori</i> error estimates	127
7.5	Numerical examples	131
7.5.1	Convergence results	131
7.5.2	A remark about the condition numbers	132
7.5.3	The optimality of the penalty parameter	137
8	Weak imposition of the essential boundary conditions for the Darcy flow: unfitted case	143
8.1	Model problem and notation	143
8.2	Interpolation strategy	145
8.3	The stabilized formulation	145
8.3.1	Stability estimates	149
8.3.2	<i>A priori</i> error estimates	152
8.4	The condition number	155
8.5	The pure natural case	157
8.6	Numerical examples	158
8.6.1	Convergence rates	158
8.6.2	Condition number	160
8.6.3	On mass conservation	161
	Summary of Part II	163
A	Appendix	165
A.1	Useful inequalities	165
A.2	Technical proofs	168
	Bibliography	173
	Curriculum Vitae	181

Notation

In this chapter we introduce some definitions and notations which will be frequently employed in the manuscript.

With a slight abuse of notation, we will use the same symbol $|\cdot|$ to denote both the d -dimensional Lebesgue measure and the $(d-1)$ -dimensional Hausdorff measure. Given $D \subset \mathbb{R}^d$ and Σ a hypersurface of \mathbb{R}^d or a subset of it, $|D|$ and $|\Sigma|$ denote the d -dimensional Lebesgue measure of D and the $(d-1)$ -dimensional Hausdorff measure of Σ , respectively. The symbol $\#\cdot$ denotes the cardinality of a set. Given $E \subset \mathbb{R}^d$, the notations E° and $\text{int } E$ denote its interior.

A domain is an open, bounded, subset of \mathbb{R}^d , $d \in \{2, 3\}$. A domain D with boundary ∂D is said to be Lipschitz if for every $x \in \partial D$ there exists a neighborhood U of x such that $U \cap \partial D$ is the graph of a Lipschitz function. In the following D denotes a Lipschitz domain with boundary ∂D , and Σ a Lipschitz continuous surface contained in ∂D . The unit outer normal on ∂D is denoted by \mathbf{n} .

We will denote as $\mathbb{Q}_{r,s,t}$ the vector space of polynomials of degree at most r in the first variable, at most s in the second and at most t in the third one (analogously for the case $d = 2$), \mathbb{P}_u the vector space of polynomials of degree at most u , and $\tilde{\mathbb{P}}_\ell$ the vector space of polynomials of degree exactly ℓ . We may write \mathbb{Q}_k instead of $\mathbb{Q}_{k,k}$ or $\mathbb{Q}_{k,k,k}$. We will often consider the restriction of a polynomial space to a given domain D and write, for instance, $\mathbb{Q}_k(D)$ instead of $\mathbb{Q}_k|_D$.

We denote by $L^2(D)$ the space of square integrable functions on the domain D , equipped with the usual norm $\|\cdot\|_{L^2(D)}$. We denote by $L_0^2(D)$ the subspace of $L^2(D)$ of functions with zero average, where the average of $v \in L^2(D)$ is $\bar{v} := |D|^{-1} \int_D v$.

For a given $\varphi : D \rightarrow \mathbb{R}$ sufficiently regular, α a multi-index with $|\alpha| := \sum_{i=1}^d \alpha_i$, and $j \in \mathbb{N}$, we define $D^\alpha \varphi := \frac{\partial^{|\alpha|} \varphi}{\partial x_1^{\alpha_1} \dots \partial x_d^{\alpha_d}}$ and $\partial_n^j \varphi := \sum_{|\alpha|=j} D^\alpha \varphi \mathbf{n}^\alpha$, where $\mathbf{n}^\alpha := n_1^{\alpha_1} \dots n_d^{\alpha_d}$. We indicate by $H^k(D)$, for $k \in \mathbb{N}$, the standard Sobolev space of functions in $L^2(D)$ whose k -th order weak derivatives belong to $L^2(D)$, equipped with the norm $\|\varphi\|_{H^k(D)}^2 := \sum_{|\alpha| \leq k} \|D^\alpha \varphi\|_{L^2(D)}^2$. Sobolev spaces of fractional order $H^r(D)$, $r \in \mathbb{R}$, can be defined by interpolation techniques, see [3].

The space $H_{0,\Sigma}^1(D)$ consists of functions in $H^1(D)$ with vanishing trace on Σ . We write $H_0^1(D)$ instead of $H_{0,\partial D}^1(D)$.

For vector-valued functions, we denote by $\mathbf{L}^2(D) := (L^2(D))^d$ and $\mathbf{H}^k(D) := (H^k(D))^d$.

We define the Hilbert space $\mathbf{H}(\text{div}; D)$ of vector fields in $\mathbf{L}^2(D)$ with divergence in $L^2(D)$, endowed with the graph norm, denotes as $\|\cdot\|_{\mathbf{H}(\text{div}; D)}$. Moreover, we set $\mathbf{H}_{0,\Sigma}(\text{div}; D) := \{\mathbf{v} \in \mathbf{H}(\text{div}; D) : \mathbf{v} \cdot \mathbf{n} = 0 \text{ on } \Sigma\}$ and $\mathbf{H}_0(\text{div}; D) := \mathbf{H}_{0,\partial D}(\text{div}; D)$.

Let $H^{\frac{1}{2}}(\partial D)$ be the range of the trace operator of functions in $H^1(D)$ and we define its restriction to Σ as $H^{\frac{1}{2}}(\Sigma)$. Both $H^{\frac{1}{2}}(\partial D)$ and $H^{\frac{1}{2}}(\Sigma)$ can be endowed with an intrinsic norm, see [130].

The dual space of $H^{\frac{1}{2}}(\Sigma)$ is denoted by $H^{-\frac{1}{2}}(\Sigma)$. The duality pairing between $H^{\frac{1}{2}}(\Sigma)$ and $H^{-\frac{1}{2}}(\Sigma)$ will be denoted with a formal integral notation. Finally, we define $\mathbf{H}^{\frac{1}{2}}(\partial D) := \left(H^{\frac{1}{2}}(\partial D)\right)^d$, $\mathbf{H}^{\frac{1}{2}}(\Sigma) := \left(H^{\frac{1}{2}}(\Sigma)\right)^d$, and $\mathbf{H}^{-\frac{1}{2}}(\Sigma) := \left(H^{-\frac{1}{2}}(\Sigma)\right)^d$.

We will often consider the infimum or the supremum of quotients of the type $\frac{f(x)}{\|x\|}$ or $\frac{|f(x)|}{\|x\|}$

where $(E, \|\cdot\|)$ is a Hilbert space with (topological) dual E' , $x \in E$, $f \in E'$. In these cases, we shall write $\sup_{x \in K} \frac{f(x)}{\|x\|}$ instead of $\sup_{\substack{x \in K \\ x \neq 0}} \frac{f(x)}{\|x\|}$ and $\sup_{x \in K} \frac{|f(x)|}{\|x\|}$ instead of $\sup_{\substack{x \in K \\ x \neq 0}} \frac{|f(x)|}{\|x\|}$, where K is a closed subspace of E .

Finally, \mathcal{O} will denote the classical Landau symbol.

Introduction

Part I: Stabilized isogeometric discretizations on trimmed and union geometries

Motivation

Manufacturing engineering is based on a *design-through-analysis* workflow. A virtual prototype is first designed as a geometrical model using Computer-aided-design (CAD) software. Then, to understand and settle its properties, some physical problems need to be simulated, typically using a Finite element analysis (FEA) software. Despite their mutual interactions in virtual prototyping, the two fields of design and analysis grow apart as two independent communities. On the one hand, computational design has been focusing on the modeling and visualization of geometric objects. On the other, computational analysis has been developing models to approach physical problems and reliable algorithms to approximate them numerically. However, most efforts have not aimed at bridging the growing gap between these two worlds. In the usual interplay between design and analysis, the designer produces a CAD file, which needs to be defeatured, repaired, and meshed (requiring human intervention) to become an analysis-suitable geometry, finally ready to be the input of a FEA code. Most of the time (about 80% [45, 78]) of the workflow is devoted to the intermediate step of constructing the simulation-specific geometry. It is in this context that Isogeometric analysis (IGA) comes to life, from the seminal work of T. J. R. Hughes and collaborators in 2005 [78], with the ambition of filling the gap between design and analysis in industrial simulation processes. The main idea of IGA is to use the same primitives employed in CAD, typically B-splines, non-uniform rational B-splines (NURBS), or some other extensions, as basis functions for the Galerkin discretization of the partial differential equations (PDEs). Progress in recent years has been remarkable, so it can be said that IGA is now a mature field of research; see the review papers [1, 19]. The mathematical study of IGA initiated with [17] and among its major successes, let us recall the development of IGA-tailored assembly and quadrature strategies [120], the recent progress in adaptivity [23, 29], and the steps towards the understanding of the superior approximation properties of higher-order spline spaces [26, 56]. However, we are still a long way from achieving the so-called *isogeometric paradigm* in practice: the geometries constructed by CAD software are not ready to be used for IGA-based-simulations. Their conversion to IGA-suitable geometric models remains an unsolved issue, and the required analysis time is a major bottleneck in the design-through-analysis workflow. Indeed, CAD geometries are described as collections of their boundary surfaces according to the so-called boundary representation (B-rep) [93, 109, 128]. These surfaces, often independently parametrized as tensor-product splines or NURBS, are joined, intersected, or trimmed. These Boolean operations act on the original surfaces to obtain a more complex surface, but they cannot be exactly performed, introducing gaps and overlaps. On the other hand, all developments of IGA rely on strong requirements on the underlying geometric models and, in general, do not support CAD geometries after Boolean operations.

Several efforts have been undertaken in the last years to improve the usability of CAD geometries in the solution of PDEs. From its side, the geometric modeling community provided essential inputs to this scientific challenge [43, 60, 95, 117]. In what follows, we briefly review some of the state-of-the-art techniques adopted by the IGA community, allowing to deal with typical CAD geometric descriptions. One of the first attempts to overcome the tensor product structure is the “multi-patch” representation, where the domain is represented by gluing many patches, each the image of the d -dimensional cube [32, 44, 45]. This description is natural when the geometry is made of different materials or when dealing with multi-physics problems. T-splines, introduced in [124] as a generalization of B-splines allowing T-junctions, can also be used, as in [123], for a watertight representation of the CAD geometry. Another idea is to convert the B-rep of the CAD object into a single NURBS-compatible subdivision surface, namely, a control polygon whose limit (in a suitable sense) is the original object itself [125]. We refer to [83, 132] for some isogeometric methods on subdivision surfaces. These strategies fall in the class of the so-called “global approaches” [93], where the geometric model is modified before the numerical simulation.

Another way is to follow a “local approach” [93], hence keeping the B-rep model as it is, and instead adapt the analysis in order to deal with it. Here, we describe some of the most promising strategies in this direction, mainly focused on geometries obtained via a trimming operation. The finite cell method [47, 105, 114] is a fictitious domain approach [65], where the domain is immersed into a larger domain with a simpler geometry that is readily meshed. An artificial stiffness parameter, discontinuously varying from 1 inside the physical domain to a small value ε outside, is introduced in order to weakly penalize the contribution from the non-physical part of the domain. The actual geometry is considered only in the integration process of the cut cells for which suitable quadrature rules need to be developed. Extended B-splines have been introduced in [77] in the context of a fictitious domain B-splines-based finite element method and have been later successfully applied within the isogeometric paradigm in [92, 94]. The main idea is to cure the instabilities deriving from the basis functions truncated by the trimming by systematically substituting the degenerate degrees of freedom. In this case, as well, particular care should be taken for performing integration in the cut elements. Other successful strategies in the literature are for sure [84, 101], even though these approaches are limited to the 2D case. Let us mention as well the Volumetric Representation (V-Rep), which in a sense is neither a global nor a local approach. V-rep, introduced in [95] and later proposed as an alternative framework for IGA in [4], is a new paradigm aiming to replace the B-rep in CAD software: the geometrical models are described by their occupied volumes. However, Boolean operations (this time among trivariate blocks) are still the fundamental ingredient to build complex domains and a source of issues for the numerical discretization of PDEs.

Main contributions

The goal of this dissertation is to study and develop robust solvers for isogeometric discretizations set on geometries coming from CAD software and constructed via Boolean operations (see the discussion in the previous section). We observe that our research applies to both the B-rep and V-rep paradigms. In particular, we restrict our focus to two kinds of constructions.

Trimmed geometries. Set difference, also known as “trimming”, acts on geometrical objects by removing unwanted parts. Given Ω_0 a spline patch, *i.e.*, homeomorphic to the d -unit cube through a spline mapping, and $\Omega_1, \dots, \Omega_N$ domains of \mathbb{R}^d , we let

$$\Omega = \Omega_0 \setminus \bigcup_{i=1}^N \overline{\Omega}_i, \quad (1)$$

and call it *trimmed domain*. Let us observe that while Ω_0 is endowed with a Bézier mesh

induced by its spline parametrization, Ω does not have any canonical mesh of its own. This means that when discretizing a PDE on Ω , we would have to work with the underlying mesh of Ω_0 , unfitted with the domain, hence to deal with cut Bézier elements, see Figure 1.

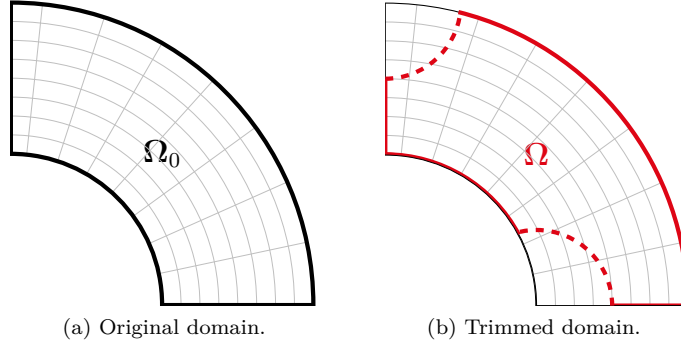


Figure 1 – Illustration of the trimming operation.

Union geometries. With the union, different objects are put together, giving rise to a new one. Given $\Omega_0^*, \dots, \Omega_N^*$ spline patches, we let

$$\bar{\Omega} = \bigcup_{i=0}^N \bar{\Omega}_i^*, \quad (2)$$

and call it *union domain*. We observe that we allow in (2) the patches to glue with overlaps, hence let

$$\Omega_i = \Omega_i^* \setminus \bigcup_{\ell=i+1}^N \bar{\Omega}_\ell^*, \quad i = 0, \dots, N,$$

be the visible parts of the patches, which are trimmed domains, see Figure 2. It follows that $\bar{\Omega} = \bigcup_{i=0}^N \bar{\Omega}_i$. The isogeometric discretization of a PDE in Ω will require an *ad hoc* strategy to glue the visible parts through their interfaces, and to deal with their cut meshes as well.

We recall that the following are necessary requirements for a numerical method in order to be robust:

- (i) it must rely on suitable quadrature rules in the trimmed elements;
- (ii) the conditioning of the resulting linear system needs to be under control;
- (iii) its discrete formulation has to be stable or well-posed. The precise definition is problem-dependent and will be given in the corresponding chapter.

The focus of this thesis is point (iii), while (i) and (ii) are only partially addressed. For what concerns (i), we rely on the technique developed in [4]. After identifying the cut and non-cut Bézier elements through a “slicing” procedure, with given geometric precision, every cut element is reparametrized as the union of high order Lagrange polynomials (of the same degree as the B-splines employed for discretizing the unknowns) composed of tetrahedra or hexahedra. This

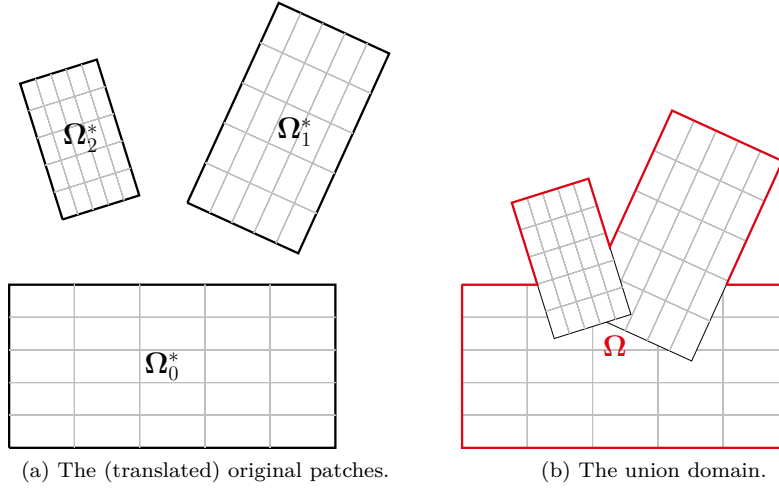


Figure 2 – Illustration of the union operation.

new mesh is used only to place the quadrature points: a Gauss-Legendre rule for hexahedra and a collapsed Gauss-Legendre rule for tetrahedra. Similarly, a thorough study of the conditioning of the final linear system is out of the scope of this work. In the numerical experiments, we will restrict ourselves to a simple left-right Jacobi preconditioner, which turns out to be a very effective solution in the presence of trimmed elements. However, as much as it helps to improve the conditioning of the stiffness matrix significantly, it does not completely eliminate the dependence of the conditioning number on the way the mesh elements are cut.

Our starting point is the isogeometric discretization of the Poisson problem in a trimmed geometry, like (1), whose boundary does not fit with the underlying physical Bézier mesh. As it is customary in the fictitious domain finite element method, we use Nitsche's method, a penalty-based formulation, to weakly impose the Dirichlet boundary conditions. We show its lack of well-posedness through a numerical experiment where the computational domain is trimmed so that sliver cut elements appear. It turns out that the main culprit for this loss of stability is the lack of an inverse inequality that is robust for trimming. We propose a stabilization technique, mainly inspired by [73], based on local modifications of the variational formulation of the discrete problem. In particular, we replace the evaluation of the normal derivatives through the boundaries of the badly trimmed elements with a suitable stable evaluation. In doing so, we do not add any additional parameters. In particular, we propose two classes of stabilizations: one whereby the stable evaluation of the fluxes is done in the parametric domain and then pushed forward to the physical domain, and another directly in the physical domain. The stabilization in the parametric domain is closely related to the weighted extended B-splines di [77] and suffers from sub-optimality in the case of an isogeometric map with low inter-regularity. The stabilization procedure in the physical domain, on the other hand, gives rise to a formulation with optimal approximation properties.

Then, we consider the Poisson problem in a union geometry, like (2). We assume that the patches overlay one on top of the other according to a given hierarchy. In this way, for each internal interface between two trimmed patches, one lies on top, and another lies below. We use the Nitsche method to enforce the transmission conditions at the internal interfaces and couple the patches. It turns out that the evaluation of the fluxes through a given interface, required by the transmission conditions, may involve the presence of cut elements. Similar to the case of a single trimmed patch, this causes instabilities to the discrete formulation. To resolve them,

we resort to the stabilization in the physical domain developed for the case of a single trimmed geometry. We rigorously prove the stability of the method and derive optimal *a priori* error estimates. All estimates track the dependence of the number of overlaps.

We carry on with the Stokes problem in a trimmed geometry, like (1). As in the elliptic case, the first issue we need to face is the imposition of the essential boundary conditions on the trimmed part of the boundary of the physical domain, which is addressed by using Nitsche's method. Again, evaluations of velocity fluxes along the boundaries of the trimmed elements cause instabilities that are resolved by applying a generalization of the stabilization used for the Poisson problem, adapted to the particular choice of the isogeometric element. This time, we must also fully stabilize the pressure space to get rid of the degrees of freedom corresponding to badly trimmed elements. We show that the coercivity of the bilinear form of the velocities is recovered. However, a mathematical proof of the inf-sup stability is still missing; hence we assume it for the subsequent analysis. We show that our method, combined with the isogeometric Raviart-Thomas, Nédélec, and Taylor-Hood elements, is well-posed and, consequently, we derive optimal *a priori* error estimates.

Outline

In Chapter 1 we introduce the fundamentals of isogeometric analysis. We give the definition of B-splines and spline spaces in the one-dimensional case and quickly move to the tensor product case. Then, the main assumptions on the parametrization and on the mesh used throughout the manuscript are given.

In Chapter 2 we focus on the isogeometric discretization of the Poisson problem on trimmed geometries. We show that the resulting discrete formulation suffers a lack of stability even when Dirichlet boundary conditions are weakly enforced using Nitsche's method. Then, we develop two novel stabilization techniques based on a modification of the variational formulation, allowing us to recover well-posedness and guaranteeing accuracy.

Chapter 3 focuses on the union operation, which involves multiple independent, trimmed spline patches, overlaid one on top of each other. We employ Nitsche's method to weakly couple independent patches through the visible internal interfaces. Moreover, we propose a stabilization method to address the instability issue that arises on the interfaces shared by arbitrary small trimmed elements. We prove that the proposed method recovers stability and guarantees the well-posedness of the problem as well as optimal error estimates.

In Chapter 4 the isogeometric approximation of the Stokes problem in a trimmed domain is studied. Different isogeometric elements are taken into consideration. We employ the Nitsche method to weakly impose the essential boundary conditions on the trimmed part of the boundary. Again, we show that the formulation requires appropriate stabilization. We introduce our stabilization procedure and partially prove (a proof of the inf-sup stability is still missing, but numerical results look promising) that in this way, we can recover the well-posedness of the method and, accordingly, optimal *a priori* error estimates.

In Chapter 5 we study the discretization of the Stokes problem in a union geometry. As in Chapter 3, we resort to the Nitsche method to weakly enforce the transmission conditions between the interfaces of the patches. The stabilization of Chapter 4 developed for the single patch case is extended to this setting. By assuming that some local inf-sup conditions are satisfied in each patch, we show that our stabilized formulation is stable and that optimal convergence rates are retained for different choices of isogeometric elements.

A note on the numerical implementation

The numerical experiments in Chapters 2 and 4 were designed and performed by the author of this manuscript by using the Matlab library GeoPDEs [131]. Regarding this part, we are grateful to Dr. Pablo Antolín for providing us with an automatic routine for performing integration in the trimmed elements to add to our code. Numerical experiments in Chapters 3 and 5 were designed in collaboration by the author, Dr. Pablo Antolín, and Dr. Xiaodong Wei and conducted by Dr. Xiaodong Wei using the C++ library igatools [106].

Part II: Weak imposition of the boundary conditions for the Darcy flow

Motivation

Mesh generation is one of the major bottlenecks for the classical finite element method (FEM) for the numerical solution of partial differential equations (PDEs). It is a very costly process because it necessitates not only important computational power but also human intervention. Mathematical problems for which mesh generation becomes a very demanding task are, in general, problems set in complicated geometries or for which the computational domain changes during the simulation. Typical examples arise in both computational fluid dynamics and mechanics: time-dependent flow problems described in Lagrangian coordinates, multiphase flows where the interfaces significantly vary, problems of fluid-structure interaction with large displacements, fracture propagation in porous media are some examples.

In the last few decades, many efforts have been devoted to developing robust numerical methods to tackle this issue. One of the most popular approaches is the so-called fictitious domain method where the possibly complicated domain Ω is immersed in a much simpler geometry $\Omega_{\mathcal{T}}$, for which the generation of the mesh is a simple task. Its origin traces back to the pioneering work [107], where a novel method for a fluid-structure interaction problem in heart physiology was proposed. Since then, a zoo of variants of this method have appeared in the mathematical and engineering literature, typically with names like “immersed methods”, “immersed boundary methods”, “unfitted methods”, or some combinations of the previous names.

Since the boundary (or the interface) of the physical domain is not resolved by the computational mesh, a common feature of the fictitious domain approaches is the weak imposition of the boundary conditions (or transmission conditions at the interface) through Lagrange multipliers [8], the penalty method [9], or Nitsche’s method [103].

We briefly review some of the most known fictitious domain methods. Among the first mathematical studies, let us recall the works of J. W. Barrett and C. M. Elliott, [12, 13, 14] on unfitted finite element methods for elliptic equations with different types of boundary conditions. In particular, in [13] the authors study the case of Dirichlet boundary conditions weakly imposed with the penalty method and prove optimal convergence rates in the energy norm, under extra regularity assumptions of the analytic solution, for a suitable choice of the penalty parameter with piecewise linear elements. Similarly, in [64] a fictitious domain finite element method based on the weak imposition of the Dirichlet boundary conditions with Lagrange multipliers is studied. Optimal convergence rates for piecewise linear polynomials are derived, provided that the ratio between the boundary mesh size and the mesh size in the domain is large enough.

Another successful class of methods is the Generalized Finite Element Method (GFEM) [10, 11] also appearing in the literature as Extended Finite Element Method (XFEM) [48, 98], addressing

at the same time the mesh generation issue and the approximation of irregular solutions of elliptic problems. Its main idea is the enrichment of the finite element space with non-polynomial functions living in a neighborhood of the unfitted boundary or the interface, based on the *a priori* knowledge of the behavior of the analytic solution. Integration, conditioning, and the imposition of the essential boundary conditions remain open problems in GFEM. This class of methods has been mainly applied to model crack propagations and, in general, for discontinuous phenomena.

In the last few years, the Cut Finite Element Method (CutFEM) [36] gained much attention and showed its potential in different applications in science and engineering [39, 72, 97]. CutFEM relies on solid theoretical foundations, and its key feature is to add weakly consistent stabilization operators [35] to the variational formulation of the discrete problem to transfer the stability and approximation properties from the finite element scheme constructed on the background mesh to its cut finite element counterpart.

Main contributions

In the second part of the thesis, we consider the Darcy flow as model problem, and we study the weak imposition of the essential boundary conditions. An important difference between the variational formulations of the Poisson and the Darcy problems is that the Dirichlet boundary conditions that were enforced by modifying the trial space in the primal case are now natural, *i.e.*, they appear as an integral on the right hand side, and the Neumann boundary conditions, that were before natural, have to be enforced as essential boundary conditions in the Darcy case.

The weak imposition of essential boundary conditions for elliptic problems is a quite well-understood matter; let us refer, for instance, to [53, 61, 126]. On the other hand, the problem of weakly imposing the essential boundary conditions for the Darcy problem, to the best of our knowledge, has not been deeply explored yet, either in standard boundary-fitted methods or in the fictitious domain setting.

Our analysis is based on the classical $\mathbf{H}(\text{div})$ -conforming Raviart-Thomas mixed element defined in simplicial and quadrilateral meshes. For the boundary-fitted case, we present two families of methods to weakly enforce the essential boundary conditions for the Darcy equations. The first one belongs to Nitsche-type consistent methods, and the second one is a penalty method derived from a perturbation of the strong problem. Both classes of methods are presented in symmetric and non-symmetric versions. The main advantage of the non-symmetric versions is to exploit the well-known commuting diagram property satisfied by the Raviart-Thomas element. The discrete functional setting is somehow unusual since it is based on mesh-dependent norms scaling as $\mathbf{H}^1 \times H^1$, instead of the usual $\mathbf{H}(\text{div}) \times L^2$. Moreover, we observe that a superpenalty parameter is imposed on the flux variable along the essential part of the boundary in both formulations. Through standard arguments for the mixed element approximation of saddle point problems, we derive *a priori* error estimates for the velocity and pressure fields which are optimal for the chosen topologies but not for the usual ones. The orthogonality along the boundary of the interpolation operator for the velocity allows us to prove a superconvergence result enabling us to recover the usual optimal convergence rates for the velocity in the \mathbf{L}^2 -norm. What has been said above applies to both methods. However, for the penalty method, to avoid technicalities arising from the regularity theory of elliptic equations with essential boundary conditions, the estimates are restricted to the case of an analytic solution for the velocity in \mathbf{H}^1 . We observe that we set equal to one the dimensionless parameter related to the enforcement of the boundary conditions, in contrast to the Poisson problem case where these quantities have to be taken large enough. A discussion on the conditioning of the finite element stiffness matrices is carried out. We show through numerical experiments that the Nitsche method is preferable to the penalty method as its effects on the condition numbers are much milder.

Introduction

In the last chapter we study the case of a fictitious domain finite element discretization of the Darcy problem. We focus on the Nitsche method presented for the boundary fitted case and study its extension to the unfitted setting. The discrete formulation is very ill-posed because the geometry can cut through the mesh arbitrarily. We show that this affects the accuracy of the approximation scheme and the conditioning of the arising linear system. Our strategy, in line with [35, 37, 38], consists of adding to the variational formulation at the discrete level two weakly consistent operators acting separately on the velocity and the pressure fields. Once again, the choice of the norms for the discrete spaces gives rise to suboptimal orders of convergence for the usual $\mathbf{H}(\text{div}) \times L^2$ topology. The orthogonality argument that allowed us to recover the optimal L^2 -estimate for the velocities is no more available because of the mismatch between mesh and boundary. On the other hand, we can prove an upper bound for the condition number of the stabilized stiffness matrix. Our numerical studies show that our method delivers optimal convergence rates with respect to the L^2 -norm for both velocity and pressure. However, our stabilization procedure pollutes the divergence of the numerical solution for the velocity and the numerical scheme preserves the mass only approximately.

Outline

In Chapter 6 we introduce the Darcy problem and its standard approximation with the Raviart-Thomas element for both triangular and quadrilateral meshes.

In Chapter 7 we propose two methods, a Nitsche-type and a penalty-type, for the weak imposition of the essential boundary conditions for the Darcy problem. We rigorously analyze their stability and deliver *a priori* error estimates for both velocity and pressure, which are optimal with respect to the chosen norms. In the case of the velocity, we also derive optimal error estimates for the L^2 -norm.

The aim of Chapter 8 is to study the extension of the Nitsche formulation of the previous chapter to the unfitted setting. We propose a fictitious domain method approach that fits the CutFEM paradigm and uses ghost penalty operators to recover the stability and keep the linear system's conditioning under control.

A note on the numerical implementation

The numerical experiments in Chapter 7 were implemented in FreeFem++ [74] and in the Matlab library GeoPDEs [131]. For the experiments in the unfitted case in Chapter 8, we tested our method on quadrilateral meshes in GeoPDEs. We thank Dr. Pablo Antolín for providing us with an automatic routine for performing integration in the cut elements to add to our code.

Stabilized isogeometric
discretizations on trimmed and
union
geometries

Part I

1 Preliminaries

In this chapter, we briefly review the construction of isogeometric spline and NURBS spaces for the discretization of PDEs. The Poisson and Stokes equations, the model problems for this part of the manuscript, are introduced and discretized. Let us observe that there are several comprehensive IGA-oriented introductions to splines in the literature; we refer the interested reader, for instance, to [19, 45, 78].

1.1 Isogeometric analysis: B-splines, mesh and parametrization

1.1.1 The univariate case

Given two positive integers p and n , we say that $\Xi := \{\xi_1, \dots, \xi_{n+p+1}\}$ is a p -open knot vector if

$$\xi_1 = \dots = \xi_{p+1} < \xi_{p+2} \leq \dots \leq \xi_n < \xi_{n+1} = \dots = \xi_{n+p+1}.$$

We assume $\xi_1 = 0$ and $\xi_{n+p+1} = 1$. We also introduce $Z := \{\zeta_1, \dots, \zeta_M\}$, the set of *breakpoints*, or knots without repetitions, which forms a partition of the unit interval $(0, 1)$. Note that

$$\Xi = \underbrace{\{\zeta_1, \dots, \zeta_1\}}_{m_1 \text{ times}}, \underbrace{\{\zeta_2, \dots, \zeta_2\}}_{m_2 \text{ times}}, \dots, \underbrace{\{\zeta_M, \dots, \zeta_M\}}_{m_M \text{ times}},$$

where m_j is the multiplicity of the breakpoint ζ_j and $\sum_{i=1}^M m_i = n + p + 1$. Moreover, we assume $m_j \leq p$ for every internal knot, and we denote $I_i := (\zeta_i, \zeta_{i+1})$ and its measure $h_i := \zeta_{i+1} - \zeta_i$, $i = 1, \dots, M - 1$.

We denote as $\widehat{B}_{i,p} : [0, 1] \rightarrow \mathbb{R}$ the i th B -spline, $1 \leq i \leq n$, obtained using the *Cox-de Boor formula*

$$\begin{aligned} \widehat{B}_{i,0}(\zeta) &:= \begin{cases} 1, & \text{if } \zeta \in [\xi_i, \xi_{i+1}), \\ 0, & \text{otherwise,} \end{cases} \\ \widehat{B}_{i,p}(\zeta) &:= \frac{\zeta - \xi_i}{\xi_{i+p} - \xi_i} \widehat{B}_{i,p-1}(\zeta) + \frac{\xi_{i+p+1} - \zeta}{\xi_{i+p+1} - \xi_{i+1}} \widehat{B}_{i+1,p-1}(\zeta), \quad p \geq 1, \end{aligned}$$

with the convention that $\frac{0}{0} = 0$. Moreover, let $S_{\alpha}^p(\Xi) := \text{span}\{\widehat{B}_{i,p} : 1 \leq i \leq n\}$ be the vector space of univariate splines of degree p . $S_{\alpha}^p(\Xi)$ can also be characterized as the space of piecewise

polynomials of degree p with $\alpha_j := p - m_j$ continuous derivatives at the breakpoints ζ_j , $1 \leq j \leq M$ (*Curry-Schoenberg Theorem* [91]). The number of continuous derivatives at the breakpoints is collected in the *regularity vector* $\alpha := (\alpha_j)_{j=1}^M$. A knot multiplicity $m_j = p + 1$ corresponds to a regularity $\alpha_j = -1$, i.e., a discontinuity at the breakpoint ζ_j . Since the knot vector is open, it holds $\alpha_1 = \alpha_M = -1$. For the sake of simplicity of the notation we assume that the basis functions have the same regularity at the internal knots, namely $\alpha_j = \alpha$ for $2 \leq j \leq M - 1$. Note that the derivatives of spines are splines too when $p \geq 1$ and $\alpha \geq 0$ and, for $\Xi' := \{\xi_2, \dots, \xi_{n+p}\}$, the operator $\frac{d}{dx} : S_{\alpha}^p(\Xi) \rightarrow S_{\alpha-1}^{p-1}(\Xi')$ is surjective., where $\alpha - 1$ denotes the regularity vector $(\alpha_j - 1)_{j=1}^M$.

Let us define univariate NURBS. Given the positive coefficients $w_j > 0$, $1 \leq j \leq n$, we define the *weight* $W(\zeta) := \sum_{i=1}^n w_i \hat{B}_{i,p}(\zeta)$, and the basis functions

$$\hat{N}_{j,p}(\zeta) := \frac{w_j \hat{B}_{j,p}(\zeta)}{W(\zeta)}, \quad j = 1, \dots, n,$$

which are called *non-rational uniform B-splines* (NURBS) and span the NURBS space $N_{\alpha}^p(\Xi, W) := \text{span}\{\hat{N}_{i,p} : i = 1, \dots, n\}$.

Moreover, given an interval $I_j = (\zeta_j, \zeta_{j+1}) = (\xi_i, \xi_{i+1})$, we define its *support extension* \tilde{I}_j as

$$\tilde{I}_j := \text{int} \bigcup \{\text{supp}(\hat{B}_{k,p}) : \text{supp}(\hat{B}_{k,p}) \cap I_j \neq \emptyset, 1 \leq k \leq n\} = (\xi_{i-p}, \xi_{i+p+1}).$$

1.1.2 The multivariate case

Let $d \in \{2, 3\}$ denote the space dimension and $M_{\ell}, n_{\ell}, p_{\ell} \in \mathbb{N}$, $\Xi_{\ell} = \{\xi_{\ell,1}, \dots, \xi_{\ell,n_{\ell}+p_{\ell}+1}\}$, $Z_{\ell} = \{\zeta_{\ell,1}, \dots, \zeta_{\ell,M_{\ell}}\}$ be given, for every $1 \leq \ell \leq d$. We set the degree vector $\mathbf{p} := (p_1, \dots, p_d)$, the regularity vectors α_{ℓ} , $1 \leq \ell \leq d$, and $\Xi := \Xi_1 \times \dots \times \Xi_d$. As in the univariate case, we assume that the same regularity holds at the internal knots for every parametric direction, hence we drop the bold font once for all and write α_{ℓ} , $1 \leq \ell \leq d$. Note that the breakpoints of Z_{ℓ} form a Cartesian grid in the *parametric domain* $\hat{\Omega}_0 := (0, 1)^d$, namely the *parametric Bézier mesh*

$$\hat{\mathcal{M}}_{0,h} := \{Q_{\mathbf{j}} = I_{1,j_1} \times \dots \times I_{d,j_d} : I_{\ell,j_{\ell}} = (\zeta_{\ell,j_{\ell}}, \zeta_{\ell,j_{\ell}+1}) : 1 \leq j_{\ell} \leq M_{\ell} - 1\},$$

where each $Q_{\mathbf{j}}$ is called a *parametric Bézier element*, with $h_{Q_{\mathbf{j}}} := \text{diam}(Q_{\mathbf{j}})$. Let $h := \max\{h_Q : Q \in \hat{\mathcal{M}}_{0,h}\}$.

Assumption 1.1.1. The family of meshes $\{\hat{\mathcal{M}}_{0,h}\}_h$ is assumed to be *shape-regular*, that is, the ratio between the smallest edge of $Q \in \hat{\mathcal{M}}_{0,h}$ and its diameter h_Q is uniformly bounded with respect to Q and h .

Remark 1.1.2. Shape-regularity implies that the mesh is *locally quasi-uniform*, i.e., the ratio of the sizes of two neighboring elements is uniformly bounded (see [17]). Also note that it allows us to assign h_Q as the unique size of the element, without the necessity of dealing with the length of its edges separately.

Let $\mathbf{I} := \{\mathbf{i} = (i_1, \dots, i_d) : 1 \leq i_{\ell} \leq n_{\ell}\}$ be a set of multi-indices. For each $\mathbf{i} = (i_1, \dots, i_d)$, we define the set of *multivariate B-splines* $\{\hat{B}_{\mathbf{i},\mathbf{p}}(\zeta) = \hat{B}_{i_1,p_1}(\zeta_1) \dots \hat{B}_{i_d,p_d}(\zeta_d) : \mathbf{i} \in \mathbf{I}\}$. The *multivariate spline space* in $\hat{\Omega}$ is defined as $S_{\alpha_1, \dots, \alpha_d}^{\mathbf{p}}(\Xi) := \text{span}\{\hat{B}_{\mathbf{i},\mathbf{p}} : \mathbf{i} \in \mathbf{I}\}$, which can also be seen as the space

of piecewise multivariate polynomials of degree \mathbf{p} and with regularity across the Bézier elements given by the knot multiplicities. Note that $S_{\alpha_1, \dots, \alpha_d}^{\mathbf{p}}(\Xi) = S_{\alpha_1, \dots, \alpha_d}^{\mathbf{p}}(\Xi_1, \dots, \Xi_d) = \bigotimes_{\ell=1}^d S_{\alpha_\ell}^{p_\ell}(\Xi_\ell)$.

Given a collection of positive coefficients $\{w_{\mathbf{j}} : \mathbf{j} \in \mathbf{I}\}$, we set the weight $W(\zeta) := \sum_{\mathbf{i} \in \mathbf{I}} w_{\mathbf{i}} \hat{B}_{\mathbf{i}, \mathbf{p}}(\zeta)$, and the *multivariate NURBS*

$$\hat{N}_{\mathbf{j}, \mathbf{p}}(\zeta) := \frac{w_{\mathbf{j}} \hat{B}_{\mathbf{j}, \mathbf{p}}(\zeta)}{W(\zeta)}, \quad \mathbf{j} \in \mathbf{I}.$$

The *multivariate NURBS space* is defined as $N_{\alpha_1, \dots, \alpha_d}^{\mathbf{p}}(\Xi, W) := \text{span}\{\hat{N}_{\mathbf{i}, \mathbf{p}}(\zeta) : \mathbf{i} \in \mathbf{I}\}$.

Moreover, for an arbitrary Bézier element $Q_{\mathbf{j}} \in \widehat{\mathcal{M}}_{0, h}$, we define its *support extension* $\tilde{Q}_{\mathbf{j}} := \tilde{I}_{1, j_1} \times \dots \times \tilde{I}_{d, j_d}$, where \tilde{I}_{l, j_ℓ} is the univariate support extension of the univariate case defined above.

1.1.3 Parametrization and physical domain

Let \mathbf{p}, Ξ be a degree and a knot vector at a coarse level of discretization. We recall that for splines *h*-refinement and *p*-refinement are obtained, respectively, via *knot insertion* and *degree elevation* [19]. Given a spline space $S_{\alpha_1, \dots, \alpha_d}^{\mathbf{p}}(\Xi) = \text{span}\{\hat{B}_{\mathbf{i}, \mathbf{p}} : \mathbf{i} \in \mathbf{I}\}$ and *control points* $\{\mathbf{c}_{\mathbf{j}} : \mathbf{j} \in \mathbf{I}\}$, we may define the *spline parametrization* or *isogeometric mapping*

$$\mathbf{F}(\zeta) := \sum_{\mathbf{i} \in \mathbf{I}} \mathbf{c}_{\mathbf{i}} \hat{B}_{\mathbf{i}, \mathbf{p}}(\zeta), \quad \zeta \in \hat{\Omega}_0,$$

such that $\Omega_0 = \mathbf{F}(\hat{\Omega}_0)$, where Ω_0 is the so-called *physical domain*. Similarly, given a NURBS space $N_{\alpha_1, \dots, \alpha_d}^{\mathbf{p}}(\Xi, \mathbf{W}) = \text{span}\{\hat{N}_{\mathbf{i}, \mathbf{p}} : \mathbf{i} \in \mathbf{I}\}$, we define the *NURBS parametrization*

$$\mathbf{F}(\zeta) := \sum_{\mathbf{i} \in \mathbf{I}} \mathbf{c}_{\mathbf{i}} \hat{N}_{\mathbf{i}, \mathbf{p}}(\zeta), \quad \zeta \in \hat{\Omega}_0.$$

We define the *physical Bézier mesh* as the image of the elements in $\widehat{\mathcal{M}}_{0, h}$ through \mathbf{F}

$$\mathcal{M}_{0, h} := \{K \subset \Omega : K = \mathbf{F}(Q), Q \in \widehat{\mathcal{M}}_{0, h}\}.$$

We denote $h_K := \text{diam}(K)$ for each $K \in \mathcal{M}_{0, h}$. To prevent the existence of singularities in the parametrization, we make the following assumption.

Assumption 1.1.3. The parametrization $\mathbf{F} : \hat{\Omega}_0 \rightarrow \Omega_0$ is bi-Lipschitz. Moreover, $\mathbf{F}|_{\bar{Q}} \in C^\infty(\bar{Q})$ for every $Q \in \widehat{\mathcal{M}}_{0, h}$ and $\mathbf{F}^{-1}|_{\bar{K}} \in C^\infty(\bar{K})$ for every $K \in \mathcal{M}_{0, h}$.

Some consequences of Assumption 1.1.3 are the following.

1. $h_Q \approx h_K$, i.e., there exist $C_1 > 0, C_2 > 0$ such that $C_1 h_K \leq h_Q \leq C_2 h_K$;
2. there exists $C > 0$ such that, for all $Q \in \widehat{\mathcal{M}}_{0, h}$ such that $\mathbf{F}(Q) = K$, it holds $\|D\mathbf{F}\|_{L^\infty(Q)} \leq C$ and $\|D\mathbf{F}^{-1}\|_{L^\infty(K)} \leq C$;
3. there exist $C_1 > 0, C_2 > 0$ such that $C_1 \leq |\det(D\mathbf{F}(\zeta))| \leq C_2$ for all $\zeta \in \hat{\Omega}_0$.

Moreover, note that Assumption 1.1.3 implies that if the parametric mesh is shape-regular, then the physical mesh is shape-regular too. With an abuse of notation, we may denote $h := \max_{K \in \mathcal{M}_{0,h}} h_K$, even if the same symbol has been used for the maximum diameter of the parametric mesh. We define $h : \Omega_0 \rightarrow (0, +\infty)$ to be the piecewise constant mesh-size function assigning to each active element $K \in \mathcal{M}_{0,h}$ its diameter, namely $h|_K := h_K$.

Remark 1.1.4. Even though in this thesis we are mainly going to deal with spline spaces, everything is easily generalizable to the case of NURBS [45].

1.2 Isogeometric discretization of the Poisson problem on untrimmed geometries

Let Γ_0 denote the boundary of Ω_0 with unit outer normal \mathbf{n}_0 and such that $\Gamma_0 = \bar{\Gamma}_D \cup \bar{\Gamma}_N$, where Γ_D and Γ_N are non-empty, open, and disjoint.

Assumption 1.2.1. We assume that $\hat{\Gamma}_D, \hat{\Gamma}_D := \mathbf{F}^{-1}(\Gamma_D)$, is the union of full faces of the parametric domain $\hat{\Omega}_0$.

The Poisson problem is a second-order linear elliptic partial differential equation describing the diffusion of a given quantity (for instance, a temperature, a mass, or an electric charge distribution) subjected to an external force or source term and suitable boundary conditions. Given the source term $f \in L^2(\Omega_0)$, the Dirichlet datum $g_D \in H^{\frac{1}{2}}(\Gamma_D)$ and the Neumann datum $g_N \in H^{-\frac{1}{2}}(\Gamma_N)$, we look for $u : \Omega_0 \rightarrow \mathbb{R}$ such that

$$\begin{aligned} -\Delta u &= f, & \text{in } \Omega_0, \\ u &= g_D, & \text{on } \Gamma_D, \\ \frac{\partial u}{\partial n} &= g_N, & \text{on } \Gamma_N. \end{aligned} \tag{1.1}$$

In what follows, we will use the subscript 0 to refer to the fact that we are discretizing in the untrimmed domain Ω_0 . We define the isogeometric approximation space in the physical domain

$$V_{0,h} := \{v_h \circ \mathbf{F}^{-1} : v_h \in \hat{V}_{0,h}\},$$

where $\hat{V}_{0,h} := S_{\alpha_1, \dots, \alpha_d}^{\mathbf{p}}(\Xi)$ is the approximation space in the parametric domain, Ξ is the same knot vector (or a refinement of it) used for the geometry at a coarse level of discretization with degree \mathbf{p} and internal regularities α_i , $1 \leq i \leq d$.

We say that $\xi \in L^2(\Gamma_D)$ is a *discrete Dirichlet datum* if there exists $v_h \in V_{0,h}$ such that $v_h|_{\Gamma_D} = \xi$. We define

$$V_{0,h}^{\xi} := \{v_h \in V_{0,h} : v_h|_{\Gamma_D} = \xi\}.$$

Note that if g_D is a discrete Dirichlet datum, then $V_{0,h}^{g_D}$ is readily defined. Otherwise, we assume to have an approximation $g_{h,D}$ of it which is a Dirichlet datum and, by abuse of notation, we set $V_{0,h}^{g_D} := V_{0,h}^{g_{h,D}}$. We can construct such an approximation with an L^2 -projection of g_D on the dofs associated with Γ_D as described in [131].

We are finally ready to discretize (1.1).

Find $u_h \in V_{0,h}^{g_D}$ such that

$$a(u_h, v_h) = F(v_h), \quad \forall v_h \in V_{0,h}^0, \tag{1.2}$$

1.3. Isogeometric discretization of the Stokes problem on untrimmed geometries

where

$$\begin{aligned} a(w_h, v_h) &:= \int_{\Omega_0} \nabla w_h \cdot \nabla v_h, & w_h, v_h \in V_{0,h}, \\ F(v_h) &:= \int_{\Omega_0} f v_h + \int_{\Gamma_N} g_N v_h, & v_h \in V_{0,h}. \end{aligned}$$

Remark 1.2.2. The writing in (1.2) should be interpreted as a shortcut for the usual *lifting* of the Dirichlet datum, see [112].

Another way to impose the Dirichlet boundary conditions, instead of manipulating the discrete space, is to incorporate them in the variational formulation of the problem. The Nitsche method, originally proposed in [103], and later rediscovered in [126], is a consistent penalty method that enjoys optimal approximation properties.

Find $u_h \in V_{0,h}$ such that

$$a_h(u_h, v_h) = F_h(v_h), \quad \forall v_h \in V_{0,h}, \quad (1.3)$$

where

$$\begin{aligned} a_h(w_h, v_h) &:= \int_{\Omega_0} \nabla w_h \cdot \nabla v_h - \int_{\Gamma_D} \frac{\partial w_h}{\partial n} v_h - \underbrace{\int_{\Gamma_D} w_h \frac{\partial v_h}{\partial n}}_{\text{symmetry}} + \underbrace{\beta \int_{\Gamma_D} \mathbf{h}^{-1} w_h v_h}_{\text{stability}}, & w_h, v_h \in V_{0,h}, \\ F_h(v_h) &:= \int_{\Omega_0} f v_h + \int_{\Gamma_N} g_N v_h - \underbrace{\int_{\Gamma_D} g_D \frac{\partial v_h}{\partial n} + \beta \int_{\Gamma_D} \mathbf{h}^{-1} g_D v_h}_{\text{consistency}}, & v_h \in V_{0,h}, \end{aligned}$$

$\beta > 0$ being a penalty parameter.

1.3 Isogeometric discretization of the Stokes problem on untrimmed geometries

As in the Poisson case, we assume that the boundary of Ω_0 , Γ_0 , has unit outer normal \mathbf{n}_0 and can be written as $\Gamma_0 = \bar{\Gamma}_D \cup \bar{\Gamma}_N$, with Γ_D satisfying Assumption 1.2.1.

The Stokes equations are a linear system that can be derived as a simplification of the Navier-Stokes equations. They describe the flow of a fluid under incompressibility and slow motion regimes. Given the body force $\mathbf{f} \in \mathbf{L}^2(\Omega_0)$, the mass production rate $g \in L^2(\Omega_0)$, the Dirichlet datum $\mathbf{u}_D \in \mathbf{H}^{\frac{1}{2}}(\Gamma_D)$ and the Neumann datum $\mathbf{u}_N \in \mathbf{H}^{-\frac{1}{2}}(\Gamma_N)$, we look for the *velocity* $\mathbf{u} : \Omega_0 \rightarrow \mathbb{R}^d$ and *pressure* $p : \Omega_0 \rightarrow \mathbb{R}$ such that

$$\begin{aligned} -\mu \Delta \mathbf{u} + \nabla p &= \mathbf{f}, & \text{in } \Omega_0, \\ \operatorname{div} \mathbf{u} &= g, & \text{in } \Omega_0, \\ \mathbf{u} &= \mathbf{u}_D, & \text{on } \Gamma_D, \\ \boldsymbol{\sigma}(\mathbf{u}, p) \mathbf{n} &= \mathbf{u}_N, & \text{on } \Gamma_N, \end{aligned} \quad (1.4)$$

where $\mu > 0$ is the *viscosity coefficient*, $\boldsymbol{\sigma}(\mathbf{u}, p) := \mu D\mathbf{u} - p\mathbf{I}$ is the *Cauchy stress tensor*, $(D\mathbf{u})_{ij} := \frac{\partial u_i}{\partial x_j}$, $i, j = 1, \dots, d$. The first equation is known as the *conservation of the momentum* and is nothing else than Newton's Second Law, relating the external forces acting on the fluid to the rate of change of its momentum, the second one is the *conservation of mass* (when $g \equiv 0$).

We need to construct compatible spaces for velocity and pressure for the discretization of the Stokes problem (see [28]). To define the isogeometric spaces in the parametric domain, we need to resort to the following cumbersome notation. For every $1 \leq \ell \leq d$, let Ξ_ℓ be a knot vector of degree k and regularity vector α , with $\Xi = \Xi_1 \times \cdots \times \Xi_\ell$ is the knot vector used for the geometry. We construct $\tilde{\Xi}_\ell$, a knot vector of degree $k+1$ and regularity $\alpha+1$, from Ξ_ℓ by adding one repetition of the first and last knots. By increasing the multiplicity of the internal knots Ξ_ℓ by one, we obtain $\tilde{\Xi}_\ell$, a knot vector of degree $k+1$ and regularity α .

We define the following approximation spaces in the parametric domain.

$$\begin{aligned} \widehat{V}_{0,h}^{\text{RT}} &:= \begin{cases} S_{\alpha+1,\alpha}^{k+1,k}(\tilde{\Xi}_1, \Xi_2) \times S_{\alpha,\alpha+1}^{k,k+1}(\Xi_1, \tilde{\Xi}_2), & \text{if } d = 2, \\ S_{\alpha+1,\alpha,\alpha}^{k+1,k,k}(\tilde{\Xi}_1, \Xi_2, \Xi_3) \times S_{\alpha,\alpha+1,\alpha}^{k,k+1,k}(\Xi_1, \tilde{\Xi}_2, \Xi_3) \times S_{\alpha,\alpha,\alpha+1}^{k,k,k+1}(\Xi_1, \Xi_2, \tilde{\Xi}_3), & \text{if } d = 3, \end{cases} \\ \widehat{V}_{0,h}^{\text{N}} &:= \begin{cases} S_{\alpha+1,\alpha}^{k+1,k+1}(\tilde{\Xi}_1, \tilde{\Xi}_2) \times S_{\alpha,\alpha+1}^{k+1,k+1}(\tilde{\Xi}_1, \tilde{\Xi}_2), & \text{if } d = 2, \\ S_{\alpha+1,\alpha,\alpha}^{k+1,k+1,k+1}(\tilde{\Xi}_1, \tilde{\Xi}_2, \tilde{\Xi}_3) \times S_{\alpha,\alpha+1,\alpha}^{k+1,k+1,k+1}(\tilde{\Xi}_1, \tilde{\Xi}_2, \tilde{\Xi}_3) \times S_{\alpha,\alpha,\alpha+1}^{k+1,k+1,k+1}(\tilde{\Xi}_1, \tilde{\Xi}_2, \tilde{\Xi}_3), & \text{if } d = 3, \end{cases} \\ \widehat{V}_{0,h}^{\text{TH}} &:= \begin{cases} S_{\alpha,\alpha}^{k+1,k+1}(\tilde{\Xi}_1, \tilde{\Xi}_2) \times S_{\alpha,\alpha}^{k+1,k+1}(\tilde{\Xi}_1, \tilde{\Xi}_2), & \text{if } d = 2, \\ S_{\alpha,\alpha,\alpha}^{k+1,k+1,k+1}(\tilde{\Xi}_1, \tilde{\Xi}_2, \tilde{\Xi}_3) \times S_{\alpha,\alpha,\alpha}^{k+1,k+1,k+1}(\tilde{\Xi}_1, \tilde{\Xi}_2, \tilde{\Xi}_3) \times S_{\alpha,\alpha,\alpha}^{k+1,k+1,k+1}(\tilde{\Xi}_1, \tilde{\Xi}_2, \tilde{\Xi}_3), & \text{if } d = 3, \end{cases} \\ \widehat{Q}_{0,h} &:= \begin{cases} S_{\alpha,\alpha}^{k,k}(\Xi_1, \Xi_2), & \text{if } d = 2, \\ S_{\alpha,\alpha,\alpha}^{k,k,k}(\Xi_1, \Xi_2, \Xi_3), & \text{if } d = 3. \end{cases} \end{aligned}$$

It holds $\widehat{V}_{0,h}^{\text{RT}} \subset \widehat{V}_{0,h}^{\text{N}} \subset \widehat{V}_{0,h}^{\text{TH}}$, see [28]. We note that, for $\alpha = -1$, $\widehat{V}_{0,h}^{\text{RT}}$ and $\widehat{V}_{0,h}^{\text{N}}$ recover the classical Raviart-Thomas finite element and Nédélec finite element of the second kind, respectively. For $\alpha = 0$, $\widehat{V}_{0,h}^{\text{TH}}$ represents the classical Taylor-Hood finite element space. Henceforth we assume $\alpha \geq 0$, otherwise $\widehat{V}_{0,h}^\square$, $\square \in \{\text{RT}, \text{N}, \text{TH}\}$, is a discontinuous space (of *jump type*) and it does not provide a suitable discretization for the velocity solution of the Stokes problem, since it is not \mathbf{H}^1 -conforming.

The isogeometric spaces in the physical domain Ω_0 read as follows

$$\begin{aligned} V_{0,h}^{\text{RT}} &:= \{\mathbf{v}_h : \iota_v(\mathbf{v}_h) \in \widehat{V}_{0,h}^{\text{RT}}\}, \quad V_{0,h}^{\text{N}} := \{\mathbf{v}_h : \iota_v(\mathbf{v}_h) \in \widehat{V}_{0,h}^{\text{N}}\}, \quad V_{0,h}^{\text{TH}} := \{\mathbf{v}_h : \mathbf{v}_h \circ \mathbf{F} \in \widehat{V}_{0,h}^{\text{TH}}\}, \\ Q_{0,h}^{\text{RT}} = Q_{0,h}^{\text{N}} &:= \{q_h : \iota_p(q_h) \in \widehat{Q}_{0,h}\}, \quad Q_{0,h}^{\text{TH}} := \{q_h : q_h \circ \mathbf{F} \in \widehat{Q}_{0,h}\}, \end{aligned}$$

where ι_v and ι_p are, respectively, the divergence-preserving and integral-preserving transformations, defined as

$$\begin{aligned} \iota_v : \mathbf{H}(\text{div}; \Omega_0) &\rightarrow \mathbf{H}(\text{div}; \widehat{\Omega}_0), & \iota_v(\mathbf{v}) &:= \det(D\mathbf{F}) D\mathbf{F}^{-1}(\mathbf{v} \circ \mathbf{F}), \\ \iota_p : L^2(\Omega_0) &\rightarrow L^2(\widehat{\Omega}_0), & \iota_p(q) &:= \det(D\mathbf{F})(q \circ \mathbf{F}). \end{aligned}$$

We are going to refer to the pairs $V_{0,h}^{\text{RT}} - Q_{0,h}^{\text{RT}}$, $V_{0,h}^{\text{N}} - Q_{0,h}^{\text{N}}$, $V_{0,h}^{\text{TH}} - Q_{0,h}^{\text{TH}}$ as the *isogeometric Raviart-Thomas*, *Nédélec* and *Taylor-Hood* elements, respectively. To further alleviate the notation, we adopt the convention to omit the superscript $\square \in \{\text{RT}, \text{N}, \text{TH}\}$ when what said does not depend from the particular finite element choice. Let us observe that, in the physical domain, $V_{0,h}^{\text{RT}} \subset V_{0,h}^{\text{N}} \not\subset V_{0,h}^{\text{TH}}$.

For the Taylor-Hood element, the spaces satisfying boundary conditions $V_{0,h}^{\text{TH}, \mathbf{u}_D}$ and $V_{0,h}^{\text{TH}, \mathbf{0}}$ can be constructed, in general, by using an L^2 -projection on the dofs associated with Γ_D , as explained for the discretization of the Poisson problem. Hence, we can discretize (1.4) as follows.

Find $(\mathbf{u}_h, p_h) \in V_{0,h}^{\text{TH}, \mathbf{u}_D} \times Q_{0,h}^{\text{TH}}$ such that

$$\begin{aligned} a(\mathbf{u}_h, \mathbf{v}_h) + b(\mathbf{v}_h, p_h) &= F(\mathbf{v}_h), & \forall \mathbf{v}_h \in V_{0,h}^{\text{TH}, \mathbf{0}}, \\ b(\mathbf{u}_h, q_h) &= G(q_h), & \forall q_h \in Q_{0,h}^{\text{TH}}, \end{aligned} \tag{1.5}$$

1.3. Isogeometric discretization of the Stokes problem on untrimmed geometries

where

$$\begin{aligned}
a(\mathbf{w}_h, \mathbf{v}_h) &:= \int_{\Omega_0} \mu D\mathbf{w}_h : D\mathbf{v}_h, & \mathbf{w}_h, \mathbf{v}_h &\in V_{0,h}^{\text{TH}}, \\
b(\mathbf{v}_h, q_h) &:= - \int_{\Omega_0} q_h \operatorname{div} \mathbf{v}_h, & \mathbf{v}_h &\in V_{0,h}^{\text{TH}}, \quad q_h \in Q_{0,h}^{\text{TH}} \\
F(\mathbf{v}_h) &:= \int_{\Omega_0} \mathbf{f} \cdot \mathbf{v}_h + \int_{\Gamma_N} \mathbf{u}_N \cdot \mathbf{v}_h, & \mathbf{v}_h &\in V_{0,h}^{\text{TH}}, \\
G(q_h) &:= - \int_{\Omega_0} g q_h, & q_h &\in Q_{0,h}^{\text{TH}}.
\end{aligned}$$

We observe that the imposition of the non-homogeneous Dirichlet boundary conditions in (1.5) should be done with a *lifting*.

We recall that the Raviart-Thomas isogeometric element satisfies $\operatorname{div} V_{0,h}^{\text{RT}} = Q_{0,h}^{\text{RT}}$ [34]. This property still holds when *no-penetration* boundary conditions are prescribed to the velocity fields and, consequently, constant discrete pressures are filtered out, namely $\operatorname{div} (V_{0,h}^{\text{RT}} \cap \mathbf{H}_0(\operatorname{div}; \Omega_0)) = Q_{0,h}^{\text{RT}} \cap L_0^2(\Omega_0)$. However, $\operatorname{div} (V_{0,h}^{\text{RT}} \cap \mathbf{H}_0^1(\Omega_0)) \subsetneq Q_{0,h}^{\text{RT}} \cap L_0^2(\Omega_0)$, meaning that the discrete inf-sup condition is lost when the *no-slip* boundary conditions are strongly imposed [58].

Motivated by this observation and by the inclusion $V_{0,h}^{\text{RT}} \subset V_{0,h}^{\text{N}}$, we follow [58, 59, 131] and impose the tangential component of the boundary conditions in a weak sense through the Nitsche method [63]. Let us define $V_{0,h}^{\text{RT}, \mathbf{u}_D}$, $V_{0,h}^{\text{N}, \mathbf{u}_D}$ and $V_{0,h}^{\text{RT}, \mathbf{0}}$, $V_{0,h}^{\text{N}, \mathbf{0}}$, but this time the L^2 -projection acts just on the normal component of the datum on the dofs living on the Dirichlet part of the boundary. At this point, we consider the following Nitsche formulation.

Find $(\mathbf{u}_h, p_h) \in V_{0,h}^{\square, \mathbf{u}_D} \times Q_{0,h}^{\square}$ such that

$$\begin{aligned}
a_h(\mathbf{u}_h, \mathbf{v}_h) + b_1(\mathbf{v}_h, p_h) &= F_h(\mathbf{v}_h), & \forall \mathbf{v}_h &\in V_{0,h}^{\square, \mathbf{0}}, \\
b_1(\mathbf{u}_h, q_h) &= G_1(q_h), & \forall q_h &\in Q_{0,h}^{\square},
\end{aligned} \tag{1.6}$$

where

$$\begin{aligned}
a_h(\mathbf{w}_h, \mathbf{v}_h) &:= \int_{\Omega_0} \mu D\mathbf{w}_h : D\mathbf{v}_h - \int_{\Gamma_D} \mu D\mathbf{w}_h \mathbf{n} \cdot \mathbf{v}_h - \underbrace{\int_{\Gamma_D} \mu \mathbf{w}_h \cdot D\mathbf{v}_h \mathbf{n}}_{\text{symmetry}} \\
&\quad + \underbrace{\gamma \int_{\Gamma_D} h^{-1} \mu \mathbf{w}_h \cdot \mathbf{v}_h}_{\text{stability}}, & \mathbf{w}_h, \mathbf{v}_h &\in V_{0,h}^{\square}, \\
b_1(\mathbf{v}_h, q_h) &:= - \int_{\Omega_0} q_h \operatorname{div} \mathbf{v}_h + \int_{\Gamma_D} q_h \mathbf{v}_h \cdot \mathbf{n}, & \mathbf{v}_h &\in V_{0,h}^{\square}, \quad q_h \in Q_{0,h}^{\square} \\
F_h(\mathbf{v}_h) &:= \int_{\Omega_0} \mathbf{f} \cdot \mathbf{v}_h + \int_{\Gamma_N} \mathbf{u}_N \cdot \mathbf{v}_h \\
&\quad - \underbrace{\int_{\Gamma_D} \mu \mathbf{u}_D \cdot D\mathbf{v}_h \mathbf{n} + \gamma \int_{\Gamma_D} h^{-1} \mu \mathbf{u}_D \cdot \mathbf{v}_h}_{\text{consistency}}, & \mathbf{v}_h &\in V_{0,h}^{\square}, \\
G_1(q_h) &:= - \int_{\Omega_0} g q_h + \underbrace{\int_{\Gamma_D} q_h \mathbf{u}_D \cdot \mathbf{n}}_{\text{consistency}}, & q_h &\in Q_{0,h}^{\square},
\end{aligned}$$

Chapter 1. Preliminaries

where $\gamma > 0$ is a penalty parameter and $\square \in \{\text{RT}, \text{N}\}$.

Alternatively, it is possible to use the Nitsche method to enforce the “whole” Dirichlet boundary conditions (both the penetration and slip parts) in a weak sense. In this way, we get a unified formulation for the different choices of isogeometric elements.

Find $(\mathbf{u}_h, p_h) \in V_{0,h}^\square \times Q_{0,h}^\square$ such that

$$\begin{aligned} a_h(\mathbf{u}_h, \mathbf{v}_h) + b_1(\mathbf{v}_h, p_h) &= F_h(\mathbf{v}_h), & \forall \mathbf{v}_h \in V_{0,h}^\square, \\ b_1(\mathbf{u}_h, q_h) &= G_1(q_h), & \forall q_h \in Q_{0,h}^\square, \end{aligned} \tag{1.7}$$

where $\square \in \{\text{RT}, \text{N}, \text{TH}\}$.

2 Stabilized isogeometric discretization of the Poisson problem on trimmed geometries

This chapter is devoted to the numerical analysis of the isogeometric discretization of the Poisson problem in trimmed domains.

As we have already mentioned in the introduction, for the discretization of a PDE to be robust to the trimming operation, the following points need to be addressed:

- quadrature rules to integrate in the trimmed elements must be available;
- the conditioning of the resulting linear system needs to be under control;
- its discrete formulation has to be stable or well-posed.

The problem of integration here goes by the wayside as we adopt the strategy proposed in [4] where the cut elements are locally reparameterized by a piecewise polynomial approximation with the same degree as the spline basis used for the discretization of the space.

Concerning the conditioning issue, we do not have a sound solution to the problem, but we constructed tests to check the behavior of the condition number of the stiffness matrix. Numerical evidence shows that a rescaling of the stiffness matrix, coupled with our stabilization, dramatically reduces the condition number. However it does not solve the conditioning issue in all configurations (see Section 2.4.4). A clear theoretical understanding of the issue is beyond the scope of this work, and, in this regard, the interested reader is referred to [100] and to [50, 51].

The main contribution of this chapter is proposing a novel stabilization technique, inspired by [73], which locally modifies the discrete formulation while keeping the discrete functional space unaffected, in compliance with the so-called *isogeometric paradigm*. This stabilization is “minimal”, in the sense that it does not introduce additional parameters, in contrast with the CutFEM [37], and finite cell methods [47]. The main idea, inspired by [73], is to modify the evaluation of the normal derivatives of the basis functions at the “bad” cut elements. We present two different versions of the stabilization. The first one is based on polynomial extrapolation in the parametric domain, which is easier to implement from the numerical point of view but suboptimal in some cases. The second is a projection-based stabilization performed directly on the physical domain, which allows us to recover optimal *a priori* error estimates.

The chapter is organized as follows. In Section 2.1 we set the notation for the isogeometric discretization and introduce the Nitsche formulation of the Poisson problem on a trimmed domain. After having explained in detail in Section 2.2 the causes for the lack of stability of the Nitsche

Chapter 2. Stabilized isogeometric discretization of the Poisson problem on trimmed geometries

formulation in trimmed geometries, in Section 2.3 we present our stabilization technique. Two possible constructions of the stabilization operator are suggested and analyzed in Sections 2.3.1–2.3.4, and error estimates are provided in Section 2.3.5. Finally, we conclude by showing some numerical examples in Section 2.4, obtained using the MATLAB library GeoPDEs [131], confirming the theoretical results.

C will denote generic positive constants that may change with each occurrence throughout the chapter but are always independent of the local mesh size and the position of the trimming curve (surface, if $d = 3$) unless otherwise specified.

This chapter is based on the publication [33].

2.1 Isogeometric discretization

2.1.1 Parametrization, mesh and approximation space in the trimmed domain

For the sake of convenience, we will partially re-define some of the notations already introduced in Chapter 1. Let Ξ be a knot-vector at the coarsest level of discretization, \mathbf{p} a degree-vector, and α_ℓ , $1 \leq \ell \leq d$, regularity vectors. The induced parametric Bézier mesh in $\widehat{\Omega}_0 = (0, 1)^d$ is denoted by $\widehat{\mathcal{M}}_{0,h}$ and is required to satisfy Assumption 1.1.1, allowing us to assign h_Q as a unique measure to each element and to use the Bramble-Hilbert type results developed in [17]. Finer meshes can be constructed by *knot insertion*, as explained in [19], and allow us to obtain a sequence of nested meshes $(\widehat{\mathcal{M}}_{0,h})_{h>0}$.

Let $\Omega_0 \subset \mathbb{R}^d$ be the untrimmed domain, homeomorphic to $\widehat{\Omega}_0 = (0, 1)^d$ through the isogeometric mapping $\mathbf{F} \in (S_{\alpha_1, \dots, \alpha_d}^{\mathbf{p}}(\Xi))^d$, which is given from the CAD description of the geometry and, to prevent singularities, is required to satisfy Assumption 1.1.3. Moreover, let $\Omega_1, \dots, \Omega_N$ be domains of \mathbb{R}^d and assume that $\bigcup_{i=1}^N \overline{\Omega}_i$ are to be cut away from Ω_0 , *i.e.*,

$$\Omega = \Omega_0 \setminus \bigcup_{i=1}^N \overline{\Omega}_i. \quad (2.1)$$

We call Ω a *trimmed domain* and assume that its boundary Γ is Lipschitz with outer unit normal vector \mathbf{n} . We observe that, after trimming, the parametrization of the original patch remains unchanged; that is, the elements and basis functions fit the boundary of Ω_0 instead of that of Ω , see Figure 2.1.

For the sake of simplicity of the presentation, but without loss of generality, we assume $N = 1$ in (2.1). Moreover, we let $\Gamma = \overline{\Gamma}_D \cup \overline{\Gamma}_N$, where Γ_D and Γ_N are non-empty, open and disjoint. The *trimming curve* (respectively, *trimming surface* if $d = 3$) is $\Gamma_T := \Gamma \cap \partial\Omega_1$.

We define the isogeometric space in the parametric domain, namely $\widehat{V}_{0,h} := S_{\alpha_1, \dots, \alpha_d}^{\mathbf{p}}(\Xi)$, where Ξ is the same knot vector of the geometry or a refinement of it. Throughout the chapter we are going to consider $p = p_1 = \dots = p_d$ and $\alpha = \alpha_1 = \dots = \alpha_d$, hence we may write p instead of \mathbf{p} .

Remark 2.1.1. We observe that the previous construction and what follows could be done in a more general setting by considering different but fixed degrees and regularities for each parametric direction. In that case, all the constants appearing in the inequalities of the theoretical results would depend on the difference between the degrees and possibly explode if this difference is not kept bounded. Further generalizations to the anisotropic setting, either in terms of the mesh or

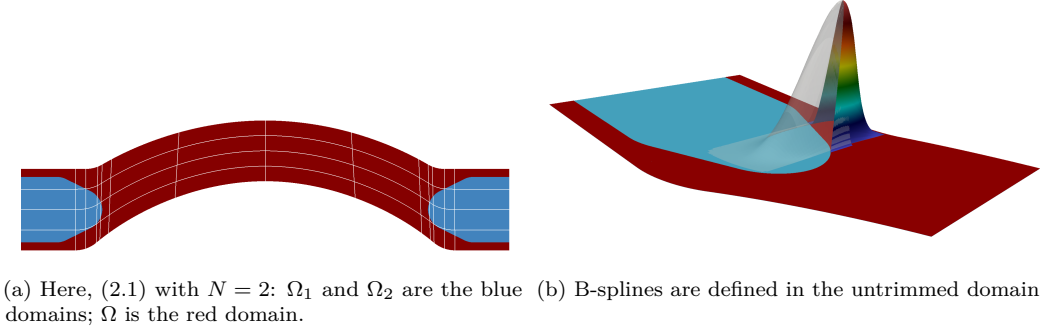


Figure 2.1 – An example of trimmed domain. Images courtesy of Dr. Pablo Antolín.

in terms of the degree, would rely on the approximation theory in anisotropic Sobolev spaces (see, for instance, [20, 46]). These extensions are far from trivial and out of the scope of this work.

Let us recall that the *physical Bézier mesh* is the collection of the images of the elements in $\widehat{\mathcal{M}}_{0,h}$ through \mathbf{F} , namely $\mathcal{M}_{0,h} := \{K : K = \mathbf{F}(Q), Q \in \widehat{\mathcal{M}}_{0,h}\}$. It will be convenient to define the *active physical Bézier mesh* $\mathcal{M}_h := \{K \in \mathcal{M}_{0,h} : K \cap \Omega \neq \emptyset\}$, and, similarly, the *active parametric Bézier mesh* $\widehat{\mathcal{M}}_h := \{Q : Q = \mathbf{F}^{-1}(K), K \in \mathcal{M}_h\}$. For every $K \in \mathcal{M}_h$, let $h_K := \text{diam}(K)$ and $h := \max_{K \in \mathcal{M}_h} h_K$. We define $h : \Omega \rightarrow (0, +\infty)$ to be the piecewise constant mesh-size function assigning to the active part of each element $K \in \mathcal{M}_h$ its whole diameter, namely $h|_{K \cap \Omega} := h_K$. The elements whose interiors are cut by the trimming curve (or surface) are denoted as \mathcal{G}_h , namely, $\mathcal{G}_h := \{K \in \mathcal{M}_h : \Gamma_K \neq \emptyset\}$, where $\Gamma_K := \Gamma_T \cap K$. Note that in the rest of the chapter we often write Γ_K and it should be clear from the context to which part of the boundary we are referring to. We are also going to denote $\widehat{\Gamma} := \mathbf{F}^{-1}(\Gamma)$, $\widehat{\Gamma}_D := \mathbf{F}^{-1}(\Gamma_D)$, $\widehat{\Gamma}_T := \mathbf{F}^{-1}(\Gamma_T)$ and as $\widehat{\mathbf{n}}$ the respective outward unit normal. By pushing forward through \mathbf{F} the isogeometric space in the parametric domain to the physical domain Ω_0 and then restricting it to the active part of the domain, we obtain the following discrete spaces, suitable for the discretization of (2.3) in Ω ,

$$V_h = \{v_h|_{\Omega} : v_h \in V_{0,h}\}, \quad V_{0,h} = \{v_h : v_h \circ \mathbf{F} \in \widehat{V}_{0,h}\}.$$

We introduce the following mesh-dependent scalar product in V_h

$$(w_h, v_h)_{1,h} := \int_{\Omega} \nabla w_h \cdot \nabla v_h + \int_{\Gamma_D} h^{-1} w_h v_h, \quad w_h, v_h \in V_h,$$

inducing the norm

$$\|v_h\|_{1,h}^2 := \|\nabla v_h\|_{L^2(\Omega)}^2 + \left\| h^{-\frac{1}{2}} v_h \right\|_{L^2(\Gamma_D)}^2, \quad v_h \in V_h. \quad (2.2)$$

2.1.2 Variational formulation using Nitsche's method

Our model problem is the Poisson problem already introduced in (1.1) in the context of a standard boundary-fitted discretization in the untrimmed domain Ω_0 . Let us restate it for the sake of convenience. Given $f \in L^2(\Omega)$, $g_D \in H^{\frac{1}{2}}(\Gamma_D)$ and $g_N \in H^{-\frac{1}{2}}(\Gamma_N)$, we look for $u : \Omega \rightarrow \mathbb{R}$ such

that

$$\begin{aligned} -\Delta u &= f, & \text{in } \Omega, \\ u &= g_D, & \text{on } \Gamma_D, \\ \frac{\partial u}{\partial n} &= g_N, & \text{on } \Gamma_N. \end{aligned} \tag{2.3}$$

Our approach is closely related to the fictitious domain methods, where the active part of the domain Ω , with a possibly complicated topology, is immersed into a simpler, but unfitted, background mesh. Similarly to fictitious domain methods, we need to be able to impose the Dirichlet boundary conditions when the mesh is not fitted with the boundary. Following [61, 126], we decide to employ *Nitsche's method*, which reads as follows in its symmetric form.

Find $u_h \in V_h$ such that

$$a_h(u_h, v_h) = F_h(v_h), \quad \forall v_h \in V_h, \tag{2.4}$$

where

$$\begin{aligned} a_h(w_h, v_h) &:= \int_{\Omega} \nabla w_h \cdot \nabla v_h - \int_{\Gamma_D} \frac{\partial w_h}{\partial n} v_h - \underbrace{\int_{\Gamma_D} w_h \frac{\partial v_h}{\partial n}}_{\text{symmetry}} + \underbrace{\beta \int_{\Gamma_D} h^{-1} w_h v_h}_{\text{stability}}, & w_h, v_h \in V_h, \\ F_h(v_h) &:= \int_{\Omega} f v_h + \int_{\Gamma_N} g_N v_h - \underbrace{\int_{\Gamma_D} g_D \frac{\partial v_h}{\partial n}}_{\text{consistency}} + \beta \int_{\Gamma_D} h^{-1} g_D v_h, & v_h \in V_h, \end{aligned}$$

$\beta > 0$ being a penalty parameter.

Remark 2.1.2. We emphasize that, in order to simplify the presentation, in formulation (2.4) we impose the Dirichlet boundary conditions in a weak sense on the whole Γ_D . In the case where there is $\tilde{\Gamma} \subset \Gamma_D$ such that $\mathbf{F}^{-1}(\tilde{\Gamma})$ is a union of full faces of the parametric domain $\hat{\Omega}_0$, then one could have strongly imposed Dirichlet's conditions on $\tilde{\Gamma}$ by appropriately modifying the discrete velocity spaces, see Section 1.2.

Remark 2.1.3. The imposition of the Neumann boundary conditions can be done as usual even if the mesh is not aligned with Γ_N . These conditions are natural for the Poisson problem, *i.e.*, they can be enforced through a boundary integral as long as suitable quadrature rules in the cut elements are available, see [4].

Motivated by the previous remark, we henceforth assume that $\Gamma_N \cap \Gamma_T = \emptyset$, so that $\Gamma_T \subseteq \Gamma_D$.

Our main goal is to provide a minimal stabilization that makes formulation (2.4) uniformly *stable* (or *well-posed*) with respect not only to the mesh-size but also the relative position of mesh and trimming curve.

2.2 Lack of stability of Nitsche's method

Firstly, let us clarify what we actually mean by *stability* or *well-posedness* of the discrete variational problem (2.4).

Definition 2.2.1. We say that problem (2.4) is *stable* (or *well-posed*) if there exist $\bar{\beta} > 0$ and $\alpha > 0$ such that, for every $\beta \geq \bar{\beta}$, it holds that

$$\alpha \|v_h\|_{1,h}^2 \leq a_h(v_h, v_h), \quad \forall v_h \in V_h,$$

and for every fixed $\beta \geq \bar{\beta}$ there exists $\gamma > 0$ such that

$$a_h(w_h, v_h) \leq \gamma \|w_h\|_{1,h} \|v_h\|_{1,h}, \quad \forall w_h, v_h \in V_h.$$

Remark 2.2.2. The main point of Definition 2.2.1 is to find $\bar{\beta}$, α , and γ that do not depend on the trimming configuration. In the following lines, we will show with a numerical example that formulation (2.4) is not stable.

Remark 2.2.3. In Definition 2.2.1 we followed [126]. Note that the coercivity constant only depends on $\bar{\beta}$, while the continuity constant depends on the penalty parameter β , and in particular it grows with β . This dependence of the constant on β also occurs in Theorem 2.3.17 and in Proposition 2.3.20. In practice, β has to be chosen large enough (*i.e.*, larger than $\bar{\beta}$), but as close as possible to $\bar{\beta}$, to avoid that the continuity constant deteriorates.

Proposition 2.2.4. *If for all $K \in \mathcal{G}_h$ we have $\Gamma_K = \emptyset$, then problem (2.4) is stable.*

Proof. The proof is quite standard, but we include it for the sake of completeness. Since we work in the boundary-fitted regime, the following discrete trace inequality holds

$$\left\| \mathbf{h}^{\frac{1}{2}} \frac{\partial v_h}{\partial n} \right\|_{L^2(\Gamma_K)} \leq C_I \|\nabla v_h\|_{L^2(K)}, \quad \forall v_h \in V_h. \quad (2.5)$$

see Theorem 4.2 of [57]. Let us start with the coercivity. For $v_h \in V_h$, it holds

$$a_h(v_h, v_h) = \|\nabla v_h\|_{L^2(\Omega)}^2 - 2 \int_{\Gamma_D} \frac{\partial v_h}{\partial n} v_h + \beta \left\| \mathbf{h}^{-\frac{1}{2}} v_h \right\|_{L^2(\Gamma_D)}^2.$$

From Cauchy-Schwarz's and Young's inequalities together with (2.5), we have

$$2 \int_{\Gamma_D} \frac{\partial v_h}{\partial n} v_h \leq \frac{1}{\varepsilon} C_I^2 \|\nabla v_h\|_{L^2(\Omega)}^2 + \varepsilon \left\| \mathbf{h}^{-\frac{1}{2}} v_h \right\|_{L^2(\Gamma_D)}^2, \quad \varepsilon > 0.$$

Hence,

$$a_h(v_h, v_h) \geq \left(1 - \frac{1}{\varepsilon} C_I^2\right) \|\nabla v_h\|_{L^2(\Omega)}^2 + (\beta - \varepsilon) \left\| \mathbf{h}^{-\frac{1}{2}} v_h \right\|_{L^2(\Gamma_D)}^2.$$

It suffices to choose $\varepsilon > 0$ such that $C_I^2 < \varepsilon < \beta$. Let $w_h, v_h \in V_h$, then

$$\begin{aligned} a_h(w_h, v_h) &\leq \|\nabla w_h\|_{L^2(\Omega)} \|\nabla v_h\|_{L^2(\Omega)} + \left\| \mathbf{h}^{\frac{1}{2}} \frac{\partial w_h}{\partial n} \right\|_{L^2(\Gamma_D)} \left\| \mathbf{h}^{-\frac{1}{2}} v_h \right\|_{L^2(\Gamma_D)} \\ &\quad + \left\| \mathbf{h}^{\frac{1}{2}} \frac{\partial v_h}{\partial n} \right\|_{L^2(\Gamma_D)} \left\| \mathbf{h}^{-\frac{1}{2}} w_h \right\|_{L^2(\Gamma_D)} + \beta \left\| \mathbf{h}^{-\frac{1}{2}} w_h \right\|_{L^2(\Gamma_D)} \left\| \mathbf{h}^{-\frac{1}{2}} v_h \right\|_{L^2(\Gamma_D)} \\ &\leq \|\nabla w_h\|_{L^2(\Omega)} \|\nabla v_h\|_{L^2(\Omega)} + C_I \|\nabla w_h\|_{L^2(\Omega)} \left\| \mathbf{h}^{-\frac{1}{2}} v_h \right\|_{L^2(\Gamma_D)} \\ &\quad + C_I \|\nabla v_h\|_{L^2(\Omega)} \left\| \mathbf{h}^{-\frac{1}{2}} w_h \right\|_{L^2(\Gamma_D)} + \beta \left\| \mathbf{h}^{-\frac{1}{2}} w_h \right\|_{L^2(\Gamma_D)} \left\| \mathbf{h}^{-\frac{1}{2}} v_h \right\|_{L^2(\Gamma_D)}. \end{aligned}$$

Hence, it suffices to take $\gamma \geq \max\{1, 2C_I, \beta\}$. \square

The following numerical experience shows that there exists a trimming configuration for which the formulation (2.4) is not stable according to Definition 2.2.1. In particular we show that for every fixed β the continuity constant γ may be arbitrarily large for a given $h > 0$. First, we notice that if γ_β is the continuity constant corresponding to β , then $\gamma_\beta > \gamma_1$ for every $\beta > 1$. So, we fix $\beta = 1$ and show that γ_1 can be arbitrarily large.

Let us consider the following generalized eigenvalue problem.

Chapter 2. Stabilized isogeometric discretization of the Poisson problem on trimmed geometries

Find $(u_h, \lambda_h) \in V_h \setminus \{0\} \times \mathbb{R}$ such that

$$\int_{\Omega} \nabla u_h \cdot \nabla v_h - \int_{\Gamma_D} \frac{\partial u_h}{\partial n} v_h - \int_{\Gamma_D} u_h \frac{\partial v_h}{\partial n} + \int_{\Gamma_D} h^{-1} u_h v_h = \lambda_h (u_h, v_h)_{1,h}, \quad \forall v_h \in V_h. \quad (2.6)$$

As the problem is symmetric, the continuity constant γ_1 equals the maximum eigenvalue of (2.6).

Let us consider $\Omega_0 = (0, 1)^2$ and as trimmed domain $\Omega = (0, 1) \times (0, 0.757)$. We fix $h = 2^{-5}$ as mesh size and $p = 3$ as degree. We construct a sequence of discrete spaces $(V_{h,\varepsilon})_{\varepsilon>0}$ of degree p and of class C^2 at the internal knots, starting from the uniform knot vectors Ξ_x, Ξ_y and substituting in the latter the knot 0.75 with $\tilde{\xi} = 0.757 - \varepsilon$. Basically, the horizontal knot line $\{(x, y) : y = 0.75\}$ is replaced by $\{(x, y) : y = \tilde{\xi}\}$, which is such that the smaller $\varepsilon > 0$ is, the closer to the trimming curve it becomes. In Figure 2.2(a) we plot $\Omega = (0, 1) \times (0, 0.757)$ (in red), $\{(x, y) : y = \tilde{\xi}\}$ (in solid blue), $\{(x, y) : y = 0.75\}$ (in dotted gray).

In Figure 2.2(b) we can see the dependence of the spectrum of (2.6) on the magnitude of ε . In particular, the magnitude of the largest generalized eigenvalue goes to infinity as ε goes to 0, implying that the discrete formulation (2.4) is not stable, as the continuity constant can be made arbitrarily large by reducing ε . Going through the proof of stability, we clearly miss a

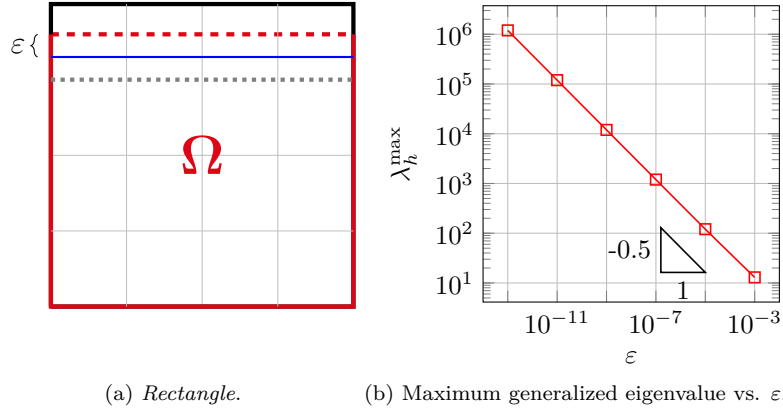


Figure 2.2 – Testing the lack of stability of formulation (2.4) with respect to trimming.

discrete trace inequality like (2.5) which is uniform with respect to any mesh-trimming curve configuration, namely,

$$\left\| h^{\frac{1}{2}} \frac{\partial v_h}{\partial n} \right\|_{L^2(\Gamma_K)} \leq C \|\nabla v_h\|_{L^2(K \cap \Omega)},$$

where C does not depend on the shape and diameter of $K \cap \Omega$.

At this point, in order to be able to deal with a stable problem, we want to find a way to improve this discrete trace inequality, where the constant does not depend on how the trimmed boundary intersects the mesh.

2.3 The stabilized formulation and its analysis

The goal of this section is to present a new stabilization technique for the problem (2.4). Our construction is inspired by the work of J. Haslinger and Y. Renard in [73] and mainly follows three steps:

- (1) distinguishing good and bad elements depending on how elements are cut;
- (2) finding a good neighbor for each bad element;
- (3) stabilizing the normal derivatives at the bad elements with the help of the good neighbor.

Let us start partitioning the elements of the Bézier mesh into two disjoint subfamilies.

Definition 2.3.1. Let $\theta \in (0, 1]$ be the *volume-ratio threshold* and $Q \in \widehat{\mathcal{M}}_h$. We say that Q is a *good element* if

$$\frac{|\widehat{\Omega} \cap Q|}{|Q|} \geq \theta.$$

Otherwise, Q is a *bad element*. Thanks to the regularity Assumption 1.1.3 on \mathbf{F} , this classification on the parametric elements naturally induces a classification on the physical elements. \mathcal{M}_h^g stands for the collection of the good physical Bézier elements and \mathcal{M}_h^b for the one of the bad physical elements. Note that $\mathcal{M}_h \setminus \mathcal{G}_h \subseteq \mathcal{M}_h^g$ and $\mathcal{M}_h^b \subseteq \mathcal{G}_h$. We denote the set of *neighbors* of K as

$$\mathcal{N}(K) := \{K' \in \mathcal{M}_h : \text{dist}(K, K') \leq Ch\} \setminus \{K\}, \quad (2.7)$$

where C does not depend on the mesh size nor on the trimming configuration.

The following assumption is not restrictive since it holds true if the mesh is sufficiently refined.

Assumption 2.3.2. We assume that for any $K \in \mathcal{M}_h^b$, there exists $K' \in \mathcal{N}(K) \cap \mathcal{M}_h^g$. From now on we will refer to such K' as a *good neighbor* of K .

In what follows, we will use Assumption 2.3.2 to construct a stable representation of the normal flux of discrete functions. Let us assume that there exists an operator

$$R_h : V_h \rightarrow L^2(\Gamma_D),$$

which approximates the normal derivative on Γ_D in a sense that will be specified. We propose the following stabilized formulation of problem (2.4).

Find $u_h \in V_h$ such that

$$\bar{a}_h(u_h, v_h) = \bar{F}_h(v_h), \quad \forall v_h \in V_h, \quad (2.8)$$

where

$$\begin{aligned} \bar{a}_h(w_h, v_h) &:= \int_{\Omega} \nabla w_h \cdot \nabla v_h - \int_{\Gamma_D} R_h(w_h) v_h - \int_{\Gamma_D} w_h R_h(v_h) + \beta \int_{\Gamma_D} \mathbf{h}^{-1} w_h v_h, & w_h, v_h \in V_h, \\ \bar{F}_h(v_h) &:= \int_{\Omega} f v_h + \int_{\Gamma_N} g_N v_h - \int_{\Gamma_D} g_D R_h(v_h) + \beta \int_{\Gamma_D} \mathbf{h}^{-1} g_D v_h, & v_h \in V_h. \end{aligned}$$

Theorem 2.3.3. Suppose R_h satisfies the following stability property. Given $\theta \in (0, 1]$, there exists $C > 0$ such that, for every $K \in \mathcal{G}_h$,

$$\left\| \mathbf{h}^{\frac{1}{2}} R_h(v_h) \right\|_{L^2(\Gamma_K)} \leq C \|\nabla v_h\|_{L^2(\Omega \cap K')}, \quad \forall v_h \in V_h, \quad (2.9)$$

where K' is a good neighbor if $K \in \mathcal{M}_h^b$, $K' = K$ if $K \in \mathcal{M}_h^g$. Then problem (2.8) is stable in the sense of Definition 2.2.1 (modified accordingly).

Proof. For the continuity, let $w_h, v_h \in V_h$, and estimate

$$\begin{aligned}
 |\bar{a}_h(w_h, v_h)| &\leq \|\nabla w_h\|_{L^2(\Omega)} \|\nabla v_h\|_{L^2(\Omega)} + \left\| h^{\frac{1}{2}} R_h(w_h) \right\|_{L^2(\Gamma_D)} \left\| h^{-\frac{1}{2}} v_h \right\|_{L^2(\Gamma_D)} \\
 &\quad + \left\| h^{\frac{1}{2}} R_h(v_h) \right\|_{L^2(\Gamma_D)} \left\| h^{-\frac{1}{2}} w_h \right\|_{L^2(\Gamma_D)} + \beta \left\| h^{-\frac{1}{2}} w_h \right\|_{L^2(\Gamma_D)} \left\| h^{-\frac{1}{2}} v_h \right\|_{L^2(\Gamma_D)} \\
 &\leq \|w_h\|_{1,h} \|v_h\|_{1,h} + C \|\nabla w_h\|_{L^2(\Omega)} \|v_h\|_{1,h} + C \|\nabla v_h\|_{L^2(\Omega)} \|w_h\|_{1,h} \\
 &\quad + \beta \|w_h\|_{1,h} \|v_h\|_{1,h} \leq C \|w_h\|_{1,h} \|v_h\|_{1,h},
 \end{aligned}$$

where we employed the Cauchy–Schwarz inequality, the definition of the norm (2.2) and the stability property (2.9). Take $v_h \in V_h$. By using the Young inequality, with $\delta > 0$, and, again, the stability property (2.9), we obtain

$$\begin{aligned}
 \bar{a}_h(v_h, v_h) &\geq \|\nabla v_h\|_{L^2(\Omega)}^2 - \frac{1}{\delta} \left\| h^{\frac{1}{2}} R_h(v_h) \right\|_{L^2(\Gamma_D)}^2 - \delta \left\| h^{-\frac{1}{2}} v_h \right\|_{L^2(\Gamma_D)}^2 \\
 &\quad + \beta \left\| h^{-\frac{1}{2}} v_h \right\|_{L^2(\Gamma_D)}^2 \geq \left(1 - \frac{C}{\delta}\right) \|\nabla v_h\|_{L^2(\Omega)}^2 + (\beta - \delta) \left\| h^{-\frac{1}{2}} v_h \right\|_{L^2(\Gamma_D)}^2,
 \end{aligned}$$

from which we deduce the coercivity, provided $C < \delta < \beta$. \square

Remark 2.3.4. Let us observe once for all that the subsequent constants related to the stabilization operator R_h will depend on the threshold parameter θ .

In order for the solution of (2.8) to be a good approximation of u , it is clear that we will also need to quantify the error between $R_h(u_h)$ and $\frac{\partial u}{\partial n}$. This issue will be addressed in the next section.

2.3.1 Construction of the stabilization operator

The definition of the operator R_h is not unique. As already observed, we seek a stable approximation of the normal derivative on the trimmed part of the boundary, namely, on Γ_K for every $K \in \mathcal{G}_h$. Here, we propose two different constructions of such an operator.

- *A stabilization in the parametric domain:* for each $K \in \mathcal{M}_h^b$ we take the canonical polynomial extension of the pull-back of the functions of V_h from $Q' := \mathbf{F}^{-1}(K')$ to $Q := \mathbf{F}^{-1}(K)$, where K' is a good neighbor.
- *A stabilization in the physical domain:* for each $K \in \mathcal{M}_h^b$, we first L^2 -project the functions restricted to the good neighbor K' onto the polynomial space $\mathbb{Q}_p(K')$; then we take their canonical polynomial extension up to K .

Definition 2.3.5 (Stabilization in the parametric domain). We define the operator $R_h : V_h \rightarrow L^2(\Gamma_D)$ locally as $R_h(v_h)|_K := R_K(v_h)$ for all $K \in \mathcal{G}_h$ and $v_h \in V_h$, where

- if $K \in \mathcal{M}_h^g$,

$$R_K(v_h) := \frac{\partial v_h|_K}{\partial n};$$

- if $K \in \mathcal{M}_h^b$,

$$R_K(v_h) := \frac{\partial \left(\mathcal{E}_{Q',Q} \left(\hat{v}_h|_{Q'} \right) \circ \mathbf{F}^{-1} \right)}{\partial n},$$

where $\mathcal{E}_{Q',Q} : \mathbb{Q}_p(Q') \rightarrow \mathbb{Q}_p(Q' \cup Q)$ is the canonical polynomial extension and K' a good neighbor of K .

An alternative stabilization operator can be defined by using the L^2 -projection in the physical domain.

Definition 2.3.6 (Stabilization in the physical domain). We define the operator $R_h : V_h \rightarrow L^2(\Gamma_D)$ locally as $R_h(v_h)|_K := R_K(v_h)$ for all $K \in \mathcal{G}_h$ and $v_h \in V_h$:

- if $K \in \mathcal{M}_h^g$,

$$R_K(v_h) := \frac{\partial v_h|_K}{\partial n};$$

- if $K = \mathbf{F}(Q) \in \mathcal{M}_h^b$, $K' \in \mathcal{N}(K) \cap \mathcal{M}_h^g$,

$$R_K(v_h) := \frac{\partial \left(\mathcal{E}_{K',K} \left(\Pi_{K'}(v_h)|_{K'} \right) \right)}{\partial n},$$

where $\Pi_{K'} : L^2(K') \rightarrow \mathbb{Q}_p(K')$ is the L^2 -orthogonal projection, $\mathcal{E}_{K',K} : \mathbb{Q}_p(K') \rightarrow \mathbb{Q}_p(K' \cup K)$ is the natural polynomial extension and K' a good neighbor of K .

Remark 2.3.7. Note that in the trivial case where there is no isogeometric map, namely $\mathbf{F} = \mathbf{Id}$, the L^2 -projection $\Pi_{K'}$ reduces to the identity operator, and the two stabilizations coincide.

Before analyzing the properties of the two stabilization operators, let us formalize our quasi-interpolation technique. The target function, living in the trimmed domain Ω , is extended up to the mesh-fitted domain Ω_0 , hence quasi-interpolated with standard techniques.

2.3.2 The quasi-interpolation strategy

Let us follow an interpolation procedure similar to the one of [37]. We define for $m \geq 1$,

$$\Pi_h : H^m(\Omega) \rightarrow V_h, \quad v \mapsto \Pi_h^0 \left(E(v)|_{\Omega_0} \right)|_{\Omega},$$

where $E : H^m(\Omega) \rightarrow H^m(\mathbb{R}^d)$ is the Sobolev-Stein extension operator, independent of m (see Section 3.2 of [104]) and Π_h^0 is the spline quasi-interpolant onto V_h^0 , see [30, 87]. Let us prove that Π_h enjoys optimal approximation properties.

Theorem 2.3.8. *There exists $C > 0$ such that, for every $v \in H^m(\Omega)$ with $m \geq 1$,*

$$\|v - \Pi_h v\|_{1,h} \leq Ch^s \|v\|_{H^m(\Omega)},$$

where $s := \min\{p, m - 1\}$.

Proof. First of all, we apply the trace inequality of Lemma A.1.2. Then, we proceed by employing the standard approximation properties of Π_h^0 and the boundedness of the Sobolev-Stein extension

operator.

$$\begin{aligned}
\|v - \Pi_h v\|_{1,h}^2 &= \|\nabla(v - \Pi_h v)\|_{L^2(\Omega)}^2 + \|\mathbf{h}^{-\frac{1}{2}}(v - \Pi_h v)\|_{L^2(\Gamma_D)}^2 \leq \|\nabla(E(v) - \Pi_h^0 E(v))\|_{L^2(\Omega_0)}^2 \\
&\quad + C \sum_{K \in \mathcal{G}_h} \|\mathbf{h}^{-1}(E(v) - \Pi_h^0 E(v))\|_{L^2(K)} \|E(v) - \Pi_h^0 E(v)\|_{H^1(K)} \\
&\leq Ch^{2s} \|E(v)\|_{H^m(\Omega_0)}^2 \\
&\quad + C \sum_{K \in \mathcal{G}_h} \|\mathbf{h}^{-1}(E(v) - \Pi_h^0 E(v))\|_{L^2(K)} \|E(v) - \Pi_h^0 E(v)\|_{H^1(K)} \\
&\leq Ch^{2s} \|v\|_{H^m(\Omega)}^2 + \|\mathbf{h}^{-1}(E(v) - \Pi_h^0 E(v))\|_{L^2(\Omega_0)} \|E(v) - \Pi_h^0 E(v)\|_{H^1(\Omega_0)} \\
&\leq Ch^{2s} \|v\|_{H^m(\Omega)}^2.
\end{aligned}$$

□

2.3.3 Stabilization operator in the parametric domain

We are now up to verify if the stabilization operator in the parametric domain R_h verifies the stability property (2.9). Its proof relies on a series of quite technical results that are reported in the appendix.

Theorem 2.3.9. *The stability property (2.9) holds for R_h defined as in Definition 2.3.5, i.e., there exists $C > 0$ such that, for every $K \in \mathcal{G}_h$,*

$$\left\| \mathbf{h}^{\frac{1}{2}} R_h(v_h) \right\|_{L^2(\Gamma_K)} \leq C \|\nabla v_h\|_{L^2(\Omega \cap K')}, \quad \forall v_h \in V_h,$$

where $K' \in \mathcal{M}_h^g$ is a good neighbor if $K \in \mathcal{M}_h^b$, $K' = K$ if $K \in \mathcal{M}_h^g$.

Proof. We can restrict ourselves to the case $K \in \mathcal{M}_h^b$ with good neighbor K' . Let $v_h \in V_h$ and $\bar{v}_h := \mathcal{E}_{Q',Q}(\widehat{v}_h|_{Q'}) \circ \mathbf{F}^{-1}$, where $Q := \mathbf{F}^{-1}(K)$ and $Q' := \mathbf{F}^{-1}(K')$. It is enough to prove

$$\left\| \mathbf{h}^{\frac{1}{2}} \bar{v}_h \right\|_{L^2(\Gamma_K)} \leq C \|v_h\|_{L^2(\Omega \cap K')}.$$

It holds that

$$\begin{aligned}
\|\bar{v}_h\|_{L^2(\Gamma_K)}^2 &= \int_{\Gamma_K} |\bar{v}_h|^2 = \int_{\mathbf{F}^{-1}(\Gamma_K)} |\widehat{v}_h|^2 |\det(D\mathbf{F})| \|D\mathbf{F}^{-1}\widehat{\mathbf{n}}\| \\
&\leq C \int_{\mathbf{F}^{-1}(\Gamma_K)} |\widehat{v}_h|^2 = C \|\widehat{v}_h\|_{L^2(\widehat{\Gamma}_D \cap Q)}^2,
\end{aligned} \tag{2.10}$$

where we used $\mathbf{F}^{-1}(\Gamma_K) = \mathbf{F}^{-1}(\Gamma_D) \cap \mathbf{F}^{-1}(K) = \widehat{\Gamma}_D \cap Q$, because \mathbf{F} preserves boundaries (as homeomorphisms do). Hence, we have, by the Hölder inequality,

$$\|\widehat{v}_h\|_{L^2(\widehat{\Gamma}_D \cap Q)} \leq \left| \widehat{\Gamma}_D \cap Q \right|^{\frac{1}{2}} \|\widehat{v}_h\|_{L^\infty(\widehat{\Gamma}_D \cap Q)} \leq \left| \widehat{\Gamma}_D \cap Q \right|^{\frac{1}{2}} \|\widehat{v}_h\|_{L^\infty(Q)}.$$

Now, we employ Lemma A.1.4 and Lemma A.1.1:

$$\|\widehat{v}_h\|_{L^2(\widehat{\Gamma}_D \cap Q)}^2 \leq C \left| \widehat{\Gamma}_D \cap Q \right|^{\frac{1}{2}} \|\widehat{v}_h\|_{L^\infty(Q')} \leq Ch^{\frac{d-1}{2}} \|\widehat{v}_h\|_{L^\infty(Q')}.$$

2.3. The stabilized formulation and its analysis

At this point, notice that we can use Lemma A.1.5 because $\frac{|\Omega \cap K'|}{|K'|} \geq \theta$ implies $\frac{|\hat{\Omega} \cap Q'|}{|Q'|} \geq C\theta$, where C depends just on \mathbf{F} , thanks to Assumption 1.1.3. Moreover, let us push forward to the physical domain

$$\|\hat{v}_h\|_{L^2(\hat{\Gamma}_D \cap Q)} \leq Ch^{-\frac{1}{2}} \|\hat{v}_h\|_{L^2(\hat{\Omega} \cap Q')} \leq Ch^{-\frac{1}{2}} \|v_h\|_{L^2(\Omega \cap K')}. \quad (2.11)$$

Gathering together (2.10) and (2.11), the proof is finished. \square

In what follows, we analyze the approximation properties of the stabilization operator in the parametric domain R_h and provide estimates that will be used in Section 2.3.5 to deduce a complete error estimate.

Proposition 2.3.10. *There exists $C > 0$ such that, for every $K \in \mathcal{G}_h$,*

- if $2 \leq m < p + \frac{1}{2}$, for every $v \in H^m(\Omega)$,

$$\left\| h^{\frac{1}{2}} \left(R_h(\Pi_h(v)) - \frac{\partial v}{\partial n} \right) \right\|_{L^2(\Gamma_K)} \leq Ch^{m-1} \left(\|E(v)\|_{H^m(\tilde{K}')} + \|E(v)\|_{H^m(B_K)} \right);$$

- if $m \geq \max\{p + \frac{1}{2}, 2\}$ and each internal knot line is not repeated, for every $v \in H^m(\Omega)$, for all $\varepsilon > 0$,

$$\left\| h^{\frac{1}{2}} \left(R_h(\Pi_h(v)) - \frac{\partial v}{\partial n} \right) \right\|_{L^2(\Gamma_K)} \leq Ch^{p-\frac{1}{2}-\varepsilon} \left(\|E(v)\|_{H^m(\tilde{K}')} + \|E(v)\|_{H^m(B_K)} \right).$$

Here, K' is a good neighbor if $K \in \mathcal{M}_h^b$, $K' = K$ if $K \in \mathcal{M}_h^g$, $B_K := \mathbf{F}(B_Q)$, and B_Q is the minimal bounding box enclosing $Q \cup Q'$, $Q := \mathbf{F}^{-1}(K)$, $Q' := \mathbf{F}^{-1}(K')$.

Proof. Let $K \in \mathcal{G}_h$ and distinguish two cases: either $K \in \mathcal{M}_h^g$ or $K \in \mathcal{M}_h^b$. If $K \in \mathcal{M}_h^g$, we use Corollary A.1.3, Young's inequality, and standard approximation results:

$$\begin{aligned} \left\| h^{\frac{1}{2}} \left(R_h(\Pi_h(v)) - \frac{\partial v}{\partial n} \right) \right\|_{L^2(\Gamma_K)}^2 &= \left\| h^{\frac{1}{2}} \frac{\partial}{\partial n} (\Pi_h(v) - v) \right\|_{L^2(\Gamma_K)}^2 \\ &\leq C \left\| \nabla (\Pi_h^0(E(v)) - E(v)) \right\|_{L^2(K)} \left\| \nabla (\Pi_h^0(E(v)) - E(v)) \right\|_{H^1(K)} \\ &\leq Ch^{2s} \|E(v)\|_{H^m(\tilde{K})}^2, \end{aligned} \quad (2.12)$$

where $s := \min\{p, m-1\}$. If $K = \mathbf{F}(Q) \in \mathcal{M}_h^b$ and $K' = \mathbf{F}(Q') \in \mathcal{N}(K) \cap \mathcal{M}_h^g$ is its good neighbor, we proceed by pulling back to the parametric domain and triangular inequality

$$\begin{aligned} \left\| h^{\frac{1}{2}} \left(R_h(\Pi_h(v)) - \frac{\partial v}{\partial n} \right) \right\|_{L^2(\Gamma_K)} &\leq C \left\| h^{\frac{1}{2}} \frac{\partial}{\partial n} \left(\mathcal{E}_{Q',Q} \left(\Pi_h(v) \circ \mathbf{F} \Big|_{Q'} \right) - \hat{v} \right) \right\|_{L^2(\hat{\Gamma}_D \cap Q)} \\ &\leq C \left(\left\| h^{\frac{1}{2}} \frac{\partial}{\partial n} \left(\mathcal{E}_{Q',Q} \left(\Pi_h(v) \circ \mathbf{F} \Big|_{Q'} \right) - \hat{q} \right) \right\|_{L^2(\hat{\Gamma}_D \cap Q)} + \left\| h^{\frac{1}{2}} \frac{\partial}{\partial n} (\hat{q} - \hat{v}) \right\|_{L^2(\hat{\Gamma}_D \cap Q)} \right), \end{aligned} \quad (2.13)$$

where $\hat{v} := E(v) \circ \mathbf{F}$ and $\hat{q} \in \mathbb{Q}_p(B_Q)$ (where B_Q is the minimal bounding box containing $Q \cup Q'$) to be chosen. We observe that $\mathcal{E}_{Q',Q} \left(\hat{q} \Big|_{Q'} \right) = \hat{q}$. Hence, by Theorem 2.3.9 (in the parametric domain), the first term of (2.13) becomes

$$\left\| h^{\frac{1}{2}} \frac{\partial}{\partial n} \left(\mathcal{E}_{Q',Q} \left(\Pi_h(v) \circ \mathbf{F} \Big|_{Q'} \right) - \hat{q} \right) \right\|_{L^2(\hat{\Gamma}_D \cap Q)} \leq \left\| \nabla (\Pi_h(v) \circ \mathbf{F} - \hat{q}) \right\|_{L^2(\hat{\Omega} \cap Q')}. \quad (2.14)$$

Chapter 2. Stabilized isogeometric discretization of the Poisson problem on trimmed geometries

By the triangular inequality, the optimal approximation properties of spline quasi-interpolants [30], and the norm equivalence between parametric and physical domain, (2.14) becomes

$$\begin{aligned} & \left\| \mathbf{h}^{\frac{1}{2}} \frac{\partial}{\partial n} \left(\mathcal{E}_{Q',Q} \left(\Pi_h(v) \circ \mathbf{F} \Big|_{Q'} \right) - \hat{q} \right) \right\|_{L^2(\hat{\Gamma}_D \cap Q)} \\ & \leq \|\nabla(\Pi_h(v) \circ \mathbf{F} - \hat{v})\|_{L^2(\hat{\Omega} \cap Q')} + \|\nabla(\hat{v} - \hat{q})\|_{L^2(\hat{\Omega} \cap Q')} \\ & \leq Ch^s \|E(v)\|_{H^m(\tilde{K}')} + \|\nabla(\hat{v} - \hat{q})\|_{L^2(\hat{\Omega} \cap Q')}, \end{aligned} \quad (2.15)$$

where $s := \min\{p, m-1\}$. From Corollary A.1.3, the second term of (2.13) can be bounded as:

$$\left\| \mathbf{h}^{\frac{1}{2}} \frac{\partial}{\partial n} (\hat{q} - \hat{v}) \right\|_{L^2(\hat{\Gamma}_D \cap Q)} \leq C \|\nabla(\hat{q} - \hat{v})\|_{L^2(Q)}^{\frac{1}{2}} \|\mathbf{h} \nabla(\hat{q} - \hat{v})\|_{H^1(Q)}^{\frac{1}{2}}. \quad (2.16)$$

Thus, by combining (2.13)–(2.16), we obtain

$$\begin{aligned} \left\| \mathbf{h}^{\frac{1}{2}} \left(R_h(\Pi_h(v)) - \frac{\partial v}{\partial n} \right) \right\|_{L^2(\Gamma_K)} & \leq Ch^s \|E(v)\|_{H^m(\tilde{K}')} + \|\nabla(\hat{v} - \hat{q})\|_{L^2(\hat{\Omega} \cap Q')} \\ & \quad + C \|\nabla(\hat{q} - \hat{v})\|_{L^2(Q)}^{\frac{1}{2}} \|\mathbf{h} \nabla(\hat{q} - \hat{v})\|_{H^1(Q)}^{\frac{1}{2}} \\ & \leq Ch^s \|E(v)\|_{H^m(\tilde{K}')} + \|\nabla(\hat{v} - \hat{q})\|_{L^2(B_Q)} \\ & \quad + C \|\nabla(\hat{q} - \hat{v})\|_{L^2(B_Q)}^{\frac{1}{2}} \|\mathbf{h} \nabla(\hat{q} - \hat{v})\|_{H^1(B_Q)}^{\frac{1}{2}}. \end{aligned} \quad (2.17)$$

We want to apply the Deny-Lions Lemma (Theorem 3.4.1 of [112]) on B_Q . By the theory of *bent Sobolev spaces* (see [17]), we have $E(v) \in H^m(\Omega_0)$, but, in general, $\hat{v}|_{B_Q} \notin H^m(B_Q)$, since it is bent by \mathbf{F} , a spline of degree p and regularity $p-1$ (under the assumption that internal knot lines are not repeated). It holds, indeed, that $\hat{v}|_{B_Q} \in H^r(B_Q)$, where $r := \min\{p + \frac{1}{2} - \varepsilon, m\}$. So, there exists $\hat{q} \in \mathbb{Q}_p(B_Q)$ such that

$$\|\hat{q} - \hat{v}\|_{H^1(B_Q)} \leq Ch^{r-1} \|\hat{v}\|_{H^r(B_Q)}, \quad \|\hat{q} - \hat{v}\|_{H^2(B_Q)} \leq Ch^{r-2} \|\hat{v}\|_{H^r(B_Q)},$$

where C depends on the shape-regularity of B_Q through Theorem 3.4.1 of [112] (see Remark 2.3.11). By pushing forward to the physical domain,

$$\|\hat{q} - \hat{v}\|_{H^1(B_Q)} \leq Ch^{r-1} \|E(v)\|_{H^r(B_K)}, \quad \|\hat{q} - \hat{v}\|_{H^2(B_Q)} \leq Ch^{r-2} \|E(v)\|_{H^r(B_K)}, \quad (2.18)$$

where $B_K = \mathbf{F}(B_Q)$. From (2.17) and (2.18), it holds

$$\left\| \mathbf{h}^{\frac{1}{2}} \left(R_h(\Pi_h(v)) - \frac{\partial v}{\partial n} \right) \right\|_{L^2(\Gamma_K)} \leq Ch^s \|E(v)\|_{H^m(\tilde{K}')} + Ch^{r-1} \|E(v)\|_{H^r(B_K)}, \quad (2.19)$$

where $s := \min\{p, m-1\}$ and $r := \min\{p + \frac{1}{2} - \varepsilon, m\}$. We want to rewrite inequality (2.19) by distinguishing two cases.

- $2 \leq m < p + \frac{1}{2}$. In this case,

$$\left\| \mathbf{h}^{\frac{1}{2}} \left(R_h(\Pi_h(v)) - \frac{\partial v}{\partial n} \right) \right\|_{L^2(\Gamma_K)} \leq Ch^{m-1} \left(\|E(v)\|_{H^m(\tilde{K}')} + \|E(v)\|_{H^m(B_K)} \right).$$

- $m \geq \max\{p + \frac{1}{2}, 2\}$. Then, for any $\varepsilon > 0$,

$$\left\| \mathbf{h}^{\frac{1}{2}} \left(R_h(\Pi_h(v)) - \frac{\partial v}{\partial n} \right) \right\|_{L^2(\Gamma_K)} \leq Ch^{p-\frac{1}{2}-\varepsilon} \left(\|E(v)\|_{H^m(\tilde{K}')} + \|E(v)\|_{H^m(B_K)} \right).$$

□

Remark 2.3.11. Let $N_K := \#\{K^* \in \mathcal{M}_h : K^* \cap B_K \neq \emptyset\}$ and $N_Q := \#\{Q^* \in \widehat{\mathcal{M}}_h : Q^* \cap B_Q \neq \emptyset\}$, given $K \in \mathcal{M}_h$ and $Q = \mathbf{F}^{-1}(K) \in \widehat{\mathcal{M}}_h$. Note that $N_K = N_Q$. N_K may vary according to the constant C appearing in (2.7) and the space dimension d , but it is uniformly bounded with respect to h thanks to the regularity of \mathbf{F} and, in particular, to the shape-regularity of \mathcal{M}_h (see Assumptions 1.1.3, 1.1.1). The shape-regularity of \mathcal{M}_h also implies that, given $K \in \mathcal{M}_h$, $\#\{B_{\tilde{K}} : B_{\tilde{K}} \cap K \neq \emptyset, \tilde{K} \in \mathcal{M}_h\}$ is uniformly bounded with respect to h . The uniform bound for N_Q implies the shape-regularity of B_Q . In other words, given $\rho_{B_Q} := \sup\{\text{diam}(B) : B \text{ is a ball contained in } B_Q\}$ and $h_{B_Q} := \text{diam}(B_Q)$, the geometric quantity $\frac{h_{B_Q}}{\rho_{B_Q}} \sim \frac{h}{\rho_{B_Q}}$ is uniformly bounded with respect to $Q \in \widehat{\mathcal{M}}_h$. Hence, we can seamlessly apply Theorem 3.4.1 of [112] in the proof of Proposition 2.3.10.

Remark 2.3.12. Note that if $2 \leq m < p + \frac{1}{2}$, the estimate is optimal. In the case $m \geq \max\{p + \frac{1}{2}, 2\}$ the estimate is suboptimal, instead. As already mentioned in the proof, this is due to the fact that $E(v) \in H^m(B_K)$ does not imply $E(v) \circ \mathbf{F} \in H^m(B_Q)$: if one of the knot lines between Q and Q' is not repeated, namely, $\mathbf{F} \in C^{p-1}(B_Q)$, then it holds that $E(v) \circ \mathbf{F} \in H^r(B_Q)$ with $r := \min\{m, p + \frac{1}{2} - \varepsilon\}$. Moreover, if the parametrization is less regular than requested in the hypotheses of Proposition 2.3.10, then the suboptimality may be even worse. More precisely, if $\mathbf{F} \in C^{p-k}(B_Q)$, which is the case if one of knot lines between Q and Q' is repeated k times, then we have $r := \min\{m, p - k + \frac{3}{2} - \varepsilon\}$. We will see an example of this suboptimal behavior in the worst case scenario of $k = p$ in Section 2.4.3.

Remark 2.3.13. Any method based on polynomial extrapolation of the B-splines in the parametric domain may also suffer this suboptimality depending on the regularity of the isogeometric map \mathbf{F} because the theory of bent Sobolev spaces from [17] cannot be applied. In particular, the method of extended B-splines, which works very well in the parametric domain [77], may suffer a lack of accuracy in the isogeometric setting [92, 94].

2.3.4 Stabilization operator in the physical domain

Theorem 2.3.14. *The stability property (2.9) holds for R_h defined as in Definition 2.3.6, i.e., there exists $C > 0$ such that, for every $K \in \mathcal{G}_h$,*

$$\left\| h^{\frac{1}{2}} R_h(v_h) \right\|_{L^2(\Gamma_K)} \leq C \|\nabla v_h\|_{L^2(\Omega \cap K')}, \quad \forall v_h \in V_h,$$

where $K' \in \mathcal{M}_h^g$ is a good neighbor if $K \in \mathcal{M}_h^b$, $K' = K$ if $K \in \mathcal{M}_h^g$.

Proof. Let us start by applying the Hölder inequality and Lemma A.1.4:

$$\begin{aligned} \|R_h(v_h)\|_{L^2(\Gamma_K)} &= \left\| \frac{\partial}{\partial n} \mathcal{E}_{K',K} \left(\Pi_{K'}(v_h|_{K'}) \right) \right\|_{L^2(\Gamma_K)} \leq |\Gamma_K|^{\frac{1}{2}} \left\| \frac{\partial}{\partial n} \mathcal{E}_{K',K} \left(\Pi_{K'}(v_h|_{K'}) \right) \right\|_{L^\infty(\Gamma_K)} \\ &\leq |\Gamma_K|^{\frac{1}{2}} \left\| \nabla \mathcal{E}_{K',K} \left(\Pi_{K'}(v_h|_{K'}) \right) \right\|_{L^\infty(K)} \leq C |\Gamma_K|^{\frac{1}{2}} \left\| \nabla \Pi_{K'}(v_h|_{K'}) \right\|_{L^\infty(K')}. \end{aligned}$$

Then, we use Lemma A.1.5, Lemma A.1.1, and the stability of the L^2 -orthogonal projection $\Pi_{K'}$ (see, for instance, [24]):

$$\begin{aligned} \left\| h^{\frac{1}{2}} R_h(v_h) \right\|_{L^2(\Gamma_K)} &\leq C h^{-\frac{d}{2}} |\Gamma_K|^{\frac{1}{2}} \left\| h^{\frac{1}{2}} \nabla \Pi_{K'}(v_h|_{K'}) \right\|_{L^2(\Omega \cap K')} \\ &\leq C \|\nabla \Pi_{K'}(v_h)\|_{L^2(\Omega \cap K')} \leq C \|\nabla v_h\|_{L^2(K')}. \end{aligned}$$

Chapter 2. Stabilized isogeometric discretization of the Poisson problem on trimmed geometries

Now, let us use the equivalence of norms between parametric and physical spaces, the Hölder inequality, Lemma A.1.5, and again the norm equivalence between parametric and physical spaces. We have

$$\begin{aligned} \left\| h^{\frac{1}{2}} R_h(v_h) \right\|_{L^2(\Gamma_K)} &\leq C \|\nabla \hat{v}_h\|_{L^2(Q')} \leq C h^{\frac{d}{2}} \|\nabla \hat{v}_h\|_{L^\infty(Q')} \\ &\leq C \|\nabla \hat{v}_h\|_{L^2(\hat{\Omega} \cap Q')} \leq C \|\nabla v_h\|_{L^2(\Omega \cap K')}, \end{aligned}$$

where $Q' := \mathbf{F}^{-1}(K')$ and C depends on θ through Lemma A.1.5. \square

Proposition 2.3.15. *There exists $C > 0$ such that, for every $K \in \mathcal{G}_h$ and $v \in H^m(\Omega)$ with $m \geq 2$,*

$$\left\| h^{\frac{1}{2}} \left(R_h(\Pi_h(v)) - \frac{\partial v}{\partial n} \right) \right\|_{L^2(\Gamma_K)} \leq C h^s \left(\|E(v)\|_{H^m(\tilde{K}')} + \|E(v)\|_{H^m(B_K)} \right),$$

where $s := \min\{p, m-1\}$, $K' \in \mathcal{M}_h^g$ is a good neighbor if $K \in \mathcal{M}_h^b$, $K' = K$ if $K \in \mathcal{M}_h^g$, and B_K is the minimal bounding box enclosing K and K' .

Proof. Without loss of generality, we can focus on the case $K \in \mathcal{M}_h^b$ with good neighbor K' .

$$\left\| h^{\frac{1}{2}} \left(R_h(\Pi_h(v)) - \frac{\partial v}{\partial n} \right) \right\|_{L^2(\Gamma_K)} \leq \left\| h^{\frac{1}{2}} \left(R_h(\Pi_h(v)) - \frac{\partial q}{\partial n} \right) \right\|_{L^2(\Gamma_K)} + \left\| h^{\frac{1}{2}} \frac{\partial}{\partial n} (q - v) \right\|_{L^2(\Gamma_K)}. \quad (2.20)$$

Let $q \in \mathbb{Q}_p(B_K)$, where B_K is the minimal bounding box enclosing K and K' , so that $R_h(q) = \frac{\partial q}{\partial n}$, and focus on the first term. We apply the stability property proved in Theorem 2.3.14 and, again, the triangular inequality:

$$\begin{aligned} \left\| h^{\frac{1}{2}} (R_h(\Pi_h(v)) - q) \right\|_{L^2(\Gamma_K)} &\leq C \|\nabla(\Pi_h(v) - q)\|_{L^2(\Omega \cap K')} \\ &\leq C \left(\|\nabla(q - v)\|_{L^2(\Omega \cap K')} + \|\nabla(v - \Pi_h(v))\|_{L^2(\Omega \cap K')} \right) \\ &\leq C \left(\|\nabla(q - E(v))\|_{L^2(K')} + \|\nabla(E(v) - \Pi_h(v))\|_{L^2(K')} \right) \\ &\leq C h^s \left(\|E(v)\|_{H^m(B_K)} + \|E(v)\|_{H^m(\tilde{K}')} \right), \end{aligned} \quad (2.21)$$

with $s := \min\{p, m-1\}$ and C depends on the shape-regularity of B_K (see Remark 2.3.16). In (2.21), we used the Deny-Lions Lemma (Theorem 3.4.1 of [112]) on B_K and the optimal approximation properties of spline quasi-interpolants (together with the regularity of the mapping, i.e., Assumption 1.1.3). Let us study the convergence of the second term of (2.20). Corollary A.1.3 together with Theorem 3.4.1 of [112], entail

$$\begin{aligned} \left\| h^{\frac{1}{2}} \frac{\partial}{\partial n} (q - E(v)) \right\|_{L^2(\Gamma_K)}^2 &\leq C \left\| h^{\frac{1}{2}} \nabla (q - E(v)) \right\|_{L^2(K)} \left\| h^{\frac{1}{2}} \nabla (q - E(v)) \right\|_{H^1(K)} \\ &\leq C h^{2s} \|E(v)\|_{H^m(B_K)}^2, \end{aligned} \quad (2.22)$$

where $s := \min\{p, m-1\}$ and C depends on the shape-regularity of B_K . Note that, as in the proof of Proposition 2.3.10, we can choose the same q in (2.21) and (2.22). By combining the previous passages, we readily get

$$\left\| h^{\frac{1}{2}} \left(R_h(\Pi_h(v)) - \frac{\partial v}{\partial n} \right) \right\|_{L^2(\Gamma_K)} \leq C h^s \left(\|E(v)\|_{H^m(B_K)} + \|E(v)\|_{H^m(\tilde{K}')} \right),$$

with $s := \min\{p, m-1\}$ and C depends on the shape-regularity of B_K . \square

Remark 2.3.16. Let $N_K := \#\{K^* \in \mathcal{M}_h : K^* \cap B_K \neq \emptyset\}$, given $K \in \mathcal{M}_h$. N_K may vary according to the constant C appearing in (2.7) and the space dimension d (analogous reasoning as in Remark 2.3.11). Still, it is uniformly bounded with respect to h thanks to the shape-regularity of the physical mesh and, in particular, depends on \mathbf{F} . Indeed, if we assume that for every $N \in \mathbb{N}$ there exist $\bar{h} > 0$ and $\bar{K} \in \mathcal{M}_h$ such that $N_{\bar{K}} > N$, then this would contradict the shape-regularity of \mathcal{M}_h and the existence of uniform constant C in (2.7). The shape-regularity of \mathcal{M}_h also implies that, given $K \in \mathcal{M}_h$, $\#\{B_{\tilde{K}} : B_{\tilde{K}} \cap K \neq \emptyset, \tilde{K} \in \mathcal{M}_h\}$ is uniformly bounded with respect to h . Moreover, given $\rho_{B_K} := \sup\{\text{diam}(B) : B \text{ is a ball contained in } B_K\}$ and $h_{B_K} := \text{diam}(B_K)$, then the geometric quantity $\frac{h_{B_K}}{\rho_{B_K}} \sim \frac{h}{\rho_{B_K}}$ is also uniformly bounded with respect to $K \in \mathcal{M}_h$.

2.3.5 A priori error estimates

The preparatory results of Propositions 2.3.10 and 2.3.15 were needed in order to prove the following convergence results.

Theorem 2.3.17. *There exists $\bar{\beta} > 0$ such that, for every $\beta \geq \bar{\beta}$, if $u \in H^m(\Omega)$ with $m \geq 2$ is the solution to (2.3) and $u_h \in V_h$ is the solution to (2.8), then*

$$\|u - u_h\|_{1,h} \leq C \left(h^s \|u\|_{H^m(\Omega)} + h^{r-1} \|E(u)\|_{H^r(S_h)} \right), \quad (2.23)$$

where S_h is the strip of width Ch , $C > 0$, such that $S_h \supseteq \bigcup_{K \in \mathcal{M}_h^b} B_K$, $s := \min\{m-1, p\}$, r and B_K are defined as

- $r := \min\{m, p + \frac{1}{2} - \varepsilon\}$, $\varepsilon > 0$, if we choose the stabilization in the parametric domain of Definition 2.3.5 (if $m \geq p + \frac{1}{2}$, we assume that each internal knot line is not repeated, otherwise we shall refer to Remark 2.3.12). In this case $B_K = \mathbf{F}(B_Q)$, B_Q is the minimal bounding box enclosing $Q \cup Q'$, $K' = \mathbf{F}(Q') \in \mathcal{M}_h^g$ is a good neighbor of $K = \mathbf{F}(Q)$;
- $r := s + 1$, if we choose the stabilization in the physical domain of Definition 2.3.6, and B_K is the minimal bounding box enclosing $K \cup K'$, where $K' \in \mathcal{M}_h^g$ is a good neighbor of K .

Proof. From Theorems 2.3.3, 2.3.9, and 2.3.14 we know that, for both choices of stabilization, $\bar{a}_h(\cdot, \cdot)$ is coercive w.r.t. $\|\cdot\|_{1,h}$, i.e., there exists $\alpha > 0$ such that, for every $v_h \in V_h$,

$$\sup_{\substack{w_h \in V_h \\ w_h \neq 0}} \frac{\bar{a}_h(v_h, w_h)}{\|w_h\|_{1,h}} \geq \alpha \|v_h\|_{1,h}.$$

Let $v_h \in V_h$. Using the triangular inequality and coercivity, we get

$$\begin{aligned} \|u - u_h\|_{1,h} &\leq \|u - v_h\|_{1,h} + \|v_h - u_h\|_{1,h} \\ &\leq \|u - v_h\|_{1,h} + \frac{1}{\alpha} \sup_{\substack{w_h \in V_h \\ w_h \neq 0}} \frac{\bar{a}_h(v_h - u_h, w_h)}{\|w_h\|_{1,h}}. \end{aligned} \quad (2.24)$$

Then, recalling that u_h solves (2.8), we get

$$\begin{aligned} \bar{a}_h(v_h - u_h, w_h) &= \bar{a}_h(v_h, w_h) - \bar{a}_h(u_h, w_h) = \bar{a}_h(v_h, w_h) - \bar{F}_h(w_h) \\ &= \int_{\Omega} \nabla v_h \cdot \nabla w_h - \int_{\Gamma_D} R_h(v_h) w_h - \int_{\Gamma_D} v_h R_h(w_h) + \beta \int_{\Gamma_D} h^{-1} v_h w_h \\ &\quad - \int_{\Omega} f w_h + \int_{\Gamma_D} g_D R_h(w_h) - \beta \int_{\Gamma_D} h^{-1} g_D w_h. \end{aligned}$$

Chapter 2. Stabilized isogeometric discretization of the Poisson problem on trimmed geometries

Since u solves (2.3), $\int_{\Omega} f w_h = \int_{\Omega} \nabla u \cdot \nabla w_h - \int_{\Gamma_D} \frac{\partial u}{\partial n} w_h$ and $u|_{\Gamma_D} = g_D$. Hence,

$$\begin{aligned} \bar{a}_h(v_h - u_h, w_h) &= \underbrace{\int_{\Omega} \nabla(v_h - u) \cdot \nabla w_h}_I - \underbrace{\int_{\Gamma_D} (R_h(v_h) - \frac{\partial u}{\partial n}) w_h}_{II} \\ &\quad + \underbrace{\int_{\Gamma_D} (u - v_h) R_h(w_h)}_{III} + \underbrace{\beta \int_{\Gamma_D} h^{-1} (v_h - u) w_h}_{IV}. \end{aligned}$$

Let us now estimate the four terms separately. We will leave II for last since its analysis depends on the choice of the stabilization. Clearly

$$I + IV \leq C \|u - v_h\|_{1,h} \|w_h\|_{1,h},$$

where $C = \mathcal{O}(\beta) > 0$. Note that this will not compromise the uniformity of the resulting constant, provided that β is chosen as close as possible to $\bar{\beta}$ (see the discussion in Remark 2.2.3). Using the stability property (2.9), we get

$$\begin{aligned} III^2 &\leq \left\| h^{-\frac{1}{2}} (u - v_h) \right\|_{L^2(\Gamma_D)}^2 \sum_{K \in \mathcal{G}_h} \left\| h^{\frac{1}{2}} R_h(w_h) \right\|_{L^2(\Gamma_K)}^2 \\ &\leq \|u - v_h\|_{1,h}^2 C \sum_{K \in \mathcal{G}_h} \|\nabla w_h\|_{L^2(K' \cap \Omega)}^2 \leq C \|u - v_h\|_{1,h}^2 \|w_h\|_{1,h}^2, \end{aligned}$$

where K' is a good neighbor if $K \in \mathcal{M}_h^b$, $K' = K$ if $K \in \mathcal{M}_h^g$. Let us estimate the term II . By definition of the norm $\|\cdot\|_{1,h}$,

$$II \leq \left\| h^{\frac{1}{2}} \left(R_h(v_h) - \frac{\partial u}{\partial n} \right) \right\|_{L^2(\Gamma_D)} \|w_h\|_{1,h}.$$

Now, we choose $v_h = \Pi_h(u)$ and distinguish two cases.

- If we use the stabilization in the parametric domain of Definition 2.3.5, hence applying Proposition 2.3.10, we get

$$\begin{aligned} &\sum_{K \in \mathcal{G}_h} \left\| h^{\frac{1}{2}} \left(R_h(\Pi_h(u)) - \frac{\partial u}{\partial n} \right) \right\|_{L^2(\Gamma_K)} \|w_h\|_{1,h} \\ &\leq \sum_{K \in \mathcal{G}_h} C \left(h^s \|E(u)\|_{H^m(\tilde{K}')} + h^{r-1} \|E(u)\|_{H^r(B_K)} \right) \|w_h\|_{1,h}, \end{aligned}$$

with $s := \min\{p, m-1\}$ and $r := \min\{m, p + \frac{1}{2} - \varepsilon\}$, $\varepsilon > 0$. See the statement of the theorem for the definition of B_K .

- Employing the stabilization in the physical domain of Definition 2.3.6, hence applying Proposition 2.3.15, we obtain

$$\begin{aligned} &\sum_{K \in \mathcal{G}_h} \left\| h^{\frac{1}{2}} \left(R_h(\Pi_h(u)) - \frac{\partial u}{\partial n} \right) \right\|_{L^2(\Gamma_K)} \|w_h\|_{1,h} \\ &\leq \sum_{K \in \mathcal{G}_h} C h^s \left(\|E(u)\|_{H^m(\tilde{K}')} + \|E(u)\|_{H^m(B_K)} \right) \|w_h\|_{1,h}, \end{aligned}$$

with $s := \min\{p, m-1\}$. See the statement of the theorem for the definition of B_K .

2.3. The stabilized formulation and its analysis

By using, respectively, Remarks 2.3.11 and 2.3.16 (the number of elements in each bounding box and the number of boxes containing a particular element are uniformly bounded), we have

$$II \leq C \left(h^s \|u\|_{H^m(\Omega)} + h^{r-1} \|E(u)\|_{H^r(S_h)} \right) \|w_h\|_{1,h},$$

where S_h is the strip of width Ch , $C > 0$, such that $S_h \supseteq \bigcup_{K \in \mathcal{M}_h^b} B_K$, $s := \min\{p, m-1\}$, and

- $r := \min\{m, p + \frac{1}{2} - \varepsilon\}$, $\varepsilon > 0$, if we use the stabilization in the parametric domain, hence apply Proposition 2.3.10;
- $r := s + 1$ if we use the one in the physical domain and use Proposition 2.3.15.

Therefore, we get

$$\begin{aligned} \bar{a}_h(\Pi_h(u) - u_h, w_h) &\leq C \|u - \Pi_h(u)\|_{1,h} \|w_h\|_{1,h} \\ &\quad + C \left(h^s \|u\|_{H^m(\Omega)} + h^{r-1} \|E(u)\|_{H^r(S_h)} \right) \|w_h\|_{1,h}. \end{aligned} \quad (2.25)$$

We now combine (2.25) with (2.24), to obtain

$$\begin{aligned} \|u - u_h\|_{1,h} &\leq \|u - \Pi_h(u)\|_{1,h} + \frac{1}{\alpha} \sup_{\substack{w_h \in V_h \\ w_h \neq 0}} \frac{\bar{a}_h(\Pi_h(u) - u_h, w_h)}{\|w_h\|_{1,h}} \\ &\leq \left(1 + \frac{C}{\alpha} \right) \|u - \Pi_h(u)\|_{1,h} + \frac{C}{\alpha} \left(h^s \|u\|_{H^m(\Omega)} + h^{r-1} \|E(u)\|_{H^r(S_h)} \right). \end{aligned}$$

Applying Theorem 2.3.8, we conclude

$$\|u - u_h\|_{1,h} \leq C \left(h^s \|u\|_{H^m(\Omega)} + h^{r-1} \|E(u)\|_{H^r(S_h)} \right),$$

where s and r have been defined above. \square

Remark 2.3.18. As already observed in Remark 2.3.12, when $u \in H^m(\Omega)$, with $2 \leq m < p + \frac{1}{2}$, both stabilizations give rise to optimal *a priori* error estimates. When $u \in H^m(\Omega)$, with $m \geq p + \frac{1}{2}$ and $m \geq 2$, instead, stabilization in Definition 2.3.5 is suboptimal. In this case the estimate can be modified and improved using the following result.

Lemma 2.3.19. *Given $\varepsilon > 0$, let S_h be defined as in Theorem 2.3.17, there exists $C > 0$ such that*

$$\|E(u)\|_{H^r(S_h)} \leq Ch^{\frac{1}{2}-\varepsilon} \|u\|_{H^{p+\frac{3}{2}-\varepsilon}(\Omega)}, \quad \forall u \in H^{p+\frac{3}{2}-\varepsilon}(\Omega), \quad \forall 0 \leq r < p + \frac{1}{2}.$$

Proof. Using the fact that $r < p + 1$, we are able to recover an integer order for the Sobolev norm and so to apply Lemma A.1.8 with $s = \frac{1}{2} - \varepsilon$:

$$\|E(u)\|_{H^r(S_h)} \leq \|E(u)\|_{H^{p+1}(S_h)} \leq Ch^{\frac{1}{2}-\varepsilon} \|E(u)\|_{H^{p+\frac{3}{2}-\varepsilon}(\Omega_0)} \leq Ch^{\frac{1}{2}-\varepsilon} \|u\|_{H^{p+\frac{3}{2}-\varepsilon}(\Omega)}.$$

In the last inequality, we used the boundedness of the Sobolev-Stein extension operator. \square

Proposition 2.3.20. *Let $u \in H^p(\Omega)$ be the solution of (2.3) and $u_h \in V_h$ the solution of (2.8), obtained using the stabilization in the parametric domain of Definition 2.3.5 under the hypothesis that each internal knot line is not repeated. Then, the following error estimate holds:*

$$\|u - u_h\|_{1,h} \leq Ch^{p'} \|u\|_{H^{p'+\frac{3}{2}}(\Omega)} \quad \forall 0 \leq p' < p - 1.$$

Proof. It immediately follows by combining Theorem 2.3.17 and Lemma 2.3.19. \square

Remark 2.3.21. At the prize of slightly higher regularity request, the optimal convergence rate is to be also expected for the stabilization in the parametric domain of Definition 2.3.5 (when we assume that each internal knot line is not repeated).

2.4 Numerical examples

2.4.1 Some details about the implementation

For accurate numerical integration, we decompose the trimmed elements into smaller quadrilateral tiles to compute the integrals. These tiles are reparametrized as Bézier surfaces of the same degree p as the approximation space used to discretize our PDE; see [4] for a detailed explanation. We remark that this reparametrization is also used to compute the boundary integrals.

In order to compute the stabilization terms appearing in (2.8), first of all for each bad trimmed element K we choose K' : among all the neighbors of K , we choose (the) one with the largest relative overlap $|K' \cap \Omega| / |K'|$. Then we need to locally project functions living in K' (or in Q') onto the space of polynomials on K' (or Q') and extend them up to Γ_K . For the stabilization in the parametric domain, by taking the Bernstein polynomials as a basis on Q' , the projection can be computed by knot insertion, while for the stabilization in the physical domain, the L^2 -projection is needed anyhow.

2.4.2 Validation of stability

Let us repeat the numerical experiment of Section 2.2 in order to validate the effectiveness of our stabilization technique. Let us solve the generalized eigenvalue problem (2.6) with the stabilization of Definition 2.3.5 (since $\mathbf{F} = \mathbf{Id}$, the two proposed stabilizations techniques are equivalent) in the trimmed domain of Figure 2.2(a) for the same values of ε used in Section 2.2. The result is shown in Figure 2.3(b). This time we observe that the maximum generalized

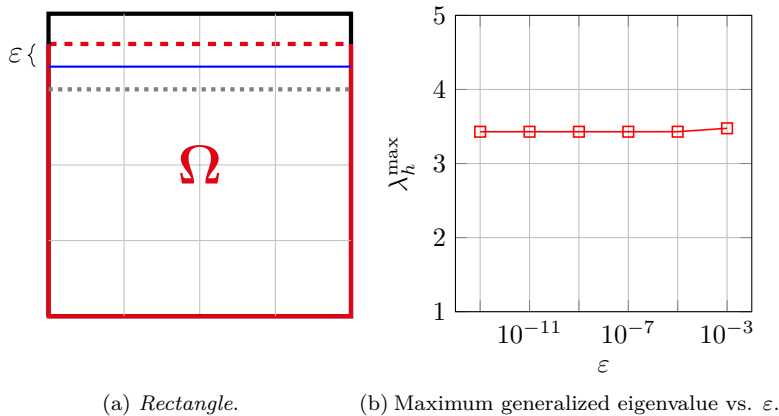


Figure 2.3 – Testing the stability of formulation (2.8) with respect to trimming.

eigenvalue remains bounded independently of ε , confirming our method to be stable.

2.4.3 Validation of *a priori* error estimates

In the following we focus on the Poisson problem (2.8) with the difference that, while we impose Dirichlet boundary conditions weakly on the trimmed parts of the boundary, on the other parts where the mesh is fitted with the boundary we impose them in the strong sense.

Test 1. Let $\Omega = \Omega_0 \setminus \overline{\Omega}_1$ be defined as in Figure 2.4(a), where $\Omega_0 = \mathbf{F}((0, 1)^2)$ is a *quarter of annulus* (\mathbf{F} is a non linear mapping) constructed with biquadratic NURBS, and Ω_1 is the image of a ball in the parametric domain through the isogeometric map, namely, $\Omega_1 = \mathbf{F}(B(0, r))$ with $r = 0.76$. We consider as a manufactured solution $u_{ex}(x, y) = e^x \sin(xy)$. We use the stabilization in the parametric domain of Definition 2.3.5, and the parameters $\beta = 1$ and $\theta = 0.1$. The results of convergence for different values of p , which are displayed Figure 2.5(a), show that we obtain the optimal order of convergence.

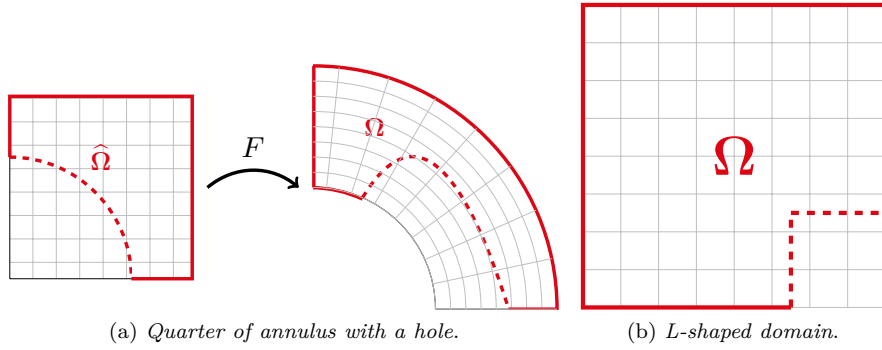


Figure 2.4 – Trimmed domains.

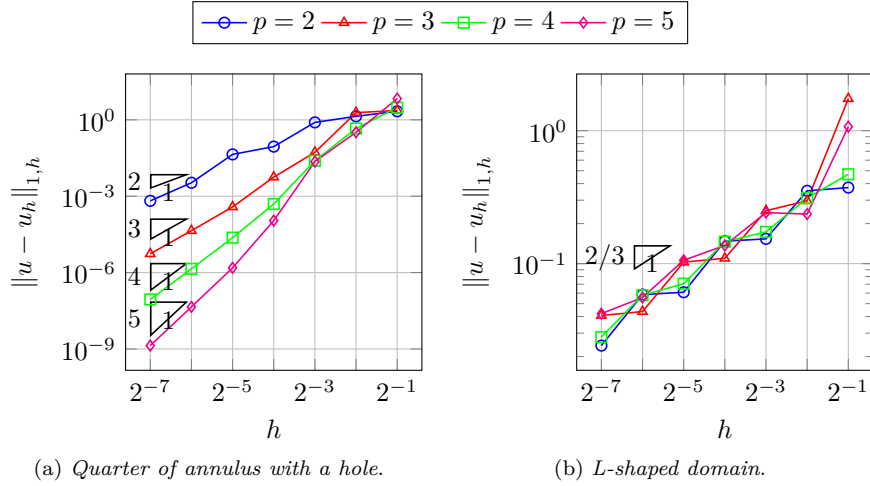


Figure 2.5 – Convergence rates of $\|u - u_h\|_{1,h}$ for Test 1 and Test 2.

Test 2. We now consider the Poisson problem in the *L-shaped domain* shown in Figure 2.4(b), given by $\Omega = \Omega_0 \setminus \overline{\Omega}_1$, where $\Omega_0 = (-2, 1) \times (-1, 2)$ and $\Omega_1 = (0, 1) \times (-1, 0)$. The exact solution is chosen as the singular function that, in polar coordinates, reads as $u(r, \varphi) = r^{\frac{2}{3}} \sin(\frac{2}{3}\varphi) \in H^{\frac{5}{3}-\delta}(\Omega)$ for every $\delta > 0$. The function has a singularity at the re-entrant corner in the origin, and the domain is chosen in such a way that the corner is always located in the interior of an element. We employ the formulation (2.8) together with the stabilization operator in Definition 2.3.5,

noting that since the parametrization is a simple scaling, the two stabilizations are equivalent. This time we set the parameters $\theta = 1$ and, due to the presence of the singularity, $\beta = (p + 1) \cdot 10$. The numerical results of Figure 2.5(b) show that the method converges with order $\frac{2}{3}$ as expected, and the suboptimal behavior is due to the low regularity of the reference solution. We note that in principle our *a priori* estimates, see Theorem 2.3.17, does not cover this case since it requires the solution to be at least in $H^2(\Omega)$.

Test 3. The goal of this test is to show that, when the regularity of the mapping \mathbf{F} is low between the trimmed elements and their neighbors, the stabilization in the physical domain is more effective than the ones based on polynomial extensions in the parametric domain (as it is the case for our stabilization in the parametric domain, but also the method proposed in [92]). Let us consider again, as domain Ω_0 , the quarter of annulus, this time parametrized with a different map \mathbf{F} : starting from the standard biquadratic NURBS parametrization, we perform knot insertion adding the knot $\xi = 0.75$, with multiplicity 2, in the direction corresponding to the angular coordinate, that corresponds to the thick black line in Figure 2.6(a). In order to get a geometry of class C^0 , we set the second coordinate of one control point, highlighted in Figure 2.6(b), equal to 0.5 in homogeneous coordinates. Note that the new parametrization is

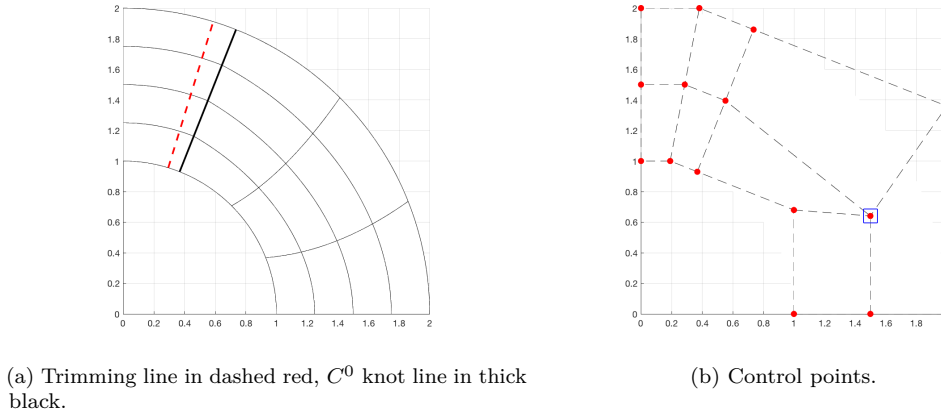
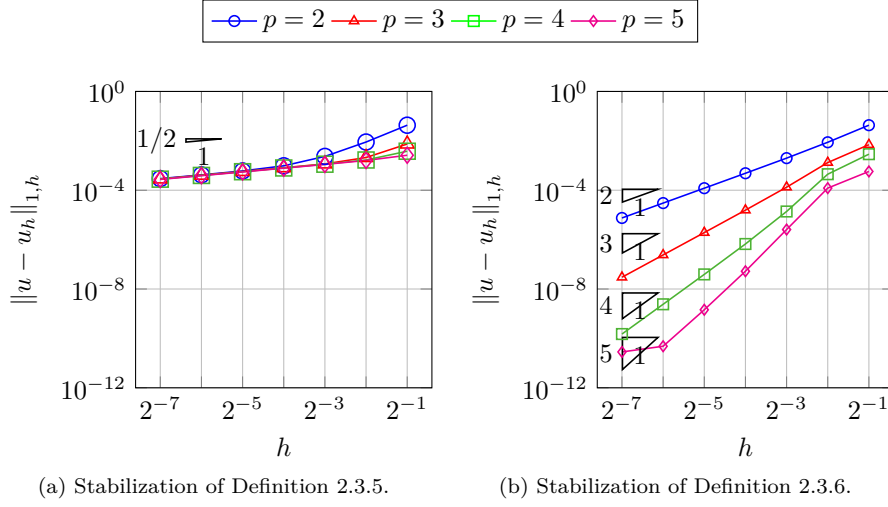


Figure 2.6 – Lower inter-regularity parametrization of the quarter of annulus.

only of class C^0 in correspondence of the knot line given by $\mathbf{F}(\{(x, y) : x \in (0, 1), y = 0.75\})$. To ensure that this knot line is located between K and K' , we define the trimmed domain as $\Omega = \mathbf{F}((0, 1) \times (0, 0.75 + \varepsilon))$ with $\varepsilon = 10^{-8}$. Here we set $\theta = 1$ and, because of the lower regularity of the parametrization, $\beta = (p + 1) \cdot 25$. We know from Remarks 2.3.12 and 2.3.13 that the convergence rate deriving from the stabilization in Definition 2.3.5 (and any stabilization based on polynomial extensions in the parametric domain) may suffer suboptimality. In particular, from Figure 2.7(a), we see that the error with the stabilization in the parametric domain is converging just as $h^{\frac{1}{2}}$ for any degree p , while in Figure 2.7(b) we observe that the desired convergence rates are reached when using the stabilization in the physical domain.

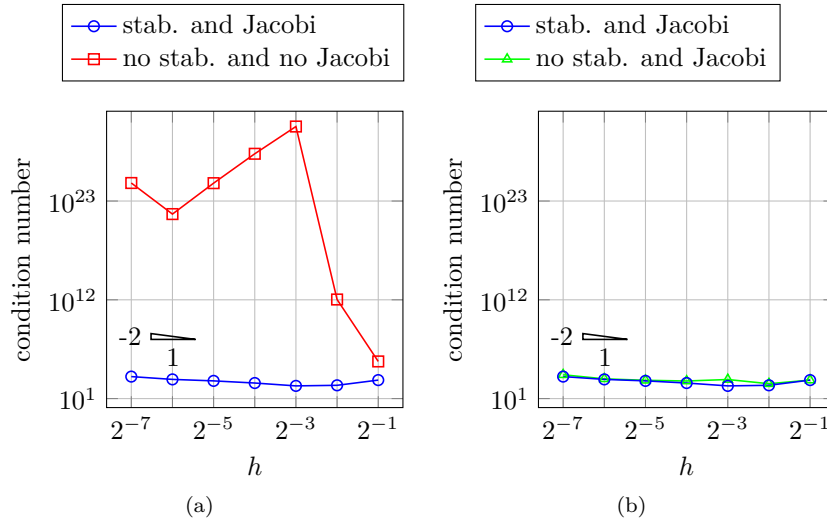
2.4.4 Conditioning

Even if an exhaustive discussion about the conditioning of the stiffness matrix in trimmed geometries is beyond the scope of this work (for a more detailed discussion on the topic, see, for instance, [50, 51]), we would like to present some numerical experiments for the sake of completeness. We focus again on the formulation (2.8) of the Poisson problem. We impose Dirichlet boundary conditions weakly on the trimmed parts of the boundary and strongly on the


 Figure 2.7 – Comparison of the two stabilizations in Test 3 when \mathbf{F} has lower regularity.

fitted parts.

Test C1. Let us come back to the *quarter of annulus with a hole*, and, as above, we employ B-splines of degree $p = 3$. In Figure 2.8(a) we show that our stabilization coupled with a simple diagonal scaling, which can be interpreted as a left-right Jacobi preconditioner, can solve the conditioning issue. In Figure 2.8(b) we compare the effectiveness of the diagonal rescaling with and without the stabilization, and we observe that the effect of the stabilization is marginal with respect to the one of the diagonal preconditioner. The stabilization used is the one in the parametric domain with $\beta = 1$ and $\theta = 0.1$.


 Figure 2.8 – Condition number study for the *quarter of annulus with a hole*, Test C1.

Test C2. Let us consider the same configuration as in the test of Figure 2.3(a), for which we notice again that the two stabilizations are equivalent. Let us take B-splines of degree $p = 3$, as mesh size $h = 2^{-5}$, and set the penalization parameter $\beta = 1$. After a simple diagonal rescaling as preconditioner, we compare the condition number of the stiffness matrix, as a function of ε , obtained for the nonstabilized ($\theta = 0$) and the stabilized ($\theta = 1$) formulations. Note that

as the ratio in Definition 2.3.1 is the same for all cut elements, it is sufficient to consider only these two values of θ . The results in Figure 2.9(a) show the diagonal rescaling is acting as a robust preconditioner with respect to the size of the trimming. Then, we perform uniform dyadic refinement, and we plot the condition number as a function of the mesh size h , obtaining the plots in Figures 2.9(b) and 2.9(c). The results suggest a better behavior of the condition number when a stabilized formulation is employed to solve the problem.

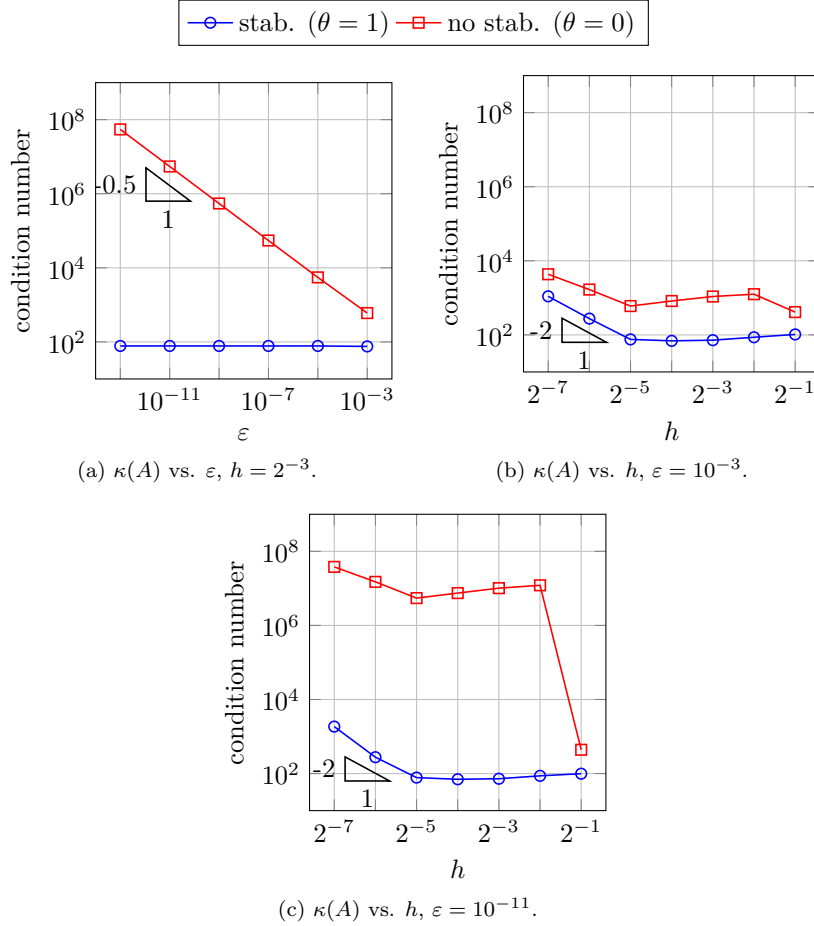


Figure 2.9 – Condition number study for the *rectangle*, Test C2.

Test C3. This test is inspired by [51]. Let us embed $\Omega = (0.19, 0.71) \times (0.19, 0.71)$ in the untrimmed domain $\Omega_0 = (0, 1)^2$ with an underlying mesh of size $h = 2^{-3}$. We consider B-splines of degree $p = 2$. Now, let us rotate Ω around its barycenter for different angles α (see Figure 2.10(a)). For each $\alpha = i \frac{\pi}{200}$, $i = 0, \dots, 100$ we face a specific trimming configuration where there may appear B-splines whose support intersects in a “pathological way” the domain Ω . Let us denote the “smallest volume fraction” $\eta := \min_{K \in \mathcal{G}_h} |\Omega \cap K|$. In Figure 2.10(b) we plot the condition number of the stiffness matrix against the smallest volume fraction, in order to compare the nonstabilized case with the stabilized (with parameter $\theta = 0.5$) and diagonally rescaled one. Let us observe that even if the behavior of the condition number appears to be much better after stabilization and diagonal rescaling, it is still strongly affected by the way the trimming curve cuts the mesh. In this regard, this is a counterexample that diagonal rescaling, together with our stabilization, is a robust preconditioner for the trimming operation.

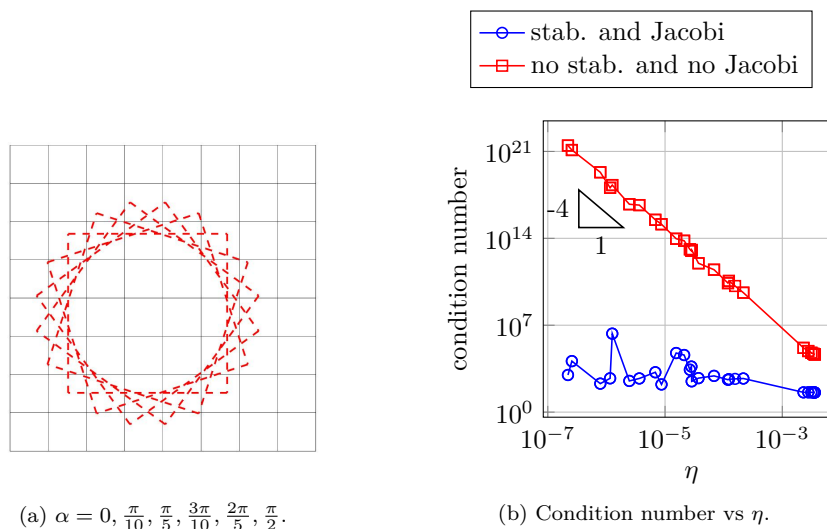


Figure 2.10 – Condition number study for the *rotating square*, Test C3.

3 Stabilized isogeometric discretization of the Poisson problem on union geometries

This chapter aims to develop a numerical method based on IGA to discretize the Poisson problem in a domain constructed via union, *i.e.*, by combining multiple independent overlapping patches. More precisely, given a series of spline patches, we overlay one on top of another in a certain order, following the same manner as in the multi-mesh finite element method [79, 80]. While we employ the Nitsche method to weakly couple these patches through the visible interfaces, the use of the stabilization technique borrowed from Chapter 2 allows us to prove the stability of the proposed approach in very general geometric configurations.

As in the trimmed case, the related major challenges include performing numerical integration in the trimmed (overlapped) elements, keeping the condition number of the arising linear system under control, and handling the stability issue caused by small trimmed elements [33, 92].

Note that while the theory is dimension-independent, the numerical experiments are performed just in 2D geometries. Indeed, creating a suitable quadrature mesh for each interface is a significant challenge, especially in 3D.

The chapter is organized as follows. Section 3.1 sets up the notations and necessary assumptions. The core of the chapter, namely the theory of overlapping multipatch isogeometric analysis, is presented in Section 3.2. In Section 3.3, we discuss how to create suitable quadrature meshes for interfaces, as well as how to implement the stabilization method. We next show several numerical examples in Section 3.4 to demonstrate the convergence and conditioning behavior of the proposed method.

C will denote generic positive constants that may change with each occurrence throughout the document but are always independent of the local mesh size and of the way the meshes are overlapped unless otherwise specified.

The results of this chapter have been published in [5].

3.1 Parametrization, mesh and approximation space for domains obtained via union

To facilitate the presentation of the content, we may re-introduce some of the notations already introduced in Chapter 1. Let $\Omega_i^* \subset \mathbb{R}^d$, $0 \leq i \leq N$ ($N \in \mathbb{N}$), $d \in \{2, 3\}$, be a *patch* or *predomain*, *i.e.*, before the union operation that will be described later on. We assume that there exists

Chapter 3. Stabilized isogeometric discretization of the Poisson problem on union geometries

a bi-Lipschitz map $\mathbf{F}_i \in \left(S_{\alpha_1^i, \dots, \alpha_d^i}^{\mathbf{p}^i}(\Xi^i) \right)^d$ such that $\Omega_i^* = \mathbf{F}_i(\widehat{\Omega})$, $\widehat{\Omega} := (0, 1)^d$, for given degree vector \mathbf{p}^i , regularity indices $\alpha_1^i, \dots, \alpha_d^i$, and knot-vector at the coarsest level of discretization Ξ^i . Hence, each Ω_i^* is homeomorphic to a square for $d = 2$, or a cube for $d = 3$, and its boundary is naturally composed of four edges or six faces respectively. We define the physical Bézier premesh as the image of the elements in $\widehat{\mathcal{M}}_i$ (the parametric Bézier mesh naturally induced on $\widehat{\Omega}$) through \mathbf{F}_i , *i.e.*,

$$\mathcal{M}_i^* := \{K \subset \Omega_i^* : K = \mathbf{F}_i(Q), Q \in \widehat{\mathcal{M}}_i\}.$$

For the sake of simplicity of the notation and the analysis, the following simplifications are made.

Assumption 3.1.1. We assume that the degree-vector is *isotropic* and that all predomains are parametrized by splines of the same degree, *i.e.*, $\mathbf{p}^i = \mathbf{p} = (p, \dots, p)$. Hence, we may write p instead of \mathbf{p} . Similarly for the regularity vectors, that is, $\alpha = \alpha_1^i = \dots = \alpha_d^i$, for all $0 \leq i \leq N$.

Let $\widehat{V}_{h,i}$ be a refinement of $S_{\alpha}^{\mathbf{p}}(\Xi^i)$ and

$$V_{h,i}^* = \text{span}\{B_{\mathbf{i},\mathbf{p}}(\mathbf{x}) := \widehat{B}_{\mathbf{i},\mathbf{p}} \circ \mathbf{F}_i^{-1}(\mathbf{x}) : \mathbf{i} \in \mathbf{I}\},$$

where $\{\widehat{B}_{\mathbf{i},\mathbf{p}} : \mathbf{i} \in \mathbf{I}\}$ is a basis of $\widehat{V}_{h,i}$. Let Ω be a domain of \mathbb{R}^d , $d \in \{2, 3\}$, with Lipschitz boundary Γ and outer unit normal \mathbf{n} , obtained through *union operation*, *i.e.*, such that $\overline{\Omega} = \bigcup_{i=0}^N \overline{\Omega}_i^*$. We define Ω_i as the *visible part* of the predomain Ω_i^*

$$\Omega_i := \Omega_i^* \setminus \bigcup_{\ell=i+1}^N \overline{\Omega}_\ell^*, \quad i = 0, \dots, N.$$

It holds $\Omega_N = \Omega_N^*$ and $\overline{\Omega} = \bigcup_{i=0}^N \overline{\Omega}_i = \bigcup_{i=0}^N \overline{\Omega}_i^*$, see Figure 3.1. Note that this choice of definition of the Ω_i 's follows [80] and implies a *hierarchy* of predomains. In particular, if $i > j$ then Ω_i^* is *on top of* Ω_j^* , in the sense that $\Omega_i^* \cap \Omega_j^*$ is hidden by $\bigcup_{k \geq i} \Omega_k$. We define

$$\Gamma_i := \partial\Omega_i^* \setminus \bigcup_{\ell=i+1}^N \overline{\Omega}_\ell^*, \quad i = 0, \dots, N,$$

i.e., the interface Γ_i is the *visible part of the external boundary* of Ω_i^* with outer unit normal n_i . Moreover, we define the *local interfaces* Γ_{ij} as

$$\Gamma_{ij} := \Gamma_i \cap \overline{\Omega}_j, \quad 0 \leq j < i \leq N,$$

i.e., Γ_{ij} is the subset of the visible boundary of Ω_i^* that intersects Ω_j , see Figure 3.1(b). We assume that each interface Γ_{ij} either has non-zero $(d-1)$ -measure or is the empty set. We also assume that Γ_{ij} inherits the orientation of Γ_i , hence it has outer unit normal \mathbf{n}_i , also denoted as \mathbf{n} when it is clear from the context to which domain is referred to. Note that Γ_{ij} is not connected in general.

Definition 3.1.2. Let $0 \leq j < i \leq N$, and

$$\delta_{ij} := \begin{cases} 1 & \text{if } \Gamma_{ij} \neq \emptyset, \\ 0 & \text{otherwise.} \end{cases}$$

For each $1 \leq i \leq N$, the quantity $\sum_{j=0}^{i-1} \delta_{ij}$ counts the number of visible parts Ω_j whose boundaries are overlapped by Γ_i and, for $0 \leq j \leq N-1$, $\sum_{i=j+1}^N \delta_{ij}$ the number of visible parts whose boundaries overlap Γ_j . We further define $N_{\Gamma}^1 := \max_{1 \leq i \leq N} \sum_{j=0}^{i-1} \delta_{ij}$, the maximum

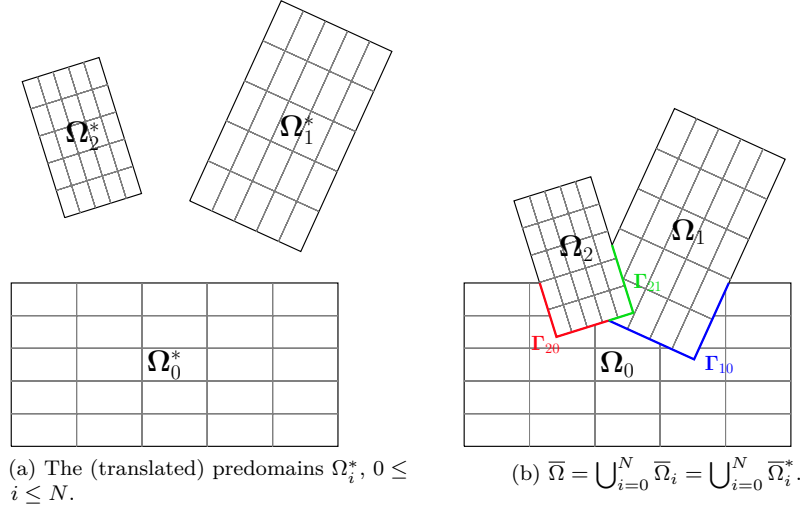


Figure 3.1 – Definitions of predomains (a), visible parts of predomains, and local interfaces (Γ_{10} , Γ_{20} and Γ_{21}) of predomain boundaries (b).

number of visible parts whose boundaries are overlapped by any visible boundary, and $N_\Gamma^\uparrow := \max_{0 \leq j \leq N-1} \sum_{i=j+1}^N \delta_{ij}$, the maximum number of visible parts whose boundaries cover any visible boundary. Hence, we let $N_\Gamma := \max\{N_\Gamma^\downarrow, N_\Gamma^\uparrow\}$ be the *maximum number of boundary overlaps* in the current configuration.

Definition 3.1.3. We let $O_{ij} := \Omega_i \cap \Omega_j^*$, $0 \leq j < i \leq N$, be the *overlap* between the j -th predomain and the i -th visible part. For every $0 \leq j < i \leq N$, we define

$$\eta_{ij} := \begin{cases} 1 & \text{if } O_{ij} \neq \emptyset, \\ 0 & \text{otherwise.} \end{cases}$$

For each $1 \leq i \leq N$, the quantity $\sum_{j=0}^{i-1} \eta_{ij}$ counts the number of predomains covered by the visible part Ω_i . We further define $N_\mathcal{O} := \max_{1 \leq i \leq N} \sum_{j=0}^{i-1} \eta_{ij}$, the maximum number of predomains covered by any visible part.

We observe that $N_\Gamma, N_\mathcal{O} \leq N$; see Figure 3.2. Moreover, in applications we expect $N_\Gamma, N_\mathcal{O} \ll N$. We refer to $\mathcal{M}_i := \{K \in \mathcal{M}_i^* : K \cap \Omega_i \neq \emptyset\}$, $i = 0, \dots, N$, as the i -th *extended mesh*, consisting of all visible elements (not necessarily fully visible) of the i -th premesh \mathcal{M}_i^* . We define $h_i : \Omega_i \rightarrow \mathbb{R}^+$ to be the piecewise constant mesh size function of \mathcal{M}_i assigning to each visible element its whole diameter (rather than the diameter of its visible part), namely $h_i|_{K \cap \Omega} := h_{i,K}$, where $h_{i,K} := \text{diam}(K)$ for every $K \in \mathcal{M}_i$, $0 \leq i \leq N$. Moreover let us denote $h_i := \max_{K \in \mathcal{M}_i} h_{i,K}$ and $h := \max_{0 \leq i \leq N} h_i$. Finally, we denote by $h : \Omega \rightarrow \mathbb{R}^+$ the piecewise constant function defined as $h|_{\Omega_i} := h_i$.

Throughout the chapter, we are going to rely on the shape-regularity hypothesis on each premesh (in the spirit of Chapter 2) and on the assumption that adjacent sub-domains are discretized with similar mesh sizes.

Assumption 3.1.4. For every $0 \leq i \leq N$, the family of meshes \mathcal{M}_i (parameterized on the mesh size) is assumed to be *shape-regular*, see Assumption 1.1.1. Moreover, the meshes locally have

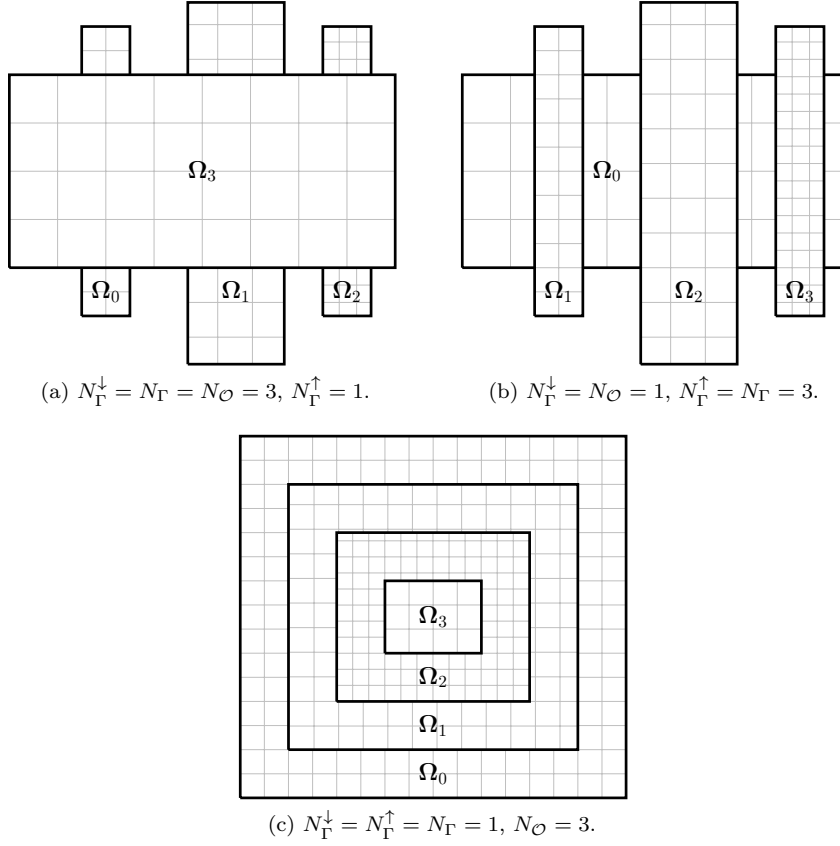


Figure 3.2 – Illustration of N_Γ^\downarrow , N_Γ^\uparrow , N_Γ , $N_\mathcal{O}$.

compatible sizes in the following sense. There exist $c, C > 0$ such that for every $\Gamma_{ij} \neq \emptyset$, with $1 \leq j < i \leq N$, $K_i \in \mathcal{M}_i$ such that $\overline{K}_i \cap \Gamma_{ij} \neq \emptyset$ and $K_j \in \mathcal{M}_j$ such that $\overline{K}_j \cap \Gamma_{ij} \neq \emptyset$, it holds

$$ch_j \Big|_{K_j} \leq h_i \Big|_{K_i} \leq Ch_j \Big|_{K_j}.$$

Finally, let us make a mild assumption on the roughness of the interfaces Γ_{ij} .

Assumption 3.1.5. All the interfaces Γ_{ij} , $1 \leq j < i \leq N$, are Lipschitz-regular.

Remark 3.1.6. Assumption 3.1.5 combined with Lemma A.1.1 insures that there exists $C > 0$ such that for every $1 \leq j < i \leq N$ and $K \in \mathcal{M}_j$ it holds $|\Gamma_{ij} \cap \overline{K}| \leq Ch_j^{d-1} \Big|_K$.

Note that in what follows, we are going to refer to elements $K \in \mathcal{M}_i$, $i = 0, \dots, N$, such that $|\Omega_i \cap K| < |K|$ as *cut elements*. Moreover, integrals and norms will be defined on sets like Γ_{ij} , $\Gamma_{ij} \cap \overline{K}$ and they are meant to be on their interior in a suitable sense.

C will denote generic positive constants that may change with each occurrence throughout the chapter but are always independent of the local mesh size, the position of the visible interfaces with respect to the meshes, and the number of patches, unless otherwise specified.

3.2 Isogeometric analysis on union geometries

3.2.1 Model problem and its variational formulation

Let us consider the Poisson equation as the model problem. The goal is to solve it in the *union domain* Ω . Given $f \in L^2(\Omega)$, $g_D \in H^{\frac{1}{2}}(\Gamma_D)$ and $g_N \in H^{-\frac{1}{2}}(\Gamma_N)$, find $u : \Omega \rightarrow \mathbb{R}$ such that

$$\begin{aligned} -\Delta u &= f, & \text{in } \Omega, \\ u &= g_D, & \text{on } \Gamma_D, \\ \frac{\partial u}{\partial n} &= g_N, & \text{on } \Gamma_N, \end{aligned} \tag{3.1}$$

where Γ_D, Γ_N are non-empty, open, disjoint subsets of $\partial\Omega$, $\Gamma := \partial\Omega = \bar{\Gamma}_D \cup \bar{\Gamma}_N$, and \mathbf{n} denotes, as usual, the unit outward normal on Γ .

Proceeding similarly to [18, 127], we rewrite problem (3.1) in the following multipatch form. Find $u : \Omega \rightarrow \mathbb{R}$ such that

$$-\Delta u_i = f, \quad \text{in } \Omega_i, \quad i = 0, \dots, N, \tag{3.2a}$$

$$u_i - u_j = 0, \quad \text{on } \Gamma_{ij}, \quad 0 \leq j < i \leq N, \tag{3.2b}$$

$$\frac{\partial u_i}{\partial n_i} + \frac{\partial u_j}{\partial n_j} = 0, \quad \text{on } \Gamma_{ij}, \quad 0 \leq j < i \leq N, \tag{3.2c}$$

$$u_i = g_D, \quad \text{on } \Gamma_D \cap \Gamma_i, \quad i = 0, \dots, N, \tag{3.2d}$$

$$\frac{\partial u_i}{\partial n_i} = g_N, \quad \text{on } \Gamma_N \cap \Gamma_i, \quad i = 0, \dots, N, \tag{3.2e}$$

where $u_i := u|_{\Omega_i}$, $i = 0, \dots, N$. Equations (3.2b) and (3.2c) are commonly known as *transmission conditions* at the local interfaces.

Proposition 3.2.1. *Problems (3.1) and (3.2a)–(3.2e) are equivalent.*

Proof. The proof is straightforward. We refer the interested reader to Chapter 1 of [113]. \square

Let us introduce, for each visible part Ω_i , the *local isogeometric space*

$$V_{h,i} = \text{span}\{B_{\mathbf{i},\mathbf{p}}|_{\Omega_i} : \mathbf{i} \in \mathbf{I}\},$$

and glue together the local spaces to form the *union isogeometric space*

$$V_h := \bigoplus_{i=0}^N V_{h,i}.$$

Elements of V_h are $(N+1)$ -tuples $v_h = (v_0, \dots, v_N)$. In practice, we can treat them as scalar functions thanks to the embedding

$$V_h \hookrightarrow L^2(\Omega), \quad v_h(x) \mapsto v_i(x), \quad x \in \Omega_i, \quad i = 0, \dots, N.$$

In order to impose Dirichlet boundary conditions in a strong sense, some assumptions are needed.

Assumption 3.2.2. 1. There exists $0 \leq i \leq N$ such that $\hat{\Gamma}_i, \hat{\Gamma}_i := \mathbf{F}_i^{-1}(\Gamma_i)$, contains a full face of the parametric domain $\hat{\Omega}$.

Chapter 3. Stabilized isogeometric discretization of the Poisson problem on union geometries

2. For every $0 \leq i \leq N$, $\widehat{\Gamma}_D := \mathbf{F}^{-1}(\Gamma_D)$, $\widehat{\Gamma}_D \cap \widehat{\Gamma}_i$ is either empty or the union of full faces of $\widehat{\Omega}$.

The spaces V_h^{gD} and V_h^0 are readily defined as in Section 1.2. Note that in case Assumption 3.2.2 does not hold, we can combine the technique in this chapter with the one detailed in [33] and in Chapter 2, to deal with the imposition of Dirichlet boundary conditions in a weak sense.

Let us endow V_h with the following mesh dependent norm:

$$\|v_h\|_{1,h}^2 := \sum_{i=0}^N \|\nabla v_i\|_{L^2(\Omega_i)}^2 + \sum_{i=1}^N \sum_{j=0}^{i-1} \left\| h^{-\frac{1}{2}} [v_h] \right\|_{L^2(\Gamma_{ij})}^2, \quad v_h \in V_h, \quad (3.3)$$

where $[v_h] := v_i|_{\Gamma_{ij}} - v_j|_{\Gamma_{ij}}$ denotes the *jump term* on Γ_{ij} , $i > j$. Hereafter, we also make use of the approximation of the normal flux through Γ_{ij} , denoted as $\langle \frac{\partial v_h}{\partial n} \rangle_t := t \frac{\partial v_i}{\partial n_i} + (1-t) \frac{\partial v_j}{\partial n_j}$, $t \in \{\frac{1}{2}, 1\}$. When $t = \frac{1}{2}$ the latter is a *symmetric average flux*, while when $t = 1$ we choose the *one-sided flux* on the Ω_i side, in the spirit of [71], i.e., on the side of the domain which is “on top” of the other. As the choice $t = 1$ will turn out to be the most convenient one, we may drop the index t when it is equal to 1.

We propose the following weak formulation for the discrete counterpart of problem (3.2a)–(3.2e), which is obtained enforcing the transmission conditions in a weak sense using Nitsche’s method (as initially proposed in [127]).

Find $u_h \in V_h^{gD}$ such that

$$a_h(u_h, v_h) = F_h(v_h), \quad \forall v_h \in V_h^0, \quad (3.4)$$

where

$$\begin{aligned} a_h(w_h, v_h) := & \sum_{i=0}^N \int_{\Omega_i} \nabla w_i \cdot \nabla v_i - \sum_{i=1}^N \sum_{j=0}^{i-1} \int_{\Gamma_{ij}} \left(\langle \frac{\partial w_h}{\partial n} \rangle_t [v_h] + [w_h] \langle \frac{\partial v_h}{\partial n} \rangle_t \right) \\ & + \beta \sum_{i=1}^N \sum_{j=0}^{i-1} \int_{\Gamma_{ij}} h^{-1} [w_h] [v_h], \end{aligned} \quad (3.5)$$

with $t \in \{\frac{1}{2}, 1\}$, and

$$F_h(v_h) := \sum_{i=0}^N \int_{\Omega_i} f v_i + \int_{\Gamma_N} g_N v_h.$$

Note that $\beta > 0$ is a penalty parameter related to the spline degree, and its specific choice will be discussed in Section 3.4.

Proposition 3.2.3. *The discrete variational formulation in equation (3.4) is consistent, i.e., the solution u of the problem (3.1) satisfies problem (3.4) as well.*

Proof. The proof is quite classical. See for instance [18, 71]. □

3.2.2 Quasi-interpolation strategy

Before analyzing problem (3.4), we need some technical results. First, we generalize the interpolation strategy employed in [33] and in Chapter 2. Given a Sobolev function living in the whole physical domain Ω , we consider its restrictions to the predomains Ω_i^* in order to be able to interpolate on each premesh \mathcal{M}_i^* , restrict them in their turn to the visible parts Ω_i , and finally glue together the interpolated functions.

We construct a spline quasi-interpolant operator for each local space $V_{h,i}$. Given $m \geq 1$ and $v \in H^m(\Omega)$, for every $i \in \{0, \dots, N\}$, we define

$$\Pi_h^i : H^m(\Omega_i) \rightarrow V_{h,i}, \quad v \mapsto \Pi_h^{i,*} \left(v \Big|_{\Omega_i^*} \right) \Big|_{\Omega_i},$$

where $\Pi_h^{i,*} : H^m(\Omega_i^*) \rightarrow V_{h,i}^*$ is a standard quasi-interpolation operator [19]. Then, we glue together the local operators as

$$\Pi_h : H^m(\Omega) \rightarrow V_h, \quad v \mapsto \bigoplus_{i=0}^N \Pi_h^i(v_i),$$

where $v_i(x) := v(x)$ for every $x \in \Omega_i$, $i = 0, \dots, N$.

Theorem 3.2.4 (Interpolation error estimate). *There exists $C > 0$ such that, for every $v \in H^m(\Omega)$ with $m \geq 1$,*

$$\|v - \Pi_h v\|_{1,h} \leq Ch^s \|v\|_{H^m(\Omega)},$$

where $s := \min\{p, m - 1\}$.

Proof. The proof is rather standard and we omit it. □

3.2.3 Minimal stabilization procedure

It has been shown in Chapter 2 that problem (3.4), in the case of only one cut subdomain, may suffer from instability due to the evaluation of the normal derivatives in bad cut elements. In the two-patch situation, such as in Figure 3.3(a), we do not have the instability issue as soon as we are using the one-sided flux from top elements that are not cut. However, we do have this issue in general cases with many patches; see Figure 3.3(b), where the one-sided flux regarding the interface Γ_{ij} may come from the red element, a, possibly bad, cut element. In this regard, the stabilization technique introduced in Chapter 2 (specifically, the stabilization in the physical domain) needs to be accommodated in the context of multipatches that overlap. For each extended Bézier mesh \mathcal{M}_i , $i = 0, \dots, N$, we partition its elements into two disjoint sub-families.

Definition 3.2.5. Fix $\theta \in (0, 1]$, the *area-ratio threshold*. For every $K \in \mathcal{M}_i$, $i = 0, \dots, N$, we say that K is a *good element* if

$$\frac{|\Omega_i \cap K|}{|K|} \geq \theta.$$

Otherwise, K is a *bad element*.

We denote as \mathcal{M}_i^g and \mathcal{M}_i^b the collection of good and bad physical Bézier elements, respectively. Note that all the uncut elements in \mathcal{M}_i are good elements, and all its bad elements are cut elements. Moreover, it holds $\mathcal{M}_N^g = \mathcal{M}_N$ and $\mathcal{M}_N^b = \emptyset$.

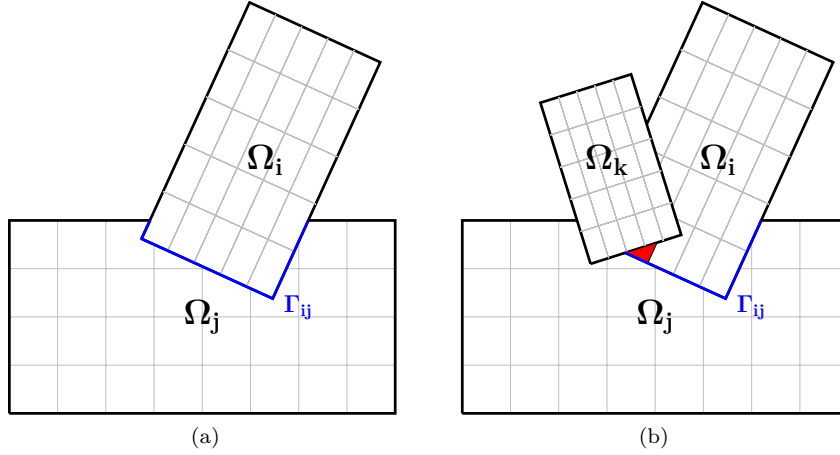


Figure 3.3 – Two-patch and three-patch overlapping along the interface Γ_{ij} .

Definition 3.2.6. Given $K \in \mathcal{M}_i$, $i = 0, \dots, N-1$, the set of its *neighbors* is

$$\mathcal{N}(K) := \{K' \in \mathcal{M}_k : \text{dist}(K, K') \leq Ch|_K, k = 0, 1, \dots, N\} \setminus \{K\}, \quad (3.6)$$

where $C > 0$ does not depend on the mesh sizes.

Next, for each bad cut element $K \in \mathcal{M}_i^b$, $0 \leq i < N$, we want to associate a *good neighbor* K' (a neighbor that is a good element). Note that in principle we allow $K' \in \mathcal{M}_k$ with $i \neq k$, *i.e.*, a good neighbor can belong to the mesh of another domain. For every $K \in \mathcal{M}_i^b$, $0 \leq i < N$, its associated good neighbor K' is chosen according to the procedure in Algorithm 1.

Algorithm 1: Find good neighbor

```

Given  $K \in \mathcal{M}_i^b$ ,  $0 \leq i < N$ ;
for  $k = i, \dots, N$  do
    if  $\mathcal{N}(K) \cap \mathcal{M}_k^g \neq \emptyset$  then
         $K' \leftarrow$  any element of  $\mathcal{N}(K) \cap \mathcal{M}_k^g$ ;
        break
    end
end
return  $K'$ ;

```

If Algorithm 1 does not produce any output, then it suffices to relax the definition of the good neighbor by taking a larger constant C in Definition 3.2.6. Figure 3.4 shows two choices of good neighbor. In Figure 3.4(b) there is clearly no neighbor of K in \mathcal{M}_1^g , and the algorithm chooses it in \mathcal{M}_2^g . Let us quantify through some suitable constants how many times any element can be chosen as a good neighbor. Some of the estimates derived in the sequel will depend upon these quantities.

Definition 3.2.7. Let $K \in \mathcal{M}_k$, $0 \leq i \leq N$.

$$\mathfrak{C}_{i,k}(K) := \#\{\check{K} \in \mathcal{M}_i : K \in \mathcal{N}(\check{K})\}$$

gives an upper bound for the number of times K can be chosen as a good neighbor from any element of the i -th mesh. Similarly, $\mathfrak{C}_{i,k} := \max_{K \in \mathcal{M}_k} \mathfrak{C}_{i,k}(K)$ is an upper bound for the number of times any element of the k -th mesh can be chosen as good neighbor from any element of the

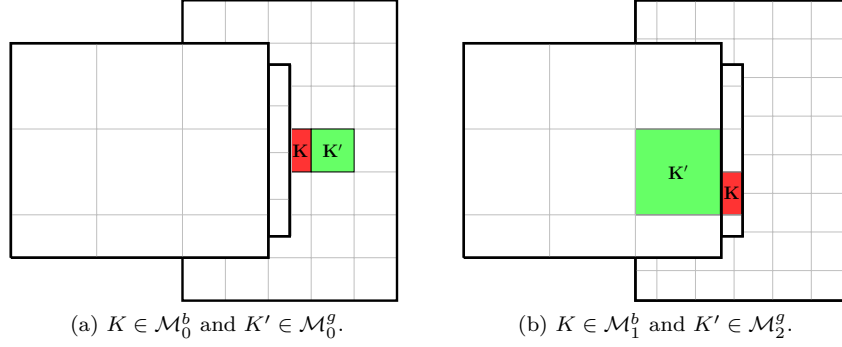


Figure 3.4 – The good neighbor K' located in the same domain as K (a), and in a different (top) domain (b).

i -th mesh. Then, $\mathfrak{C}_k := \sum_{i=0}^k \mathfrak{C}_{i,k}$ is an upper bound for the number of times any element of the k -th mesh can be chosen as good neighbor. Finally, $\mathfrak{C} := \max_{0 \leq k \leq N} \mathfrak{C}_k$ is an upper bound for the number of times any element can be chosen as good neighbor from any other element.

Remark 3.2.8. The constants introduced in Definition 3.2.7 depend on the constant C appearing in Definition 3.2.6. Moreover, the fact that all the meshes are shape-regular and have compatible sizes, namely Assumption 3.1.4, implies that \mathfrak{C} is uniformly bounded with respect to h .

For $0 \leq j < i \leq N$, $\ell \in \{i, j\}$, let us define $R_\ell : V_h \rightarrow L^2(\Gamma_{ij})$ locally. For every $K \in \mathcal{M}_\ell$ such that $\bar{\Gamma}_{ij} \cap \bar{K} = \bar{\gamma}$, $\gamma \neq \emptyset$, we distinguish two cases:

- if $K \in \mathcal{M}_\ell^g$, then

$$R_\ell(v_h)|_\gamma := \frac{\partial v_\ell}{\partial n_\ell}|_\gamma,$$

- if $K \in \mathcal{M}_\ell^b$, $K' \in \mathcal{M}_k^g$, $0 \leq \ell \leq k \leq N$ its good neighbor, then

$$R_\ell(v_h)|_\gamma := \frac{\partial \mathcal{E}_{K',K} \left(\Pi_{K'} \left(v_k|_{K'} \right) \right)}{\partial n_\ell}|_\gamma,$$

where $\Pi_{K'} : L^2(K') \rightarrow \mathbb{Q}_p(K')$ is the L^2 -orthogonal projection onto $\mathbb{Q}_p(K')$ and $\mathcal{E}_{K',K} : \mathbb{Q}_p(K') \rightarrow \mathbb{Q}_p(K' \cup K)$ is the canonical polynomial extension.

Let us denote, for $0 \leq j < i \leq N$ such that $\Gamma_{ij} \neq \emptyset$ and $t \in \{\frac{1}{2}, 1\}$,

$$\langle R_{ij}(v_h) \rangle_t := t R_i(v_h)|_{\Gamma_{ij}} + (1-t) R_j(v_h)|_{\Gamma_{ij}}. \quad (3.7)$$

In what follows we prove two main results on the operators R_ℓ (using the same strategies employed in Chapter 2).

Lemma 3.2.9 (Stability property). *Given $\theta \in (0, 1]$, there exists $C_S > 0$ such that for every $v_h \in V_h$, $0 \leq j < i \leq N$, $K \in \mathcal{M}_\ell$, $\ell \in \{i, j\}$, we have*

$$\left\| h_\ell^{\frac{1}{2}} R_\ell(v_h) \right\|_{L^2(\Gamma_{ij} \cap \bar{K})} \leq C_S \|\nabla v_k\|_{L^2(\Omega_k \cap K')},$$

where $K' \in \mathcal{M}_k^g$ is a good neighbor if $K \in \mathcal{M}_\ell^b$, $K' = K$ if $K \in \mathcal{M}_\ell^g$.

Chapter 3. Stabilized isogeometric discretization of the Poisson problem on union geometries

Proof. Let us restrict to the case $K \in \mathcal{M}_\ell^b$ with K' is a good neighbor. We apply, respectively, Hölder inequality, Remark 3.1.6, Lemmas A.1.4, A.1.5, and the H^1 -stability of the L^2 -projection [24].

$$\begin{aligned}
\left\| h_\ell^{\frac{1}{2}} R_\ell(v_h) \right\|_{L^2(\Gamma_{ij} \cap \bar{K})} &= \left\| h_\ell^{\frac{1}{2}} \frac{\partial}{\partial n_\ell} \mathcal{E}_{K',K} \left(\Pi_{K'} \left(v_h|_{K'} \right) \right) \right\|_{L^2(\Gamma_{ij} \cap \bar{K})} \\
&\leq |\Gamma_{ij} \cap \bar{K}|^{\frac{1}{2}} \left\| h_\ell^{\frac{1}{2}} \frac{\partial}{\partial n_\ell} \mathcal{E}_{K',K} \left(\Pi_{K'} \left(v_h|_{K'} \right) \right) \right\|_{L^\infty(\Gamma_{ij} \cap \bar{K})} \\
&\leq Ch_i^{\frac{d-1}{2}} \left\| h_\ell^{\frac{1}{2}} \right\|_K \left\| \nabla \mathcal{E}_{K',K} \left(\Pi_{K'} \left(v_h|_{K'} \right) \right) \right\|_{L^\infty(K)} \\
&\leq Ch_\ell^{\frac{d}{2}} \left\| \nabla \Pi_{K'} \left(v_h|_{K'} \right) \right\|_{L^\infty(K')} \\
&\leq C \left\| \nabla \Pi_{K'} \left(v_k|_{K'} \right) \right\|_{L^2(\Omega_k \cap K')} \leq C \left\| \nabla v_k \right\|_{L^2(K')}.
\end{aligned}$$

Now, let us use the equivalence of norms between parametric and physical spaces, the Hölder inequality, Lemma A.1.5, and again the norm equivalence between parametric and physical spaces. We have, for $\hat{v}_k := v_h \circ \mathbf{F}_k$ and $Q' := \mathbf{F}_k^{-1}(K')$,

$$\begin{aligned}
\left\| h_\ell^{\frac{1}{2}} R_\ell(v_h) \right\|_{L^2(\Gamma_{ij} \cap \bar{K})} &\leq C \left\| \nabla \hat{v}_k \right\|_{L^2(Q')} \leq Ch^{\frac{d}{2}} \left\| \nabla \hat{v}_k \right\|_{L^\infty(Q')} \\
&\leq C \left\| \nabla \hat{v}_k \right\|_{L^2(\hat{\Omega} \cap Q')} \leq C \left\| \nabla v_k \right\|_{L^2(\Omega_k \cap K')},
\end{aligned}$$

where C depends on θ through Lemma A.1.5. Moreover, we observe that the local quasi-uniformity, consequence of Assumption 3.1.4 itself has been employed as well. \square

Proposition 3.2.10. *There exists $C > 0$, depending on N_Γ and \mathfrak{C} , such that for every $v_h \in V_h$, we have*

$$\sum_{i=1}^N \sum_{j=0}^{i-1} \left\| h^{\frac{1}{2}} \langle R_{ij}(v_h) \rangle_t \right\|_{L^2(\Gamma_{ij})}^2 \leq C \sum_{i=0}^N \left\| \nabla v_i \right\|_{L^2(\Omega_i)}^2.$$

Proof. Young's inequality entails

$$\begin{aligned}
\sum_{i=1}^N \sum_{j=0}^{i-1} \left\| h^{\frac{1}{2}} \langle R_{ij}(v_h) \rangle_t \right\|_{L^2(\Gamma_{ij})}^2 &\leq 2t^2 \sum_{i=1}^N \sum_{j=0}^{i-1} \left\| h_i^{\frac{1}{2}} R_i(v_h) \right\|_{L^2(\Gamma_{ij})}^2 + 2(1-t)^2 \sum_{i=1}^N \sum_{j=0}^{i-1} \left\| h_j^{\frac{1}{2}} R_j(v_h) \right\|_{L^2(\Gamma_{ij})}^2 \\
&\leq 2t^2 \underbrace{\sum_{i=1}^N \sum_{j=0}^{i-1} \delta_{ij} \sum_{\substack{\Gamma_{ij} \cap \bar{K} \neq \emptyset \\ K \in \mathcal{M}_i}} \left\| h_i^{\frac{1}{2}} R_i(v_h) \right\|_{L^2(\Gamma_{ij} \cap \bar{K})}^2}_I \\
&\quad + 2(1-t)^2 \underbrace{\sum_{i=1}^N \sum_{j=0}^{i-1} \delta_{ij} \sum_{\substack{\Gamma_{ij} \cap \bar{K} \neq \emptyset \\ K \in \mathcal{M}_j}} \left\| h_j^{\frac{1}{2}} R_j(v_h) \right\|_{L^2(\Gamma_{ij} \cap \bar{K})}^2}_{II}.
\end{aligned} \tag{3.8}$$

In the following lines we will use Lemma 3.2.9 and the constants introduced in Definitions 3.1.2,

and 3.2.7. Let us focus on I , when the elements are in \mathcal{M}_i^g . We have

$$\begin{aligned}
 \sum_{i=1}^N \sum_{j=0}^{i-1} \delta_{ij} \sum_{\substack{\Gamma_{ij} \cap \bar{K} \neq \emptyset \\ K \in \mathcal{M}_i^g}} \left\| h_i^{\frac{1}{2}} R_i(v_h) \right\|_{L^2(\Gamma_{ij} \cap \bar{K})}^2 &\leq C_S^2 \sum_{i=1}^N \sum_{j=0}^{i-1} \delta_{ij} \sum_{\substack{\Gamma_{ij} \cap \bar{K} \neq \emptyset \\ K \in \mathcal{M}_i^g}} \|\nabla v_i\|_{L^2(\Omega_i \cap K)}^2 \\
 &\leq C_S^2 \sum_{i=1}^N \sum_{j=0}^{i-1} \delta_{ij} \|\nabla v_i\|_{L^2(\Omega_i)}^2 \\
 &\leq C_S^2 \left(\max_{1 \leq i \leq N} \sum_{j=0}^{i-1} \delta_{ij} \right) \sum_{i=1}^N \|\nabla v_i\|_{L^2(\Omega_i)}^2 \\
 &= C_S^2 N_\Gamma^\downarrow \sum_{i=1}^N \|\nabla v_i\|_{L^2(\Omega_i)}^2.
 \end{aligned}$$

For the bad elements in \mathcal{M}_i^b , we have

$$\begin{aligned}
 \sum_{i=1}^N \sum_{j=0}^{i-1} \delta_{ij} \sum_{\substack{\Gamma_{ij} \cap \bar{K} \neq \emptyset \\ K \in \mathcal{M}_i^b}} \left\| h_i^{\frac{1}{2}} R_i(v_h) \right\|_{L^2(\Gamma_{ij} \cap \bar{K})}^2 &\leq C_S^2 \sum_{i=1}^N \sum_{j=0}^{i-1} \delta_{ij} \sum_{\substack{\Gamma_{ij} \cap \bar{K} \neq \emptyset \\ K \in \mathcal{M}_i^b}} \|\nabla v_k\|_{L^2(\Omega_k \cap K')}^2 \\
 &\leq C_S^2 \sum_{k=1}^N \sum_{i=1}^k \mathfrak{C}_{i,k} \|\nabla v_k\|_{L^2(\Omega_k)}^2 \sum_{j=0}^{i-1} \delta_{ij} \\
 &\leq C_S^2 \left(\max_{1 \leq i \leq N} \sum_{j=0}^{i-1} \delta_{ij} \right) \sum_{k=1}^N \|\nabla v_k\|_{L^2(\Omega_k)}^2 \sum_{i=1}^k \mathfrak{C}_{i,k} \\
 &\leq C_S^2 N_\Gamma^\downarrow \mathfrak{C} \sum_{k=1}^N \|\nabla v_k\|_{L^2(\Omega_k)}^2.
 \end{aligned}$$

Let us move to II and consider elements in \mathcal{M}_j^g . It holds

$$\begin{aligned}
 \sum_{i=1}^N \sum_{j=0}^{i-1} \delta_{ij} \sum_{\substack{\Gamma_{ij} \cap \bar{K} \neq \emptyset \\ K \in \mathcal{M}_j^g}} \left\| h_j^{\frac{1}{2}} R_j(v_h) \right\|_{L^2(\Gamma_{ij} \cap \bar{K})}^2 &\leq C_S^2 \sum_{i=1}^N \sum_{j=0}^{i-1} \delta_{ij} \sum_{\substack{\Gamma_{ij} \cap \bar{K} \neq \emptyset \\ K \in \mathcal{M}_j^g}} \|\nabla v_j\|_{L^2(\Omega_j \cap K)}^2 \\
 &\leq C_S^2 \sum_{i=1}^N \sum_{j=0}^{i-1} \delta_{ij} \|\nabla v_j\|_{L^2(\Omega_j)}^2 \\
 &\leq C_S^2 \sum_{i=1}^N \sum_{j=0}^N \delta_{ij} \|\nabla v_j\|_{L^2(\Omega_j)}^2 \\
 &\leq C_S^2 \left(\max_{0 \leq j \leq N-1} \sum_{i=j+1}^N \delta_{ij} \right) \sum_{j=0}^N \|\nabla v_j\|_{L^2(\Omega_j)}^2 \\
 &= C_S^2 N_\Gamma^\uparrow \sum_{j=0}^N \|\nabla v_j\|_{L^2(\Omega_j)}^2.
 \end{aligned}$$

For the bad elements in \mathcal{M}_j^b , it holds

$$\begin{aligned}
\sum_{i=1}^N \sum_{j=0}^{i-1} \delta_{ij} \sum_{\substack{\Gamma_{ij} \cap \bar{K} \neq \emptyset \\ K \in \mathcal{M}_j^b}} \left\| h_j^{\frac{1}{2}} R_j(v_h) \right\|_{L^2(\Gamma_{ij} \cap \bar{K})}^2 &\leq C_S^2 \sum_{i=1}^N \sum_{j=0}^{i-1} \delta_{ij} \sum_{\substack{\Gamma_{ij} \cap \bar{K} \neq \emptyset \\ K \in \mathcal{M}_j^b}} \|\nabla v_k\|_{L^2(\Omega_k \cap K')}^2 \\
&\leq C_S^2 \sum_{k=0}^N \sum_{j=0}^k \mathfrak{C}_{j,k} \|\nabla v_k\|_{L^2(\Omega_k)}^2 \sum_{i=j+1}^N \delta_{ij} \\
&\leq C_S^2 \left(\max_{0 \leq j \leq N-1} \sum_{i=j+1}^N \delta_{ij} \right) \sum_{k=0}^N \|\nabla v_k\|_{L^2(\Omega_k)}^2 \sum_{j=0}^k \mathfrak{C}_{j,k} \\
&\leq C_S^2 N_\Gamma^\uparrow \max_{0 \leq k \leq N} \mathfrak{C}_k \sum_{k=0}^N \|\nabla v_k\|_{L^2(\Omega_k)}^2 \\
&= C_S^2 N_\Gamma^\uparrow \mathfrak{C} \sum_{k=0}^N \|\nabla v_k\|_{L^2(\Omega_k)}^2.
\end{aligned}$$

Hence, coming back to (3.8), we get

$$\sum_{i=1}^N \sum_{j=0}^{i-1} \left\| h_j^{\frac{1}{2}} \langle R_{ij}(v_h) \rangle_t \right\|_{L^2(\Gamma_{ij})}^2 \leq C \sum_{i=0}^N \|\nabla v_i\|_{L^2(\Omega_i)}^2,$$

where C depends, in particular, on N_Γ and on \mathfrak{C} . \square

In the sequel $E : H^m(\Omega) \rightarrow \mathbb{R}^d$, $m \geq 1$, will denote the Sobolev-Stein extension operator (see Section 3.2 in [104]).

Lemma 3.2.11 (Approximation property). *There exists $C_A > 0$ such that for every $v \in H^m(\Omega)$, $m \geq 2$, $0 \leq j < i \leq N$, $K \in \mathcal{M}_\ell$, $\ell \in \{i, j\}$, it holds*

$$\left\| h_\ell^{\frac{1}{2}} \left(R_\ell(\Pi_h(v)) - \frac{\partial v_\ell}{\partial n_\ell} \right) \right\|_{L^2(\Gamma_{ij} \cap \bar{K})} \leq C_A h^s \left(\|v\|_{H^m(\tilde{K}')} + \|E(v)\|_{H^m(B_K)} \right),$$

where K' is a good neighbor if $K \in \mathcal{M}_\ell^b$, $K' = K$ if $K \in \mathcal{M}_\ell^g$, B_K is the minimal bounding box enclosing K and K' , $s := \min\{p, m-1\}$.

Proof. Again, let us restrict ourselves to the case where $K \in \mathcal{M}_\ell^b$, with K' its good neighbor, and take $q \in \mathbb{Q}_p(B_K)$, where B_K is the minimal bounding box enclosing K and K' .

$$\begin{aligned}
&\left\| h_\ell^{\frac{1}{2}} \left(R_\ell(\Pi_h v) - \frac{\partial v_\ell}{\partial n_\ell} \right) \right\|_{L^2(\Gamma_{ij} \cap \bar{K})} \\
&\leq \underbrace{\left\| h_\ell^{\frac{1}{2}} \left(R_\ell(\Pi_h v) - \frac{\partial q}{\partial n_\ell} \right) \right\|_{L^2(\Gamma_{ij} \cap \bar{K})}}_{\text{I}} + \underbrace{\left\| h_\ell^{\frac{1}{2}} \frac{\partial}{\partial n_\ell} (q - v_\ell) \right\|_{L^2(\Gamma_{ij} \cap \bar{K})}}_{\text{II}}.
\end{aligned}$$

Let us focus on I. We note that $R_\ell(q) = \frac{\partial q}{\partial n_\ell}$, then apply Lemma 3.2.9 and the triangular inequality:

$$\begin{aligned}
\text{I} &= \left\| h_\ell^{\frac{1}{2}} (R_\ell(\Pi_h v - q)) \right\|_{L^2(\Gamma_{ij} \cap \bar{K})} \leq C_S \|\nabla(\Pi_h^k v_k - q)\|_{L^2(\Omega_k \cap K')} \\
&\leq C_S \left(\|\nabla(\Pi_h^k v_k - v_k)\|_{L^2(\Omega_k \cap K')} + \|\nabla(v_k - q)\|_{L^2(\Omega_k \cap K')} \right).
\end{aligned}$$

We employ the approximation properties of Π_h^k (Theorem 2.3.8) and the standard Deny-Lions Lemma on B_K (Theorem 3.4.1 of [112]):

$$I \leq Ch^s \left(\|v\|_{H^m(\tilde{K}')} + \|E(v)\|_{H^m(B_K)} \right),$$

where $s := \min\{p, m-1\}$ and C depends on the shape-regularity of B_K , see Remark 3.2.12. I can be estimated by using Corollary A.1.3 and Theorem 3.4.1 of [112] as follows:

$$\begin{aligned} \Pi^2 &= \left\| h_\ell^{\frac{1}{2}} \frac{\partial}{\partial n_\ell} (q - v_\ell) \right\|_{L^2(\Gamma_{ij} \cap \bar{K})}^2 \\ &\leq C \left\| h_\ell^{\frac{1}{2}} \nabla (q - E(v)) \right\|_{L^2(K)} \left\| h_\ell^{\frac{1}{2}} \nabla (q - E(v)) \right\|_{H^1(K)} \\ &\leq Ch_\ell^{2s} \left\| E(v) \right\|_{H^m(B_K)}^2, \end{aligned}$$

with $s := \min\{p, m-1\}$ and C depending on the shape-regularity of B_K . Putting everything together, the proof is finished. \square

Remark 3.2.12. Let $N_K := \#\{K^* \in \mathcal{M}_i : K^* \cap B_K \neq \emptyset, 0 \leq i \leq N\}$, given $K \in \mathcal{M}_\ell$. We observe that N_K depends on C appearing in Definition 3.2.6 and on the space dimension d . It is uniformly bounded with respect to h thanks to Assumption 3.1.4. As in Remark 3.2.8, we deduce that the number of times any element can be chosen as member of a minimal bounding box is uniformly bounded with respect to h . Moreover, given $\rho_{B_K} := \sup\{\text{diam}(B) : B \text{ is a ball contained in } B_K\}$ and $h_{B_K} := \text{diam}(B_K)$, the geometric quantity $\frac{h_{B_K}}{\rho_{B_K}} \sim \frac{h}{\rho_{B_K}}$ is also uniformly bounded with respect to $K \in \mathcal{M}_\ell$.

Proposition 3.2.13. *There exists $C > 0$, depending on N_Γ , $N_\mathcal{O}$, and \mathfrak{C} , such that, for every $v \in H^m(\Omega)$, $m \geq 2$, we have*

$$\sum_{i=1}^N \sum_{j=0}^{i-1} \left\| h_i^{\frac{1}{2}} \langle R_{ij}(\Pi_h(v)) - \frac{\partial v}{\partial n} \rangle_t \right\|_{L^2(\Gamma_{ij})}^2 \leq Ch^{2s} \|v\|_{H^m(\Omega)}^2,$$

where $s := \min\{p, m-1\}$.

Proof. The triangular and Young's inequality entail

$$\begin{aligned} \sum_{i=1}^N \sum_{j=0}^{i-1} \left\| h_i^{\frac{1}{2}} \langle R_{ij}(\Pi_h(v)) - \frac{\partial v}{\partial n} \rangle_t \right\|_{L^2(\Gamma_{ij})}^2 &\leq 2t^2 \sum_{i=1}^N \sum_{j=0}^{i-1} \left\| h_i^{\frac{1}{2}} \left(R_i(\Pi_h(v)) - \frac{\partial v_i}{\partial n_i} \right) \right\|_{L^2(\Gamma_{ij})}^2 \\ &\quad + 2(1-t)^2 \sum_{i=1}^N \sum_{j=0}^{i-1} \left\| h_j^{\frac{1}{2}} \left(R_j(\Pi_h(v)) - \frac{\partial v_j}{\partial n_j} \right) \right\|_{L^2(\Gamma_{ij})}^2 \end{aligned} \tag{3.9}$$

By using Lemma 3.2.11, and recalling Definition 3.1.2,

$$\begin{aligned} \sum_{i=1}^N \sum_{j=0}^{i-1} \left\| h_i^{\frac{1}{2}} \left(R_i(\Pi_h(v)) - \frac{\partial v_i}{\partial n_i} \right) \right\|_{L^2(\Gamma_{ij})}^2 &= \sum_{i=1}^N \sum_{j=0}^{i-1} \delta_{ij} \sum_{\substack{\Gamma_{ij} \cap \bar{K} \neq \emptyset \\ K \in \mathcal{M}_i}} \left\| h_i^{\frac{1}{2}} \left(R_i(\Pi_h(v)) - \frac{\partial v_i}{\partial n_i} \right) \right\|_{L^2(\Gamma_{ij} \cap \bar{K})}^2 \\ &\leq 2C_A^2 h^{2s} \max_{1 \leq i \leq N} \sum_{i=1}^N \sum_{j=0}^{i-1} \delta_{ij} \sum_{\substack{\Gamma_{ij} \cap \bar{K} \neq \emptyset \\ K \in \mathcal{M}_i}} \left(\|E(v)\|_{H^m(B_K)}^2 + \|v\|_{H^m(\tilde{K}')}^2 \right), \end{aligned}$$

Chapter 3. Stabilized isogeometric discretization of the Poisson problem on union geometries

where the factor 2 comes from the inequality $(a+b)^2 \leq 2(a^2 + b^2)$, $a, b \in \mathbb{R}$. Without loss of generality, let us focus on elements in \mathcal{M}_i^b . We have

$$\begin{aligned} & \sum_{i=1}^N \sum_{j=0}^{i-1} \delta_{ij} \sum_{\substack{\Gamma_{ij} \cap \bar{K} \neq \emptyset \\ K \in \mathcal{M}_i^b}} \left\| \mathbf{h}_i^{\frac{1}{2}} \left(R_i(\Pi_h(v)) - \frac{\partial v_i}{\partial n_i} \right) \right\|_{L^2(\Gamma_{ij} \cap \bar{K})}^2 \\ & \leq 2C_A^2 h^{2s} \sum_{i=1}^N \sum_{j=0}^{i-1} \delta_{ij} \sum_{\substack{\Gamma_{ij} \cap \bar{K} \neq \emptyset \\ K \in \mathcal{M}_i^b}} \|E(v)\|_{H^m(B_K)}^2 + 2C_A^2 h^{2s} \sum_{i=1}^N \sum_{j=0}^{i-1} \delta_{ij} \sum_{\substack{\Gamma_{ij} \cap \bar{K} \neq \emptyset \\ K \in \mathcal{M}_i^b}} \|v\|_{H^m(\tilde{K}')}^2 \\ & \leq 2CN_\Gamma^\downarrow C_A^2 h^{2s} \|v\|_{H^m(\Omega)}^2, \end{aligned}$$

where $s := \min\{p, m-1\}$. Here, C depends on $d, p, N_\mathcal{O}, \mathfrak{C}, \mathbf{F}$, on the constants in Assumption 3.1.4, on the fact that the bounding boxes overlap a finite number of times (see Remark 3.2.12), and on the boundedness of the Sobolev-Stein extension. Similarly, it holds

$$\begin{aligned} & \sum_{i=1}^N \sum_{j=0}^{i-1} \left\| \mathbf{h}_j^{\frac{1}{2}} \left(R_j(\Pi_h(v)) - \frac{\partial v_j}{\partial n_j} \right) \right\|_{L^2(\Gamma_{ij})}^2 = \sum_{i=1}^N \sum_{j=0}^{i-1} \delta_{ij} \sum_{\substack{\Gamma_{ij} \cap \bar{K} \neq \emptyset \\ K \in \mathcal{M}_j}} \left\| \mathbf{h}_j^{\frac{1}{2}} \left(R_j(\Pi_h(v)) - \frac{\partial v_j}{\partial n_j} \right) \right\|_{L^2(\Gamma_{ij} \cap \bar{K})}^2 \\ & \leq 2C_A^2 h^{2s} \max_{1 \leq i \leq N} \sum_{i=1}^N \sum_{j=0}^{i-1} \delta_{ij} \sum_{\substack{\Gamma_{ij} \cap \bar{K} \neq \emptyset \\ K \in \mathcal{M}_j}} \left(\|E(v)\|_{H^m(B_K)}^2 + \|v\|_{H^m(\tilde{K}')}^2 \right). \end{aligned}$$

Again, without loss of generality, we focus on elements in \mathcal{M}_j^b :

$$\begin{aligned} & \sum_{i=1}^N \sum_{j=0}^{i-1} \delta_{ij} \sum_{\substack{\Gamma_{ij} \cap \bar{K} \neq \emptyset \\ K \in \mathcal{M}_j^b}} \left\| \mathbf{h}_j^{\frac{1}{2}} \left(R_j(\Pi_h(v)) - \frac{\partial v_j}{\partial n_j} \right) \right\|_{L^2(\Gamma_{ij} \cap \bar{K})}^2 \\ & \leq 2C_A^2 h^{2s} \sum_{i=1}^N \sum_{j=0}^{i-1} \delta_{ij} \sum_{\substack{\Gamma_{ij} \cap \bar{K} \neq \emptyset \\ K \in \mathcal{M}_j^b}} \|E(v)\|_{H^m(B_K)}^2 + 2C_A^2 h^{2s} \sum_{i=1}^N \sum_{j=0}^{i-1} \delta_{ij} \sum_{\substack{\Gamma_{ij} \cap \bar{K} \neq \emptyset \\ K \in \mathcal{M}_j^b}} \|v\|_{H^m(\tilde{K}')}^2 \\ & \leq 2CC_A^2 N_\Gamma^\uparrow h^{2s} \|v\|_{H^m(\Omega)}^2, \end{aligned}$$

where $s := \min\{p, m-1\}$, C has the same dependencies as above. We conclude by putting everything together. \square

We propose the following stabilized weak formulation.

Find $u_h \in V_h^{gD}$ such that

$$\bar{a}_h(u_h, v_h) = F_h(v_h), \quad \forall v_h \in V_h^0. \quad (3.10)$$

Here, the bilinear form is defined, for $t \in \{\frac{1}{2}, 1\}$, as

$$\begin{aligned} \bar{a}_h(w_h, v_h) &:= \sum_{i=0}^N \int_{\Omega_i} \nabla w_i \cdot \nabla v_i - \sum_{i=1}^N \sum_{j=0}^{i-1} \int_{\Gamma_{ij}} (\langle R_{ij}(w_h) \rangle_t [v_h] + [w_h] \langle R_{ij}(v_h) \rangle_t) \\ & \quad + \beta \sum_{i=1}^N \sum_{j=0}^{i-1} \int_{\Gamma_{ij}} \mathbf{h}^{-1} [w_h] [v_h], \end{aligned} \quad (3.11)$$

where $\beta > 0$ is a penalty parameter.

Remark 3.2.14. Note that, by the choice of the hierarchy of the predomains made in Section 3.1 and the definition of the global stabilization operator (3.7), the one-sided flux approximation is better than the symmetric average. It allows indeed to modify the weak formulation much less frequently.

3.2.4 Stability analysis and *a priori* error estimates

Our goal is to show that problem (3.10) is well-posed in the sense of the following definition.

Definition 3.2.15. Problem (3.10) is *stable* if, given $\theta \in (0, 1]$, there exist $\bar{\beta} > 0$ and $\alpha > 0$ such that for every $\beta \geq \bar{\beta}$, for every $h > 0$, it holds

$$\alpha \|v_h\|_{1,h,\Omega}^2 \leq \bar{a}_h(v_h, v_h), \quad \forall v_h \in V_h,$$

and for every fixed $\beta \geq \bar{\beta}$ there exists $\gamma > 0$ such that, for every $h > 0$, it holds

$$|\bar{a}_h(w_h, v_h)| \leq \gamma \|w_h\|_{1,h,\Omega} \|v_h\|_{1,h,\Omega}, \quad \forall w_h, v_h \in V_h.$$

Theorem 3.2.16. Problem (3.10) is stable in the sense of Definition 3.2.15.

Proof. Let us start with continuity. For $w_h, v_h \in V_h$, we have

$$\begin{aligned} |\bar{a}_h(w_h, v_h)| &\leq \underbrace{\sum_{i=0}^N \|\nabla w_i\|_{L^2(\Omega_i)} \|\nabla v_i\|_{L^2(\Omega_i)}}_{\text{I}} + C \underbrace{\sum_{i=1}^N \sum_{j=0}^{i-1} \left(\left\| \mathbf{h}^{\frac{1}{2}} \langle R_{ij}(w_h) \rangle_t \right\|_{L^2(\Gamma_{ij})} \left\| \mathbf{h}^{-\frac{1}{2}} [v_h] \right\|_{L^2(\Gamma_{ij})} \right)}_{\text{II}} \\ &+ \underbrace{\left\| \mathbf{h}^{-\frac{1}{2}} [w_h] \right\|_{L^2(\Gamma_{ij})} \left\| \mathbf{h}^{\frac{1}{2}} \langle R_{ij}(v_h) \rangle_t \right\|_{L^2(\Gamma_{ij})}}_{\text{III}} + \underbrace{\beta \sum_{i=1}^N \sum_{j=0}^{i-1} \left\| \mathbf{h}^{-\frac{1}{2}} [w_h] \right\|_{L^2(\Gamma_{ij})} \left\| \mathbf{h}^{-\frac{1}{2}} [v_h] \right\|_{L^2(\Gamma_{ij})}}_{\text{IV}}. \end{aligned}$$

It is straightforward to bound I and IV. We focus on II, whereas taking care of III is analogous. By using the Cauchy-Schwarz inequality and Proposition 3.2.10, we have

$$\begin{aligned} \text{II} &= \sum_{i=1}^N \sum_{j=0}^{i-1} \left\| \mathbf{h}^{\frac{1}{2}} \langle R_{ij}(w_h) \rangle_t \right\|_{L^2(\Gamma_{ij})} \left\| \mathbf{h}^{-\frac{1}{2}} [v_h] \right\|_{L^2(\Gamma_{ij})} \\ &\leq \left(\sum_{i=1}^N \sum_{j=0}^{i-1} \left\| \mathbf{h}^{\frac{1}{2}} \langle R_{ij}(w_h) \rangle_t \right\|_{L^2(\Gamma_{ij})}^2 \right)^{\frac{1}{2}} \left(\sum_{i=1}^N \sum_{j=0}^{i-1} \left\| \mathbf{h}^{-\frac{1}{2}} [v_h] \right\|_{L^2(\Gamma_{ij})}^2 \right)^{\frac{1}{2}} \\ &\leq C \left(\sum_{i=1}^N \|\nabla w_i\|_{L^2(\Omega_i)}^2 \right)^{\frac{1}{2}} \|v_h\|_{1,h} \leq C \|w_h\|_{1,h} \|v_h\|_{1,h}, \end{aligned} \tag{3.12}$$

with C depending on N_Γ and \mathfrak{C} . Hence, it holds $|\bar{a}_h(w_h, v_h)| \leq \gamma \|w_h\|_{1,h} \|v_h\|_{1,h}$, where γ depends on N_Γ and \mathfrak{C} , and it increases as N_Γ and \mathfrak{C} grow. Now, let us prove the coercivity. Given $v_h \in V_h$, it holds

$$\bar{a}_h(v_h, v_h) = \sum_{i=0}^N \|\nabla v_i\|_{L^2(\Omega_i)}^2 - 2 \sum_{i=1}^N \sum_{j=0}^{i-1} \int_{\Gamma_{ij}} \langle R_{ij}(v_h) \rangle_t [v_h] + \beta \sum_{i=1}^N \sum_{j=0}^{i-1} \left\| \mathbf{h}^{-1} [v_h] \right\|_{L^2(\Gamma_{ij})}^2.$$

Chapter 3. Stabilized isogeometric discretization of the Poisson problem on union geometries

Cauchy-Schwartz's inequality, Young's inequality, and Proposition 3.2.10 imply

$$\begin{aligned} 2 \sum_{i=1}^N \sum_{j=0}^{i-1} \int_{\Gamma_{ij}} \langle R_{ij}(v_h) \rangle_t [v_h] &\leq \sum_{i=1}^N \sum_{j=0}^{i-1} \left(\frac{1}{\varepsilon} \left\| \mathbf{h}^{\frac{1}{2}} \langle R_{ij}(v_h) \rangle_t \right\|_{L^2(\Gamma_{ij})}^2 + \varepsilon \left\| \mathbf{h}^{-\frac{1}{2}} [v_h] \right\|_{L^2(\Gamma_{ij})}^2 \right) \\ &\leq \frac{C}{\varepsilon} \sum_{i=1}^N \|\nabla v_i\|_{L^2(\Omega_i)}^2 + \varepsilon \sum_{i=1}^N \sum_{j=0}^{i-1} \left\| \mathbf{h}^{-\frac{1}{2}} [v_h] \right\|_{L^2(\Gamma_{ij})}^2, \end{aligned}$$

for any $\varepsilon > 0$ and C depending on N_Γ and \mathfrak{C} . Thus,

$$\bar{a}_h(v_h, v_h) \geq \left(1 - \frac{C}{\varepsilon}\right) \sum_{i=0}^N \|\nabla v_i\|_{L^2(\Omega_i)}^2 + (\beta - \varepsilon) \sum_{i=1}^N \sum_{j=0}^{i-1} \left\| \mathbf{h}^{-1} [v_h] \right\|_{L^2(\Gamma_{ij})}^2,$$

from which we deduce coercivity provided that $C < \varepsilon < \beta$. Hence, the coercivity constant α depends on N_Γ and \mathfrak{C} , and it decreases as N_Γ and \mathfrak{C} grow. \square

Theorem 3.2.17 (*A priori error estimate*). *Let $u \in H^m(\Omega)$, $m \geq 2$, be the solution of the continuous problem (3.1) and $u_h \in V_h$ the solution of (3.10). Then, there exists $C > 0$, depending on N_Γ and \mathfrak{C} , such that*

$$\|u - u_h\|_{1,h} \leq Ch^s \|u\|_{H^m(\Omega)}, \quad (3.13)$$

where $s := \min\{p, m - 1\}$.

Proof. Let u be the solution of the strong problem (3.1), $a_h(\cdot, \cdot)$ and $\bar{a}_h(\cdot, \cdot)$ be the bilinear forms defined in (3.5) and in (3.11), respectively. The triangular inequality and the coercivity of $\bar{a}_h(\cdot, \cdot)$ entail

$$\begin{aligned} \|u - u_h\|_{1,h} &\leq \|u - v_h\|_{1,h} + \|v_h - u_h\|_{1,h} \\ &\leq \|u - v_h\|_{1,h} + \alpha^{-1} \sup_{\substack{w_h \in V_h \\ w_h \neq 0}} \frac{\bar{a}_h(v_h - u_h, w_h)}{\|w_h\|_{1,h}}, \end{aligned} \quad (3.14)$$

where $\alpha > 0$ is the coercivity constant. Recalling that u solves (3.4) and u_h solves (3.10) and properly rearranging the terms, we have

$$\begin{aligned} \bar{a}_h(v_h - u_h, w_h) &= \bar{a}_h(v_h, w_h) - \bar{a}_h(u_h, w_h) = \bar{a}_h(v_h, w_h) - a_h(u, w_h) \\ &= \sum_{i=0}^N \int_{\Omega_i} \nabla(v_i - u_i) \cdot \nabla w_i - \sum_{i=1}^N \sum_{j=0}^{i-1} \int_{\Gamma_{ij}} \left(\langle R_{ij}(v_h) - \frac{\partial u}{\partial n} \rangle_t [w_h] + \langle R_{ij}(w_h) \rangle_t [v_h] - \langle \frac{\partial w_h}{\partial n} \rangle_t [u] \right) \\ &\quad + \beta \sum_{i=1}^N \sum_{j=0}^{i-1} \int_{\Gamma_{ij}} \mathbf{h}^{-1} [v_h - u] [w_h]. \end{aligned} \quad (3.15)$$

Reminding that $[u] = 0$, we have

$$\int_{\Gamma_{ij}} \langle R_{ij}(w_h) \rangle_t [v_h] = \int_{\Gamma_{ij}} \langle R_{ij}(w_h) \rangle_t [v_h - u].$$

Hence,

$$\begin{aligned}
 \bar{a}_h(v_h - u_h, w_h) &= \underbrace{\sum_{i=0}^N \int_{\Omega_i} \nabla(v_i - u_i) \cdot \nabla w_i}_I \\
 &\quad - \underbrace{\sum_{i=1}^N \sum_{j=0}^{i-1} \int_{\Gamma_{ij}} \left(\langle R_{ij}(v_h) - \frac{\partial u}{\partial n} \rangle_t [w_h] + \langle R_{ij}(w_h) \rangle_t [v_h - u] \right)}_{\text{II} \quad \& \quad \text{III}} \\
 &\quad + \underbrace{\beta \sum_{i=1}^N \sum_{j=0}^{i-1} \int_{\Gamma_{ij}} h^{-1} [v_h - u] [w_h]}_{\text{IV}}
 \end{aligned} \tag{3.16}$$

First of all, we note that

$$I + IV \leq C \|v_h - u\|_{1,h} \|w_h\|_{1,h}. \tag{3.17}$$

Then, in order to bound III, we use Cauchy-Schwarz inequality and Proposition 3.2.10

$$\begin{aligned}
 \text{III} &\leq \sum_{i=1}^N \sum_{j=0}^{i-1} \left\| h^{\frac{1}{2}} \langle R_{ij}(w_h) \rangle_t \right\|_{L^2(\Gamma_{ij})} \left\| h^{-\frac{1}{2}} [u - v_h] \right\|_{L^2(\Gamma_{ij})} \\
 &\leq \left(\sum_{i=1}^N \sum_{j=0}^{i-1} \left\| h^{\frac{1}{2}} \langle R_{ij}(w_h) \rangle_t \right\|_{L^2(\Gamma_{ij})}^2 \right)^{\frac{1}{2}} \left(\sum_{i=1}^N \sum_{j=0}^{i-1} \left\| h^{-\frac{1}{2}} [u - v_h] \right\|_{L^2(\Gamma_{ij})}^2 \right)^{\frac{1}{2}} \\
 &\leq C \left(\sum_{i=1}^N \|\nabla w_i\|_{L^2(\Omega_i)}^2 \right)^{\frac{1}{2}} \|u - v_h\|_{1,h} \leq C \|w_h\|_{1,h} \|u - v_h\|_{1,h},
 \end{aligned} \tag{3.18}$$

with C depending on N_Γ and \mathfrak{C} . Let us choose $v_h := \Pi_h u$. By using Proposition 3.2.13 and proceeding as in (3.18), we have

$$\begin{aligned}
 \text{II} &\leq \sum_{i=1}^N \sum_{j=0}^{i-1} \left\| h^{\frac{1}{2}} \langle R_{ij}(\Pi_h u) - \frac{\partial u}{\partial n} \rangle_t \right\|_{L^2(\Gamma_{ij})} \left\| h^{-\frac{1}{2}} [w_h] \right\|_{L^2(\Gamma_{ij})} \\
 &\leq C h^s \|u\|_{H^m(\Omega)} \|w_h\|_{1,h},
 \end{aligned} \tag{3.19}$$

where $s := \min\{p, m - 1\}$ and C depends on N_Γ and \mathfrak{C} . Coming back to (3.14) and using Theorem 3.2.4, we get

$$\|u - u_h\|_{1,h} \leq (1 + \alpha^{-1} C) h^s \|u\|_{H^m(\Omega)},$$

where $s := \min\{p, m - 1\}$ and C depends on N_Γ and \mathfrak{C} . \square

Remark 3.2.18. We note that the constant C appearing in (3.13) depends on N_Γ and \mathfrak{C} , in particular it degenerates as these quantities grow. As already observed, we expect N_Γ to be small in practice. Interested readers may further refer to [79] (the accompanying work of [80]) for numerical results with a growing number of domains.

3.3 Implementation aspects of the union operation

Union, subtraction (*i.e.*, trimming), and intersection are three common Boolean operations in CAD systems. Generally speaking, subtraction and intersection can be handled in the same

manner. Given two *predomains* (Ω_0^* and Ω_1^*) in 2D, the trimmed region $\Omega_0^* \setminus \Omega_1^*$ is bounded by a set of counterclockwise-oriented curves that forms a closed *wire*. Such curves come from $\partial\Omega_0^*$ and $\partial\Omega_1^*$. The same argument applies to the intersected region $\Omega_0^* \cap \Omega_1^*$, where the difference from subtraction lies in the involved curves as well as their orientations.

On the other hand, recall that we create union by first trimming Ω_0^* with Ω_1^* , and then weakly coupling the *visible part* of Ω_0^* , *i.e.*, $\Omega_0 := \Omega_0^* \setminus \Omega_1^*$, with Ω_1^* through their interface. While the integration on cut elements has been discussed in [4] (see also [86, 114, 119]), here we focus on dealing with interfaces, which includes creating a quadrature mesh for each interface as well as stabilizing bad cut elements that are adjacent to the union interface. In what follows, we explain the related algorithms in 2D and will also comment on the extension to 3D.

3.3.1 Generation of the interface quadrature mesh

The key to creating an interface quadrature mesh is to find mesh intersections on the interface; see a 2D example in Figure 3.5. Each visible interface is shared by two patches, one on the top and the other on the bottom. Recall that we denote the interface, the top patch, and the bottom patch as Γ_{ij} , Ω_i and Ω_j ($i > j$), respectively. According to our construction of unions, Γ_{ij} is always part of the boundary of Ω_i , so its geometric mapping is the same as that of Ω_i and it naturally has the mesh information of Ω_i . Now the aim is to find out how the mesh of Ω_j intersects with Γ_{ij} . We find these intersections primarily in the parametric domain $\hat{\Omega}_j := \mathbf{F}_j^{-1}(\Omega_j)$

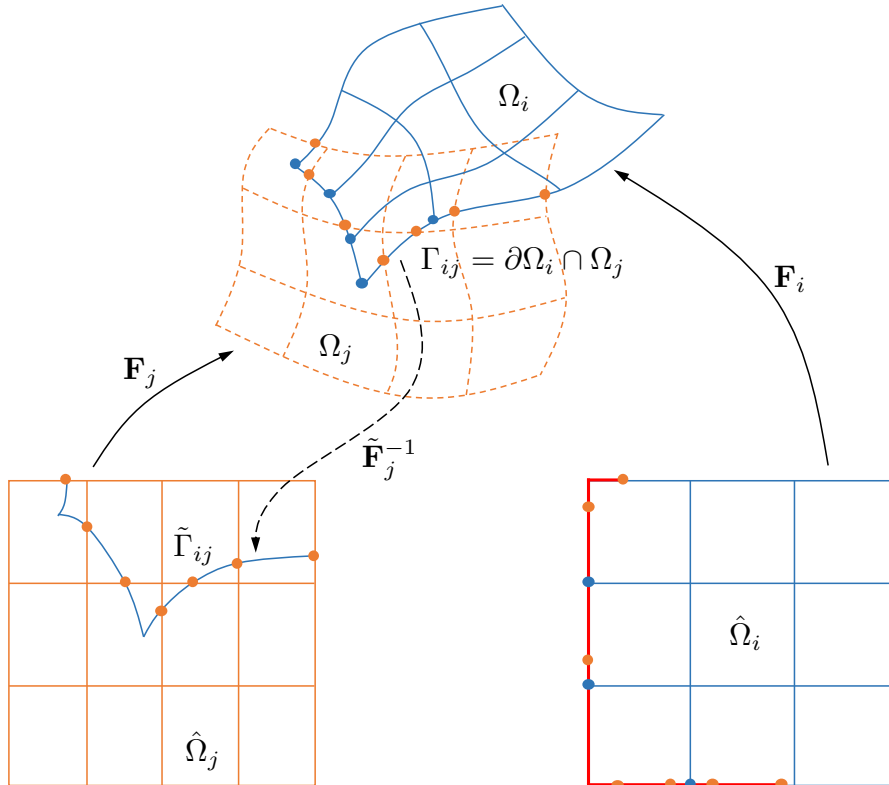


Figure 3.5 – Mesh intersections of a top patch (blue lines) and a bottom patch (orange lines) on their interface. The mesh intersections are marked in blue and orange dots. The parametric domain of the interface is marked as red lines.

3.3. Implementation aspects of the union operation

following three steps. First, we obtain an approximate preimage of Γ_{ij} with respect to $\widehat{\Omega}_j$ through the inversion algorithm (Chapter 6 of [108]), *i.e.*, $\widetilde{\Gamma}_{ij} := \widetilde{\mathbf{F}}_j^{-1}(\Gamma_{ij})$, where the tilde indicates the approximation nature of the inversion algorithm. Second, in $\widehat{\Omega}_j$ we find the intersections of $\widetilde{\Gamma}_{ij}$ with the axis-aligned knot lines of $\widehat{\Omega}_j$, which is easier compared to the general curve-curve intersection; see the bottom left figure in Figure 3.5. Third, we map these intersections to the physical domain through \mathbf{F}_j . However, the resulting points generally do not lie on Γ_{ij} , again due to the approximation of the inversion algorithm. Therefore, we further project these points onto Γ_{ij} to get the final intersections; see orange and blue dots in Figure 3.5.

With all the intersections, we are ready to create the interface quadrature mesh and compute the interface integral. We here emphasize two aspects that can improve the computation in terms of accuracy and efficiency. First, as the Nitsche method needs the normal information of Γ_{ij} , we compute it using Ω_i where the geometric information is exact. In contrast, if we compute it using Ω_j , we will lose accuracy because it relies on $\widetilde{\Gamma}_{ij}$, which is only an approximation. Second, when evaluating basis functions from Ω_j in the interface integral, it involves finding corresponding quadrature points in $\widehat{\Omega}_j$ through the approximate inverse mapping $\widetilde{\mathbf{F}}_j^{-1}$, so there is an unnecessary coupling of the geometric operation (*i.e.*, the inversion operation) and analysis. Instead, we precompute and store those quadrature points in $\widehat{\Omega}_j$ such that later analysis can be performed without repeatedly appealing to the inversion operation.

Remark 3.3.1. We use OpenCASCADE [2], an open-source CAD system, to perform geometric surface operations, including creating the union of multiple spline patches and finding the mesh intersections on each interface. To the author's knowledge, the default geometric tolerance in OpenCASCADE is around 10^{-8} in trimming-related operations and cannot be further reduced. Its influence will be seen in a numerical example in Section 3.4, where the geometric error induced by this tolerance begins to dominate once the approximation error (in L^2 norm) reaches 10^{-8} .

3.3.2 Implementation of the minimal stabilization

The minimal stabilization method introduced in Section 3.2.3 mainly needs to: (1) find a list of bad-to-good element pairs and (2) replace the basis functions of each bad element with extended polynomials from its good neighbor. In the following, we explain the procedure in 2D terminologies, but the extension to 3D is straightforward.

Simply speaking, a bad element is a cut element with a “small” effective area on which we have to compute fluxes, *i.e.*, normal derivatives at its boundary. All the other active elements are good. In practice, we compute element areas in the parametric domain and use a given threshold to identify bad elements, which serves as an approximate criterion to Definition 3.2.5. Then we follow the procedure described in Section 3.2.3.

Next, we take a look at the interface integral that contributes to the stiffness matrix. Let $\mathcal{T}(\Gamma_{ij})$ denote the quadrature mesh of the interface Γ_{ij} , and $e \in \mathcal{T}(\Gamma_{ij})$ be a quadrature element. The two elements adjacent to e are denoted as $K_i^e \in \Omega_i$ and $K_j^e \in \Omega_j$. The index set of basis functions $B_{\mathbf{k},i}$ with support on K_i^e is denoted as $I_{K_i^e}$; similarly, $I_{K_j^e}$ corresponds to K_j^e . Note that we neglect the degree information in the notation of basis functions as it is fixed. We are particularly interested in the terms involving normal derivatives, and such a term takes the following form when the one-sided flux from the top patch Ω_i is used,

$$\int_e \frac{\partial B_{\mathbf{k},i}}{\partial n_i} B_{\ell,i}, \quad \int_e \frac{\partial B_{\mathbf{k},i}}{\partial n_i} B_{\mathbf{m},j}, \quad (3.20)$$

where $\ell, \mathbf{k} \in I_{K_i^e}$, and $\mathbf{m} \in I_{K_j^e}$. The stability issue originates from $\frac{\partial B_{\ell,i}}{\partial n_i}$ if K_i^e is badly cut;

Chapter 3. Stabilized isogeometric discretization of the Poisson problem on union geometries

otherwise equation (3.20) contributes to the matrix entries corresponding to the indices (\mathbf{k}, ℓ) and (\mathbf{k}, \mathbf{m}) , respectively.

In the following, we focus on the case that K_i^e is badly cut. The minimal stabilization consists in replacing $\frac{\partial B_{\ell,i}}{\partial n_i}$ with a stabilized version that involves function extension from the good neighbor $(K_i^e)'$ of K_i^e . In other words, we need to extend basis functions defined on $(K_i^e)'$ to K_i^e and use the extended functions to evaluate the involved normal derivatives. Specifically, we follow three steps. First, we find the Cartesian bounding box $(K_i^e)'_b$ of $(K_i^e)'$ in the physical domain and define on it a set of bi-degree- p Bernstein polynomials \mathbf{b}_r , where $r \in \{1, 2, \dots, (p+1)^2\}$, and p is the degree. Second, let $I_{(K_i^e)'}$ be the index set of basis functions with support on $(K_i^e)'$, and we compute a L^2 -projection of each $B_{\mathbf{k}',i}$ ($\mathbf{k}' \in I_{(K_i^e)'}$) using these Bernstein polynomials. As a result, we have

$$\Pi_{(K_i^e)'}(B_{\mathbf{k}',i}) = \sum_{r=1}^{(p+1)^2} c_{\mathbf{k}'r} \mathbf{b}_r,$$

where $\Pi_{(K_i^e)'}$ stands for the L^2 -orthogonal projection onto $\mathbb{Q}_p((K_i^e)').$ Note that $c_{\mathbf{k}'r} \in \mathbb{R}$ are obtained by solving a local system of linear equations $\sum_{r=1}^{(p+1)^2} M_{mr} c_{\mathbf{k}'r} = F_m$ for $m = 1, \dots, (p+1)^2$, where

$$M_{mr} = \int_{(K_i^e)'} \mathbf{b}_m \mathbf{b}_r, \quad F_m = \int_{(K_i^e)'} B_{\mathbf{k}',i} \mathbf{b}_m.$$

Third, we define the extension of $B_{\mathbf{k}',i}$ to be $\Pi_{(K_i^e)'}(B_{\mathbf{k}',i})$ and enlarge the definition domain of the Bernstein polynomials by including the bounding box $(K_i^e)_b$ of the bad element K_i^e as well, that is,

$$\mathcal{E}(\Pi_{(K_i^e)'}(B_{\mathbf{k}',i}(\mathbf{x}))) := \sum_{r=1}^{(p+1)^2} c_{\mathbf{k}'r} \mathbf{b}_r(\mathbf{x}), \quad \mathbf{x} \in (K_i^e)'_b \cup (K_i^e)_b.$$

Finally, the stabilized interface integral corresponding to equation (3.20) becomes

$$\int_e \frac{\partial \mathcal{E}(\Pi_{(K_i^e)'}(B_{\mathbf{k}',i}))}{\partial n_i} B_{\ell,i}, \quad \int_e \frac{\partial \mathcal{E}(\Pi_{(K_i^e)'}(B_{\mathbf{k}',i}))}{\partial n_i} B_{\mathbf{m},j}, \quad (3.21)$$

where recall that $\mathbf{k}' \in I_{(K_i^e)'}$, $\ell \in I_{K_i^e}$, and $\mathbf{m} \in I_{K_j^e}$. Therefore, when K_i^e is a bad element, it is equation (3.21) rather than equation (3.20) that contributes to the stiffness matrix. Particularly, it contributes to the entries corresponding to the indices (\mathbf{k}', ℓ) and $(\mathbf{k}', \mathbf{m})$.

We have discussed the stabilization with the one-sided flux. Following a similar procedure, we can obtain the stabilization with the symmetric average flux as well, which, however, generally requires to stabilize more elements. More specifically, with the symmetric average flux, the term we need to stabilize becomes

$$\int_e \frac{\partial B_{\ell,i}}{\partial n_i} B_{\ell,i}, \quad \int_e \frac{\partial B_{\ell,i}}{\partial n_i} B_{\mathbf{m},j}, \quad \int_e \frac{\partial B_{\mathbf{m},j}}{\partial n_i} B_{\ell,i}, \quad \int_e \frac{\partial B_{\mathbf{m},j}}{\partial n_i} B_{\mathbf{m},j},$$

where the integral involves normal derivatives from both patches. Therefore, in addition to $\frac{\partial B_{\ell,i}}{\partial n_i}$, the flux $\frac{\partial B_{\mathbf{m},j}}{\partial n_i}$ also needs stabilization if K_j^e is badly cut.

Remark 3.3.2. Conditioning is another important issue related to trimming. As already observed, the guarantee of stability does not necessarily imply a well-conditioned stiffness matrix due to the presence of cut basis functions. A proper preconditioner is needed to ensure a reliable

solution. In the next set of numerical experiments, the simple diagonal scaling preconditioner was used. Another alternative is the recent work on the multigrid preconditioner [50], which can deliver cut-element independent convergence rates in the context of immersed isogeometric analysis. However, further investigation, especially theoretically, is needed to advance our knowledge on this challenging issue.

3.4 Numerical examples

This section presents three examples to demonstrate the convergence and conditioning by solving the Poisson equation on various domains obtained through the union operation. We then show the geometric flexibility of our proposed method by solving the linear elasticity problem on a more complex 2D geometry. In all the numerical tests, we set the penalty parameter β in Nitsche's formulation as $6p^2$, where p is the degree of the spline discretization. The area-ratio threshold is set to be 10% to identify bad elements, *i.e.*, $\theta = 0.1$.

3.4.1 Convergence and conditioning under bad cuts

We start with a two-patch union that forms a unit square. This simple test is meant to show that the minimal stabilization works robustly even when there are extremely small cut elements involved. As shown in Figure 3.6(a), the bottom patch Ω_0^* is a unit square $[0, 1]^2$ with a 4×3 mesh (orange lines), whereas the top patch Ω_1^* covers the region $[0.5 + \varepsilon, 1] \times [0, 1]$ with a 2×2 mesh (blue lines). The parameter $\varepsilon \in (0, 10^{-2})$ controls trimming of the bottom patch, or equivalently, ε is the width of the cut elements in the bottom patch. Both patches are B-spline patches. Particularly, we set $\varepsilon = 10^{-6}$ to perform a convergence study with bases of degrees 2, 3 and 4 in all the patches. We consider the manufactured solution: $u(x, y) = \sin(\pi x/2) \cos(\pi y)$, $(x, y) \in [0, 1]^2$, with homogeneous Dirichlet and Neumann boundary conditions imposed according to Figure 3.6(a). Figure 3.6(b) shows the solution obtained on the input mesh using the quadratic basis, where the cut elements are invisible due to their small scale. The convergence plots in the L^2 -norm and in the H^1 -broken norm error are shown in Figures 3.6(c), 3.6(d), where we observe expected optimal convergence rates in both norms. With “ H^1 -broken norm” we mean

$$\|v_h\|_{H^1(\Omega), \text{broken}}^2 := \sum_{i=0}^N \|v_i\|_{H^1(\Omega_i)}^2, \quad v_h \in V_h.$$

Note that we have used two types of fluxes $\langle \frac{\partial v_h}{\partial n} \rangle_t$, $t \in \{\frac{1}{2}, 1\}$, to show that they behave almost the same in terms of convergence and conditioning. We should also note that the symmetric average flux involves the flux from the bad cut elements and thus needs to be stabilized through the minimal stabilization method. On the other hand, the one-sided flux comes from a non-cut domain, so it does not need stabilization. Indeed, we observe in Figures 3.6(c), 3.6(d) that the convergence curves are indistinguishable using both types of fluxes.

Next, we study the conditioning of global stiffness matrices in three cases:

- (i) the symmetric average flux without stabilization;
- (ii) the symmetric average flux with stabilization;
- (iii) the one-sided flux (no need for stabilization).

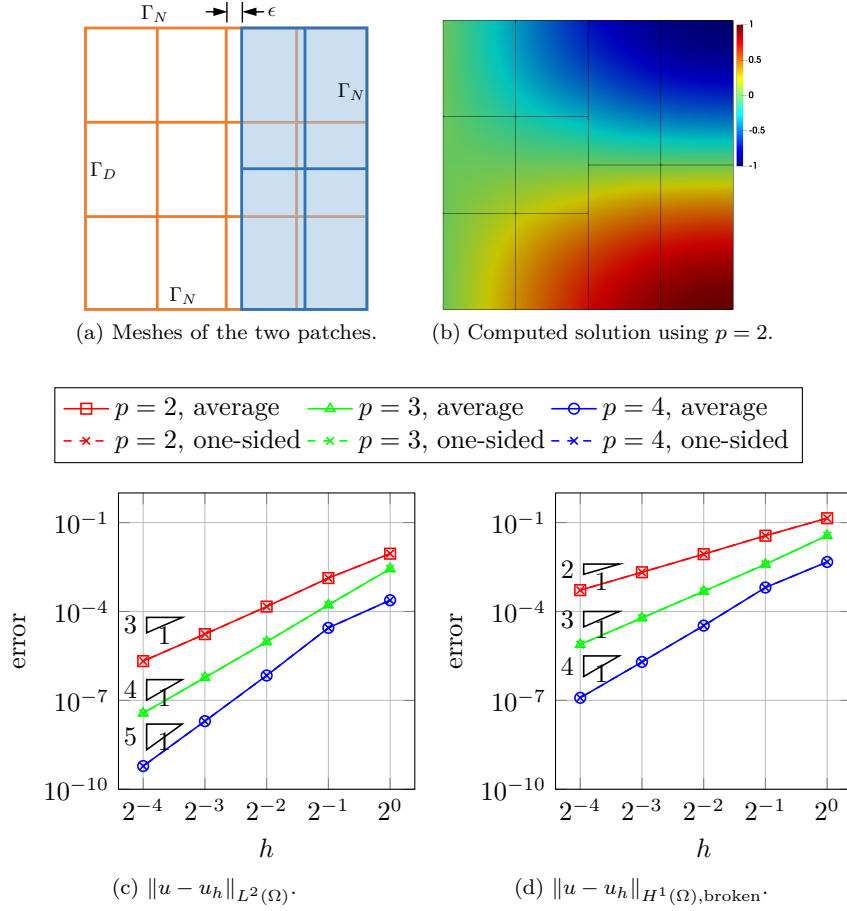
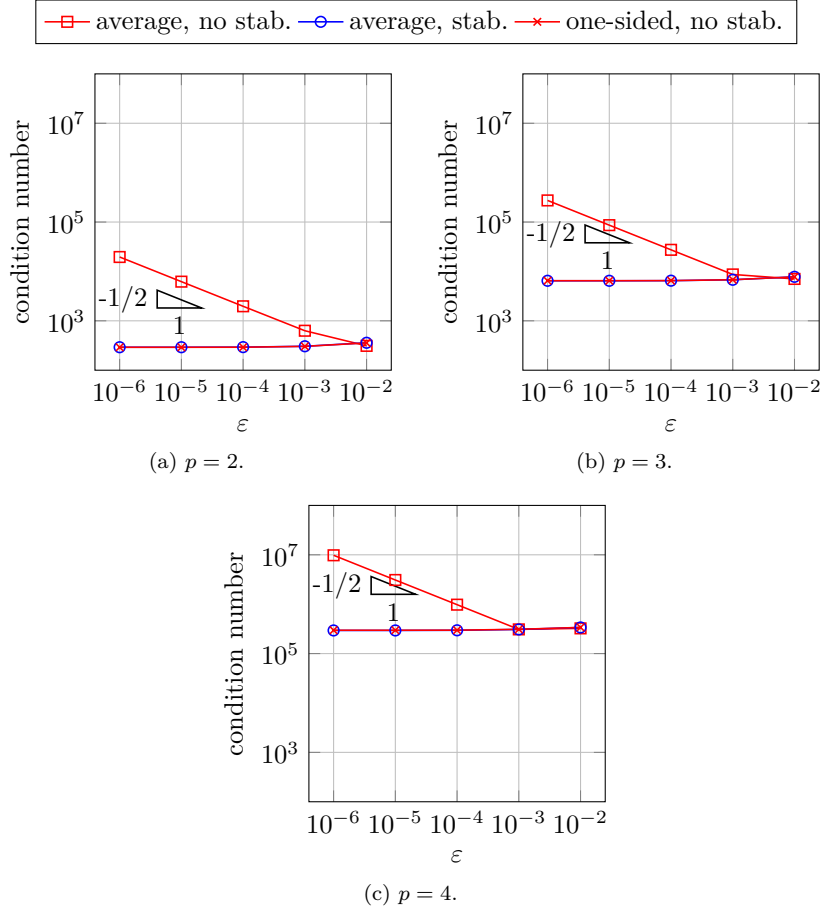


Figure 3.6 – The unit square example by a two-patch union. Here ε is set to 10^{-6} .

We compute the condition number of the rescaled stiffness matrix $D_s^{-1/2} K_s D_s^{-1/2}$, where K_s is the stiffness matrix and D_s denotes $\text{diag}(K_s)$. We test both the influence of ε on a fixed mesh and the influence of the mesh size h with a fixed small ε . First, given the input mesh shown in Figure 3.6(a) and bases of different degrees (2, 3 and 4), we compute their corresponding condition numbers changing ε from 10^{-2} down to 10^{-6} . The result is summarized in Figure 3.7. We observe that in cases (ii) and (iii), the condition number is independent from trimming, that is, it almost remains constant as ε decreases. Moreover, the condition numbers obtained in these two cases are indistinguishable. In contrast, the condition number in case (i) increases as $\mathcal{O}(\varepsilon^{-\frac{1}{2}})$ (see [51] for a more involved discussion about the dependence of the condition number on ε). We now fix ε to be 10^{-6} in the initial mesh and change the mesh size h (via global refinement) to further compare conditioning. First, we observe in Figure 3.8 that for all the degrees considered, the condition number in cases (ii) and (iii) is constantly lower than that in case (i). Second, higher-degree splines generally yield higher condition numbers under the same mesh size in all the cases. Third, in the low degree case (e.g., $p = 2$), the condition number tends to be controlled by the mesh size h , and it increases in the order of h^{-2} as h decreases, as it is expected. On the other hand, in the high degree case (e.g., $p = 4$), the condition number is higher but does not enter the asymptotic regime yet (this is a known behavior in IGA, see, for instance, Tables 2,3 in [31]). As h goes down, the effective area ratio of a cut element actually becomes larger, and this is why the condition number in case (i) decreases as h decreases, whereas it remains almost constant in cases (ii) and (iii); see Figure 3.8(c).


 Figure 3.7 – Condition number vs. ε for the domain of Figure 3.6.

In both the convergence and condition tests, we have shown that the one-sided flux works almost the same as the symmetric average flux with stabilization. The one-sided flux is chosen in the following tests as it generally needs to stabilize fewer elements than the symmetric average flux case.

3.4.2 Influence of patch ordering

We next study a disk geometry centered at $(0,0)$ with a radius of 2. It is formed by the union of an annulus with a rectangle, and we focus on a quarter of it due to symmetry. The annulus is represented by a NURBS patch with an inner radius of 1 and an outer radius of 2, which has a 5×5 mesh. The rectangle is a B-spline patch covering the region $[0, 1.13] \times [0, 1.17]$ with a 4×4 mesh. We consider two arrangements of patches to check if there is a difference in the numerical performance:

- (i) the rectangle on top of the annulus,
- (ii) the annulus on top of the rectangle;

see Figures 3.9(a), 3.9(b). In the convergence study, we take the manufactured solution $u(x, y) = (4 - x^2 - y^2) \cos(\pi x) \cos\left(\frac{\pi y}{2}\right)$ ($x \geq 0, y \geq 0, x^2 + y^2 \leq 4$), see Figure 3.9(c), and use bases of

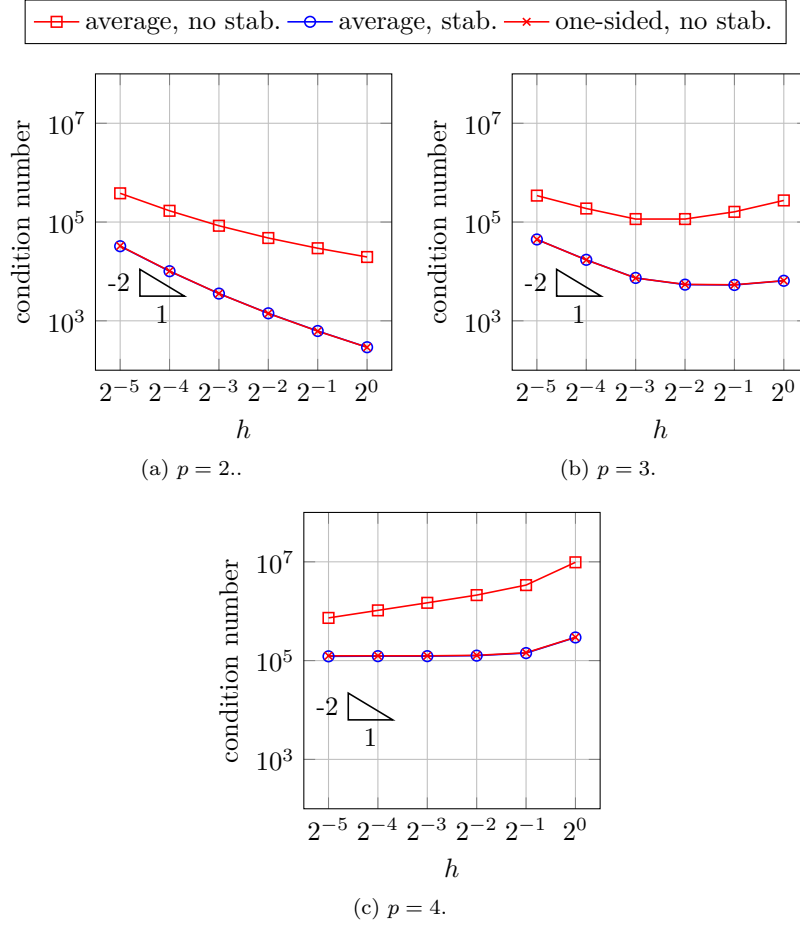


Figure 3.8 – Condition number vs. h for the domain of Figure 3.6a. Here ε is set to 10^{-6} .

degrees 2, 3 and 4 everywhere. Homogeneous Dirichlet and Neumann boundary conditions are imposed as shown in Figures 3.9(a), 3.9(b). In Figures 3.9(d), 3.9(e), we observe the expected optimal convergence in all the cases before the error reaches 10^{-8} . Afterwards we observe a deteriorated behavior due to the dominance of the geometric error, which is induced by the fixed tolerance setting ($\sim 10^{-8}$) in OpenCASCADE. Moreover, in all the convergence plots, we do not find distinguishable differences in the two different arrangements before the L^2 -norm error hits the geometric tolerance; compare dashed and solid lines.

3.4.3 Multiple overlapped patches

We further study an example that involves multiple overlapping patches; see Figure 3.10(a). In particular, there is a region where three patches overlap; see the intersection region of orange, blue, and green patches. All the patches are B-spline patches. We take the manufactured solution $u(x, y) = \sin(2\pi x) \sin(\pi y)$ for the convergence test, and we use bases of degrees 2, 3 and 4 to solve Poisson's problem. The homogeneous Dirichlet boundary condition is imposed according to Figure 3.10(a), whereas the Neumann boundary condition is imposed on all the other boundaries. Again, we observe the expected optimal convergence for all the degrees considered; see Figures 3.10(c), 3.10(d). Note that the blue patch provides the one-sided flux to the orange patch, and it is in the meanwhile cut by the green patch, so generally it needs stabilization. Recall

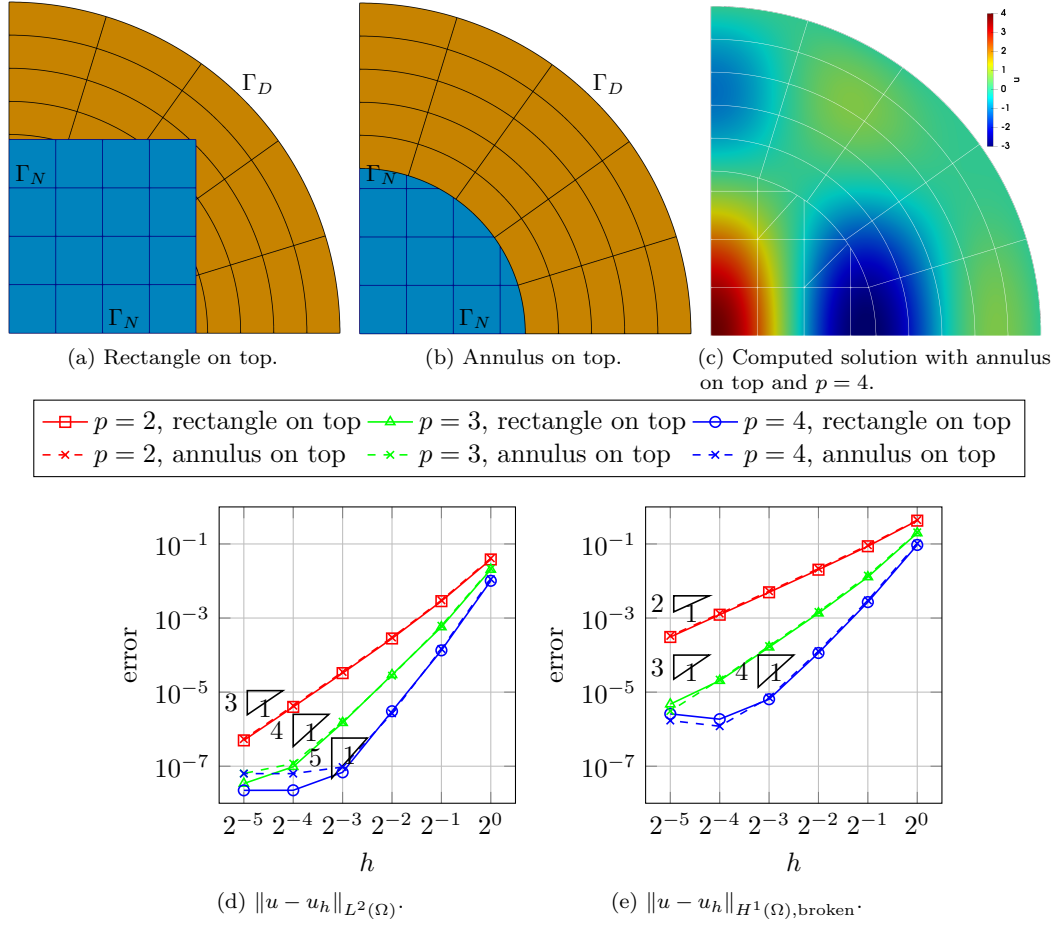


Figure 3.9 – The quarter of disk example by a two-patch union.

that we set the area-ratio threshold to be 10%. In our test cases, we observe that around 3% to 7% of cut elements are usually identified as bad elements. In other words, stabilization is only needed for a small number of elements. Moreover, let us observe that the elements depicted in Figure 3.10(b) are just used to set up quadrature rules.

3.4.4 A complex geometry obtained via Boolean operations

As the last example, we consider a more complex geometry, a toy car wheel model in the planar domain as shown in Figure 3.11(a), to show the potential capability of the proposed method. Such a geometry can be easily created with a combination of trimming and union operations, more specifically, by first generating two annuli, putting handles on top of them via union, and finally creating holes of different sizes via trimming. Two boundary conditions are shown in Figure 3.11(a), whereas the homogeneous Neumann boundary condition is imposed on all the other boundaries. We use quadratic splines to solve the linear elasticity problem on a series of meshes under the plane strain assumption, where the material is homogeneous and isotropic with Young's modulus and Poisson's ratio being 1 and 0.3, respectively. In particular, we show the displacement field on the initial mesh and the von Mises stress on the mesh after three steps of global refinement; see Figure 3.11(b) and Figure 3.11(c), respectively. As expected, we observe

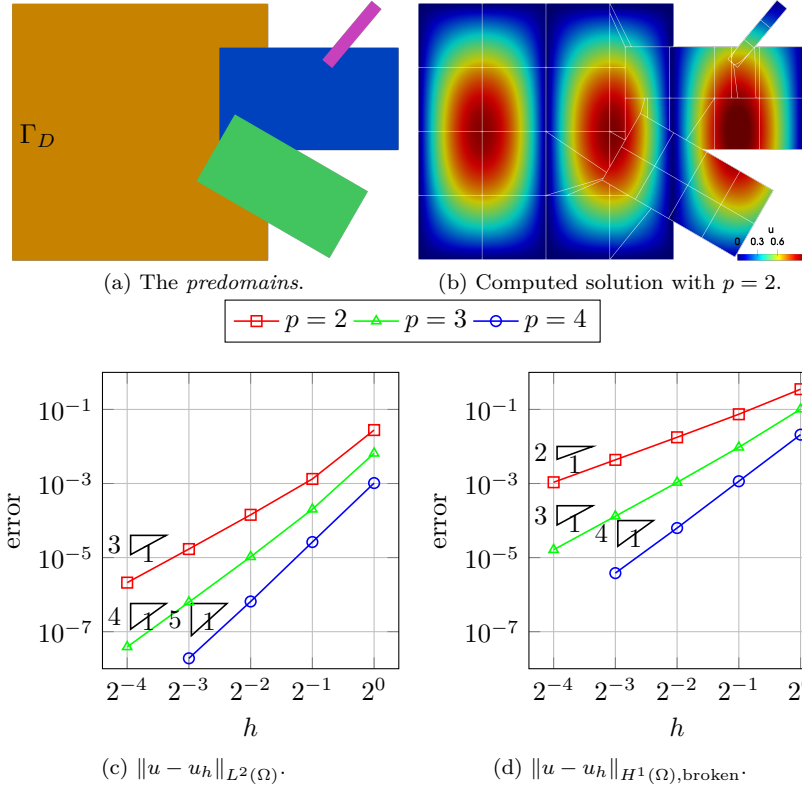


Figure 3.10 – An example of multipatch overlapped domain.

stress concentrations around holes as well as sharp corners. Moreover, our computational tool is robust in reparameterizing cut elements and handling union interfaces, and it can be easily adapted to solving different elliptic PDEs.

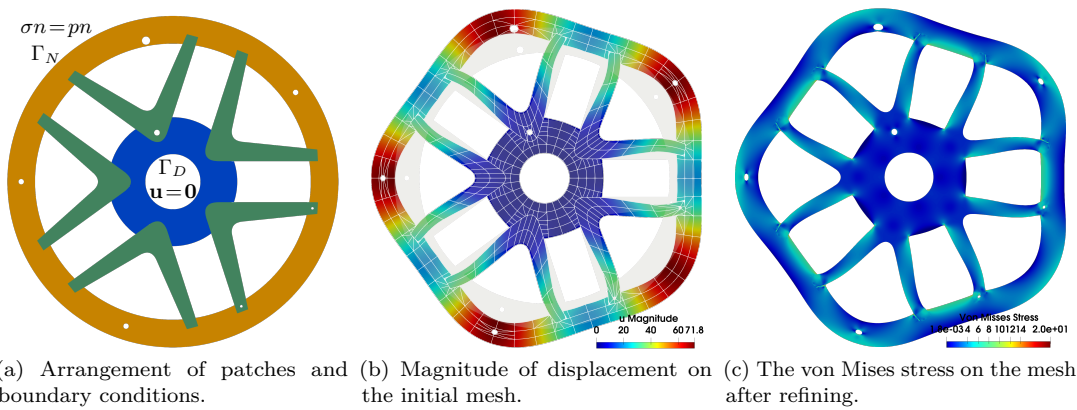


Figure 3.11 – A toy car wheel example in the planar domain. σ is the stress tensor, $p = 1$ is the pressure, n is the outward unit normal, and \mathbf{u} is the displacement vector. The results are visualized on deformed geometries. The white lines represent both the Bézier mesh and the quadrature mesh for cut elements.

4 Stabilized isogeometric discretization of the Stokes problem on trimmed geometries

Here, we extend the analysis developed in Chapter 2 from second-order elliptic PDEs to flow problems, focusing on the isogeometric discretization of the Stokes problem in trimmed domains. As we already observed in the introduction, the main issues for the numerical analysis are integration, conditioning, and stability. For what concerns integration, namely the construction of suitable quadrature rules on the trimmed geometries, we rely on the technique developed in [4], where the cut elements are subdivided into tiles which are reparametrized with piecewise polynomials of the same degree of the spline basis employed for the space discretization. The conditioning issue is also out of the scope of this work: herein, we limit ourselves to applying a Jacobi preconditioner. Our goal is to address the stability of incompressible flow problems in trimmed geometries. As in the Poisson problem, we rely on Nitsche’s method for the weak imposition of the Dirichlet boundary conditions. After empirically demonstrating the lack of stability of this formulation, we propose our stabilization. On the one hand, just as in the elliptic case, we modify the evaluation of the normal derivatives of the velocities at the “bad” cut elements. At the same time, stabilization is applied to the whole space of pressures.

The chapter is structured as follows. After having introduced in Section 4.1 some notations and the strong formulation of the Stokes problem, in Section 4.2 we provide the basic notions on IGA: we introduce three families of isogeometric elements (Raviart-Thomas, Nédélec, and Taylor-Hood) and use them to discretize the considered equations in a trimmed domain using Nitsche’s method for the imposition of the essential boundary conditions. In Section 4.3 we show through numerical experiments that the Nitsche formulation is not stable with respect to the trimming operation. Then, in Section 4.4, we introduce our stabilization procedure together with its key properties and the stabilized discrete formulation. In Section 4.5, we develop our stability analysis: we observe that one of the cardinal steps of the proof of stability, namely the inf-sup stability, is missing. In Section 4.6, we prove that optimal *a priori* error estimates hold. In the last section, we provide numerical experiments to validate the theory, emphasizing the validation of the inf-sup stability of our method.

The results of this chapter are collected in the preprint [111], which has been submitted for publication.

4.1 Model problem

We let $\Omega_0 \subset \mathbb{R}^d$ (here $d = 2, 3$) be the starting domain parametrized by a bijective spline map $\mathbf{F} : (0, 1)^d \rightarrow \Omega_0$, *i.e.*, a *patch* in the isogeometric terminology, and let $\Omega_1, \dots, \Omega_N$ be Lipschitz

Chapter 4. Stabilized isogeometric discretization of the Stokes problem on trimmed geometries

domains in \mathbb{R}^d . We assume that Ω_i , $i = 1, \dots, N$, are to be cut away from Ω_0 and that our computational domain reads:

$$\Omega = \Omega_0 \setminus \bigcup_{i=1}^N \overline{\Omega}_i. \quad (4.1)$$

For simplicity, let us assume that Ω is a Lipschitz domain that has been obtained via trimming operations, as in (4.1) with $N = 1$, namely $\Omega = \Omega_0 \setminus \overline{\Omega}_1$. Let Γ be its boundary such that $\Gamma = \overline{\Gamma}_D \cup \overline{\Gamma}_N$, where Γ_D and Γ_N are open and disjoint. We denote the *trimming curve* (*trimming surface* if $d = 3$) as $\Gamma_T = \Gamma \cap \partial\Omega_1$.

Given the body force $\mathbf{f} : \Omega \rightarrow \mathbb{R}^d$, the mass production rate $g : \Omega \rightarrow \mathbb{R}$, the Dirichlet datum $\mathbf{u}_D : \Omega \rightarrow \mathbb{R}^d$ and the Neumann datum $\mathbf{u}_N : \Omega \rightarrow \mathbb{R}^d$, we look for the *velocity* $\mathbf{u} : \Omega \rightarrow \mathbb{R}^d$ and *pressure* $p : \Omega \rightarrow \mathbb{R}$ such that

$$\begin{aligned} -\mu \Delta \mathbf{u} + \nabla p &= \mathbf{f}, & \text{in } \Omega, \\ \operatorname{div} \mathbf{u} &= g, & \text{in } \Omega, \\ \mathbf{u} &= \mathbf{u}_D, & \text{on } \Gamma_D, \\ \boldsymbol{\sigma}(\mathbf{u}, p) \mathbf{n} &= \mathbf{u}_N, & \text{on } \Gamma_N, \end{aligned} \quad (4.2)$$

where $\mu \in \mathbb{R}$, $\mu > 0$ is the *viscosity coefficient*, $\boldsymbol{\sigma}(\mathbf{u}, p) = \mu D\mathbf{u} - p\mathbf{I}$ is the *Cauchy stress tensor*, $(D\mathbf{u})_{ij} := \frac{\partial u_i}{\partial x_j}$, $i, j = 1, \dots, d$. For the sake of simplicity of the exposition, we set $\mu \equiv 1$.

C will denote generic positive constants that may change with each occurrence throughout the chapter but are always independent of the local mesh size and the position of the trimming curve (surface, if $d = 3$) unless otherwise specified.

4.2 Isogeometric discretization

4.2.1 Isogeometric spaces on trimmed geometries

Let us consider the isogeometric mixed elements defined in the untrimmed domain Ω_0 , which have been introduced in Section 1.3. We recall that $V_{0,h}^{\text{RT}} - Q_{0,h}^{\text{RT}}$, $V_{0,h}^{\text{N}} - Q_{0,h}^{\text{N}}$, and $V_{0,h}^{\text{TH}} - Q_{0,h}^{\text{TH}}$ denote the Raviart-Thomas, the Nédélec, and the Taylor-Hood isogeometric elements, respectively. Let us restrict them to the active part of the domain, *i.e.*,

$$\begin{aligned} V_h^{\text{RT}} &:= \{\mathbf{v}_h \Big|_{\Omega} : \mathbf{v}_h \in V_{0,h}^{\text{RT}}\}, \quad V_h^{\text{N}} := \{\mathbf{v}_h \Big|_{\Omega} : \mathbf{v}_h \in V_{0,h}^{\text{N}}\}, \quad V_h^{\text{TH}} := \{\mathbf{v}_h \Big|_{\Omega} : \mathbf{v}_h \in V_{0,h}^{\text{TH}}\}, \\ Q_h^{\text{RT}} &= Q_h^{\text{N}} := \{q_h \Big|_{\Omega} : q_h \in Q_{0,h}^{\text{RT}}\}, \quad Q_h^{\text{TH}} := \{q_h \Big|_{\Omega} : q_h \in Q_{0,h}^{\text{TH}}\}. \end{aligned}$$

We observe that in general, in the physical domain, $V_h^{\text{RT}} \subset V_h^{\text{N}} \not\subset V_h^{\text{TH}}$.

To alleviate the notation, we may omit the superscript $\square \in \{\text{RT}, \text{N}, \text{TH}\}$ when what said does not depend from the particular isogeometric element choice. Moreover, for the notation about the mesh, mesh-size, and cut elements, we refer the reader to Section 2.1.1.

We endow the discrete spaces of the velocities with the scalar product

$$(\mathbf{w}_h, \mathbf{v}_h)_{1,h} := \int_{\Omega} D\mathbf{w}_h : D\mathbf{v}_h + \int_{\Gamma_D} \mathbf{h}^{-1} \mathbf{w}_h \cdot \mathbf{v}_h, \quad \mathbf{w}_h, \mathbf{v}_h \in V_h,$$

inducing the mesh-dependent norm

$$\|\mathbf{v}_h\|_{1,h}^2 := \|D\mathbf{v}_h\|_{L^2(\Omega)}^2 + \left\| \mathbf{h}^{-\frac{1}{2}} \mathbf{v}_h \right\|_{L^2(\Gamma_D)}^2, \quad \mathbf{v}_h \in V_h.$$

We also equip the discrete spaces of the pressures with the mesh-dependent norm

$$\|q_h\|_{0,h}^2 := \|q_h\|_{L^2(\Omega)}^2 + \left\| h^{\frac{1}{2}} q_h \right\|_{L^2(\Gamma_D)}^2, \quad q_h \in Q_h.$$

We consider the following *Nitsche's formulations* as discretizations of problem (4.2).

Find $(\mathbf{u}_h, p_h) \in V_h \times Q_h$ such that

$$\begin{aligned} a_h(\mathbf{u}_h, \mathbf{v}_h) + b_1(\mathbf{v}_h, p_h) &= F_h(\mathbf{v}_h), & \forall \mathbf{v}_h \in V_h, \\ b_m(\mathbf{u}_h, q_h) &= G_m(q_h), & \forall q_h \in Q_h, \end{aligned} \quad (4.3)$$

where $m \in \{0, 1\}$ and

$$\begin{aligned} a_h(\mathbf{w}_h, \mathbf{v}_h) &:= \int_{\Omega} D\mathbf{w}_h : D\mathbf{v}_h - \int_{\Gamma_D} D\mathbf{w}_h \mathbf{n} \cdot \mathbf{v}_h - \int_{\Gamma_D} \mathbf{w}_h \cdot D\mathbf{v}_h \mathbf{n} \\ &\quad + \gamma \int_{\Gamma_D} h^{-1} \mathbf{w}_h \cdot \mathbf{v}_h, & \mathbf{w}_h, \mathbf{v}_h \in V_h, \\ b_m(\mathbf{v}_h, q_h) &:= - \int_{\Omega} q_h \operatorname{div} \mathbf{v}_h + m \int_{\Gamma_D} q_h \mathbf{v}_h \cdot \mathbf{n}, & \mathbf{v}_h \in V_h, q_h \in Q_h, \\ F_h(\mathbf{v}_h) &:= \int_{\Omega} \mathbf{f} \cdot \mathbf{v}_h + \int_{\Gamma_N} \mathbf{u}_N \cdot \mathbf{v}_h - \int_{\Gamma_D} \mathbf{u}_D \cdot D\mathbf{v}_h \mathbf{n} + \gamma \int_{\Gamma_D} h^{-1} \mathbf{u}_D \cdot \mathbf{v}_h, & \mathbf{v}_h \in V_h, \\ G_m(q_h) &:= - \int_{\Omega} g q_h + m \int_{\Gamma_D} q_h \mathbf{u}_D \cdot \mathbf{n}, & q_h \in Q_h, \end{aligned}$$

$\gamma > 0$ being a penalty parameter.

Remark 4.2.1. In the literature, the Nitsche formulation of the Stokes problem was introduced in [63] with $m = 1$ and allows to weakly impose the Dirichlet boundary conditions without manipulating the discrete velocity space (see also Section 1.3). The choice $m = 0$ allows for an exactly divergence-free numerical solution for the velocity field in the case of $g \equiv 0$ and the Raviart-Thomas isogeometric element, see Remark 4.4.9.

Remark 4.2.2. We observe that, in order to simplify the presentation, in formulation (4.3) we impose Dirichlet conditions weakly everywhere. In the case where there is $\tilde{\Gamma} \subset \Gamma_D$ such that $\mathbf{F}^{-1}(\tilde{\Gamma})$ is a union of full faces of $\hat{\Omega}_0$, then one could have strongly imposed Dirichlet's conditions on $\tilde{\Gamma}$ by appropriately modifying the discrete velocity spaces: the traces for V_h^{TH} and the normal components for V_h^{RT} and V_h^{N} (the tangential components are weakly imposed in the spirit of [59]).

Remark 4.2.3. The imposition of the Neumann boundary conditions does not pose any particular problem in a mesh that is not aligned with Γ_N . These kinds of conditions are natural for the Stokes problem, *i.e.*, they can be enforced through a boundary integral as long as suitable quadrature rules in the cut elements are available, see [4].

Motivated by the previous remark, we henceforth assume that $\Gamma_N \cap \Gamma_T = \emptyset$, so that $\Gamma_T \subseteq \Gamma_D$, *i.e.*, we impose Dirichlet boundary conditions on the trimming curve.

4.3 Lack of stability of Nitsche's method

Throughout this section, we want to show with some numerical experiences that the Nitsche formulation of the Stokes problem (4.3), discretized with Raviart-Thomas, Nédélec, and Taylor-Hood elements, lacks stability when working on trimmed geometries. It is well-known (see [21, 102]) that the following are necessary conditions for the well-posedness of formulation (4.3) for both $m \in \{0, 1\}$.

1. There exists $\bar{\gamma} > 0$ such that, for every fixed $\gamma \geq \bar{\gamma}$, there exists $M_a > 0$ such that

$$|a_h(\mathbf{w}_h, \mathbf{v}_h)| \leq M_a \|\mathbf{w}_h\|_{1,h} \|\mathbf{v}_h\|_{1,h}, \quad \forall \mathbf{w}_h, \mathbf{v}_h \in V_h. \quad (4.4)$$

2. There exist $\beta_1 > 0, \beta_0 > 0$ such that

$$\inf_{q_h \in Q_h} \sup_{\mathbf{v}_h \in V_h} \frac{b_1(\mathbf{v}_h, q_h)}{\|q_h\|_{0,h} \|\mathbf{v}_h\|_{1,h}} \geq \beta_1, \quad (4.5)$$

$$\inf_{q_h \in Q_h} \sup_{\mathbf{v}_h \in V_h} \frac{b_0(\mathbf{v}_h, q_h)}{\|q_h\|_{0,h} \|\mathbf{v}_h\|_{1,h}} \geq \beta_0. \quad (4.6)$$

Remark 4.3.1. We observe that M_a depends (and grows dependently) on γ , which has to be taken sufficiently large, *i.e.*, $\gamma \geq \bar{\gamma}$, but at the same time as small as possible, *i.e.*, close to $\bar{\gamma}$, in order not to end up with a too-large continuity constant.

We want to show that the stability constants in the previous estimates, M_a, β_1, β_0 , can be arbitrarily negatively influenced by the relative position between the mesh and the trimming curve; hence they are not uniform with respect to the trimming operation. Note that in the following essential boundary conditions are enforced on the whole boundary, and they are weakly imposed on the parts unfitted with the mesh. Let us proceed in order.

1. The breakdown example for the robustness of the continuity constant M_a is the following. Let $\Omega_0 = (0, 1)^2$, $\Omega_1 = (0, 1) \times (0.75 + \varepsilon, 1)$ and $\Omega = \Omega_0 \setminus \bar{\Omega}_1$, as illustrated in Figure 4.1(a). Note that the continuity constant of $a_h(\cdot, \cdot)$ corresponding to $\gamma = 1$ is smaller than the one related to $\gamma > 1$, *i.e.*, $M_a^\gamma > M_a^1$ for every $\gamma > 1$. Hence, in order to verify that the continuity constant also degenerates with the cut, it is sufficient to show that M_a^1 grows as ε gets smaller. M_a^1 can be estimated as the largest eigenvalue of the subsequent generalized eigenvalue problem.

Find $(\mathbf{u}_h, \lambda_h) \in V_h \setminus \{0\} \times \mathbb{R}$ such that

$$a_h(\mathbf{u}_h, \mathbf{v}_h) = \lambda_h (\mathbf{u}_h, \mathbf{v}_h)_{1,h}, \quad \forall \mathbf{v}_h \in V_h. \quad (4.7)$$

Assume that the mesh is uniform and let us fix the degree $k = 2$.

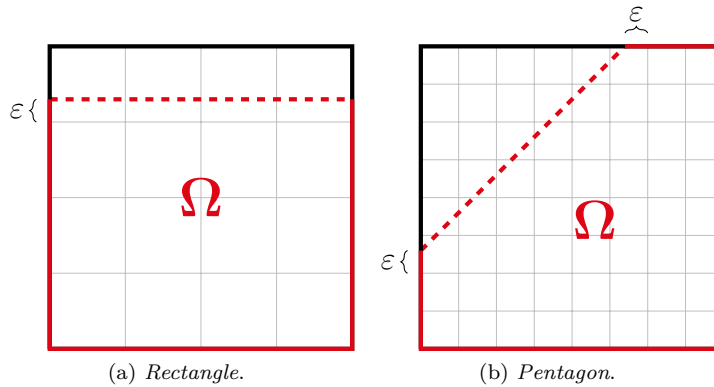


Figure 4.1 – The trimmed geometries.

Then, let us compute λ_h^{\max} for different values of ε : in each configuration we refine the mesh, see Figure 4.2. We can clearly see how the largest eigenvalue grows unboundedly as ε goes

4.3. Lack of stability of Nitsche's method

to zero, implying that the continuity constant can be made arbitrarily large by reducing ε . As already observed in Section 2.2, this is due to the lack of an inverse inequality robust with respect to the trimming operation, namely,

$$\left\| h^{\frac{1}{2}} D\mathbf{v}_h \mathbf{n} \right\|_{L^2(\Gamma_K)} \leq C \|D\mathbf{v}_h\|_{L^2(K \cap \Omega)},$$

with C independent of the shape and diameter of $K \cap \Omega$.

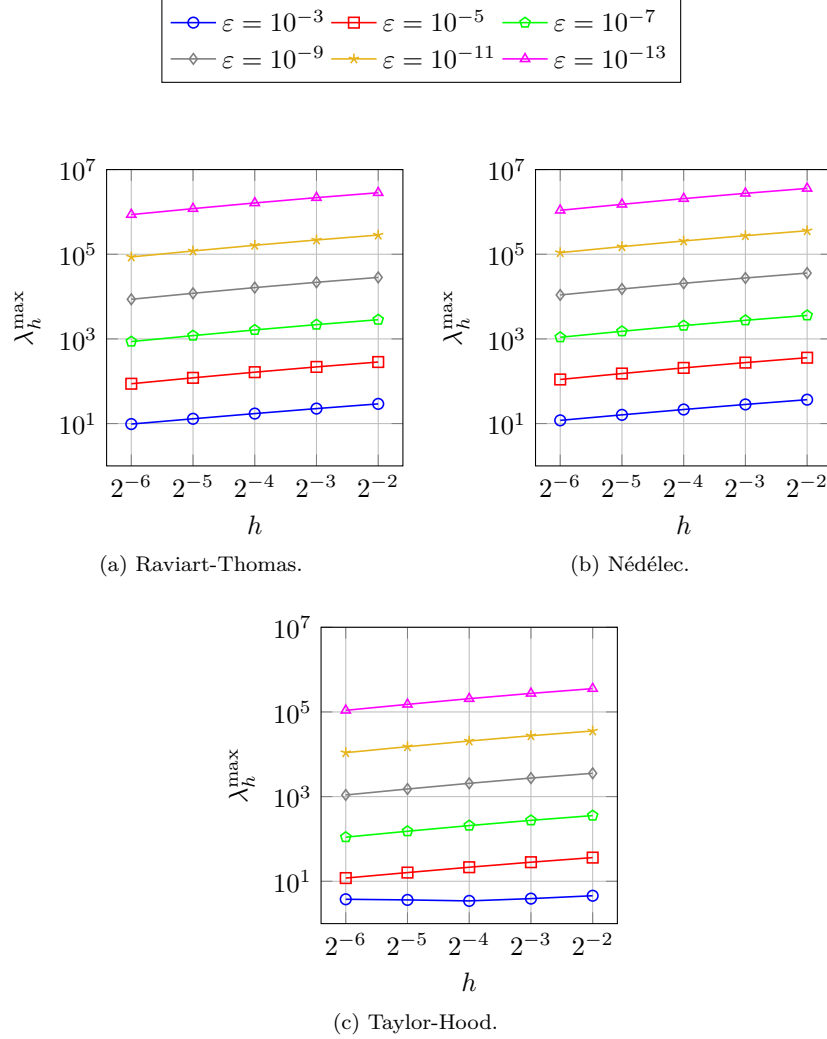


Figure 4.2 – Maximum generalized eigenvalue of (4.7) for the trimmed *rectangle*.

2. Now, we consider a different setting. Let $\Omega_0 = (0, 1)^2$, Ω_1 be the triangle with vertices $(0, 0.25 + \varepsilon) - (0, 1) - (0.75 - \varepsilon, 1)$ and $\Omega = \Omega_0 \setminus \Omega_1$, see Figure 4.1(b). We want to study the values of β_m , $m \in \{0, 1\}$, with respect to the trimming parameter ε . The inf-sup constants are numerically evaluated as explained in [15]. In Figure 4.3 we plot β_m for $k = 2$ and different values of the trimming parameter ε and the mesh-size h . The numerical experiments show the dependence of β_m on ε . This negative result is due to the presence of a *spurious pressure mode* p_h^ε (technically speaking it is not spurious since, even if $\beta_m(p_h^\varepsilon) \ll 1$, it still holds $\beta_m(p_h^\varepsilon) \neq 0$) whose support is concentrated in trimmed elements with a very small overlap with the physical domain Ω .

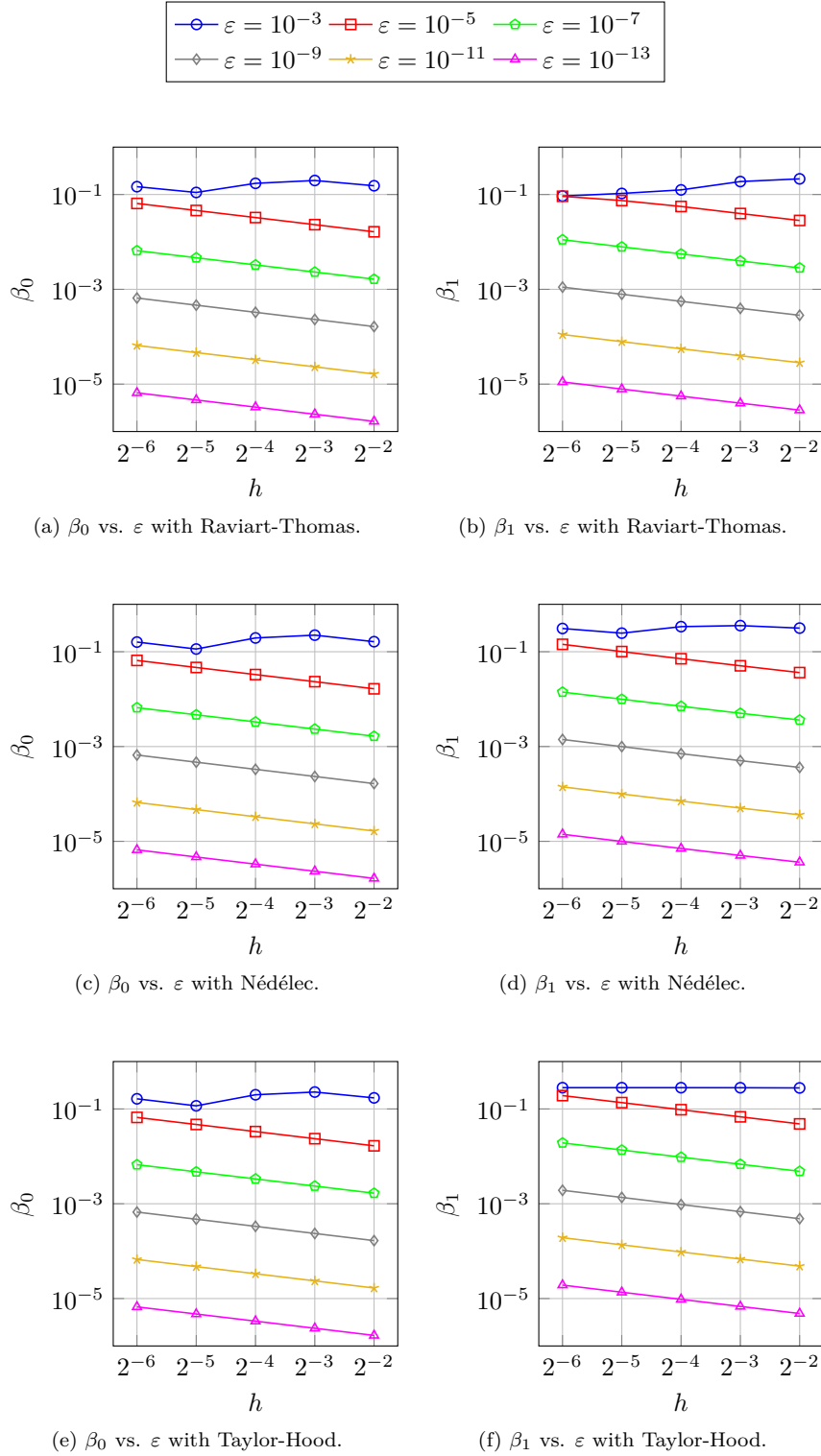


Figure 4.3 – Inf-sup constants for the trimmed *pentagon*.

Remark 4.3.2. Let us observe that in the previous numerical counterexamples, in order to

validate the lack of stability of the formulation, one should have constructed a sequence of spaces depending on ε rather than changing the domain (as it is done in [33], where the lack of stability of the Nitsche formulation for the Poisson problem on trimmed domains is shown). However, both constructions lead to the same results, and we believe that our choice makes the presentation more fluent. We also note that in the first counterexample, the inf-sup condition is not violated, and, similarly, the second configuration is not a counterexample for the continuity.

4.4 Stabilized Nitsche's formulations

4.4.1 Stabilization procedure

We start by subdividing, for each $h > 0$, the elements of the active physical Bézier mesh \mathcal{M}_h into two disjoint collections: the one of the good elements \mathcal{M}_h^g , those with sufficient overlap with the physical domain, and the one of the bad elements \mathcal{M}_h^b , a small portion of which intersect Ω . Then, for each bad element K , we select a good neighbor K' , see Definition 2.3.1. We also define $\bar{\Omega}_{I,h} = \bigcup_{K \in \mathcal{M}_h \setminus \mathcal{G}_h} \bar{K}$, the region occupied by untrimmed elements, and $S_h := \Omega \setminus \bigcup_{K \in \mathcal{M}_h^g} \bar{K} = \text{int} \bigcup_{K \in \mathcal{M}_h^b} \bar{K} \cap \bar{\Omega}$, the region occupied by bad elements.

It is well known that formulation (4.3) is stable if $\Omega = \Omega_{I,h}$. In the general case $\Omega_{I,h} \subsetneq \Omega$, the goal of the stabilization is, informally speaking, to extend the stability of the discrete problem from the internal elements of the domain to the cut ones.

Remark 4.4.1. We observe that choosing $\theta = 1$ in Definition 2.3.1 corresponds to stabilizing all cut elements, in which case it holds $\mathcal{M}_h^b = \mathcal{G}_h$, $\bar{\Omega}_{I,h} = \bigcup_{K \in \mathcal{M}_h^g} \bar{K}$ and $S_h = \Omega \setminus \bar{\Omega}_{I,h}$.

The following assumption is not restrictive and is satisfied whenever the mesh is sufficiently refined, and we take C large enough in (2.7).

Assumption 4.4.2. For every $K \in \mathcal{M}_h^b$, there exists $K' \in \mathcal{N}(K) \cap \mathcal{M}_h^g$. From now on we will refer to such K' as a *good neighbor* of K .

Let us start by stabilizing the pressures. We define the operator $R_h^p : Q_h \rightarrow L^2(\Omega)$ locally as $R_h^p(q_h)|_K := R_K^p(q_h)$, for every $K \in \mathcal{M}_h$ and all $q_h \in Q_h$, as follows:

- if $K \in \mathcal{M}_h^g$, then

$$R_K^p(q_h) := q_h|_K,$$

- if $K \in \mathcal{M}_h^b$, then

$$R_K^p(q_h) := \mathcal{E}_{K',K} \left(\Pi_{K'} \left(q_h|_{K'} \right) \right)|_K,$$

where $\Pi_{K'} : L^2(K') \rightarrow \mathbb{Q}_k(K')$ is the local L^2 -projection and $\mathcal{E}_{K',K} : \mathbb{Q}_k(K') \rightarrow \mathbb{Q}_k(K' \cup K)$ is the canonical polynomial extension. K' is a good neighbor of K .

Proposition 4.4.3 (Stability property of R_h^p). *Given $\theta \in (0, 1]$, there exist $C_1, C_2 > 0$ such that, for every $K \in \mathcal{M}_h$ and $h > 0$,*

$$\begin{aligned} \left\| h^{\frac{1}{2}} R_h^p(q_h) \right\|_{L^2(\Gamma_K)} &\leq C_1 \|q_h\|_{L^2(K' \cap \Omega)}, & \forall q_h \in Q_h, \\ \|R_h^p(q_h)\|_{L^2(K \cap \Omega)} &\leq C_2 \|q_h\|_{L^2(K' \cap \Omega)}, & \forall q_h \in Q_h, \end{aligned}$$

where K' is a good neighbor if $K \in \mathcal{M}_h^b$, $K' = K$ and if $K \in \mathcal{M}_h^g$.

Chapter 4. Stabilized isogeometric discretization of the Stokes problem on trimmed geometries

Proof. Let $q_h \in Q_h^\square$, $\square \in \{\text{TH}, \text{RT}, \text{N}\}$, and $K \in \mathcal{M}_h$. We first assume $K \in \mathcal{M}_h^g$ and let $Q = \mathbf{F}^{-1}(K)$, $\widehat{q}_h = q_h \circ \mathbf{F}$ if $\square = \text{TH}$, $q_h = \det(D\mathbf{F})^{-1} \widehat{q}_h \circ \mathbf{F}^{-1}$ if $\square \in \{\text{RT}, \text{N}\}$. Hölder's inequality, Lemma A.1.5, and Lemma A.1.1 imply

$$\begin{aligned} \left\| h^{\frac{1}{2}} q_h \right\|_{L^2(\Gamma_K)} &= h_K^{\frac{1}{2}} \|q_h\|_{L^2(\Gamma_K)} \leq h_K^{\frac{1}{2}} |\Gamma_K|^{\frac{1}{2}} \|q_h\|_{L^\infty(\Gamma_K)} \leq h_K^{\frac{1}{2}} |\Gamma_K|^{\frac{1}{2}} \|q_h\|_{L^\infty(K)} \\ &\leq C_\square h_K^{\frac{1}{2}} |\Gamma_K|^{\frac{1}{2}} \|\widehat{q}_h\|_{L^\infty(Q)} \leq C_\square h_K^{\frac{1}{2}} |\Gamma_K|^{\frac{1}{2}} h_K^{-\frac{d}{2}} \|\widehat{q}_h\|_{L^2(Q \cap \widehat{\Omega})} \leq C C_\square \overline{C}_\square \|q_h\|_{L^2(K \cap \Omega)}, \end{aligned}$$

where $C_{\text{TH}} = 1$, $C_{\text{RT}} = C_{\text{N}} = \|\det D\mathbf{F}^{-1}\|_{L^\infty(K)}$, $\overline{C}_{\text{TH}} = \|\det D\mathbf{F}^{-1}\|_{L^\infty(K \cap \Omega)}^{\frac{1}{2}}$, $\overline{C}_{\text{RT}} = \overline{C}_{\text{N}} = \|\det D\mathbf{F}\|_{L^\infty(Q \cap \widehat{\Omega})}^{\frac{1}{2}}$, and C depends on k , and on θ . Now, let $K \in \mathcal{M}_h^b$ with good neighbor K' . We employ, respectively, Hölder's inequality, Lemma A.1.1, and Lemma A.1.4, and we get

$$\begin{aligned} \left\| h^{\frac{1}{2}} R_K^p(q_h) \right\|_{L^2(\Gamma_K)} &= h_K^{\frac{1}{2}} \|\mathcal{E}_{K',K}(\Pi_{K'}(q_h))\|_{L^2(\Gamma_K)} \leq h_K^{\frac{1}{2}} |\Gamma_K|^{\frac{1}{2}} \|\mathcal{E}_{K',K}(\Pi_{K'}(q_h))\|_{L^\infty(\Gamma_K)} \\ &\leq C h_K^{\frac{d}{2}} \|\mathcal{E}_{K',K}(\Pi_{K'}(q_h))\|_{L^\infty(K)} \leq C h_K^{\frac{d}{2}} \|\Pi_{K'}(q_h)\|_{L^\infty(K')}. \end{aligned}$$

We can now use Lemma A.1.6, the boundedness of the L^2 -projection with respect to $\|\cdot\|_{L^2}$ and the local quasi-uniformity of the mesh, to obtain

$$\left\| h^{\frac{1}{2}} R_K^p(q_h) \right\|_{L^2(\Gamma_K)} \leq C h_K^{\frac{d}{2}} h_{K'}^{-\frac{d}{2}} \|\Pi_{K'}(q_h)\|_{L^2(K')} \leq C \|q_h\|_{L^2(K')},$$

with C depending on k . By applying Hölder's inequality, moving to the parametric domain, using Lemma A.1.5, and moving back to the physical domain, we get

$$\begin{aligned} \left\| h^{\frac{1}{2}} R_K^p(q_h) \right\|_{L^2(\Gamma_K)} &\leq C h_K^{\frac{d}{2}} \|q_h\|_{L^\infty(K')} \leq C_\square h_K^{\frac{d}{2}} \|\widehat{q}_h\|_{L^\infty(Q')} \\ &\leq C C_\square h_K^{\frac{d}{2}} h_{Q'}^{-\frac{d}{2}} \|\widehat{q}_h\|_{L^\infty(Q' \cap \widehat{\Omega})} \leq C C_\square \overline{C}_\square \|q_h\|_{L^2(K' \cap \Omega)}, \end{aligned} \tag{4.8}$$

where C depends, in particular, on k and θ , and C_\square , \overline{C}_\square have been defined above.

Let us move to the proof of the other inequality of the statement. If $K \in \mathcal{G}_h^g$, then there is nothing to prove. Let $K \in \mathcal{G}_h^b$ and K' its good neighbor.

$$\begin{aligned} \|R_h^p(q_h)\|_{L^2(K \cap \Omega)} &\leq |K \cap \Omega|^{\frac{1}{2}} \|R_h^p(q_h)\|_{L^\infty(K \cap \Omega)} \leq |K \cap \Omega|^{\frac{1}{2}} \|R_h^p(q_h)\|_{L^\infty(K)} \\ &\leq C |K \cap \Omega|^{\frac{1}{2}} \|\Pi_{K'}(q_h)\|_{L^\infty(K')}, \end{aligned}$$

where we have used, respectively, Hölder's inequality and Lemma A.1.4. Note that it is trivial to check that, for every $u \in L^2(K')$, $\|\Pi_{K'}(u)\|_{L^2(K')} \leq \|u\|_{L^2(K')}$. On the other hand, by using Lemma A.1.6, and the L^2 -stability of the L^2 -projection, we have $\|\Pi_{K'}(q_h)\|_{L^\infty(K')} \leq C h_{K'}^{-\frac{d}{2}} \|\Pi_{K'}(q_h)\|_{L^2(K')} \leq C h_{K'}^{-\frac{d}{2}} \|q_h\|_{L^2(K')}$. Hence,

$$\|R_h^p(q_h)\|_{L^2(K \cap \Omega)} \leq C |K \cap \Omega|^{\frac{1}{2}} h_{K'}^{-\frac{d}{2}} \|q_h\|_{L^2(K')} \leq C |K \cap \Omega|^{\frac{1}{2}} |K|^{-\frac{1}{2}} \|q_h\|_{L^2(K')} \leq C \|q_h\|_{L^2(K')},$$

where in the second last passage of both lines we used the shape-regularity and quasi-local uniformity of the mesh, entailing $h_{K'}^{-\frac{d}{2}} \sim |K'|^{-\frac{1}{2}}$, $|K'|^{-\frac{1}{2}} \sim |K|^{-\frac{1}{2}}$. We observe that the constant C depends on k , since we relied on Lemma A.1.6. We conclude as in (4.8). \square

Now, let us move to the velocities and define, for $\square \in \{\text{RT}, \text{N}, \text{TH}\}$, the operator $R_h^v : V_h^\square \rightarrow \mathbf{L}^2(\Omega)$ locally as $R_h^v(\mathbf{v}_h) \Big|_K := R_K^v(\mathbf{v}_h)$ for every $K \in \mathcal{M}_h$ and all $\mathbf{v}_h \in V_h^\square$:

- if $K \in \mathcal{M}_h^g$, then

$$R_K^v(\mathbf{v}_h) := \mathbf{v}_h|_K,$$

- if $K \in \mathcal{M}_h^b$, then

$$R_K^v(\mathbf{v}_h) := \mathcal{E}_{K',K} \left(\Pi_{K'} \left(\mathbf{v}_h|_{K'} \right) \right) \Big|_K,$$

where $\Pi_{K'} : \mathbf{L}^2(K') \rightarrow \mathbb{V}_k(K')$ is the L^2 -orthogonal projection onto

$$\begin{aligned} \mathbb{V}_k(K') &:= \begin{cases} \mathbb{S}_k(K'), & \text{if } \square = \text{RT}, \\ (\mathbb{Q}_{k+1}(K'))^d, & \text{if } \square \in \{\text{N}, \text{TH}\}, \end{cases} \\ \mathbb{S}_k(K') &:= \begin{cases} \mathbb{Q}_{k+1,k}(K') \times \mathbb{Q}_{k,k+1}(K'), & \text{if } d = 2, \\ \mathbb{Q}_{k+1,k,k}(K') \times \mathbb{Q}_{k,k+1,k}(K') \times \mathbb{Q}_{k,k,k+1}(K'), & \text{if } d = 3, \end{cases} \end{aligned}$$

and $\mathcal{E}_{K',K} : \mathbb{V}_h(K') \rightarrow \mathbb{V}_h(K \cup K')$ is the canonical polynomial extension. Here, $K' \in \mathcal{M}_h^g$ denotes a good neighbor of K .

Proposition 4.4.4 (Stability property of R_h^v). *Given $\theta \in (0, 1]$, there exists $C > 0$ such that, for every $K \in \mathcal{M}_h$,*

$$\left\| h^{\frac{1}{2}} D R_h^v(\mathbf{v}_h) \mathbf{n} \right\|_{L^2(\Gamma_K)} \leq C \|D \mathbf{v}_h\|_{L^2(K' \cap \Omega)}, \quad \forall \mathbf{v}_h \in V_h,$$

where $K' \in \mathcal{M}_h^g$ is a good neighbor of K if $K \in \mathcal{M}_h^b$, $K' = K$ if $K \in \mathcal{M}_h^g$.

Proof. We refer the reader to the proof of Theorem 2.3.14. The constant C will depend on \mathbf{F} accordingly to the element choice. \square

As we saw in Section 4.3, due to the unfitted configuration, the Nitsche formulation (4.3) may present some serious instabilities. Our remedy is twofold. On the one hand, we locally change the evaluation of the normal derivatives of the velocities in the weak formulation; on the other, we modify the space of the discrete pressures.

We introduce the following *stabilized pressure space*

$$\overline{Q}_h := \left\{ \varphi_h \in L^2(\Omega) : \exists q_h \in Q_h \text{ such that } \varphi_h|_{\Omega \setminus \overline{S}_h} = q_h|_{\Omega \setminus \overline{S}_h} \text{ and } \varphi_h|_{S_h} = R_h^p(q_h)|_{S_h} \right\}.$$

Remark 4.4.5. Let us stress that, while $\dim \overline{Q}_h \leq \dim Q_h$, in general, we have that \overline{Q}_h is not a subspace of Q_h since its elements are discontinuous functions. However, we observe that the discontinuities are located across the facets in the region of bad elements \overline{S}_h and, for $q_h \in Q_h$ and $R_h^p(q_h) \in \overline{Q}_h$, it holds

$$q_h|_{\Omega \setminus \overline{S}_h} = R_h^p(q_h)|_{\Omega \setminus \overline{S}_h}.$$

Remark 4.4.6. Proposition 4.4.3 entails that $\|\cdot\|_{0,h}$ and $\|\cdot\|_{L^2(\Omega \setminus \overline{S}_h)}$ are equivalent norms on \overline{Q}_h , namely there exist $c_1, c_2 > 0$, independent on h and on the way the mesh is cut by trimming curve, but in general depending on the fixed parameter $\theta \in (0, 1]$, such that

$$c_1 \|q_h\|_{L^2(\Omega \setminus \overline{S}_h)} \leq \|q_h\|_{0,h} \leq c_2 \|q_h\|_{L^2(\Omega \setminus \overline{S}_h)}, \quad \forall q_h \in \overline{Q}_h.$$

Remark 4.4.7. Let $Q_h = \{B_{\mathbf{k}}|_{\Omega} : \mathbf{k} \in \mathbf{K}\}$ and define $\tilde{Q}_h = \{B_{\mathbf{i}}|_{\Omega} : \mathbf{i} \in \mathbf{I}\}$, where $\mathbf{I} := \{\mathbf{i} \in \mathbf{K} : \exists K \in \mathcal{M}_h^g \text{ such that } K \subset \text{supp } B_{\mathbf{i}}\}$. This time \tilde{Q}_h is a subspace of Q_h . Moreover, let us observe that \overline{Q}_h and \tilde{Q}_h are isomorphic (as normed vector spaces) when equipped with $\|\cdot\|_{L^2(\Omega \setminus \overline{S}_h)}$.

We introduce the following stabilized version of formulation (4.3).

Find $(\mathbf{u}_h, p_h) \in V_h \times \overline{Q}_h$ such that

$$\begin{aligned} \bar{a}_h(\mathbf{u}_h, \mathbf{v}_h) + b_1(\mathbf{v}_h, p_h) &= \bar{F}_h(\mathbf{v}_h), & \forall \mathbf{v}_h \in V_h, \\ b_m(\mathbf{u}_h, q_h) &= G_m(q_h), & \forall q_h \in \overline{Q}_h, \end{aligned} \quad (4.9)$$

where $m \in \{0, 1\}$ and

$$\begin{aligned} \bar{a}_h(\mathbf{w}_h, \mathbf{v}_h) &:= \int_{\Omega} D\mathbf{w}_h : D\mathbf{v}_h - \int_{\Gamma_D} DR_h^v(\mathbf{w}_h) \mathbf{n} \cdot \mathbf{v}_h - \int_{\Gamma_D} \mathbf{w}_h \cdot DR_h^v(\mathbf{v}_h) \mathbf{n} \\ &\quad + \gamma \int_{\Gamma_D} \mathbf{h}^{-1} \mathbf{w}_h \cdot \mathbf{v}_h, & \mathbf{w}_h, \mathbf{v}_h \in V_h, \\ \bar{F}_h(\mathbf{v}_h) &:= \int_{\Omega} \mathbf{f} \cdot \mathbf{v}_h + \int_{\Gamma_N} \boldsymbol{\sigma} \cdot \mathbf{v}_h - \int_{\Gamma_D} \mathbf{u}_D \cdot DR_h^v(\mathbf{v}_h) \mathbf{n} + \gamma \int_{\Gamma_D} \mathbf{h}^{-1} \mathbf{u}_D \cdot \mathbf{v}_h, & \mathbf{v}_h \in V_h. \end{aligned}$$

Remark 4.4.8. We believe that this strategy is still consistent with Chapter 2 since the modification does not affect the space of the velocities, but just the one of pressures, the latter being discontinuous objects from a physical point of view.

4.4.2 Interpolation and approximation properties of the discrete spaces

From [75], there exist $\mathbf{E} : \mathbf{H}^t(\Omega) \rightarrow \mathbf{H}^t(\mathbb{R}^d)$, $t \geq 1$, and $E : H^r(\Omega) \rightarrow H^r(\mathbb{R}^d)$, $r \geq 1$, universal (degree-independent) Sobolev-Stein extensions such that $\operatorname{div} \circ \mathbf{E} = E \circ \operatorname{div}$. We define, for $\square \in \{\text{RT}, \text{N}, \text{TH}\}$ and $t \geq 1$,

$$\Pi_{V_h}^{\square} : \mathbf{H}^t(\Omega) \rightarrow V_h^{\square}, \quad \mathbf{v} \mapsto \Pi_{V_{0,h}}^{\square} \left(\mathbf{E}(\mathbf{v}) \Big|_{\Omega_0} \right) \Big|_{\Omega},$$

where $\Pi_{V_{0,h}}^{\square}$ is the spline quasi-interpolant onto $V_{0,h}^{\square}$. Similarly, for the pressures, given $r \geq 1$, we introduce

$$\Pi_{Q_h}^{\square} : H^r(\Omega) \rightarrow Q_h^{\square}, \quad q \mapsto \Pi_{Q_{0,h}}^{\square} \left(E(q) \Big|_{\Omega_0} \right) \Big|_{\Omega},$$

and further compose it with the stabilization operator for the pressures,

$$\bar{\Pi}_{Q_h}^{\square} : H^r(\Omega) \rightarrow \overline{Q}_h^{\square}, \quad q \mapsto R_h^p \left(\Pi_{Q_h}^{\square} q \right),$$

where $\Pi_{Q_{0,h}}^{\square}$ is the spline quasi-interpolant onto $Q_{0,h}^{\square}$. Let us recall that, in the Raviart-Thomas case, $\Pi_{V_{0,h}}^{\text{RT}}$ and $\Pi_{Q_{0,h}}^{\text{RT}}$ are defined so that the first diagram in (4.10) commutes (see [34]). Our construction implies that also the diagram on the right commutes.

$$\begin{array}{ccc} \mathbf{H}(\operatorname{div}; \Omega_0) & \xrightarrow{\operatorname{div}} & L^2(\Omega_0) \\ \downarrow \Pi_{V_{0,h}}^{\text{RT}} & & \downarrow \Pi_{Q_{0,h}}^{\text{RT}} \\ V_{0,h}^{\text{RT}} & \xrightarrow{\operatorname{div}} & Q_{0,h}^{\text{RT}} \end{array} \quad \begin{array}{ccc} \mathbf{H}(\operatorname{div}; \Omega) & \xrightarrow{\operatorname{div}} & L^2(\Omega) \\ \downarrow \Pi_{V_h}^{\text{RT}} & & \downarrow \Pi_{Q_h}^{\text{RT}} \\ V_h^{\text{RT}} & \xrightarrow{\operatorname{div}} & Q_h^{\text{RT}} \end{array} \quad (4.10)$$

Remark 4.4.9. Note that the commutativity of the right-hand diagram in (4.10) is lost when instead of Q_h we use the stabilized space \overline{Q}_h .

Proposition 4.4.10 (Approximation property of R_h^v). *There exists $C > 0$ such that, for every $\mathbf{v} \in \mathbf{H}^t(\Omega)$, $t \geq 2$, and $K \in \mathcal{G}_h$,*

$$\left\| \mathbf{h}^{\frac{1}{2}} D \left(\mathbf{v} - R_h^v(\Pi_{V_h}^{\square} \mathbf{v}) \right) \mathbf{n} \right\|_{L^2(\Gamma_D)} \leq Ch^s \|\mathbf{v}\|_{\mathbf{H}^t(\Omega)},$$

where $s := \min\{k, t-1\}$ if $\square = \text{RT}$ and $s := \min\{k+1, t-1\}$ if $\square \in \{\text{N}, \text{TH}\}$.

Proof. It is sufficient to apply the vectorial version of Proposition 2.3.15 and to sum over the cut elements in \mathcal{G}_h , by taking into account Remark 2.3.16. The constant C depends on \mathbf{F} accordingly to the element choice. \square

Lemma 4.4.11. *There exists $C > 0$ such that*

$$\|\Pi_{V_h} \mathbf{v}\|_{1,h} \leq C \|\mathbf{v}\|_{H^1(\Omega)}, \quad \forall \mathbf{v} \in \mathbf{H}_{0,\Gamma_D}^1(\Omega).$$

Proof. Let $\mathbf{v} \in \mathbf{H}_{0,\Gamma_D}^1(\Omega)$. Using the H^1 -stability for the quasi-interpolant in the boundary-fitted case [34], we have

$$\|\Pi_{V_h} \mathbf{v}\|_{1,h}^2 = \|D\Pi_{V_{0,h}}(\mathbf{E}(\mathbf{v}))\|_{L^2(\Omega)}^2 + \left\| \mathbf{h}^{-\frac{1}{2}} \Pi_{V_{0,h}}(\mathbf{E}(\mathbf{v})) \right\|_{L^2(\Gamma_D)}^2 \quad (4.11)$$

$$\leq C \|\mathbf{E}(\mathbf{v})\|_{H^1(\Omega_0)} + \sum_{K \in \mathcal{G}_h} h_K^{-1} \|\Pi_{V_{0,h}}(\mathbf{E}(\mathbf{v}))\|_{L^2(\Gamma_K)}^2. \quad (4.12)$$

By using $\mathbf{E}(\mathbf{v})|_{\Gamma_D} = 0$, Lemma A.1.2, and the optimal approximation properties of the quasi-interpolants on boundary-fitted meshes, it holds

$$\begin{aligned} \sum_{K \in \mathcal{G}_h} h_K^{-1} \|\Pi_{V_{0,h}}(\mathbf{E}(\mathbf{v}))\|_{L^2(\Gamma_K)}^2 &= \sum_{K \in \mathcal{G}_h} h_K^{-1} \|\Pi_{V_{0,h}}(\mathbf{E}(\mathbf{v})) - \mathbf{E}(\mathbf{v})\|_{L^2(\Gamma_K)}^2 \\ &\leq C \sum_{K \in \mathcal{G}_h} h_K^{-1} \|\Pi_{V_{0,h}}(\mathbf{E}(\mathbf{v})) - \mathbf{E}(\mathbf{v})\|_{L^2(K)} \|\Pi_{V_{0,h}}(\mathbf{E}(\mathbf{v})) - \mathbf{E}(\mathbf{v})\|_{H^1(K)} \\ &\leq C \|\mathbf{E}(\mathbf{v})\|_{H^1(\Omega_0)}^2. \end{aligned} \quad (4.13)$$

We conclude by combining (4.11) and (4.13), and using the boundedness of the Sobolev-Stein extension operator. \square

Theorem 4.4.12. *There exist $C_v, C_q > 0$ such that for every $(\mathbf{v}, q) \in \mathbf{H}^t(\Omega) \times H^r(\Omega)$, $t \geq 1$ and $r \geq 1$, it holds*

$$\left\| \mathbf{v} - \Pi_{V_h}^\square \mathbf{v} \right\|_{1,h} \leq C_v h^s \|\mathbf{v}\|_{H^t(\Omega)}, \quad \|q - \bar{\Pi}_{Q_h} q\|_{0,h} \leq C_q h^\ell \|q\|_{H^r(\Omega)},$$

where $s := \min\{k, t-1\}$ if $\square = \text{RT}$, $s := \min\{k+1, t-1\}$ if $\square \in \{\text{N}, \text{TH}\}$, and $\ell := \min\{k+1, r\}$.

Proof. For the velocities, we proceed by employing the trace inequality of Lemma A.1.2 componentwise, the standard approximation properties of $\Pi_{V_{0,h}}$, and the boundedness of the Sobolev-Stein extension operator.

$$\begin{aligned} \left\| \mathbf{v} - \Pi_{V_h}^\square \mathbf{v} \right\|_{1,h}^2 &\leq \left\| D(\mathbf{E}(\mathbf{v}) - \Pi_{V_{0,h}}^\square \mathbf{E}(\mathbf{v})) \right\|_{L^2(\Omega_0)}^2 \\ &\quad + C \sum_{K \in \mathcal{G}_h} \left\| \mathbf{h}^{-1} (\mathbf{E}(\mathbf{v}) - \Pi_{V_{0,h}}^\square \mathbf{E}(\mathbf{v})) \right\|_{L^2(K)} \left\| \mathbf{E}(\mathbf{v}) - \Pi_{V_{0,h}}^\square \mathbf{E}(\mathbf{v}) \right\|_{H^1(K)} \\ &\leq C h^{2s} \|\mathbf{E}(\mathbf{v})\|_{H^t(\Omega_0)}^2 \\ &\quad + C \sum_{K \in \mathcal{G}_h} \left\| \mathbf{h}^{-1} (\mathbf{E}(\mathbf{v}) - \Pi_{V_{0,h}}^\square \mathbf{E}(\mathbf{v})) \right\|_{L^2(K)} \left\| \mathbf{E}(\mathbf{v}) - \Pi_{V_{0,h}}^\square \mathbf{E}(\mathbf{v}) \right\|_{H^1(K)} \\ &\leq C h^{2s} \|\mathbf{v}\|_{H^t(\Omega)}^2 + \left\| \mathbf{h}^{-1} (\mathbf{E}(\mathbf{v}) - \Pi_{V_h}^\square \mathbf{v}) \right\|_{L^2(\Omega_0)} \left\| \mathbf{E}(\mathbf{v}) - \Pi_{V_h}^\square \mathbf{v} \right\|_{H^1(\Omega_0)} \\ &\leq C h^{2s} \|\mathbf{v}\|_{H^t(\Omega)}^2, \end{aligned}$$

Chapter 4. Stabilized isogeometric discretization of the Stokes problem on trimmed geometries

where $s := \min\{k, t - 1\}$ if $\square = \text{RT}$, $s := \min\{k + 1, t - 1\}$ if $\square \in \{\text{N}, \text{TH}\}$. For the pressure term, we have

$$\|q - \bar{\Pi}_{Q_h} q\|_{0,h}^2 = \|(q - \bar{\Pi}_{Q_h} q)\|_{L^2(\Omega)}^2 + \sum_{K \in \mathcal{G}_h} \left\| h^{\frac{1}{2}} (q - \bar{\Pi}_{Q_h} q) \right\|_{L^2(\Gamma_K)}^2. \quad (4.14)$$

For the volumetric term we may proceed analogously to the case of the velocities. Let us focus on the boundary part of (4.14) and take $K \in \mathcal{M}_h^g$. We employ Lemma A.1.2:

$$\begin{aligned} \left\| h^{\frac{1}{2}} (E(q) - \bar{\Pi}_{Q_h} q) \right\|_{L^2(\Gamma_K)}^2 &\leq C \|E(q) - \Pi_{Q_{0,h}} E(q)\|_{L^2(K)} \|h(E(q) - \Pi_{Q_{0,h}} E(q))\|_{H^1(K)} \\ &\leq Ch^{2\ell} \|E(q)\|_{H^r(\tilde{K})}, \end{aligned}$$

where $\ell := \min\{k + 1, r\}$. Now, let us suppose $K \in \mathcal{M}_h^b$, with $K' \in \mathcal{M}_h^g$ its good neighbor. Let $\varphi \in \mathbb{Q}_k(B_K)$, where B_K is the minimal bounding box enclosing K and K' , so that $R_K^p(\varphi) = \varphi$. We have

$$\begin{aligned} \left\| h^{\frac{1}{2}} (q - \bar{\Pi}_{Q_h} q) \right\|_{L^2(\Gamma_K)} &= \left\| h^{\frac{1}{2}} (q - R_K^p(\Pi_{Q_h} q)) \right\|_{L^2(\Gamma_K)} \\ &\leq \underbrace{\left\| h^{\frac{1}{2}} (q - \varphi) \right\|_{L^2(\Gamma_K)}}_I + \underbrace{\left\| h^{\frac{1}{2}} R_K^p(\varphi - \Pi_{Q_h} q) \right\|_{L^2(\Gamma_K)}}_{II}. \end{aligned}$$

By using Lemma A.1.2, we obtain

$$I \leq C \|E(q) - \varphi\|_{L^2(K)}^{\frac{1}{2}} \|h(E(q) - \varphi)\|_{H^1(K)}^{\frac{1}{2}} \leq C \|E(q) - \varphi\|_{L^2(B_K)}^{\frac{1}{2}} \|h(E(q) - \varphi)\|_{H^1(B_K)}^{\frac{1}{2}}.$$

On the other hand, from Proposition 4.4.3 and triangular inequality we have

$$\begin{aligned} II &= \left\| h^{\frac{1}{2}} R_K^p(\varphi - \Pi_{Q_h} q) \right\|_{L^2(\Gamma_K)} \leq C \|(\varphi - \Pi_{Q_h} q)\|_{L^2(K')} \\ &\leq C \left(\|\varphi - q\|_{L^2(K')} + \|q - \Pi_{Q_h} q\|_{L^2(K')} \right) \\ &\leq C \left(\|\varphi - E(q)\|_{L^2(B_K)} + \|E(q) - \Pi_{0,Q_h}(E(q))\|_{L^2(K')} \right). \end{aligned}$$

Let us choose φ such that the Deny-Lions Lemma (Theorem 3.4.1 of [112]) holds on B_K and use the optimal approximation properties of $\Pi_{Q_{0,h}}$. Thus

$$\left\| h^{\frac{1}{2}} (q - \bar{\Pi}_{Q_h} q) \right\|_{L^2(\Gamma_K)} \leq I + II \leq Ch^\ell \left(\|E(q)\|_{H^r(B_K)} + \|E(q)\|_{H^r(\tilde{K}')} \right), \quad (4.15)$$

where $\ell := \min\{k + 1, r\}$ and C depends on the shape-regularity of B_K (through Theorem 3.4.1 of [112]), on \mathbf{F} , and on the shape-regularity of the parametric Bézier mesh (through the approximation properties of $\Pi_{Q_{0,h}}$). Hence, we conclude by taking the sum over the cut elements. The final constant will depend on k, d , on the constant appearing in (2.7), on the shape-regularity of the parametric mesh, on \mathbf{F} , and on the boundedness of the Sobolev-Stein extension (see also Remark 2.3.16). \square

4.5 Well-posedness of the stabilized formulations

The following result gives the necessary and sufficient conditions for the existence, uniqueness and stability of the solution of (4.9). Let us denote $K_m := \{\mathbf{v}_h \in V_h : b_m(\mathbf{v}_h, q_h) = 0 \quad \forall q_h \in Q_h\}$, for $m = 0, 1$. Even if not explicitly stated in order to keep the notation lighter, the following stability constants are required to be independent of the mesh-size h and on the way \mathcal{M}_h has been cut by Γ_T .

Proposition 4.5.1. *Let us fix $m \in \{0, 1\}$, i.e., we choose either the symmetric or the non-symmetric version of (4.9).*

(i) *There exists $\bar{\gamma} > 0$ such that, for every $\gamma \geq \bar{\gamma}$, there exists $M_a > 0$ such that*

$$|\bar{a}_h(\mathbf{w}_h, \mathbf{v}_h)| \leq M_a \|\mathbf{w}_h\|_{1,h} \|\mathbf{v}_h\|_{1,h}, \quad \forall \mathbf{w}_h, \mathbf{v}_h \in V_h. \quad (4.16)$$

(ii) *There exist $M_{b_1} > 0$, $M_{b_0} > 0$ such that*

$$|b_1(\mathbf{v}_h, q_h)| \leq M_{b_1} \|\mathbf{v}_h\|_{1,h} \|q_h\|_{0,h}, \quad \forall \mathbf{v}_h \in V_h, \forall q_h \in \bar{Q}_h, \quad (4.17)$$

$$|b_0(\mathbf{v}_h, q_h)| \leq M_{b_0} \|\mathbf{v}_h\|_{1,h} \|q_h\|_{0,h}, \quad \forall \mathbf{v}_h \in V_h, \forall q_h \in \bar{Q}_h. \quad (4.18)$$

(iii) *There exist $\bar{\gamma} > 0$ and $\alpha_m > 0$ such that, for every $\gamma \geq \bar{\gamma}$, it holds*

$$\inf_{\mathbf{v}_h \in K_m} \sup_{\mathbf{w}_h \in K_1} \frac{\bar{a}_h(\mathbf{w}_h, \mathbf{v}_h)}{\|\mathbf{w}_h\|_{1,h} \|\mathbf{v}_h\|_{1,h}} \geq \alpha_m, \quad (4.19)$$

and, for all $\mathbf{w}_h \in K_1 \setminus \{0\}$,

$$\sup_{\mathbf{v}_h \in K_m} \bar{a}_h(\mathbf{w}_h, \mathbf{v}_h) > 0. \quad (4.20)$$

(iv) *There exist $\beta_1 > 0$, $\beta_0 > 0$ such that*

$$\inf_{q_h \in \bar{Q}_h} \sup_{\mathbf{v}_h \in V_h} \frac{b_1(\mathbf{v}_h, q_h)}{\|q_h\|_{0,h} \|\mathbf{v}_h\|_{1,h}} \geq \beta_1, \quad (4.21)$$

$$\inf_{q_h \in \bar{Q}_h} \sup_{\mathbf{v}_h \in V_h} \frac{b_0(\mathbf{v}_h, q_h)}{\|q_h\|_{0,h} \|\mathbf{v}_h\|_{1,h}} \geq \beta_0. \quad (4.22)$$

Conditions (i) – (iv) hold if and only if there exists a unique solution $(\mathbf{u}_h, q_h) \in V_h \times \bar{Q}_h$ to (4.9). Moreover,

$$\begin{aligned} \|\mathbf{u}_h\|_{1,h} &\leq \frac{1}{\alpha} \|\bar{F}_h\|_{-1,h} + \frac{1}{\beta_m} \left(\frac{M_a}{\alpha} + 1 \right) \|G_m\|_{-0,h}, \\ \|p_h\|_{0,h} &\leq \frac{1}{\beta_1} \left(1 + \frac{M_a}{\alpha_m} \right) \|\bar{F}_h\|_{-1,h} + \frac{M_a}{\beta_m \beta_1} \left(\frac{M_a}{\alpha_m} + 1 \right) \|G_m\|_{-0,h}, \end{aligned} \quad (4.23)$$

where $\|\cdot\|_{-1,h}$ and $\|\cdot\|_{-0,h}$ denote the dual norms with respect to $\|\cdot\|_{1,h}$ and $\|\cdot\|_{0,h}$, respectively.

Proof. We refer the interested reader to [21, 102]. \square

Remark 4.5.2. We observe that condition (4.20) can be replaced by $\dim K_m = \dim K_1$. If $m = 1$, then conditions (4.19) and (4.20) can be summarized in the coercivity of $\bar{a}_h(\cdot, \cdot)$ on K_1 . Moreover, if $g \equiv 0$, then we are no more bound to satisfy (4.22) when $m = 0$.

Lemma 4.5.3. *There exist $\bar{\gamma} > 0$ and $\alpha > 0$ such that, for every $\gamma \geq \bar{\gamma}$, it holds*

$$\alpha \|\mathbf{v}_h\|_{1,h}^2 \leq \bar{a}_h(\mathbf{v}_h, \mathbf{v}_h), \quad \forall \mathbf{v}_h \in V_h,$$

and, for every $\gamma \geq \bar{\gamma}$, there exists $M_a > 0$ such that

$$|\bar{a}_h(\mathbf{w}_h, \mathbf{v}_h)| \leq M_a \|\mathbf{w}_h\|_{1,h} \|\mathbf{v}_h\|_{1,h}, \quad \forall \mathbf{w}_h, \mathbf{v}_h \in V_h.$$

Proof. This proof is based on Proposition 4.4.4 and follows the same lines of Theorem 2.3.3. \square

During the review process of the manuscript to which this chapter refers (see [111]), we encountered an error in the proof of the conditions (4.21), (4.22). Due to the lack of time, we are compelled to require them in the form of the following assumption. The search for suitable techniques to derive such properties will be the subject of a future study.

Assumption 4.5.4. Given $\theta \in (0, 1]$, there exist $\beta_0 > 0$ and $\beta_1 > 0$ such that

$$\inf_{q_h \in \bar{Q}_h} \sup_{\mathbf{v}_h \in V_h} \frac{b_1(\mathbf{v}_h, q_h)}{\|q_h\|_{0,h} \|\mathbf{v}_h\|_{1,h}} \geq \beta_1, \quad \inf_{q_h \in \bar{Q}_h} \sup_{\mathbf{v}_h \in V_h} \frac{b_0(\mathbf{v}_h, q_h)}{\|q_h\|_{0,h} \|\mathbf{v}_h\|_{1,h}} \geq \beta_0.$$

Section 4.7 includes numerical experiments testing and confirming the validity of Assumption 4.5.4.

Theorem 4.5.5. *Let us require that Assumption 4.5.4 holds. For $m \in \{0, 1\}$, given $\theta \in (0, 1]$, there exists a unique solution $(\mathbf{u}_h, p_h) \in V_h^\square \times \bar{Q}_h$ of (4.9) satisfying the stability estimates (4.23).*

Proof. It suffices to verify the hypotheses of Proposition 4.5.1. Conditions (4.16), (4.19), (4.20) are implied by Lemma 4.5.3. The continuity bounds (4.17), (4.18) readily follow from the definitions of $\|\cdot\|_{1,h}$ and $\|\cdot\|_{0,h}$. Finally, conditions (4.17), (4.18) hold because required by Assumption 4.5.4. \square

4.6 *A priori* error estimates

The goal of this section is to demonstrate that the errors, for both the velocity and pressure fields, achieve optimal *a priori* convergence rates in the topologies induced by the norms $\|\cdot\|_{1,h}$ and $\|\cdot\|_{0,h}$, respectively.

Lemma 4.6.1. *Let us require that Assumption 4.5.4 holds. Let $(\mathbf{u}, p) \in \mathbf{H}^{\frac{3}{2}+\varepsilon}(\Omega) \times H^1(\Omega)$, $\varepsilon > 0$, and $(\mathbf{u}_h, p_h) \in V_h \times \bar{Q}_h$ be the solutions of (4.2) and (4.9) with $m \in \{0, 1\}$. Then, for every $(\mathbf{u}_I, p_I) \in V_h \times \bar{Q}_h$ the following estimates hold.*

$$\begin{aligned} \|\mathbf{u}_h - \mathbf{u}_I\|_{1,h} &\leq \frac{1}{\alpha} \left(M_a \|\mathbf{u} - \mathbf{u}_I\|_{1,h} + \left\| \mathbf{h}^{\frac{1}{2}} D(\mathbf{u} - R_h^v(\mathbf{u}_I)) \mathbf{n} \right\|_{L^2(\Gamma_D)} + M_{b_1} \|p - p_I\|_{0,h} \right) \\ &\quad + \frac{1}{\beta_m} \left(1 + \frac{M_a}{\alpha} \right) M_{b_m} \|\mathbf{u} - \mathbf{u}_I\|_{1,h}, \\ \|p_h - p_I\|_{0,h} &\leq \frac{1}{\beta_1} \left(1 + \frac{M_a}{\alpha} \right) \left(M_a \|\mathbf{u} - \mathbf{u}_I\|_{1,h} + \left\| \mathbf{h}^{\frac{1}{2}} D(\mathbf{u} - R_h^v(\mathbf{u}_I)) \mathbf{n} \right\|_{L^2(\Gamma_D)} \right. \\ &\quad \left. + M_{b_1} \|p - p_I\|_{0,h} \right) + \frac{M_a}{\beta_m \beta_1} \left(1 + \frac{M_a}{\alpha} \right) M_{b_m} \|\mathbf{u} - \mathbf{u}_I\|_{1,h}. \end{aligned}$$

Proof. Let $m \in \{0, 1\}$ and $(\mathbf{u}_I, p_I) \in V_h \times \bar{Q}_h$ be arbitrary. By linearity $(\mathbf{u}_h - \mathbf{u}_I, p_h - p_I) \in V_h \times \bar{Q}_h$ satisfies the saddle point problem

$$\begin{aligned} \bar{a}_h(\mathbf{u}_h - \mathbf{u}_I, \mathbf{v}_h) + b_1(\mathbf{v}_h, p_h - p_I) &= F_I(\mathbf{v}_h), \quad \forall \mathbf{v}_h \in V_h, \\ b_m(\mathbf{u}_h - \mathbf{u}_I, q_h) &= G_{I,m}(q_h), \quad \forall q_h \in \bar{Q}_h, \end{aligned} \tag{4.24}$$

where

$$\begin{aligned} F_I(\mathbf{v}_h) &:= \int_{\Omega} (D(\mathbf{u} - \mathbf{u}_I) : D\mathbf{v}_h - \int_{\Gamma_D} D(\mathbf{u} - R_h^v(\mathbf{u}_I)) \mathbf{n} \cdot \mathbf{v}_h + b_1(\mathbf{v}_h, p - p_I) \\ &\quad - \int_{\Omega} (\mathbf{u} - \mathbf{u}_I) \cdot DR_h^v(\mathbf{v}_h) \mathbf{n} + \gamma \int_{\Gamma_D} \mathbf{h}^{-1} (\mathbf{u} - \mathbf{u}_I) \cdot \mathbf{v}_h, \quad \mathbf{v}_h \in V_h, \\ G_{I,m}(q_h) &:= b_m(\mathbf{u} - \mathbf{u}_I, q_h), \quad q_h \in \bar{Q}_h. \end{aligned}$$

For the sake of completeness, let us show the first line of (4.24). Note that the second line follows immediately. Recall from (4.2) and (4.3) that $F(\mathbf{v}_h) = \int_{\Omega} D\mathbf{u} : D\mathbf{v}_h - \int_{\Gamma_D} D\mathbf{u}\mathbf{n} \cdot \mathbf{v}_h + b_1(\mathbf{v}_h, p)$ and $\mathbf{u}|_{\Gamma_D} = \mathbf{u}_D$. Hence

$$\begin{aligned} \bar{a}_h(\mathbf{u}_h - \mathbf{u}_I, \mathbf{v}_h) + b_1(\mathbf{v}_h, p_h - p_I) &= \bar{F}_h(\mathbf{v}_h) - \bar{a}_h(\mathbf{u}_I, \mathbf{v}_h) - b_1(\mathbf{v}_h, p_I) \\ &= F(\mathbf{v}_h) - \int_{\Omega} \mathbf{u}_D \cdot DR_h^v(\mathbf{v}_h)\mathbf{n} + \gamma \int_{\Gamma_D} \mathbf{h}^{-1} \mathbf{u}_D \cdot \mathbf{v}_h - \int_{\Omega} D\mathbf{u}_I : D\mathbf{v}_h \\ &\quad + \int_{\Gamma_D} DR_h^v(\mathbf{u}_I)\mathbf{n} \cdot \mathbf{v}_h + \int_{\Gamma_D} \mathbf{u}_I \cdot DR_h^v(\mathbf{v}_h)\mathbf{n} - \gamma \int_{\Gamma_D} \mathbf{h}^{-1} \mathbf{u}_I \cdot \mathbf{v}_h - b_1(\mathbf{v}_h, p_I) \\ &= \int_{\Omega} D(\mathbf{u} - \mathbf{u}_I) : D\mathbf{v}_h - \int_{\Gamma_D} D(\mathbf{u} - R_h^v(\mathbf{u}_I))\mathbf{n} \cdot \mathbf{v}_h + b_1(\mathbf{v}_h, p - p_I) \\ &\quad - \int_{\Gamma_D} (\mathbf{u} - \mathbf{u}_I) \cdot DR_h^v(\mathbf{v}_h)\mathbf{n} + \gamma \int_{\Gamma_D} \mathbf{h}^{-1} (\mathbf{u} - \mathbf{u}_I) \cdot \mathbf{v}_h. \end{aligned}$$

Using the stability estimates (4.23), respectively for $m = 0, 1$, we get

$$\begin{aligned} \|\mathbf{u}_h - \mathbf{u}_I\|_{1,h} &\leq \frac{1}{\alpha} \|F_I\|_{-1,h} + \frac{1}{\beta_m} \left(1 + \frac{M_a}{\alpha}\right) \|G_{I,m}\|_{-0,h}, \\ \|p_h - p_I\|_{0,h} &\leq \frac{1}{\beta_1} \left(1 + \frac{M_a}{\alpha}\right) \|F_I\|_{-1,h} + \frac{M_a}{\beta_m \beta_1} \left(1 + \frac{M_a}{\alpha}\right) \|G_{I,m}\|_{-0,h}. \end{aligned}$$

We conclude since, by definition of dual norm, we have

$$\begin{aligned} \|F_I\|_{-1,h} &\leq M_a \|\mathbf{u} - \mathbf{u}_I\|_{1,h} + \left\| \mathbf{h}^{\frac{1}{2}} D(\mathbf{u} - R_h^v(\mathbf{u}_I))\mathbf{n} \right\|_{L^2(\Gamma_D)} + M_{b_1} \|p - p_I\|_{0,h}, \\ \|G_{I,m}\|_{-0,h} &\leq M_{b_m} \|\mathbf{u} - \mathbf{u}_I\|_{1,h}. \end{aligned}$$

□

Theorem 4.6.2. *Let us require that Assumption 4.5.4 holds. Let $(\mathbf{u}, p) \in \mathbf{H}^t(\Omega) \times H^r(\Omega)$, $t \geq 2$ and $r \geq 1$, be the solution to problem (4.2). Then, the discrete solution $(\mathbf{u}_h, p_h) \in V_h^\square \times \bar{Q}_h$ of the stabilized problem (4.9) satisfies*

$$\|\mathbf{u} - \mathbf{u}_h\|_{1,h} + \|p - p_h\|_{0,h} \leq C_m h^{\min\{s, \ell\}} \left(\|\mathbf{u}\|_{H^t(\Omega)} + \|p\|_{H^r(\Omega)} \right),$$

where $s := \min\{k, t-1\}$ if $\square = \text{RT}$, $s := \min\{k+1, t-1\}$ if $\square = \text{N}$, and $\ell := \min\{k+1, r\}$, and $C_m > 0$ depends on the choice $m \in \{0, 1\}$ through the constants appearing in Lemma 4.6.1.

Proof. Given $(\mathbf{u}_I, p_I) \in V_h^\square \times \bar{Q}_h$, we proceed by triangular inequality:

$$\|\mathbf{u} - \mathbf{u}_h\|_{1,h} \leq \|\mathbf{u} - \mathbf{u}_I\|_{1,h} + \|\mathbf{u}_h - \mathbf{u}_I\|_{1,h}, \quad (4.25)$$

$$\|p - p_h\|_{0,h} \leq \|p - p_I\|_{0,h} + \|p_h - p_I\|_{0,h}. \quad (4.26)$$

Using Lemma 4.6.1, we obtain

$$\begin{aligned} \|\mathbf{u} - \mathbf{u}_h\|_{1,h} &\leq \|\mathbf{u} - \mathbf{u}_I\|_{1,h} + \frac{1}{\alpha} \left(M_a \|\mathbf{u} - \mathbf{u}_I\|_{1,h} + \left\| \mathbf{h}^{\frac{1}{2}} D(\mathbf{u} - R_h^v(\mathbf{u}_I))\mathbf{n} \right\|_{L^2(\Gamma_D)} \right. \\ &\quad \left. + M_{b_1} \|p - p_I\|_{0,h} \right) + \frac{1}{\beta_m} \left(1 + \frac{M_a}{\alpha}\right) M_{b_m} \|\mathbf{u} - \mathbf{u}_I\|_{1,h}, \\ \|p - p_h\|_{0,h} &\leq \|p_h - p_I\|_{0,h} + \frac{1}{\beta_1} \left(1 + \frac{M_a}{\alpha}\right) \left(M_a \|\mathbf{u} - \mathbf{u}_I\|_{1,h} + \left\| \mathbf{h}^{\frac{1}{2}} D(\mathbf{u} - R_h^v(\mathbf{u}_I))\mathbf{n} \right\|_{L^2(\Gamma_D)} \right. \\ &\quad \left. + M_{b_1} \|p - p_I\|_{0,h} \right) + \frac{M_a}{\beta_m \beta_1} \left(1 + \frac{M_a}{\alpha}\right) M_{b_m} \|\mathbf{u} - \mathbf{u}_I\|_{1,h}. \end{aligned}$$

Let us choose $\mathbf{u}_I := \Pi_{V_h}^\square \mathbf{u}$ and $p_I := \bar{\Pi}_{Q_h} p$ so that, by Proposition 4.4.10 and Theorem 4.4.12, we obtain

$$\begin{aligned} \|\mathbf{u} - \mathbf{u}_h\|_{1,h} &\leq C_v h^s \|\mathbf{u}\|_{H^t(\Omega)} + \frac{1}{\alpha} \max\{M_a, 1, M_{b_1}\} C h^{\min\{s, \ell\}} \left(\|\mathbf{u}\|_{H^t(\Omega)} + \|p\|_{H^r(\Omega)} \right) \\ &\quad + \frac{1}{\beta_m} \left(1 + \frac{M_a}{\alpha} \right) M_{b_m} C_v h^s \|\mathbf{u}\|_{H^t(\Omega)}, \\ \|p - p_h\|_{0,h} &\leq C_q h^\ell \|p\|_{H^r(\Omega)} \\ &\quad + \frac{1}{\beta_1} \left(1 + \frac{M_a}{\alpha} \right) \max\{M_a, 1, M_{b_1}\} C h^{\min\{s, \ell\}} \left(\|\mathbf{u}\|_{H^t(\Omega)} + \|p\|_{H^r(\Omega)} \right) \\ &\quad + \frac{M_a}{\beta_m \beta_1} \left(1 + \frac{M_a}{\alpha} \right) M_{b_m} C_v h^s \|\mathbf{u}\|_{H^t(\Omega)}. \end{aligned}$$

□

4.7 Numerical tests

The main goal of the following numerical experiments is to validate the convergence results of the Theorem 4.6.2 and to validate the inf-sup condition that we have not been able to prove theoretically.

To prevent the conditioning number of the linear system from being excessively corrupted by the presence of basis functions whose support barely intersects the physical domain, a left-right Jacobi preconditioner is employed. This approach helps for improving the conditioning, but, as previously discussed in Chapter 2, does not completely solve the problem of its dependence on the trimming configuration. A more sophisticated approach has been proposed in [49].

4.7.1 Pentagon

Let us consider as computational domain the pentagon $\Omega = \Omega_0 \setminus \bar{\Omega}_1$, where $\Omega_0 = \hat{\Omega}_0$ and Ω_1 is the triangle of vertices $(0, 0.25 + \varepsilon) - (0, 1) - (0.75 - \varepsilon, 1)$ as illustrated in Figure 4.1(b). Here $\varepsilon = 10^{-13}$. The following functions are chosen as manufactured solutions for the velocity and pressure fields:

$$\mathbf{u} = \left(xy^3, x^4 - \frac{y^4}{4} \right), \quad p = p_{\text{fun}} - \frac{1}{|\Omega|} \int_{\Omega} p_{\text{fun}}, \quad \text{where } p_{\text{fun}} = x^3 \cos(x) + y^2 \sin(x).$$

Dirichlet boundary conditions are weakly enforced on the boundary sides unfitted with the mesh, while on the rest, they are imposed in the strong sense (we recall from Remark 4.2.2 that, for the Raviart-Thomas and Nédélec element, we need to impose the tangential components in a weak sense). We compare, for different isogeometric elements, the well-posedness and accuracy of the non-symmetric, *i.e.*, with $m = 0$, non-stabilized and stabilized formulations, (4.3) and (4.9) respectively, for $k = 2$ and $\gamma = 20(k+1)^2$ (the dependency of the penalty parameter on the degree is coherent with [57]). The threshold parameter θ is set equal to 1, *i.e.*, all cut elements are stabilized.

In Table 4.1 we see the values of the inf-sup constants β_0 , β_1 , computed as in [15], in the non-stabilized and stabilized cases (subscripts *ns* and *s* respectively) for the different choices of the isogeometric element (superscripts RT, N and TH). In the stabilized case, we observe that the inf-sup constants lost their dependence on how the mesh is trimmed. In Figure 4.4 the accuracy

of the non-stabilized and stabilized formulations are compared. We observe a clear improvement in the pressure error between the non-stabilized and the stabilized case.

h	2^{-1}	2^{-2}	2^{-3}	2^{-4}	2^{-5}	2^{-6}
$\beta_{0,ns}^{RT}$	0.2437	1.6450e-07	2.3014e-07	3.2638e-07	4.6166e-07	6.5221e-07
$\beta_{1,ns}^{RT}$	0.2699	2.8358e-07	3.9759e-07	5.5849e-07	7.8738e-07	1.1108e-06
$\beta_{0,s}^{RT}$	0.4103	0.1740	0.2032	0.1850	0.1588	0.1635
$\beta_{1,s}^{RT}$	0.3923	0.2088	0.2397	0.2440	0.2441	0.2442
$\beta_{0,ns}^N$	0.2714	1.6541e-07	2.3212e-07	3.2900e-07	4.6583e-07	6.5811e-07
$\beta_{1,ns}^N$	0.3178	3.6259e-07	5.0472e-07	7.0780e-07	9.9752e-07	1.4077e-06
$\beta_{0,s}^N$	0.4142	0.2430	0.2902	0.2803	0.2809	0.2676
$\beta_{1,s}^N$	0.4118	0.2564	0.2979	0.3089	0.3096	0.3096
$\beta_{0,ns}^{TH}$	0.2672	1.6728e-07	2.3504e-07	3.3295e-07	4.7052e-07	4.7052e-07
$\beta_{1,ns}^{TH}$	0.2768	4.8359e-07	6.8222e-07	9.6265e-07	1.3581e-06	1.9189e-06
$\beta_{0,s}^{TH}$	0.3374	0.2836	0.2853	0.2853	0.2853	0.2853
$\beta_{1,s}^{TH}$	0.2994	0.2755	0.2789	0.2802	0.2807	0.2809

Table 4.1 – Inf-sup constant for the *pentagon*: stabilized vs non-stabilized formulations with $k = 2$.

4.7.2 Mapped pentagon

Let us perform an experiment similar to the previous one, this time with a non-linear isogeometric mapping \mathbf{F} . We consider $\Omega = \Omega_0 \setminus \bar{\Omega}_1$, where $\Omega_0 = \mathbf{F}((0,1)^2)$ is the quarter of annulus parametrized by a biquadratic NURBS \mathbf{F} , and $\Omega_1 = \mathbf{F}(T)$, with T the triangle with vertices $(0, 0.25 + \varepsilon)$, $(0, 1)$, $(0.75 - \varepsilon, 1)$, see Figure 4.6(a). We compare the inf-sup stability of the non-stabilized and the stabilized formulations (4.3) and (4.9) respectively, for different degrees and isogeometric elements, $\theta = 1$ (we stabilize at all cut elements), and $\varepsilon = 10^{-13}$. Dirichlet boundary conditions are imposed on the whole boundary, weakly on the unfitted parts. From Figure 4.5 we observe that the inf-sup constants of the stabilized formulation behave much better than the ones of the non-stabilized formulation. The order of magnitude of the inf-sup constants in the non-stabilized case are of the same order of the ones in Table 4.1.

4.7.3 Rotating square

Let us consider the same geometrical setting of Test C3 in Section 2.4.4. We embed $\Omega = (0.19, 0.71) \times (0.19, 0.71)$ into $\Omega_0 = (0, 1)^2$, the latter subdivided with a Cartesian grid of 8 elements per direction, and rotate Ω around its barycenter for different angles α , as illustrated in Figure 4.6(b). We choose a threshold parameter $\theta = 0.75$, and, for each angle $\alpha \in \{i \frac{\pi}{200} : i = 0, \dots, 100\}$, we compute the inf-sup constants β_0 and β_1 in the stabilized and non-stabilized cases. For every configuration we compute $\eta := \min_{K \in \mathcal{M}_h} |K \cap \Omega|$ and in Figure 4.7 we plot the inf-sup constants with respect to η for the Raviart-Thomas, the Nédélec, and the Taylor-Hood elements of degree $k = 2$. In most configurations, we can observe that the constants corresponding to the stabilized formulation perform better than those of the non-stabilized formulation, specially for small values of η .

Furthermore, we notice a greater efficiency, *i.e.*, a greater difference between stabilized and non-stabilized cases, when using the Taylor-Hood element. The configurations corresponding to a smaller η do not necessarily give rise to a worse inf-sup constant. Although stabilization does not

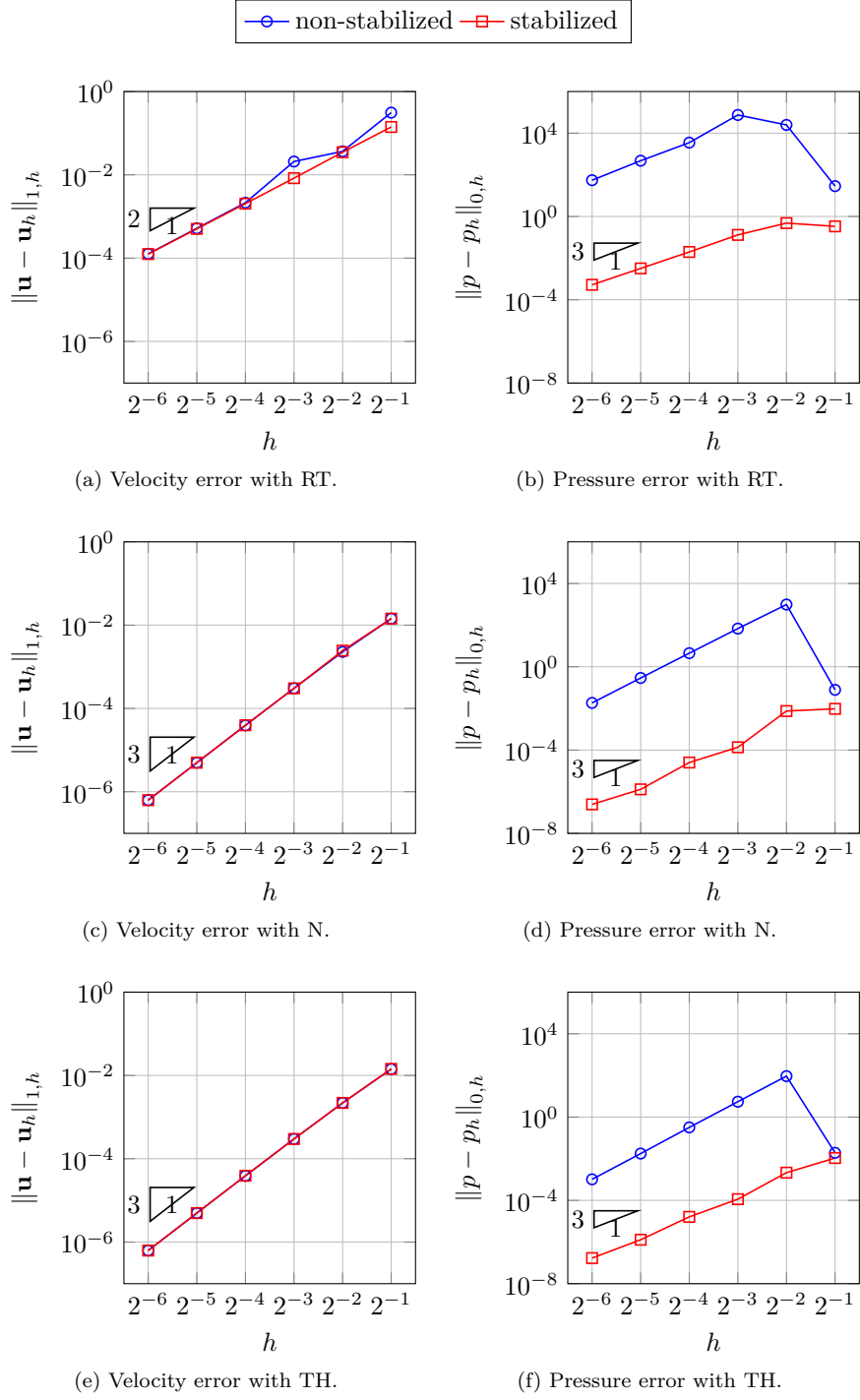


Figure 4.4 – Convergence errors for the *pentagon* with $k = 2$.

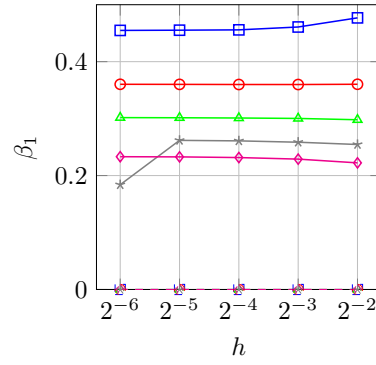
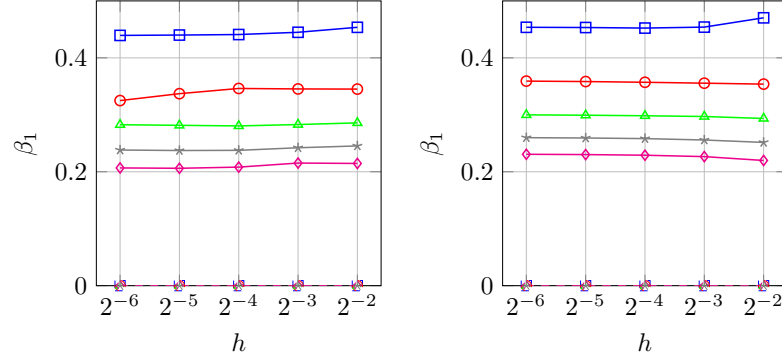
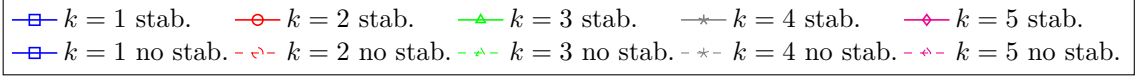
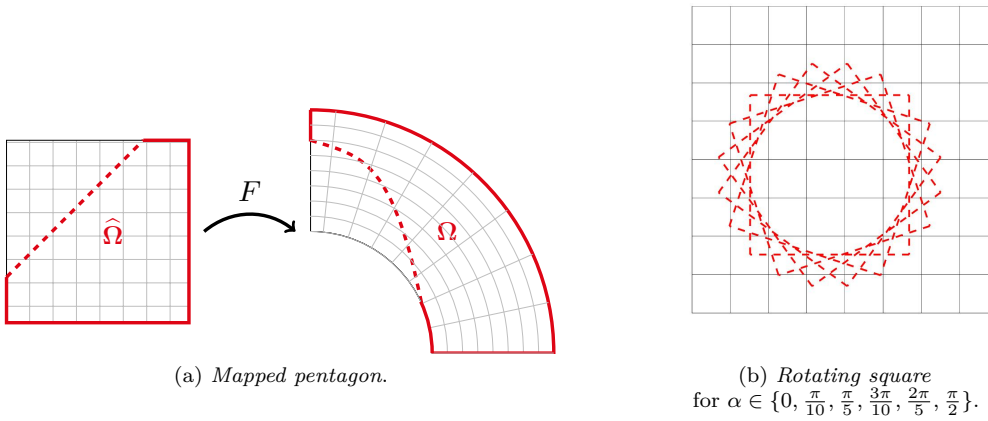

 Figure 4.5 – Inf-sup constant for the *mapped pentagon*.


Figure 4.6 – Trimmed domains.

always seem to "beat" the non-stabilized method, we observe that the configurations in which the non-stabilized inf-sup constant is greater than the stabilized one are, in general, the ones with bigger values of η , which are not the most critical ones.

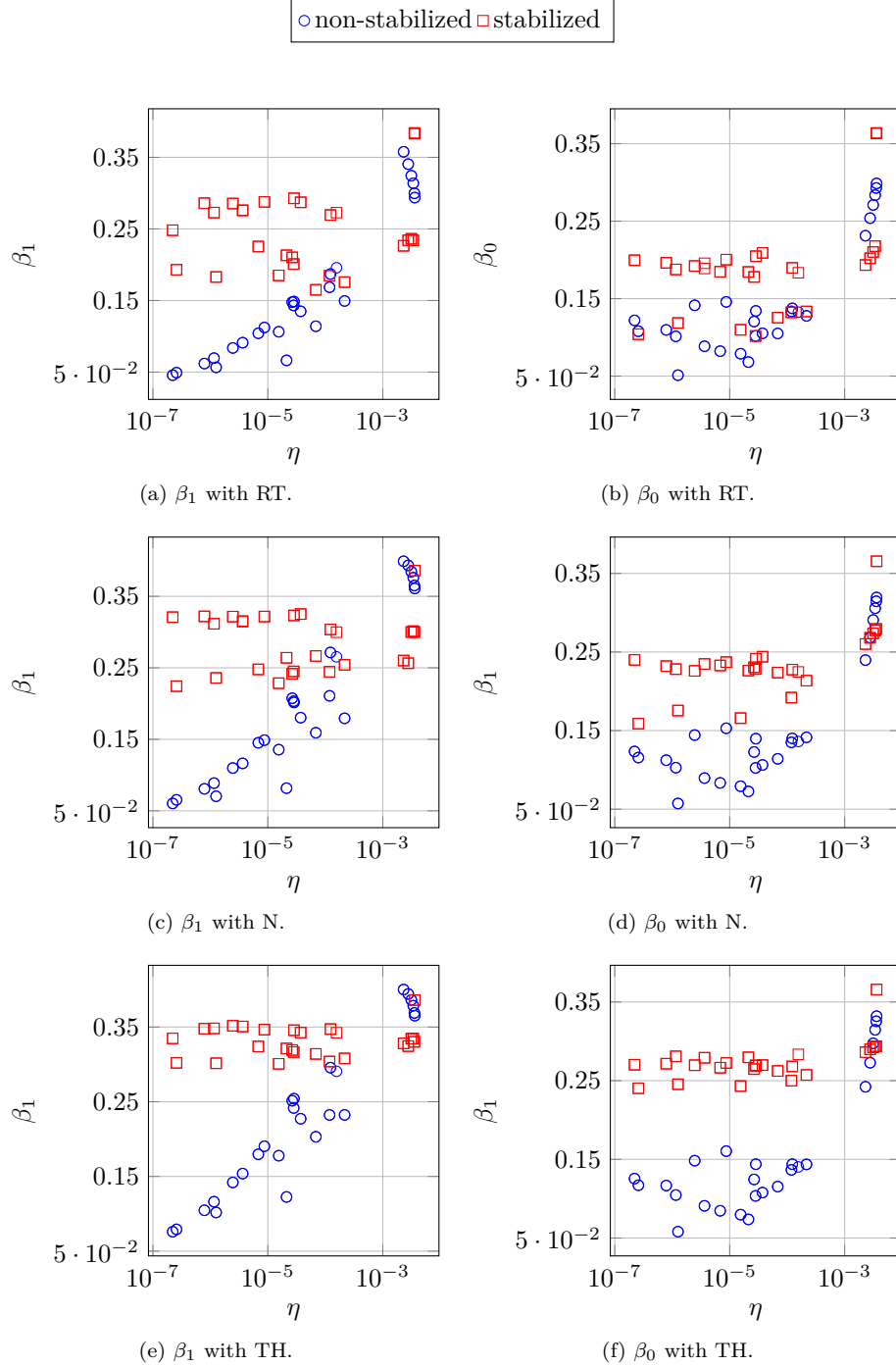


Figure 4.7 – Inf-sup constants vs. the measure of the “smallest cut element”.

4.7.4 Square with circular trimming

Let us set up another numerical experience where the physical domain is $\Omega = \Omega_0 \setminus \overline{\Omega}_1$ with $\Omega_0 = (0, 2) \times (0, 2)$ and $\Omega_1 = B(0, r)$, $r = 0.52$, as depicted in Figure 4.8(a). We take as reference solution fields

$$\mathbf{u} = \left(2y^3 \sin(x), x^3 \sin(x) - \frac{y^4 \cos(x)}{2} - 3x^2 \cos(x) \right), \quad p = \frac{x^3 y^2}{2} + \frac{y^3}{2},$$

where \mathbf{u} is a solenoidal vector field. We impose Neumann boundary conditions on the straight trimmed sides $\{(0, y) : 0 \leq y \leq 2\}$, $\{(x, 0) : 0 \leq x \leq 2\}$ and on the rest of the boundary we impose Dirichlet boundary conditions, enforced in a weak sense on $\{(r \cos \theta, r \sin \theta) : 0 \leq \theta \leq \frac{\pi}{2}\}$. We

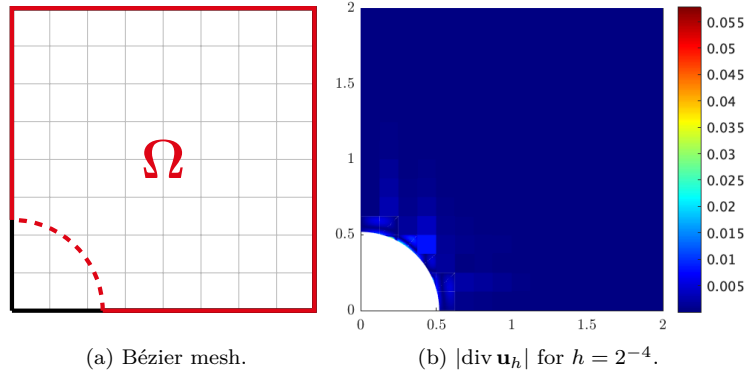


Figure 4.8 – Square with circular trimming.

solve using the non-symmetric stabilized formulation (4.9), discretized with the Raviart-Thomas element, with different degrees $k = 1, 2, 3, 4, 5$, penalty parameter $\gamma = 10(k + 2)^2$, and threshold parameter $\theta = 1$. The convergence results, validating the error estimates of Theorem 4.6.2, are shown in Figure 4.9, while the divergence of the discrete velocity field \mathbf{u}_h , for $k = 3$ and $h = 2^{-4}$, has been plotted in Figure 4.8(b). As already observed in Remark 4.4.9, our numerical scheme does not preserve exactly the incompressibility constraint since $\operatorname{div} V_h^{\text{RT}} \not\subset \overline{Q}_h$. From Figure 4.8(b), we can observe that the divergence of the numerical solution for the velocity is polluted in the vicinity of the trimmed boundary.

4.7.5 Stokes flow around a cylinder

We consider a classic benchmark example in computational fluid dynamics, *i.e.*, the so-called two-dimensional *flow around a cylinder*, proposed by [16] and already seen in the context of immersogeometric methods in [76]. The incompressible flow of a fluid around a cylinder placed in a channel is studied. The physical domain is $\Omega = \Omega_0 \setminus \overline{\Omega}_1$, where $\Omega_0 = (0, L) \times (0, H)$ and $\Omega_1 = B(x_0, R)$ with $L = 2.2$, $H = 0.41$, $x_0 = (0.2, 0.2)$ and $R = 0.05$. Let us observe that Ω_1 is not symmetric with respect to Ω_0 . As Dirichlet boundary condition on the inflow boundary $\{(0, y) : 0 \leq y \leq H\}$ a parabolic horizontal profile is prescribed:

$$\mathbf{u}(0, y) = \begin{pmatrix} 4U_m y(H - y)/H^2 \\ 0 \end{pmatrix},$$

where $U_m = 0.3$ is the maximum magnitude of the velocity field. Stress free boundary conditions, *i.e.*, $\mathbf{u}_N = \mathbf{0}$, are imposed on the outflow boundary $\{(L, y) : 0 \leq y \leq H\}$, while no slip boundary

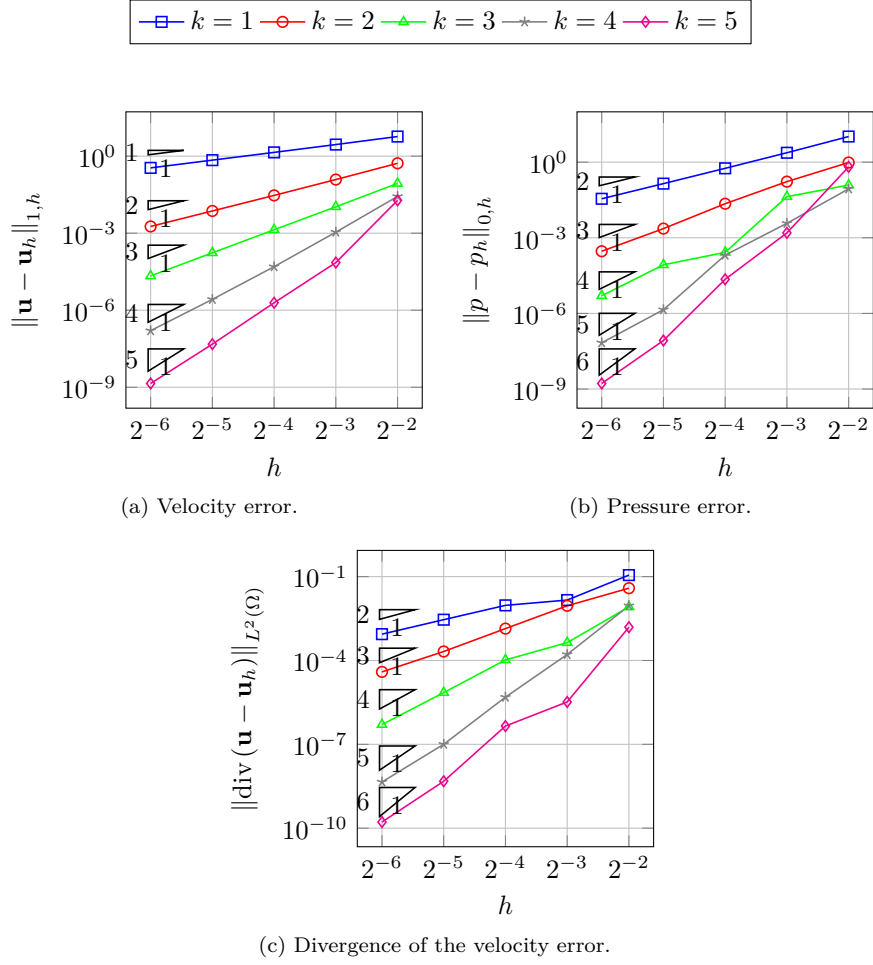


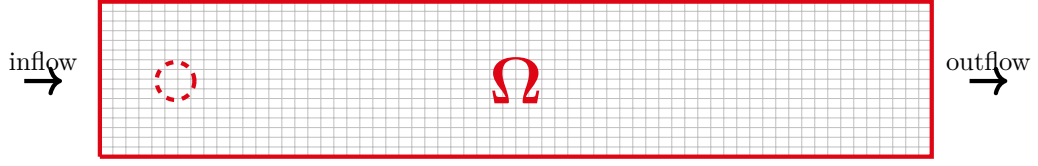
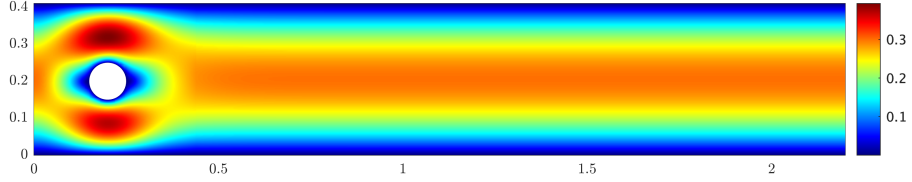
Figure 4.9 – Convergence errors for the *Square with circular trimming* with the Raviart-Thomas element.

conditions are imposed on the rest of the boundary. No external forces act on the fluid flow, *i.e.*, $\mathbf{f} = \mathbf{0}$.

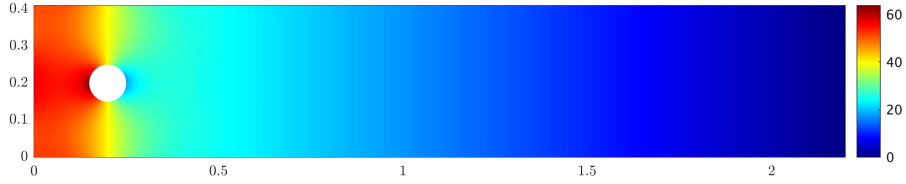
Let us set $k = 3$, $\gamma = 10(k+1)^2$ and consider the mesh configuration depicted in Figure 4.10, with 2^6 elements in the x -direction and 2^4 elements in the y -direction. In Figure 4.11 we show the magnitude of the velocity field and the pressure in the case of the stabilized formulation (4.3) for $m = 0$ with the Nédélec isogeometric element. Note that both the velocity and pressure fields do not show any spurious oscillations around the trimmed part of the boundary and seem to comply with their physical meaning.

4.7.6 Lid-driven cavity

The lid-driven cavity is another important benchmark for the Stokes problem where the incompressible flow in a confined volume is driven by the tangential in-plane motion of two opposite bounding walls [67, 129]. Here, the cavity is represented by the trimmed domain $\Omega = (-1, 1) \times (-3, 3)$ immersed in Ω_0 . Ω_0 is the rectangle with vertices $(-3, -3.5)$, $(3, -3.5)$, $(3, 3.5)$, $(-3, 3.5)$ rotated of $\frac{\pi}{6}$ counterclockwise around the origin. No-slip Dirichlet boundary conditions are imposed on

Figure 4.10 – Bézier mesh for the *flow around a cylinder*.

(a) Magnitude of the velocity.



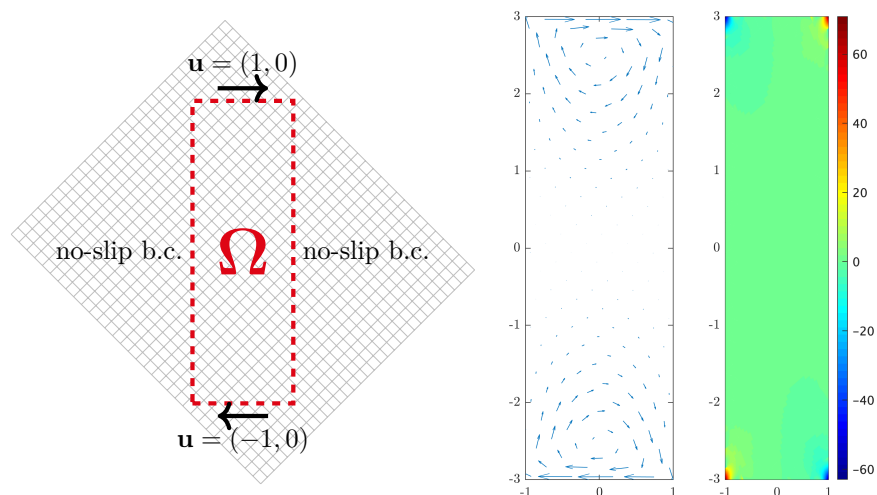
(b) Pressure.

Figure 4.11 – Numerical solutions of the non-symmetric stabilized formulation (4.9) for the *flow around a cylinder* with the Nédélec element.

the left and right sides of the cavity, while the top and bottom ones are walls sliding, respectively, to the right and left with unitary velocity magnitude, namely we enforce the non-homogenous Dirichlet boundary conditions

$$\mathbf{u}(x, 3) = \begin{pmatrix} 1 \\ 0 \end{pmatrix} \quad \text{on} \quad \{(x, 3) : x \in [-1, 1]\}, \quad \mathbf{u}(x, -3) = \begin{pmatrix} -1 \\ 0 \end{pmatrix} \quad \text{on} \quad \{(x, -3) : x \in [-1, 1]\}.$$

Since the Dirichlet boundary conditions have a jump at the corners, the trace of the solution for the velocity does not belong to $\mathbf{H}^{\frac{1}{2}}(\Gamma)$, hence $\mathbf{u} \notin \mathbf{H}^1(\Omega)$. The applied body force is $\mathbf{f} = \mathbf{0}$. We solve the problem by using the non-symmetric stabilized formulation (4.9), discretized using the Taylor-Hood element, with degree $k = 2$, penalty parameter $\gamma = 30(k + 1)^2$ and mesh-sizes $h_x = h_y = 2^{-5}$ along the first and second parametric directions respectively. The mesh employed for the numerical simulation is depicted in Figure 4.12(a). In Figures 4.12(b), 4.12(c) the numerical solutions for the velocity and the pressures are plotted: our results are qualitatively in accordance with the ones of [28, 67].



(a) Bézier mesh for the *lid-driven cavity*.

(b) Velocity.

(c) Pressure.

Figure 4.12 – Numerical solutions of the non-symmetric stabilized formulation (4.9) for the *lid-driven cavity* with the Taylor-Hood element.

5 Stabilized isogeometric discretization of the Stokes problem on union geometries

This chapter considers the isogeometric discretization of the Stokes problem in geometries obtained through a union operation. The computational domain is described as a collection of spline patches overlapping each other according to a fixed hierarchy. The discretization of the problem is based on the weak imposition of transmission conditions between the domain interfaces through the Nitsche method. As in the previous chapters, suitable strategies to address the integration, conditioning, and stability issue need to be provided. Still, the construction of integration routines in the cut elements and the design of a robust preconditioning strategy take a back seat in this chapter. As before, we borrow the integration technique of [4] and apply a simple left-right diagonal preconditioner to the resulting linear system. Our focus is instead the search for an appropriate stabilization technique.

Our numerical scheme is based on the combination of the techniques developed in Chapters 3 and 4. In particular, we stabilize the evaluation of the normal derivatives of the velocity at the interface and modify the space of the pressure corresponding to the “bad” cut elements. Under the assumption that some local inf-sup conditions hold for every patch, we prove the well-posedness of the stabilized formulation and optimal *a priori* error estimates.

Let us sketch the outline of the chapter. In Section 5.1, we introduce the notation and the geometrical setting. Section 5.2 is devoted to the proofs of stability and convergence of the method. Finally, in Section 5.3 we present some numerical experiments confirming the theoretical results.

5.1 Parametrization, mesh and approximation spaces for domains obtained via union operations

Throughout this section, we will briefly recall some of the notations already defined in Sections 1.3, 3.1. Hence we refer the reader to that part of the manuscript for more details.

Let $\Omega_i^* \subset \mathbb{R}^d$, $0 \leq i \leq N$, with $N \in \mathbb{N}$, $d \in \{2, 3\}$, be spline patches, *i.e.*, $\Omega_i^* = \mathbf{F}_i(\widehat{\Omega})$, where $\mathbf{F}_i \in \left(S_{\alpha_1^i, \dots, \alpha_d^i}^{\mathbf{p}^i}(\Xi^i) \right)^d$ and, as usual, $\widehat{\Omega} := (0, 1)^d$, for given degree vector \mathbf{p}^i , regularity indices $\alpha_1^i, \dots, \alpha_d^i$, and knot-vector at the coarsest level of discretization Ξ^i . Hence, each patch has an

Chapter 5. Stabilized isogeometric discretization of the Stokes problem on union geometries

underlying Bézier mesh \mathcal{M}_i^* , naturally induced by the map \mathbf{F}_i . For every $0 \leq i \leq N$, we define

$$\begin{aligned} V_{h,i}^{*,\text{RT}} &:= \{\mathbf{v}_h : \iota_v^i(\mathbf{v}_h) \in \widehat{V}_{0,h}^{\text{RT}}\}, & V_{h,i}^{*,\text{N}} &:= \{\mathbf{v}_h : \iota_v^i(\mathbf{v}_h) \in \widehat{V}_{0,h}^{\text{N}}\}, & V_{h,i}^{*,\text{TH}} &:= \{\mathbf{v}_h : \mathbf{v}_h \circ \mathbf{F}_i \in \widehat{V}_{0,h}^{\text{TH}}\}, \\ Q_{h,i}^{*,\text{RT}} = Q_{h,i}^{*,\text{N}} &:= \{q_h : \iota_p^i(q_h) \in \widehat{Q}_{0,h}\}, & Q_{h,i}^{*,\text{TH}} &:= \{q_h : q_h \circ \mathbf{F}_i \in \widehat{Q}_{0,h}\}, \end{aligned}$$

and the *Piola transformations*

$$\begin{aligned} \iota_v^i : \mathbf{H}(\text{div}; \Omega_i^*) &\rightarrow \mathbf{H}(\text{div}; \widehat{\Omega}), & \iota_v^i(\mathbf{v}) &:= \det(D\mathbf{F}_i) D\mathbf{F}_i^{-1}(\mathbf{v} \circ \mathbf{F}_i), \\ \iota_p^i : L^2(\Omega_i^*) &\rightarrow L^2(\widehat{\Omega}), & \iota_p^i(q) &:= \det(D\mathbf{F}_i) (q \circ \mathbf{F}_i). \end{aligned}$$

Let us consider the union domain Ω , namely $\overline{\Omega} = \cup_{i=0}^N \overline{\Omega}_i^*$. We assume that it has Lipschitz boundary Γ with outer unit normal \mathbf{n} . Moreover, for every $0 \leq i \leq N$, Ω_i will denote the visible part of Ω_i^* , *i.e.*,

$$\Omega_i := \Omega_i^* \setminus \bigcup_{\ell=i+1}^N \overline{\Omega}_\ell^*, \quad i = 0, \dots, N.$$

The unit outer normal on Γ_i is denoted as \mathbf{n}_i . We define the visible part of the external boundary of Ω_i^* as

$$\Gamma_i := \partial\Omega_i^* \setminus \bigcup_{\ell=i+1}^N \overline{\Omega}_\ell^*, \quad i = 0, \dots, N,$$

and, similarly, the local interfaces Γ_{ij} as

$$\Gamma_{ij} := \Gamma_i \cap \overline{\Omega}_j, \quad 0 \leq j < i \leq N.$$

See Figure 3.1(b) for an example. We require every interface Γ_{ij} to have either non-zero $(d-1)$ -measure or to be the empty set. The outer unit normal on Γ_{ij} inherits the orientation of Γ_i , hence it is denoted as \mathbf{n}_i . We also denote it as \mathbf{n} when it is clear from the context to which domain is referred to. Note that Γ_{ij} is not connected in general. Let us also point out that integrals and norms will be defined on sets like Γ_{ij} , $\Gamma_{ij} \cap \overline{K}$ and they are meant to be on their interior in a suitable sense. To simplify our analysis, we will adopt Assumptions 3.1.1, 3.1.4, and 3.1.5.

Let us recall the definitions of some quantities relating to the patches' configuration upon which our method's stability constants will depend.

Definition 5.1.1. Let $0 \leq j < i \leq N$, and

$$\delta_{ij} := \begin{cases} 1 & \text{if } \Gamma_{ij} \neq \emptyset, \\ 0 & \text{otherwise.} \end{cases}$$

For each $1 \leq i \leq N$, the quantity $\sum_{j=0}^{i-1} \delta_{ij}$ counts the number of visible parts Ω_j whose boundaries are overlapped by Γ_i and, for $0 \leq j \leq N-1$, $\sum_{i=j+1}^N \delta_{ij}$ the number of visible parts whose boundaries overlap Γ_j . We further define $N_\Gamma^\downarrow := \max_{1 \leq i \leq N} \sum_{j=0}^{i-1} \delta_{ij}$, the maximum number of visible parts whose boundaries are overlapped by any visible boundary, and $N_\Gamma^\uparrow := \max_{0 \leq j \leq N-1} \sum_{i=j+1}^N \delta_{ij}$, the maximum number of visible parts whose boundaries cover any visible boundary. Hence, we let $N_\Gamma := \max\{N_\Gamma^\downarrow, N_\Gamma^\uparrow\}$ be the *maximum number of boundary overlaps* in the current configuration. See Figure 3.2 for some examples.

Definition 5.1.2. We let $O_{ij} := \Omega_i \cap \Omega_j^*$, $0 \leq j < i \leq N$, be the *overlap* between the j -th predomain and the i -th visible part. For every $0 \leq j < i \leq N$, we define

$$\eta_{ij} := \begin{cases} 1 & \text{if } O_{ij} \neq \emptyset, \\ 0 & \text{otherwise.} \end{cases}$$

For each $1 \leq i \leq N$, the quantity $\sum_{j=0}^{i-1} \eta_{ij}$ counts the number of predomains covered by the visible part Ω_i . We further define $N_{\mathcal{O}} := \max_{1 \leq i \leq N} \sum_{j=0}^{i-1} \eta_{ij}$, the maximum number of predomains covered by any visible part. See Figure 3.2 for some examples.

We denote as $\mathcal{M}_i := \{K \in \mathcal{M}_i^* : K \cap \Omega_i \neq \emptyset\}$, $i = 0, \dots, N$, the i -th extended mesh, consisting of all visible elements of the i -th premesh \mathcal{M}_i^* . For $i = 0, \dots, N$, we denote $\mathcal{G}_{h,i}$ the collection of cut elements of \mathcal{M}_i , namely $\mathcal{G}_{h,i} := \{K \in \mathcal{M}_i : K \cap (\Gamma_i \setminus \overline{\partial\Omega_i^*}) \neq \emptyset\}$. We define $h_i : \overline{\Omega_i} \rightarrow \mathbb{R}^+$ to be the piecewise constant mesh size function of \mathcal{M}_i assigning to each visible element its whole diameter, namely $h_i|_{K \cap \Omega} := h_{i,K}$, where $h_{i,K} := \text{diam}(K)$ for every $K \in \mathcal{M}_i$, $0 \leq i \leq N$. Moreover let us denote $h_i := \max_{K \in \mathcal{M}_i} h_{i,K}$ and $h := \max_{0 \leq i \leq N} h_i$. Finally, we denote by $h : \Omega \rightarrow \mathbb{R}^+$ the piecewise constant function defined as $h|_{\Omega_i} := h_i$.

Throughout this chapter, C will denote generic positive constants that may change with each occurrence throughout the chapter but are always independent of the local mesh size, the position of the visible interfaces with respect to the meshes, and the number of patches, unless otherwise specified.

5.2 Isogeometric discretization on overlapping multipatch domains

5.2.1 Model Problem and its variational formulation

Let $\Gamma = \overline{\Gamma_D} \cup \overline{\Gamma_N}$, where Γ_D and Γ_N are non-empty, open, and disjoint. We consider the Stokes problem in the *union domain* Ω . Given $\mathbf{f} \in \mathbf{L}^2(\Omega)$, $\mathbf{u}_D \in \mathbf{H}^{\frac{1}{2}}(\Gamma_D)$ and $\mathbf{u}_N \in \mathbf{H}^{-\frac{1}{2}}(\Gamma_N)$, we look for the *velocity* $\mathbf{u} : \Omega \rightarrow \mathbb{R}^d$ and the *pressure* $p : \Omega \rightarrow \mathbb{R}$ such that

$$\begin{aligned} -\operatorname{div} \boldsymbol{\sigma}(\mathbf{u}, p) &= \mathbf{f}, & \text{in } \Omega, \\ \operatorname{div} \mathbf{u} &= 0, & \text{in } \Omega, \\ \mathbf{u} &= \mathbf{u}_D, & \text{on } \Gamma_D, \\ \boldsymbol{\sigma}(\mathbf{u}, p)\mathbf{n} &= \mathbf{u}_N, & \text{on } \Gamma_N, \end{aligned} \tag{5.1}$$

where $\boldsymbol{\sigma}(\mathbf{u}, q) := \mu D\mathbf{u} - p\mathbf{I}$ is the *Cauchy stress tensor* and $\mu \in \mathbb{R}$, $\mu > 0$, is the *viscosity coefficient*. For the sake of simplicity of the notation, let us set $\mu \equiv 1$.

We rewrite problem (5.1) in the following multi-patch form. Find $\mathbf{u} : \Omega \rightarrow \mathbb{R}^d$ and $p : \Omega \rightarrow \mathbb{R}$ such that

$$-\operatorname{div} \boldsymbol{\sigma}(\mathbf{u}_i, p_i) = \mathbf{f}, \quad \text{in } \Omega_i, \quad i = 0, \dots, N, \tag{5.2a}$$

$$\operatorname{div} \mathbf{u}_i = 0, \quad \text{in } \Omega_i, \quad i = 0, \dots, N, \tag{5.2b}$$

$$\mathbf{u}_i - \mathbf{u}_j = \mathbf{0}, \quad \text{on } \Gamma_{ij}, \quad 0 \leq j < i \leq N, \tag{5.2c}$$

$$\boldsymbol{\sigma}(\mathbf{u}_i, p_i)\mathbf{n}_i + \boldsymbol{\sigma}(\mathbf{u}_j, p_j)\mathbf{n}_j = \mathbf{0}, \quad \text{on } \Gamma_{ij}, \quad 0 \leq j < i \leq N, \tag{5.2d}$$

$$\mathbf{u}_i = \mathbf{u}_D, \quad \text{on } \Gamma_D \cap \Gamma_i, \quad i = 0, \dots, N, \tag{5.2e}$$

$$\boldsymbol{\sigma}(\mathbf{u}_i, p_i)\mathbf{n}_i = \mathbf{u}_N, \quad \text{on } \Gamma_N \cap \Gamma_i, \quad i = 0, \dots, N, \tag{5.2f}$$

where $\mathbf{u}_i := \mathbf{u}|_{\Omega_i}$, $p_i := p|_{\Omega_i}$, $i = 0, \dots, N$. Equations (5.2c) and (5.2d) are commonly known as *transmission conditions* at the local interfaces.

Proposition 5.2.1. *Problems (5.1) and (5.2a)–(5.2f) are equivalent.*

Chapter 5. Stabilized isogeometric discretization of the Stokes problem on union geometries

Proof. To demonstrate this result, the variational formulation of the two problems must be used. We refer the interested reader to Chapter 5 of [113]. \square

Let us introduce, for each visible part Ω_i , the *local isogeometric spaces*

$$V_{h,i}^\square := \{\mathbf{v}_h|_{\Omega_i} : \mathbf{v}_h \in V_{h,i}^{*,\square}\}, \quad Q_{h,i}^\square := \{q_h|_{\Omega_i} : q_{h,i} \in Q_{h,i}^{*,\square}\},$$

and glue them to form the *union isogeometric spaces*

$$V_h^\square := \bigoplus_{i=0}^N V_{h,i}^\square, \quad Q_h^\square := \bigoplus_{i=0}^N Q_{h,i}^\square,$$

where $\square \in \{\text{RT}, \text{N}, \text{TH}\}$. To further alleviate the notation, we adopt the convention to denote as V_h the space of the velocities and omit the superscript $\square \in \{\text{RT}, \text{N}, \text{TH}\}$ when what said does not depend from the particular finite element choice. Elements of V_h and Q_h are $(N+1)$ -tuples $\mathbf{v}_h = (\mathbf{v}_0, \dots, \mathbf{v}_N)$ and $q_h = (q_0, \dots, q_N)$, respectively. In practice, we can treat them as ordinary functions thanks to the embeddings

$$\begin{aligned} V_h &\hookrightarrow \mathbf{L}^2(\Omega), & \mathbf{v}_h(x) &\mapsto \mathbf{v}_i(x), & x \in \Omega_i, i = 0, \dots, N, \\ Q_h &\hookrightarrow L^2(\Omega), & q_h(x) &\mapsto q_i(x), & x \in \Omega_i, i = 0, \dots, N. \end{aligned}$$

In order to strongly impose Dirichlet boundary conditions, let us adopt Assumption 3.2.2. In case Assumption 3.2.2 does not hold, we can combine the technique in this chapter with that detailed in [111] and in Chapter 4 to deal with the imposition of Dirichlet boundary conditions in a weak sense.

Let $\varphi : \Omega \rightarrow \mathbb{R}$ be smooth enough and, for every $0 \leq i \leq N$, we denote its restriction to Ω_i as $\varphi_i := \varphi|_{\Omega_i}$. Then, for every interface Γ_{ij} , $0 \leq j < i \leq N$, and a.e. $x \in \Gamma_{ij}$, we define, respectively, the *average* and the *jump* of φ as

$$\begin{aligned} \langle \varphi \rangle_{t, \Gamma_{ij}}(x) &:= t\varphi_i|_{\Gamma_{ij}}(x) + (1-t)\varphi_j|_{\Gamma_{ij}}(x), & t \in \{\tfrac{1}{2}, 1\}, \\ [\varphi]_{\Gamma_{ij}}(x) &:= \varphi_i|_{\Gamma_{ij}}(x) - \varphi_j|_{\Gamma_{ij}}(x). \end{aligned}$$

We may remove the subscript Γ_{ij} when it is clear from the context to which interface we refer to. The average is said to be *symmetric* if $t = \frac{1}{2}$ and *one-sided* when $t = 1$. We define the jump and average of a vector valued function $\boldsymbol{\tau} : \Omega \rightarrow \mathbb{R}^d$ componentwise by letting $\langle \boldsymbol{\tau} \rangle_{t,k} := \langle \tau_k \rangle_t$ and $[\boldsymbol{\tau}]_k := [\tau_k]$, for $0 \leq k \leq d$.

Let us endow V_h and Q_h with the mesh dependent norms:

$$\begin{aligned} \|\mathbf{v}_h\|_{1,h}^2 &:= \sum_{i=0}^N \|D\mathbf{v}_i\|_{L^2(\Omega_i)}^2 + \sum_{i=1}^N \sum_{j=0}^{i-1} \left\| h^{-\frac{1}{2}} [\mathbf{v}_h] \right\|_{L^2(\Gamma_{ij})}^2, & \mathbf{v}_h \in V_h, \\ \|q_h\|_{0,h}^2 &:= \sum_{i=0}^N \|q_i\|_{L^2(\Omega_i)}^2 + \sum_{i=1}^N \sum_{j=0}^{i-1} \left\| h^{\frac{1}{2}} [q_h] \right\|_{L^2(\Gamma_{ij})}^2, & q_h \in Q_h. \end{aligned}$$

We propose the following weak formulation for the discrete counterpart of problem (5.2a)–(5.2f), which is obtained enforcing the transmission conditions in a weak sense using Nitsche's method.

Find $(\mathbf{u}_h, p_h) \in V_h^{\mathbf{u}^D} \times Q_h$ such that

$$\begin{aligned} a_h(\mathbf{u}_h, \mathbf{v}_h) + b(\mathbf{v}_h, q_h) &= F(\mathbf{v}_h), & \forall \mathbf{v}_h \in V_h^{\mathbf{0}}, \\ b(\mathbf{u}_h, q_h) &= 0, & \forall q_h \in Q_h, \end{aligned} \tag{5.3}$$

where

$$\begin{aligned}
 a_h(\mathbf{w}_h, \mathbf{v}_h) &:= \sum_{i=0}^N \int_{\Omega_i} D\mathbf{w}_i : D\mathbf{v}_i - \sum_{i=1}^N \sum_{j=0}^{i-1} \int_{\Gamma_{ij}} (\langle D\mathbf{w}_h \mathbf{n} \rangle_t [\mathbf{v}_h] + [\mathbf{w}_h] \langle D\mathbf{v}_h \mathbf{n} \rangle_t) \\
 &\quad + \gamma \sum_{i=1}^N \sum_{j=0}^{i-1} \int_{\Gamma_{ij}} h^{-1} [\mathbf{w}_h] [\mathbf{v}_h], \quad \mathbf{w}_h, \mathbf{v}_h \in V_h, \\
 b(\mathbf{v}_h, q_h) &:= - \sum_{i=0}^N \int_{\Omega_i} q_i \operatorname{div} \mathbf{v}_i + \sum_{i=1}^N \sum_{j=0}^{i-1} \int_{\Gamma_{ij}} \langle q_h \rangle_t [\mathbf{v}_h \cdot \mathbf{n}], \quad \mathbf{v}_h \in V_h, q_h \in Q_h,
 \end{aligned}$$

with $t \in \{\frac{1}{2}, 1\}$, and

$$F(\mathbf{v}_h) := \sum_{i=0}^N \int_{\Omega_i} \mathbf{f} \cdot \mathbf{v}_i + \int_{\Gamma_N} \mathbf{u}_N \cdot \mathbf{v}_h, \quad \mathbf{v}_h \in V_h.$$

Here, $\gamma > 0$ is a penalty parameter related to the spline degree. $V_h^{\mathbf{u}^D}$ and V_h^0 denote the discrete spaces with boundary conditions; see Section 1.3.

Proposition 5.2.2. *The discrete variational formulation in equation (5.3) is consistent, i.e., the solution $(\mathbf{u}, p) \in \mathbf{H}^{\frac{3}{2}+\varepsilon}(\Omega) \times L^2(\Omega)$, $\varepsilon > 0$, of problem (5.1) satisfies problem (5.3) as well.*

Proof. The proof is quite standard. See, for instance, Chapter 5 of [113]. \square

5.2.2 Stabilization procedure

It has been shown in Chapter 4 that problem (5.3), in the case of only one trimmed subdomain, may suffer from instability. This is primarily due to two factors. On the one hand, the evaluation of the normal derivatives of the velocity is not stable along the boundaries of the bad cut elements, and on the other hand, the functions related to the pressure in the bad cut elements cause instabilities in turn. In the two-patch situation, such as in Figure 3.3(a), we do not have the instability issue caused by the velocity as soon as we use the one-sided flux from top elements that are not cut. Nevertheless, as for the Poisson problem, we do have this issue in general cases with many patches; see Figure 3.3(b), where the one-sided flux regarding the interface Γ_{ij} comes from the red element, which may be a bad cut element. Note that the instabilities caused by the pressure are intrinsic and cannot be mitigated with the choice of t .

In this regard, the stabilization procedure, developed in the previous chapters, comes to help. In what follows, we need to accommodate this method in the context of the Stokes problem on multi-patches that overlap.

For each extended Bézier mesh \mathcal{M}_i , $i = 0, \dots, N-1$, we partition its elements into two disjoint sub-families, the collection \mathcal{M}_i^g of the good elements, i.e., the ones with a sufficiently large “active” part, and the collection \mathcal{M}_i^b of the bad elements, namely the ones which are barely visible, according to a threshold parameter $\theta \in (0, 1]$, as explained in Definition 3.2.5. For every $i = 0, \dots, N-1$ and to every bad element $K \in \mathcal{M}_i^b$ we associate a good neighboring element K' and denote the set of its good neighbors as $\mathcal{N}(K)$, see Definition 3.2.6.

The following assumption is not restrictive and is satisfied whenever the meshes of the patches are sufficiently refined, and we take C large enough in (3.6).

Assumption 5.2.3. For every $K \in \mathcal{M}_i^b$, $0 \leq i < N$, there exist $i \leq k \leq N$ and $K' \in \mathcal{N}(K) \cap \mathcal{M}_k^g$. From now on we will refer to such K' as a *good neighbor* of K .

Chapter 5. Stabilized isogeometric discretization of the Stokes problem on union geometries

For every $K \in \mathcal{M}_i^b$, $0 \leq i < N$, its associated good neighbor K' is chosen according to the procedure described in Algorithm 1 in Section 3.2.3.

As already observed, if Algorithm 1 does not produce any output, then it suffices to relax the definition of the good neighbor by taking a larger constant C in (3.6). We observe that formulation (5.3) is well-posed if there are no cut elements, *i.e.*, $\mathcal{G}_{h,k} = \emptyset$, for every $0 \leq k \leq N$. In the general case $\mathcal{G}_{h,k} \neq \emptyset$, for some $0 \leq k < N$, the goal of the stabilization is, informally speaking, to extend the stability of the discrete formulation from the internal elements of the visible parts of the patches up to their cut elements.

Let us start by stabilizing the pressure. For $0 \leq j < i \leq N$, $\ell \in \{i, j\}$, let us define $R_\ell^p : Q_h \rightarrow L^2(\Omega_\ell)$ locally. For every $q_h \in Q_h$ and $K \in \mathcal{M}_\ell$ such that $K \in \mathcal{G}_{h,\ell}$, we distinguish two cases:

- if $K \in \mathcal{M}_\ell^g$, then

$$R_\ell^p(q_h)|_K := q_\ell|_K,$$

- if $K \in \mathcal{M}_\ell^b$, then

$$R_\ell^p(q_h)|_K := \mathcal{E}_{K',K} \left(\Pi_{K'} \left(q_k|_{K'} \right) \right)|_K,$$

where $\Pi_{K'} : L^2(K') \rightarrow \mathbb{Q}_k(K')$ is the L^2 -orthogonal projection onto the space of tensor product polynomials defined on the good neighbor K' and $\mathcal{E}_{K',K} : \mathbb{Q}_k(K') \rightarrow \mathbb{Q}_k(K \cup K')$ is the canonical polynomial extension.

Lemma 5.2.4 (Stability properties of R_ℓ^p). *Given $\theta \in (0, 1]$, there exist $C_{S,1}, C_{S,2} > 0$ such that, for every $0 \leq j < i \leq N$, $K \in \mathcal{M}_\ell$, $\ell \in \{i, j\}$, and $q_h \in Q_h$, we have*

$$\left\| h_\ell^{\frac{1}{2}} R_\ell^p(q_h) \right\|_{L^2(\Gamma_{ij} \cap \bar{K})} \leq C_{S,1} \|q_k\|_{L^2(K' \cap \Omega)}, \quad \|R_\ell^p(q_h)\|_{L^2(K \cap \Omega_\ell)} \leq C_{S,2} \|q_k\|_{L^2(K' \cap \Omega)},$$

where $K' \in \mathcal{M}_k^g$ is a good neighbor of K if $K \in \mathcal{M}_\ell^b$, $K' = K$ if $K \in \mathcal{M}_\ell^g$.

Proof. The proof is analogous to the one of Proposition 4.4.3, hence we skip it. \square

Proposition 5.2.5. *There exists $C > 0$, depending on N_Γ and \mathfrak{C} , such that for every $q_h \in Q_h$, we have*

$$\sum_{i=1}^N \sum_{j=0}^{i-1} \left\| h^{\frac{1}{2}} [R_{ij}^p(q_h)] \right\|_{L^2(\Gamma_{ij})}^2 \leq C \sum_{i=0}^N \|q_h\|_{L^2(\Omega_i)}^2,$$

where $[R_{ij}^p(q_h)] := R_i^p(q_h)|_{\Gamma_{ij}} - R_j^p(q_h)|_{\Gamma_{ij}}$, for $0 \leq j < i \leq N$, and \mathfrak{C} was introduced in Definition 3.2.7.

Proof. The proof is a consequence of Lemma 5.2.4. We skip it since it follows the same lines of Proposition 3.2.10. The constant C will depend on the choice of the isogeometric element. \square

Now, let us move to the velocity. For $0 \leq j < i \leq N$, $\ell \in \{i, j\}$, let us define $R_\ell^v : V_h \rightarrow L^2(\Omega_\ell)$ locally. For every $\mathbf{v}_h \in V_h$ and $K \in \mathcal{M}_\ell$ such that $K \in \mathcal{G}_{h,\ell}$, we distinguish two cases:

- if $K \in \mathcal{M}_\ell^g$, then

$$R_\ell^v(\mathbf{v}_h)|_K := \mathbf{v}_\ell|_K,$$

- if $K \in \mathcal{M}_\ell^b$, then

$$R_\ell^v(\mathbf{v}_h)\Big|_K := \mathcal{E}_{K',K} \left(\mathbf{\Pi}_{K'} \left(\mathbf{v}_h \Big|_{K'} \right) \right) \Big|_K,$$

where $\mathbf{\Pi}_{K'} : L^2(K') \rightarrow \mathbb{V}_k(K')$ is the L^2 -orthogonal projection,

$$\begin{aligned} \mathbb{V}_k(K) &:= \begin{cases} \mathbb{S}_k(K) & \text{if } \square = \text{RT}, \\ (\mathbb{Q}_{k+1}(K))^d & \text{if } \square \in \{\text{N}, \text{TH}\}, \end{cases} \\ \mathbb{S}_k(K) &:= \begin{cases} \mathbb{Q}_{k+1,k}(K) \times \mathbb{Q}_{k,k+1}(K) & \text{if } d = 2, \\ \mathbb{Q}_{k+1,k,k}(K) \times \mathbb{Q}_{k,k+1,k}(K) \times \mathbb{Q}_{k,k,k+1}(K) & \text{if } d = 3, \end{cases} \end{aligned}$$

and $\mathcal{E}_{K',K} : \mathbb{V}_k(K') \rightarrow \mathbb{V}_k(K \cup K')$ is the canonical polynomial extension.

We denote, for $0 \leq j < i \leq N$ such that $\Gamma_{ij} \neq \emptyset$ and $t \in \{\frac{1}{2}, 1\}$,

$$\langle DR_{ij}^v(\mathbf{v}_h)\mathbf{n} \rangle_t := t DR_i^v(\mathbf{v}_h)\mathbf{n}_i \Big|_{\Gamma_{ij}} + (1-t) DR_j^v(\mathbf{v}_h)\mathbf{n}_j \Big|_{\Gamma_{ij}}. \quad (5.4)$$

In the previous definition, we used the spaces V_h and $V_{h,\ell}$. Let us point out that the stabilization operators R_ℓ^v are equally defined for the spaces with zero boundary conditions V_h^0 and $V_{h,\ell}^0$, $0 \leq \ell \leq N$, as well.

Lemma 5.2.6 (Stability property of R_ℓ^v). *Given $\theta \in (0, 1]$, there exists $C > 0$ such that for every $0 \leq j < i \leq N$, $K \in \mathcal{M}_\ell$, $\ell \in \{i, j\}$, and $\mathbf{v}_h \in V_h$, we have*

$$\left\| h_\ell^{\frac{1}{2}} DR_\ell^v(\mathbf{v}_h)\mathbf{n}_\ell \right\|_{L^2(\Gamma_{ij} \cap \bar{K})} \leq C \|D\mathbf{v}_h\|_{L^2(K' \cap \Omega)},$$

where $K' \in \mathcal{M}_k^g$ is a good neighbor of K if $K \in \mathcal{M}_\ell^b$, $K' = K$ if $K \in \mathcal{M}_\ell^g$.

Proof. We refer the interested reader to the proof of Proposition 4.4.4. \square

Proposition 5.2.7. *There exists $C > 0$, depending on N_Γ and on \mathfrak{C} , such that, for every $\mathbf{v}_h \in V_h$,*

$$\sum_{i=1}^N \sum_{j=0}^{i-1} \left\| h^{\frac{1}{2}} \langle DR_h^v(\mathbf{v}_h)\mathbf{n} \rangle_t \right\|_{L^2(\Gamma_{ij})} \leq C \sum_{i=0}^N \|D\mathbf{v}_i\|_{L^2(\Omega_i)}$$

Proof. This result is a direct consequence of Lemma 5.2.6 and is the vectorial counterpart of Proposition 3.2.10, hence we omit its proof. \square

We introduce the following stabilized space for the pressures.

$$\begin{aligned} \bar{Q}_h &= \{ \varphi_h \in L^2(\Omega) : \exists q_h \in Q_h \text{ such that } \varphi_h \Big|_K = q_h \Big|_K \ \forall K \in \mathcal{M}_i^g \\ &\quad \text{and } \varphi_h \Big|_K = R_h^p(q_h) \Big|_K \ \forall K \in \mathcal{M}_i^b, \forall 0 \leq i \leq N \}. \end{aligned}$$

We can finally propose our stabilized weak formulation.

Find $(\mathbf{u}_h, p_h) \in V_h^{\mathbf{u}D} \times \bar{Q}_h$ such that

$$\begin{aligned} \bar{a}_h(\mathbf{u}_h, \mathbf{v}_h) + b(\mathbf{v}_h, q_h) &= F(\mathbf{v}_h), & \forall \mathbf{v}_h \in V_h^0, \\ b(\mathbf{u}_h, q_h) &= 0, & \forall q_h \in \bar{Q}_h, \end{aligned} \quad (5.5)$$

where

$$\begin{aligned}\bar{a}_h(\mathbf{w}_h, \mathbf{v}_h) &:= \sum_{i=0}^N \int_{\Omega_i} D\mathbf{w}_i : D\mathbf{v}_i - \sum_{i=1}^N \sum_{j=0}^{i-1} \int_{\Gamma_{ij}} (\langle DR_{ij}^v(\mathbf{w}_h)\mathbf{n} \rangle_t [\mathbf{v}_h] + [\mathbf{w}_h] \langle DR_{ij}^v(\mathbf{v}_h)\mathbf{n} \rangle_t) \\ &\quad + \gamma \sum_{i=1}^N \sum_{j=0}^{i-1} \int_{\Gamma_{ij}} \mathbf{h}^{-1} [\mathbf{w}_h] [\mathbf{v}_h], \quad \mathbf{w}_h, \mathbf{v}_h \in V_h, \\ b(\mathbf{v}_h, q_h) &:= - \sum_{i=0}^N \int_{\Omega_i} q_i \operatorname{div} \mathbf{v}_i + \sum_{i=1}^N \sum_{j=0}^{i-1} \int_{\Gamma_{ij}} \langle q_h \rangle_t [\mathbf{v}_h \cdot \mathbf{n}], \quad \mathbf{v}_h \in V_h, q_h \in \bar{Q}_h,\end{aligned}$$

with $t \in \{\frac{1}{2}, 1\}$, and

$$F(\mathbf{v}_h) := \sum_{i=0}^N \int_{\Omega_i} \mathbf{f} \cdot \mathbf{v}_i + \int_{\Gamma_N} \mathbf{u}_N \cdot \mathbf{v}_h, \quad \mathbf{v}_h \in V_h.$$

As before $\gamma > 0$ is a penalty parameter scaling as the spline degree of the velocity.

5.2.3 Interpolation and approximation properties of the discrete spaces

Before analyzing problem (5.5), we need some technical results. Let us proceed as in Chapter 3. Giving a Sobolev function living in the whole physical domain Ω , we consider its restrictions to the predomains Ω_i^* in order to be able to interpolate on each premesh \mathcal{M}_i^* , restrict them in their turn to the visible parts Ω_i , and finally glue together the interpolated functions.

Let us start with the velocity. We construct a quasi-interpolant operator for each local space $V_{h,i}$. Given $\square \in \{\text{RT}, \text{N}, \text{TH}\}$ and $m \geq 1$, for every $i \in \{0, \dots, N\}$, we denote

$$\Pi_{V_h}^{i,\square} : \mathbf{H}^m(\Omega_i) \rightarrow V_{h,i}^\square, \quad \mathbf{v} \mapsto \Pi_{V_h}^{i,*,\square} \left(\mathbf{v} \Big|_{\Omega_i^*} \right) \Big|_{\Omega_i},$$

where $\Pi_{V_h}^{i,*,\square} : \mathbf{H}^m(\Omega_i^*) \rightarrow V_{h,i}^{*,\square}$ is a standard quasi-interpolant operator [19, 30]. Then, we glue together the local operators as

$$\Pi_{V_h}^\square : \mathbf{H}^m(\Omega) \rightarrow V_h^\square, \quad \mathbf{v} \mapsto \bigoplus_{i=0}^N \Pi_{V_h}^{i,\square}(\mathbf{v}_i),$$

where $\mathbf{v}_i(x) := \mathbf{v}(x)$ for every $x \in \Omega_i$, $i = 0, \dots, N$. For the pressures, given $r \geq 1$, we introduce the local quasi-interpolants

$$\Pi_{Q_h}^{i,\square} : H^r(\Omega_i) \rightarrow Q_{h,i}^\square, \quad q \mapsto \Pi_{Q_h}^{i,*,\square} \left(q \Big|_{\Omega_i^*} \right) \Big|_{\Omega_i},$$

where $\Pi_{Q_h}^{i,*,\square} : H^r(\Omega_i^*) \rightarrow Q_{h,i}^{*,\square}$ is a standard quasi-interpolant operator. We glue together the local operators for the pressures as

$$\Pi_{Q_h}^\square : H^r(\Omega) \rightarrow \bar{Q}_h^\square, \quad q \mapsto R_h^p \left(\bigoplus_{i=0}^N \Pi_{Q_h}^{i,\square}(q_i) \right),$$

where $q_i(x) := q(x)$ for every $x \in \Omega_i$, $i = 0, \dots, N$.

5.2. Isogeometric discretization on overlapping multipatch domains

Proposition 5.2.8 (Interpolation error estimate). *There exist $C_v, C_p > 0$ such that, for every $(\mathbf{v}, q) \in \mathbf{H}^m(\Omega) \times H^r(\Omega)$, $m \geq 1$ and $r \geq 1$, it holds*

$$\left\| \mathbf{v} - \Pi_{V_h}^\square \mathbf{v} \right\|_{1,h} \leq C_v h^s \|\mathbf{v}\|_{H^m(\Omega)}, \quad \|q - \Pi_{Q_h} q\|_{0,h} \leq C_p h^\ell \|q\|_{H^r(\Omega)},$$

where $s := \min\{k, m-1\}$ if $\square = \text{RT}$, $s := \min\{k+1, m-1\}$ if $\square \in \{\text{N}, \text{TH}\}$, and $\ell := \min\{k+1, r\}$.

Proof. The proof follows from the best approximation properties of the local quasi-interpolant operators $\Pi_{V_h}^i$ and $\Pi_{Q_h}^i$, $0 \leq i \leq N$, namely Theorem 4.4.12. \square

Lemma 5.2.9 (Approximation property of R_ℓ^v). *There exists $C > 0$, depending on N_Γ , $N_\mathcal{O}$, and \mathfrak{C} , such that, for every $\mathbf{v} \in \mathbf{H}^m(\Omega)$, $m \geq 2$, it holds*

$$\sum_{i=1}^N \sum_{j=0}^{i-1} \left\| h^{\frac{1}{2}} \langle DR_{ij}^v \left(\Pi_{V_h}^\square(\mathbf{v}) \right) \mathbf{n} - D\mathbf{v}\mathbf{n} \rangle_t \right\|_{L^2(\Gamma_{ij})}^2 \leq Ch^{2s} \|\mathbf{v}\|_{H^m(\Omega)}^2,$$

where $s := \min\{k, m-1\}$ if $\square = \text{RT}$ and $s := \min\{k+1, m-1\}$ if $\square \in \{\text{N}, \text{TH}\}$.

Proof. The proof follows the same lines of the one of Proposition 3.2.13. \square

5.2.4 Well-posedness of the stabilized formulation

Since we do not know how to prove an inf-sup condition for $b(\cdot, \cdot)$, it will be convenient for the subsequent analysis to reframe the Nitsche formulation as a stabilized Lagrange multiplier method, as done in [126]. In doing so, we find a formulation equivalent to (5.5), but whose well-posedness is easier to prove.

Remark 5.2.10. We observe that if we find a strategy for proving the inf-sup condition for the $b_1(\cdot, \cdot)$ form of Chapter 4, then we would likely have a technique for being able to prove the inf-sup condition for $b(\cdot, \cdot)$.

First of all, we observe that the transmission conditions at the interfaces (5.2b) and (5.2c) can be enforced by introducing a Lagrange multiplier living in $\Lambda := \bigoplus_{0 \leq j < i \leq N} H_{00}^{-\frac{1}{2}}(\Gamma_{ij})$, where, for $0 \leq j < i \leq N$, $H_{00}^{-\frac{1}{2}}(\Gamma_{ij}) := \left(H_{00}^{\frac{1}{2}}(\Gamma_{ij}) \right)'$ and $H_{00}^{\frac{1}{2}}(\Gamma_{ij}) := \{\varphi \in L^2(\Gamma_{ij}) : \tilde{\varphi} \in H^{\frac{1}{2}}(\Gamma_j)\}$, $\tilde{\varphi}$ denoting the extension by zero of $\varphi \in L^2(\Gamma_{ij})$ on $\Gamma_j \setminus \Gamma_{ij}$ (see Chapter 11 of [121]). Let Λ_h be a discrete subspace of Λ large enough such that, for every $(\mathbf{v}_h, q_h) \in V_h \times \overline{Q}_h$, it holds

$$h^{-1}[\mathbf{v}_h] \Big|_{\Gamma_{ij}}, \langle DR_{ij}^v(\mathbf{v}_h)\mathbf{n} \rangle_t \Big|_{\Gamma_{ij}}, \langle q_h \mathbf{n} \rangle_t \Big|_{\Gamma_{ij}} \in \Lambda_h, \quad \forall 0 \leq j < i \leq N, t \in \left\{ \frac{1}{2}, 1 \right\}. \quad (5.6)$$

For instance, let

$$\Lambda_h^\square := \bigoplus_{0 \leq j < i \leq N} \Lambda_{ij}^\square, \quad \Lambda_{ij}^\square := W_h^\square(\Gamma_{ij}) + L_h^\square(\Gamma_{ij})\mathbf{n} + N_h^\square(\Gamma_{ij})\mathbf{n}, \quad (5.7)$$

for $\square \in \{\text{TH}, \text{RT}, \text{N}\}$, where

$$\begin{aligned} W_h^\square(\Gamma_{ij}) &:= \{ \mathbf{h}^{-1} \mathbf{w}_h \Big|_{\Gamma_{ij}} : \mathbf{w}_h = \widehat{\mathbf{w}}_h \circ \mathbf{F}_\ell^{-1} \text{ if } \square = \text{TH}, \mathbf{w}_h = (\iota_v^\ell)^{-1}(\widehat{\mathbf{w}}_h) \text{ if } \square \in \{\text{RT}, \text{N}\}, \\ &\quad \widehat{\mathbf{w}}_h \in \mathbb{V}_k(Q), \forall K = \mathbf{F}(Q) \in \mathcal{M}_\ell \cap \mathcal{G}_{h,\ell}, \ell \in \{i, j\} \}, \\ L_h^\square(\Gamma_{ij}) &:= \{ D\mathbf{w}_h \Big|_{\Gamma_{ij}} : \mathbf{w}_h = \widehat{\mathbf{w}}_h \circ \mathbf{F}_\ell^{-1} \text{ if } \square = \text{TH}, \mathbf{w}_h = (\iota_v^\ell)^{-1}(\widehat{\mathbf{w}}_h) \text{ if } \square \in \{\text{RT}, \text{N}\}, \\ &\quad \widehat{\mathbf{w}}_h \in \mathbb{V}_k(Q), \forall K = \mathbf{F}(Q) \in \mathcal{M}_\ell^g \cap \mathcal{G}_{h,\ell}, \mathbf{w}_h \in \mathbb{V}_k(K), \forall K \in \mathcal{M}_\ell^b \cap \mathcal{G}_{h,\ell}, \ell \in \{i, j\} \}, \\ N_h^\square(\Gamma_{ij}) &:= \{ \varphi_h \Big|_{\Gamma_{ij}} : \varphi_h = \widehat{\varphi}_h \circ \mathbf{F}_\ell^{-1} \text{ if } \square = \text{TH}, \varphi_h = (\iota_p^\ell)^{-1}(\widehat{\varphi}_h) \text{ if } \square \in \{\text{RT}, \text{N}\}, \widehat{\varphi}_h \in \mathbb{Q}_k(Q), \\ &\quad \forall K = \mathbf{F}_\ell(Q) \in \mathcal{M}_\ell^g \cap \mathcal{G}_{h,\ell}, \varphi_h \in \mathbb{Q}_k(K), \forall K \in \mathcal{M}_\ell^b \cap \mathcal{G}_{h,\ell}, \ell \in \{i, j\} \}. \end{aligned}$$

It is easy to check that (5.7) satisfies conditions (5.6). Moreover, $\Lambda_h \neq \emptyset$. We endow Λ_h with the mesh-dependent norm

$$\|\boldsymbol{\mu}_h\|_{-\frac{1}{2},h}^2 := \sum_{i=1}^N \sum_{j=0}^{i-1} \left\| \mathbf{h}^{\frac{1}{2}} \boldsymbol{\mu}_h \right\|_{L^2(\Gamma_{ij})}^2, \quad \boldsymbol{\mu}_h \in \Lambda_h.$$

Let us introduce the following stabilized augmented Lagrangian formulation.

Find $(\mathbf{u}_h, p_h, \boldsymbol{\lambda}_h) \in V_h^{\mathbf{u}D} \times \overline{Q}_h \times \Lambda_h$ such that

$$\overline{\mathcal{A}}_h((\mathbf{u}_h, p_h, \boldsymbol{\lambda}_h); (\mathbf{v}_h, q_h, \boldsymbol{\mu}_h)) = \mathcal{F}(\mathbf{v}_h, q_h, \boldsymbol{\mu}_h), \quad \forall (\mathbf{v}_h, q_h, \boldsymbol{\mu}_h) \in V_h^{\mathbf{0}} \times \overline{Q}_h \times \Lambda_h, \quad (5.8)$$

where, for $(\mathbf{w}_h, r_h, \boldsymbol{\eta}_h), (\mathbf{v}_h, q_h, \boldsymbol{\mu}_h) \in V_h \times \overline{Q}_h \times \Lambda_h$,

$$\begin{aligned} \overline{\mathcal{A}}_h((\mathbf{w}_h, r_h, \boldsymbol{\eta}_h); (\mathbf{v}_h, q_h, \boldsymbol{\mu}_h)) &:= a(\mathbf{w}_h, \mathbf{v}_h) + b_0(\mathbf{v}_h, r_h) + b_\Gamma(\mathbf{v}_h, \boldsymbol{\eta}_h) \\ &\quad + b_0(\mathbf{w}_h, q_h) + b_\Gamma(\mathbf{w}_h, \boldsymbol{\mu}_h) \\ &\quad - \sum_{i=1}^N \sum_{j=0}^{i-1} \gamma^{-1} \int_{\Gamma_{ij}} \mathbf{h}(\boldsymbol{\eta}_h + \langle DR_{ij}^v(\mathbf{w}_h) \mathbf{n} \rangle_t - \langle r_h \mathbf{n} \rangle_t) (\boldsymbol{\mu}_h + \langle DR_{ij}^v(\mathbf{v}_h) \mathbf{n} \rangle_t - \langle q_h \mathbf{n} \rangle_t), \end{aligned}$$

$$\mathcal{F}(\mathbf{v}_h, q_h, \boldsymbol{\mu}_h) := F(\mathbf{v}_h), \quad a(\mathbf{w}_h, \mathbf{v}_h) := \sum_{i=0}^N \int_{\Omega_i} D\mathbf{w}_i : D\mathbf{v}_i,$$

$$b_0(\mathbf{v}_h, q_h) := - \sum_{i=0}^N \int_{\Omega_i} q_i \operatorname{div} \mathbf{v}_i, \quad b_\Gamma(\mathbf{v}_h, \boldsymbol{\mu}_h) := \sum_{i=1}^N \sum_{j=0}^{i-1} \int_{\Gamma_{ij}} \boldsymbol{\mu}_h[\mathbf{v}_h].$$

Proposition 5.2.11. *Let Λ_h be defined as in (5.7). Then, problem (5.8) is equivalent to the stabilized Nitsche formulation (5.5).*

Proof. We can reformulate problem (5.8) as follows.

Find $(\mathbf{u}_h, p_h, \boldsymbol{\lambda}_h) \in V_h^{\mathbf{u}D} \times \overline{Q}_h \times \Lambda_h$ such that

$$\begin{aligned} &a(\mathbf{u}_h, \mathbf{v}_h) + b_0(\mathbf{v}_h, p_h) + b_\Gamma(\mathbf{v}_h, \boldsymbol{\lambda}_h) \\ &- \sum_{i=1}^N \sum_{j=0}^{i-1} \gamma^{-1} \int_{\Gamma_{ij}} \mathbf{h}(\boldsymbol{\lambda}_h + \langle DR_{ij}^v(\mathbf{u}_h) \mathbf{n} \rangle_t - \langle p_h \mathbf{n} \rangle_t) \langle DR_{ij}^v(\mathbf{v}_h) \mathbf{n} \rangle_t = F(\mathbf{v}_h), \quad \forall \mathbf{v}_h \in V_h^{\mathbf{0}}, \\ &b_0(\mathbf{u}_h, q_h) + \sum_{i=1}^N \sum_{j=0}^{i-1} \gamma^{-1} \int_{\Gamma_{ij}} \mathbf{h}(\boldsymbol{\lambda}_h + \langle DR_{ij}^v(\mathbf{u}_h) \mathbf{n} \rangle_t - \langle p_h \mathbf{n} \rangle_t) \langle q_h \rangle_t = 0, \quad \forall q_h \in \overline{Q}_h, \\ &b_\Gamma(\mathbf{u}_h, \boldsymbol{\mu}_h) - \sum_{i=1}^N \sum_{j=0}^{i-1} \gamma^{-1} \int_{\Gamma_{ij}} \mathbf{h}(\boldsymbol{\lambda}_h + \langle DR_{ij}^v(\mathbf{u}_h) \mathbf{n} \rangle_t - \langle p_h \mathbf{n} \rangle_t) \boldsymbol{\mu}_h = 0, \quad \forall \boldsymbol{\mu}_h \in \Lambda_h. \end{aligned}$$

5.2. Isogeometric discretization on overlapping multipatch domains

From the third equation, we can *statically condensate* the Lagrange multiplier as $\boldsymbol{\lambda}_h = \sum_{i=1}^N \sum_{j=0}^{i-1} \boldsymbol{\lambda}_{ij}$, where

$$\boldsymbol{\lambda}_{ij} = \sum_{i=1}^N \sum_{j=0}^{i-1} \gamma P_{ij} (\mathbf{h}^{-1}[\mathbf{u}_h]) - P_{ij} (\langle DR_{ij}^v(\mathbf{u}_h) \mathbf{n} \rangle_t) + P_{ij} (\langle p_h \mathbf{n} \rangle_t),$$

where $P_{ij} : \mathbf{L}^2(\Gamma_{ij}) \rightarrow \Lambda_{ij}$ is the L^2 -orthogonal projection. By substituting it back to the first and second equations and using (5.7), we recover the desired formulations. \square

Remark 5.2.12. Let us observe that formulation (5.8) no longer falls within the class of saddle-point problems; hence their well-posedness needs to be proved directly by showing the invertibility of the arising global systems through the so-called *Banach-Nečas-Babuška Theorem* [54]. On the other hand, we are no longer bound to satisfy an inf-sup condition, and for this reason, we are free to choose the Lagrange multiplier space large enough so that the hypotheses of Proposition 5.2.11 are satisfied.

A fundamental ingredient for our numerical analysis is that the following *local inf-sup conditions* are satisfied on each visible part of the domain.

Assumption 5.2.13. For every $0 \leq i \leq N$, let us equip $V_{h,i}$ with

$$\|\mathbf{v}_i\|_{1,h,i}^2 := \|D\mathbf{v}_i\|_{L^2(\Omega_i)}^2 + \sum_{k=i+1}^N \left\| \mathbf{h}^{-\frac{1}{2}} \mathbf{v}_i \right\|_{L^2(\Gamma_{ki})}^2 + \sum_{j=0}^{i-1} \left\| \mathbf{h}^{-\frac{1}{2}} \mathbf{v}_i \right\|_{L^2(\Gamma_{ij})}^2, \quad \mathbf{v}_i \in V_{h,i}, \quad (5.9)$$

and $\overline{Q}_h|_{\Omega_i}$ with $\|\cdot\|_{L^2(\Omega_i)}$. We assume that, for every $0 \leq i \leq N$, there exist $C_{1,i}, C_{2,i} > 0$ such that, for every $q_i \in \overline{Q}_h|_{\Omega_i}$, there exists $\mathbf{v}_i \in V_{h,i}$ such that

$$- \int_{\Omega_i} q_i \operatorname{div} \mathbf{v}_i \geq C_{1,i} \|q_i\|_{L^2(\Omega_i)}^2, \quad \|\mathbf{v}_i\|_{1,h,i} \leq C_{2,i} \|q_i\|_{L^2(\Omega_i)}. \quad (5.10)$$

Remark 5.2.14. We observe that, because of Remark 4.4.6, the inf-sup condition for $b_0(\cdot, \cdot)$, expressed in (4.22), can be interpreted as a special case of Assumption 5.2.13. In Chapter 4, we saw that, although we cannot prove such a condition, numerical experiments seem to confirm that it holds in practice.

The following Lemma provides a norm equivalence result for the space of stabilized pressures, useful for the proof of the inf-sup stability of $b_0(\cdot, \cdot)$.

Lemma 5.2.15. *There exists $C > 0$ such that*

$$\sum_{i=0}^N \|q_i\|_{L^2(\Omega_i)}^2 \leq \|q_h\|_{0,h}^2 \leq C \sum_{i=0}^N \|q_i\|_{L^2(\Omega_i)}^2, \quad \forall q_h \in \overline{Q}_h. \quad (5.11)$$

Proof. Let us take $q_h \in \overline{Q}_h$. By definition,

$$\|q_h\|_{0,h}^2 = \sum_{i=0}^N \|q_i\|_{L^2(\Omega_i)}^2 + \sum_{i=1}^N \sum_{j=0}^{i-1} \left\| \mathbf{h}^{\frac{1}{2}} [q_h] \right\|_{L^2(\Gamma_{ij})}^2.$$

Chapter 5. Stabilized isogeometric discretization of the Stokes problem on union geometries

Hence, we use Proposition 5.2.5 so that

$$\|q_h\|_{0,h}^2 \leq C \sum_{i=0}^N \|q_i\|_{L^2(\Omega_i)}^2,$$

where, in particular, C depends on N_Γ , \mathfrak{C} , and θ . The other inequality trivially holds. \square

The following inf-sup condition for $b_0(\cdot, \cdot)$ is a key ingredient for the proof of the well-posedness of formulation (5.8).

Lemma 5.2.16. *Under Assumption 5.2.13, given $\theta \in (0, 1]$, there exists $\beta_0 > 0$ such that*

$$\inf_{q_h \in \overline{Q}_h} \sup_{\mathbf{v}_h \in V_h} \frac{b_0(\mathbf{v}_h, q_h)}{\|\mathbf{v}_h\|_{1,h} \|q_h\|_{0,h}} \geq \beta_0. \quad (5.12)$$

Proof. We prove that there exist $C_1, C_2 > 0$ such that, for every $q_h \in \overline{Q}_h$, there exists $\mathbf{v}_h \in V_h$ such that

$$b_0(\mathbf{v}_h, q_h) \geq C_1 \|q_h\|_{0,h}^2, \quad \|\mathbf{v}_h\|_{1,h} \leq C_2 \|q_h\|_{0,h}.$$

Let us fix $q_h := (q_0, \dots, q_N) \in \overline{Q}_h$. From Assumption 5.2.13, there exist $C_{1,i}, C_{2,i} > 0$ and $\mathbf{v}_i \in V_{h,i}$, $0 \leq i \leq N$, such that (5.10) holds. Let $\mathbf{v}_h := (\mathbf{v}_0, \dots, \mathbf{v}_N)$. By letting $\overline{C}_1 := \min_{0 \leq i \leq N} C_{1,i}$, we have

$$b_0(\mathbf{v}_h, q_h) \geq \overline{C}_1 \sum_{i=0}^N \|q_i\|_{L^2(\Omega_i)}^2.$$

On the other hand, from the Young inequality,

$$\|\mathbf{v}_h\|_{1,h}^2 \leq \sum_{i=0}^N \|D\mathbf{v}_i\|_{L^2(\Omega_i)}^2 + 2 \left(\sum_{i=1}^N \sum_{j=0}^{i-1} \left\| \mathbf{h}^{-\frac{1}{2}} \mathbf{v}_i \right\|_{L^2(\Gamma_{ij})}^2 + \sum_{i=1}^N \sum_{j=0}^{i-1} \left\| \mathbf{h}^{-\frac{1}{2}} \mathbf{v}_j \right\|_{L^2(\Gamma_{ij})}^2 \right).$$

Notice that $\sum_{i=1}^N \sum_{j=0}^{i-1} \left\| \mathbf{h}^{-\frac{1}{2}} \mathbf{v}_j \right\|_{L^2(\Gamma_{ij})}^2 = \sum_{i=0}^{N-1} \sum_{k=i+1}^N \left\| \mathbf{h}^{-\frac{1}{2}} \mathbf{v}_i \right\|_{L^2(\Gamma_{ki})}^2$. Hence, from the definition of $\|\cdot\|_{1,h,i}$ (5.9) and Assumption 5.2.13, it holds

$$\|\mathbf{v}_h\|_{1,h}^2 \leq C \sum_{i=0}^N \|\mathbf{v}_i\|_{1,h,i}^2 \leq \overline{C}_2^2 \sum_{i=0}^N \|q_i\|_{L^2(\Omega_i)}^2, \quad (5.13)$$

where $\overline{C}_2 := (C\tilde{C})^{\frac{1}{2}}$ and $\tilde{C} := \max_{0 \leq i \leq N} C_{2,i}$. We conclude by taking $C_1 := \overline{C}_1 C^{-1}$ and $C_2 := \overline{C}_2$, where $C > 0$ come from Lemma 5.2.15. In particular, note that C depends on θ . \square

Let us indirectly study the well-posedness of the problem (5.5) by showing that (5.8) verifies the hypotheses of the so-called Banach-Nečas-Babuška Theorem [54]. The proof of the next result is given in Appendix A.2.

Theorem 5.2.17. *Under Assumption 5.2.13, there exists $\overline{\gamma} > 0$ and $C > 0$ such that, for every $\gamma \geq \overline{\gamma}$,*

$$\inf_{(\mathbf{v}_h, q_h, \boldsymbol{\mu}_h) \in V_h \times \overline{Q}_h \times \Lambda_h} \sup_{(\mathbf{w}_h, r_h, \boldsymbol{\eta}_h) \in V_h \times \overline{Q}_h \times \Lambda_h} \frac{\overline{\mathcal{A}}_h((\mathbf{w}_h, r_h, \boldsymbol{\eta}_h); (\mathbf{v}_h, q_h, \boldsymbol{\mu}_h))}{\|(\mathbf{w}_h, r_h, \boldsymbol{\eta}_h)\| \|(\mathbf{v}_h, q_h, \boldsymbol{\mu}_h)\|} \geq C, \quad (5.14)$$

where $\|\cdot\|$ is the Euclidean product norm on $V_h \times \overline{Q}_h \times \Lambda_h$.

We can characterize the existence, uniqueness, and stability for the solution of problem (5.5) as follows.

Proposition 5.2.18. (i) *There exists $\bar{\gamma} > 0$ such that, for every fixed $\gamma \geq \bar{\gamma}$, there exists $M_a > 0$ such that*

$$|\bar{a}_h(\mathbf{w}_h, \mathbf{v}_h)| \leq M_a \|\mathbf{w}_h\|_{1,h} \|\mathbf{v}_h\|_{1,h}, \quad \forall \mathbf{w}_h, \mathbf{v}_h \in V_h.$$

(ii) *There exists $\alpha > 0$ such that, for every $\gamma \geq \bar{\gamma}$,*

$$\alpha \|\mathbf{v}_h\|_{1,h}^2 \leq \bar{a}_h(\mathbf{v}_h, \mathbf{v}_h), \quad \forall \mathbf{v}_h \in \ker B,$$

where $\ker B := \{\mathbf{v}_h \in V_h : b(\mathbf{v}_h, q_h) = 0, \quad \forall q_h \in \bar{Q}_h\}$.

(iii) *There exists $M_b > 0$ such that*

$$|b(\mathbf{v}_h, q_h)| \leq M_b \|\mathbf{v}_h\|_{1,h} \|q_h\|_{0,h}, \quad \forall \mathbf{v}_h \in V_h, \forall q_h \in \bar{Q}_h.$$

(iv) *There exists $\beta > 0$ such that*

$$\inf_{q_h \in \bar{Q}_h} \sup_{\mathbf{v}_h \in V_h} \frac{b(\mathbf{v}_h, q_h)}{\|\mathbf{v}_h\|_{1,h} \|q_h\|_{0,h}} \geq \beta.$$

(v) *There exists $M_F > 0$ such that*

$$|F(\mathbf{v}_h)| \leq M_F \|\mathbf{v}_h\|_{1,h}, \quad \forall \mathbf{v}_h \in V_h.$$

Conditions (i)-(v) hold if and only there exists a unique solution (\mathbf{u}_h, p_h) of (5.5). Moreover,

$$\|\mathbf{u}_h\|_{1,h} \leq \frac{1}{\alpha} \|F\|_{-1,h}, \quad \|p_h\|_{0,h} \leq \frac{1}{\beta} \left(1 + \frac{M_a}{\alpha}\right) \|F\|_{-1,h}, \quad (5.15)$$

where $\|\cdot\|_{-1,h}$ denotes the dual norm with respect to $\|\cdot\|_{1,h}$.

Proof. This is a standard result. See, for instance, Theorem 3.4.1 in [22]. \square

Remark 5.2.19. The most natural way to demonstrate the stability of problem (5.5) would have been to check one by one the necessary and sufficient conditions provided by Proposition 5.2.18. We observe that conditions (iii), (v) follow trivially from the definition of the norms $\|\cdot\|_{0,h}$ and $\|\cdot\|_{1,h}$. Conditions (i), (ii) can be proved in an analogous way to Theorem 3.2.16. In particular, M_a and α will depend on N_Γ , \mathfrak{C} , and, of course, on θ , and one could get the coercivity on the whole space V_h . On the other hand, it is unclear how to prove iv, even assuming that local inf-sup conditions hold. In this sense, going through the Banach-Nečas-Babuška condition allows us to circumvent the problem, thanks to the fact that Lemma 5.2.16 holds.

Theorem 5.2.20. *Under Assumption 5.2.13, given $\theta \in (0, 1]$, there exists a unique solution $(\mathbf{u}_h, p_h) \in V_h^{\mathbf{u}^D} \times \bar{Q}_h$ of the stabilized problem (5.5) satisfying the stability estimates (5.15).*

Proof. From Theorem 5.2.17 there exists a unique solution $(\mathbf{u}_h, p_h, \boldsymbol{\lambda}_h) \in V_h^{\mathbf{u}^D} \times \bar{Q}_h \times \Lambda_h$ of (5.8). Thanks to Proposition 5.2.11, (\mathbf{u}_h, p_h) is the unique solution of problem (5.5). The stability estimates follow from Proposition 5.2.18. \square

5.2.5 *A priori* error estimates

The goal of this section is to demonstrate that the errors, for both the velocity and pressure fields, achieve optimal *a priori* convergence rates in the topologies induced by the norms $\|\cdot\|_{1,h}$ and $\|\cdot\|_{0,h}$, respectively.

Lemma 5.2.21. *Given $\theta \in (0, 1]$, let $(\mathbf{u}, p) \in \mathbf{H}^{\frac{3}{2}+\varepsilon}(\Omega) \times L^2(\Omega)$, $\varepsilon > 0$, and $(\mathbf{u}_h, p_h) \in V_h \times \overline{Q}_h$ be the solutions to (5.1) and (5.5), respectively. Then, for every $(\mathbf{u}^I, p^I) \in V_h \times \overline{Q}_h$, the following estimates hold.*

$$\begin{aligned} \|\mathbf{u}_h - \mathbf{u}^I\|_{1,h} &\leq \frac{1}{\alpha} \left(M_a \|\mathbf{u} - \mathbf{u}^I\|_{1,h} + \sum_{i=1}^N \sum_{j=0}^{i-1} \left\| \mathbf{h}^{\frac{1}{2}} \langle D(\mathbf{u} - R_{ij}^v(\mathbf{u}^I)) \mathbf{n} \rangle_t \right\|_{L^2(\Gamma_{ij})} \right. \\ &\quad \left. + M_b \|p - p^I\|_{0,h} \right) + \frac{1}{\beta} \left(1 + \frac{M_a}{\alpha} \right) M_b \|\mathbf{u} - \mathbf{u}^I\|_{1,h}, \\ \|p_h - p^I\|_{0,h} &\leq \frac{1}{\beta} \left(1 + \frac{M_a}{\alpha} \right) \left(M_a \|\mathbf{u} - \mathbf{u}^I\|_{1,h} + \sum_{i=1}^N \sum_{j=0}^{i-1} \left\| \mathbf{h}^{\frac{1}{2}} \langle D(\mathbf{u} - R_{ij}^v(\mathbf{u}^I)) \mathbf{n} \rangle_t \right\|_{L^2(\Gamma_{ij})} \right. \\ &\quad \left. + M_b \|p - p^I\|_{0,h} \right) + \frac{M_a}{\beta^2} \left(1 + \frac{M_a}{\alpha} \right) M_b \|\mathbf{u} - \mathbf{u}^I\|_{1,h}. \end{aligned}$$

Proof. Let us fix $(\mathbf{u}^I, p^I) \in V_h \times \overline{Q}_h$. By linearity $(\mathbf{u}_h - \mathbf{u}^I, p_h - p^I) \in V_h \times \overline{Q}_h$ satisfies the saddle point problem

$$\begin{aligned} \bar{a}_h(\mathbf{u}_h - \mathbf{u}^I, \mathbf{v}_h) + b(\mathbf{v}_h, p_h - p^I) &= F^I(\mathbf{v}_h), \quad \forall \mathbf{v}_h \in V_h^0, \\ b(\mathbf{u}_h - \mathbf{u}^I, q_h) &= G^I(q_h), \quad \forall q_h \in \overline{Q}_h, \end{aligned} \tag{5.16}$$

where, for every $(\mathbf{v}_h, q_h) \in V_h^0 \times \overline{Q}_h$,

$$\begin{aligned} F^I(\mathbf{v}_h) &:= \sum_{i=0}^N \int_{\Omega_i} D(\mathbf{u}_i - D\mathbf{u}_i^I) : D\mathbf{v}_h - \sum_{i=1}^N \sum_{j=0}^{i-1} \int_{\Gamma_{ij}} \left(\langle D(\mathbf{u} - R_{ij}^v(\mathbf{u}^I)) \mathbf{n} \rangle_t [\mathbf{v}_h] \right. \\ &\quad \left. + \langle DR_{ij}^v(\mathbf{v}_h) \mathbf{n} \rangle_t [\mathbf{u} - \mathbf{u}^I] \right) + \gamma \sum_{i=1}^N \sum_{j=0}^{i-1} \int_{\Gamma_{ij}} \mathbf{h}^{-1} [\mathbf{u}_h - \mathbf{u}^I] [\mathbf{v}_h] + b(\mathbf{v}_h, p_h - p^I), \\ G^I(q_h) &:= b(\mathbf{u} - \mathbf{u}^I, q_h). \end{aligned}$$

Let us show the first line of (5.16). Note that the second line follows immediately. Let $\mathbf{v}_h \in V_h^0$. From Proposition 5.2.2, we know $F(\mathbf{v}_h) = a_h(\mathbf{u}, \mathbf{v}_h) + b(\mathbf{v}_h, p)$. Hence,

$$\begin{aligned} \bar{a}_h(\mathbf{u}_h - \mathbf{u}^I, \mathbf{v}_h) + b(\mathbf{v}_h, p_h - p^I) &= F(\mathbf{v}_h) - \bar{a}_h(\mathbf{u}^I, \mathbf{v}_h) - b(\mathbf{v}_h, p^I) \\ &= a_h(\mathbf{u}, \mathbf{v}_h) - \bar{a}_h(\mathbf{u}^I, \mathbf{v}_h) + b(\mathbf{v}_h, p - p^I) \\ &= \sum_{i=0}^N \int_{\Omega_i} D(\mathbf{u}_i - D\mathbf{u}_i^I) : D\mathbf{v}_h - \sum_{i=1}^N \sum_{j=0}^{i-1} \int_{\Gamma_{ij}} \left(\langle D(\mathbf{u} - R_{ij}^v(\mathbf{u}^I)) \mathbf{n} \rangle_t [\mathbf{v}_h] \right. \\ &\quad \left. + \langle DR_{ij}^v(\mathbf{v}_h) \mathbf{n} \rangle_t [\mathbf{u} - \mathbf{u}^I] \right) \\ &\quad + \gamma \sum_{i=1}^N \sum_{j=0}^{i-1} \int_{\Gamma_{ij}} \mathbf{h}^{-1} [\mathbf{u}_h - \mathbf{u}^I] [\mathbf{v}_h] + b(\mathbf{v}_h, p_h - p^I). \end{aligned}$$

5.2. Isogeometric discretization on overlapping multipatch domains

Using standard the stability estimates (5.15), we get

$$\begin{aligned}\|\mathbf{u}_h - \mathbf{u}^I\|_{1,h} &\leq \frac{1}{\alpha} \|F^I\|_{-1,h} + \frac{1}{\beta} \left(1 + \frac{M_a}{\alpha}\right) \|G^I\|_{-0,h}, \\ \|p_h - p^I\|_{0,h} &\leq \frac{1}{\beta} \left(1 + \frac{M_a}{\alpha}\right) \|F^I\|_{-1,h} + \frac{M_a}{\beta^2} \left(1 + \frac{M_a}{\alpha}\right) \|G^I\|_{-0,h},\end{aligned}$$

$\|\cdot\|_{-1,h}$ and $\|\cdot\|_{-0,h}$ being the dual norms induced by $\|\cdot\|_{1,h}$ and $\|\cdot\|_{0,h}$, respectively. Hence,

$$\begin{aligned}\|F^I\|_{-1,h} &\leq M_a \|\mathbf{u} - \mathbf{u}^I\|_1 + \sum_{i=1}^N \sum_{j=0}^{i-1} \left\| \mathbf{h}^{\frac{1}{2}} \langle D(\mathbf{u} - R_{ij}^v(\mathbf{u}^I)) \mathbf{n} \rangle_t \right\|_{L^2(\Gamma_{ij})} + M_b \|p - p^I\|_{0,h}, \\ \|G^I\|_{-0,h} &\leq M_b \|\mathbf{u} - \mathbf{u}^I\|_{-1,h}.\end{aligned}$$

□

Theorem 5.2.22. *Under Assumption 5.2.13, given $\theta \in (0, 1]$, let $(\mathbf{u}, p) \in \mathbf{H}^m(\Omega) \times H^r(\Omega)$, $m \geq 2$ and $r \geq 1$, be the solution to problem (5.1). Then, the discrete solution $(\mathbf{u}_h, p_h) \in V_h^{\square, \mathbf{u}^D} \times \overline{Q}_h^{\square}$ of the stabilized problem (5.5) satisfies*

$$\|\mathbf{u} - \mathbf{u}_h\|_{1,h} + \|p - p_h\|_{0,h} \leq Ch^{\min\{s, \ell\}} \left(\|\mathbf{u}\|_{H^m(\Omega)} + \|p\|_{H^r(\Omega)} \right),$$

where $s := \min\{k, m-1\}$ if $\square = \text{RT}$, $s := \min\{k+1, m-1\}$ if $\square \in \{\text{N}, \text{RT}\}$, $\ell := \min\{k+1, r\}$, and $C > 0$ depends on the constants appearing in Lemma 5.2.21.

Proof. Given $(\mathbf{u}^I, p^I) \in V_h^{\square} \times \overline{Q}_h$, we proceed by triangular inequality:

$$\begin{aligned}\|\mathbf{u} - \mathbf{u}_h\|_{1,h} &\leq \|\mathbf{u} - \mathbf{u}^I\|_{1,h} + \|\mathbf{u}_h - \mathbf{u}^I\|_{1,h}, \\ \|p - p_h\|_{0,h} &\leq \|p - p^I\|_{0,h} + \|p_h - p^I\|_{0,h}.\end{aligned}\tag{5.17}$$

Using Lemma 5.2.21, we obtain:

$$\begin{aligned}\|\mathbf{u} - \mathbf{u}_h\|_{1,h} &\leq \|\mathbf{u} - \mathbf{u}^I\|_{1,h} + \frac{1}{\alpha} \left(M_a \|\mathbf{u} - \mathbf{u}^I\|_{1,h} + \sum_{i=1}^N \sum_{j=0}^{i-1} \left\| \mathbf{h}^{\frac{1}{2}} \langle D(\mathbf{u} - R_{ij}^v(\mathbf{u}^I)) \mathbf{n} \rangle_t \right\|_{L^2(\Gamma_{ij})} \right. \\ &\quad \left. + M_b \|p - p^I\|_{0,h} \right) + \frac{1}{\beta} \left(1 + \frac{M_a}{\alpha} \right) M_b \|\mathbf{u} - \mathbf{u}^I\|_{1,h}, \\ \|p - p_h\|_{0,h} &\leq \|p - p^I\|_{0,h} + \frac{1}{\beta} \left(1 + \frac{M_a}{\alpha} \right) \left(M_a \|\mathbf{u} - \mathbf{u}^I\|_{1,h} + \sum_{i=1}^N \sum_{j=0}^{i-1} \left\| \mathbf{h}^{\frac{1}{2}} \langle D(\mathbf{u} - R_{ij}^v(\mathbf{u}^I)) \mathbf{n} \rangle_t \right\|_{L^2(\Gamma_{ij})} \right. \\ &\quad \left. + M_b \|p - p^I\|_{0,h} \right) + \frac{M_a}{\beta^2} \left(1 + \frac{M_a}{\alpha} \right) M_b \|\mathbf{u} - \mathbf{u}^I\|_{1,h}.\end{aligned}$$

Let us choose $\mathbf{u}^I := \Pi_{V_h}^{\square} \mathbf{u}$ and $p^I := \Pi_{Q_h}^{\square} p$ so that, by Proposition 5.2.8, and Lemma 5.2.9, we

obtain

$$\begin{aligned}\|\mathbf{u} - \mathbf{u}_h\|_{1,h} &\leq Ch^s \left(\|\mathbf{u}\|_{H^m(\Omega)} \right) + \frac{1}{\alpha} \max\{M_a, 1, M_b\} Ch^{\min\{s,\ell\}} \left(\|\mathbf{u}\|_{H^m(\Omega)} + \|p\|_{H^r(\Omega)} \right) \\ &\quad + \frac{1}{\beta} \left(1 + \frac{M_a}{\alpha} \right) M_b Ch^s \|\mathbf{u}\|_{H^m(\Omega)}, \\ \|p - p_h\|_{0,h} &\leq Ch^\ell \|p\|_{H^r(\Omega)} + \frac{1}{\beta} \left(1 + \frac{M_a}{\alpha} \right) \max\{M_a, 1, M_b\} Ch^{\min\{s,\ell\}} \left(\|\mathbf{u}\|_{H^m(\Omega)} + \|p\|_{H^r(\Omega)} \right) \\ &\quad + \frac{M_a}{\beta^2} \left(1 + \frac{M_a}{\alpha} \right) M_b Ch^s \|\mathbf{u}\|_{H^m(\Omega)}.\end{aligned}$$

□

5.3 Numerical example

We consider as computational domain $\Omega = (0, 1)^2$ constructed as $\Omega = \Omega_0 \cup \Omega_1$, where Ω_0 is Ω itself and Ω_1 is the quadrilateral of vertices $(0.125, 0.125 + \varepsilon)$, $(0.875 - \varepsilon, 0.875)$, $(0.375 - \varepsilon, 0.875)$, $(0.125, 0.625 + \varepsilon)$, where $\varepsilon > 0$ is a parameter that we can control (see Figure 5.1). We note that in the overlapped mesh \mathcal{M}_0 some elements of measure ε^2 appear. This numerical experiment aims to show that the stabilized formulation is robust to the degeneracy of the overlapping configuration, *i.e.*, as ε goes to 0. Let us solve problem (5.5) in Ω , enforcing Dirichlet boundary conditions on $\{(0, y) : 0 \leq y \leq 1\}$, $\{(1, y) : 0 \leq y \leq 1\}$ and Neumann boundary conditions on $\{(x, 0) : 0 \leq x \leq 1\}$, $\{(x, 1) : 0 \leq x \leq 1\}$. We borrow the reference solution from Example 4.1.1 of [94], namely

$$\mathbf{u} = \left(2e^x(-1+x)^2 x^2(y^2-y)(-1+2y), -e^x(-1+x)x(-2+x(3+x))(-1+y)^2 y^2 \right),$$

$$\begin{aligned}p = &-424 + 156e + (y^2 - y)(-456 + e^x(456 + x^2(228 - 5(y^2 - y)))) \\ &+ 2x(-228 + (y^2 - y)) + 2x^3(-36 + (y^2 - y)) + x^4(12 + (y^2 - y)).\end{aligned}$$

We use the Taylor-Hood isogeometric element, use $t = \frac{1}{2}$, which corresponds to the symmetric

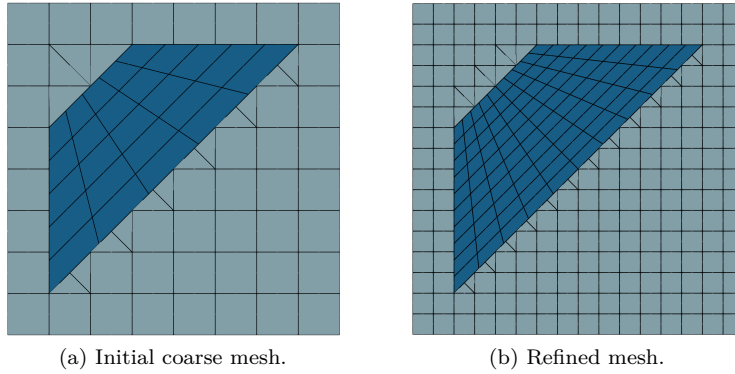


Figure 5.1 – Meshes configuration.

average, and choose threshold parameter $\theta = 1$, *i.e.*, we stabilize at all cut elements. The chosen penalty parameter is $\gamma = 10(k+2)^2$. The arising linear system is preconditioned with a left-right block-diagonal preconditioner corresponding to a rescaling with respect to $\|\cdot\|_{0,h}$ and $\|\cdot\|_{1,h}$. In

Figure 4.11 we plot the numerical solutions for the velocity and the pressure, and we can see the underlying mesh used for the numerical quadrature as well. We fix $\varepsilon = 10^{-12}$ and perform five dyadic refinements starting from the coarse mesh depicted in Figure 5.1(a). The error for the velocity and the pressure fields are shown in Figure 5.3 for degrees 2 and 3. The need for stabilization is observable from the error for the pressure. Note that the latter behaves in a similar way to the single patch trimmed case; see Section 4.7.1. The convergence rates for the stabilized case agree with the ones predicted by Theorem 5.2.22. In Figure 5.4 we also compare the condition numbers of the stabilized and non-stabilized formulations when the degree is $k = 2$. In Figure 5.4(a) we fix $\varepsilon = 10^{-12}$ and perform four dyadic refinement of the coarse meshes of Figure 5.1(a). In Figure 5.4(b) we fix the mesh sizes (one refinement of the mesh depicted in Figure 5.1(a)) and decrease the value of ε . We observe that the stabilization helps in reducing the dependence of the condition number from ε .

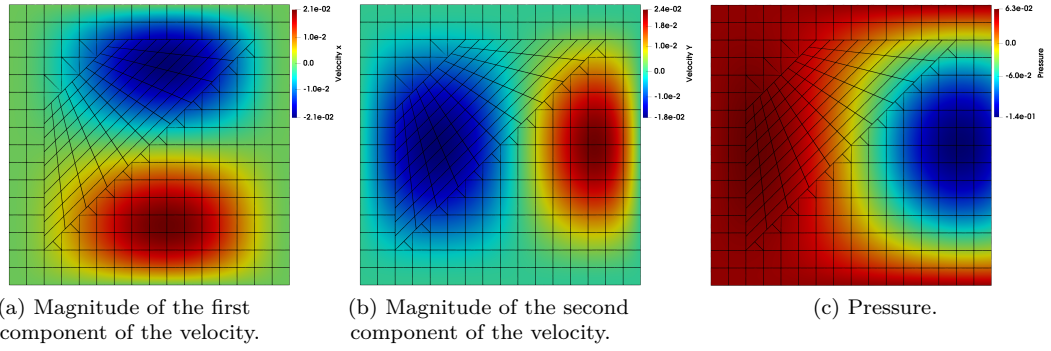


Figure 5.2 – Numerical solutions.

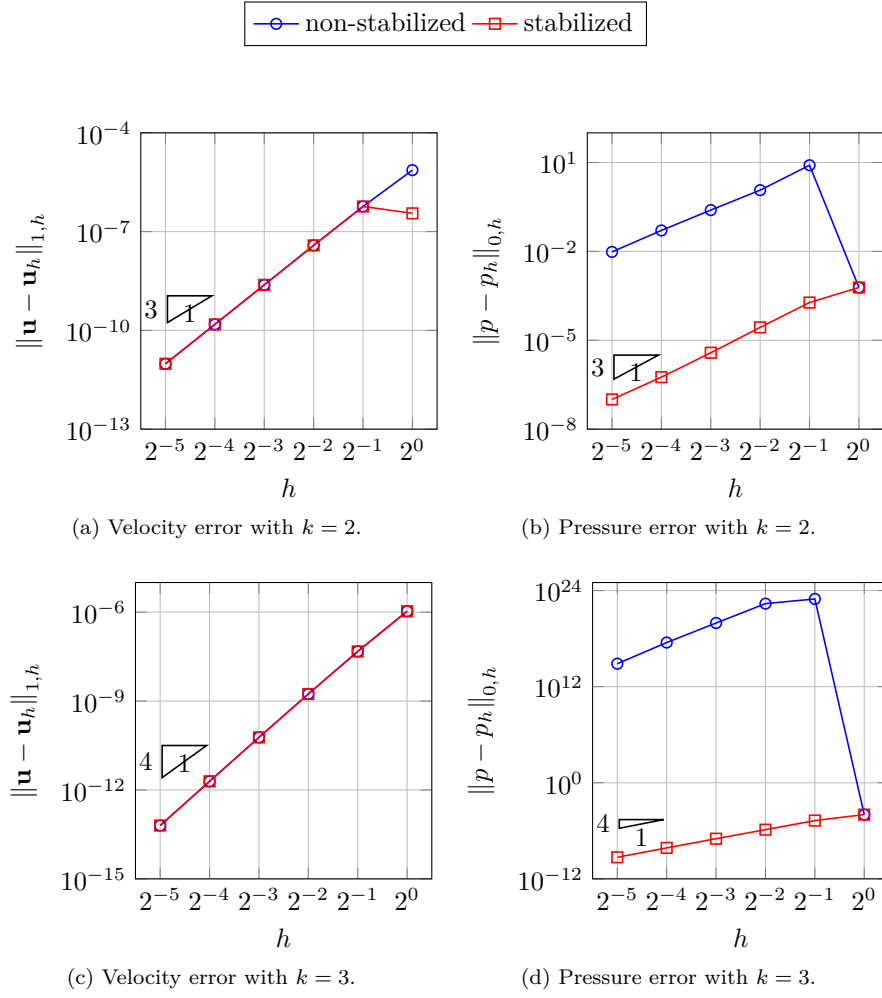


Figure 5.3 – Convergence errors.

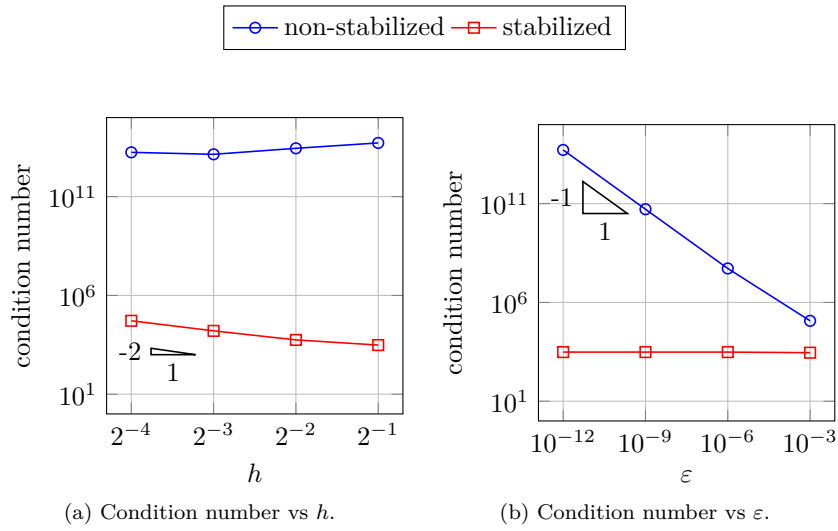


Figure 5.4 – Conditioning study.

Summary of Part I

In the first part of the dissertation, we studied the isogeometric discretization of PDEs on geometries coming from CAD software and constructed via Boolean operations. In our ideal setting, we restrict ourselves to computational domains of \mathbb{R}^d , $d \in \{2, 3\}$, obtained via trimming and union operations. The significant contributions of the thesis lie on the theoretical side, and as far as the numerical side is concerned, we restricted ourselves to the case $d = 2$.

We started by tackling the Poisson problem on trimmed domains. Our approach is a fictitious domain method making use of the Nitsche framework [103] for the imposition of the Dirichlet boundary conditions. The main contribution is a novel stabilization method to recover the well-posedness of the discrete weak formulation of the problem. In this procedure, the elements are first divided into “good elements” (sufficient intersection with the physical domain) and “bad elements” (insufficient intersection with the physical domain). Our method does not modify the basis functions and does not add any stabilization parameters to calibrate. It modifies the evaluation of the normal derivatives that appear in the discrete variational formulation at the bad elements by replacing them with the evaluation at a “good neighboring element”.

We also considered the Poisson problem on geometries obtained via union operations, treated as multipatch overlapped domains with an underlying hierarchy. We employed a Nitsche-based mortar formulation to couple the trimmed patches together. This time, the formulation was unstable due to weak coupling at the interfaces, in particular to the evaluation of the normal derivatives at the elements cut by the interfaces. We successfully adapted the stabilization technique developed for the case of a single trimmed geometry. To provide more flexibility to our method, we allowed the good neighbor, from which we evaluated the normal derivative, to belong to the mesh of another patch.

Then, we treated the Stokes problem in a trimmed geometry. For the weak imposition of the essential boundary conditions, we employed the Nitsche method. This time ill-posedness even led to a lack of accuracy for the pressure in the presence of some unfortunate mesh cuts. The extension to the vector case of the stabilization for the Poisson problem was sufficient to cure instabilities due to flux evaluations in the diffusive part of the weak formulation. To restore the discrete inf-sup stability, we locally modified the pressure space at the bad elements. In this way, we excluded the basis functions responsible for the instabilities and replaced them with an extension of those from good neighboring elements.

We considered a Nitsche-based mortar discretization of the Stokes problem in the case of multiple overlapping spline patches, following the same framework as Poisson’s problem. Similar to Poisson, we extended the stabilization technique from the trimmed case to the union case, allowing the good neighbor to be searched in a different mesh.

Several stability and error estimates have been rigorously derived throughout the different sections. These theoretical results have been confirmed and supported by the numerical experiments at

Summary of Part I

the end of every chapter.

Let us present some future directions of research that may be interesting to be investigated based on this part of the thesis.

On the theoretical side, a mathematical proof of the inf-sup stability of the stabilized Nitsche formulation of the Stokes problem in a trimmed geometry remains an open problem. In particular, the proof should cover the cases of the Raviart-Thomas, Nédélec, and Taylor-Hood isogeometric elements. In the specific case of the Raviart-Thomas isogeometric element, it would also be interesting to understand how to modify the stabilization procedure to retrieve a pointwise divergence-free numerical solution for the velocity (when $g = 0$ in (4.2)).

In this manuscript, no sound solution has been provided to the ill-conditioning problem of the final linear system due to the contribution when dealing with isogeometric methods on cut meshes. Indeed, as already said, we limited ourselves to applying a simple Jacobi preconditioner. Even though the stabilization procedure coupled with the diagonal rescaling allows for a significant improvement of the conditioning, it does not completely solve its dependency on trimming and overlapping configuration.

From a more practical side, the simulation of problems close to real applications requires extending our research code to the three-dimensional setting, which is not straightforward. Although the implementation of our stabilization procedure is readily extendable to the three-dimensional case, this is not the case for the integration strategy of the cut elements. The problem of deriving efficient quadrature rules in general curvilinear polyhedra is an active area of research; see, for instance, [6].

Weak imposition of the boundary conditions for the Darcy flow

Part II

6 The Raviart-Thomas discretization of the Darcy problem

The material in this chapter is quite standard. However, we decided to include it as a standalone chapter to make the exposition of the following chapters lighter and avoid as many overlaps as possible.

In what follows, integrals, norms, and vector spaces of functions will be defined on sets like \widehat{K} , where \widehat{K} is a closed polyhedron, and they are meant to be on their interior in a suitable sense.

Let Ω be a Lipschitz-regular domain of \mathbb{R}^d , $d \in \{2, 3\}$. We assume its boundary Γ to be partitioned into $\Gamma = \overline{\Gamma}_N \cup \overline{\Gamma}_D$, where Γ_D , Γ_N are open and disjoint. Let us consider the *Darcy problem*, a system of linear PDEs, often associated with a linearized model for the flow of groundwater through the domain Ω , here representing a saturated porous medium with permeability κ .

Given $\mathbf{f} \in \mathbf{L}^2(\Omega)$, $g \in L^2(\Omega)$, $u_N \in H^{-\frac{1}{2}}(\Gamma_N)$, $p_D \in H^{\frac{1}{2}}(\Gamma_D)$, we look for $\mathbf{u} : \Omega \rightarrow \mathbb{R}^d$ and $p : \Omega \rightarrow \mathbb{R}$ such that

$$\begin{aligned} \kappa^{-1} \mathbf{u} - \nabla p &= \mathbf{f}, & \text{in } \Omega, \\ \operatorname{div} \mathbf{u} &= g, & \text{in } \Omega, \\ \mathbf{u} \cdot \mathbf{n} &= u_N, & \text{on } \Gamma_N, \\ p &= p_D, & \text{on } \Gamma_D. \end{aligned} \tag{6.1}$$

The unknowns \mathbf{u} and p represent, respectively, the seepage velocity and the pressure of the fluid. The first equation of (6.1) is called *Darcy law* relating the velocity and the pressure gradient of the fluid, the second one expresses *mass conservation*, the third and the fourth equations are, respectively, a *essential boundary condition* for the velocity field and a *natural boundary condition* for the pressure. Moreover, $\kappa \in \mathbb{R}^{d \times d}$ is symmetric positive definite with eigenvalues λ_i such that $0 < \lambda_{\min} \leq \lambda_i \leq \lambda_{\max} < +\infty$, for every $1 \leq i \leq d$.

In order to discretize the problem (6.1), we resort to the theory of mixed finite elements. In particular, we introduce the classical Raviart-Thomas element [22, 115]. Let us follow the very classical definition of finite element *à la Ciarlet* (see [42, 99]). A finite element is defined by a triple (K, P_K, Σ_K) , where K is a geometric domain, P_K a finite-dimensional space of functions, and Σ_K a set of linear functionals on P_K , known as *degrees of freedom*. The Raviart-Thomas element is a couple of finite elements, one for the velocity and one for the pressure fields, suitable for the discretization of problem (6.1).

Let $(\mathcal{T}_h)_{h>0}$ be a family of triangular or quadrilateral meshes of Ω . For every $K \in \mathcal{T}_h$, $h > 0$, let $h_K := \operatorname{diam}(K)$ and $h := \max_{K \in \mathcal{T}_h} h_K$. We assume the mesh family to be *shape-regular*, i.e., there exists $\sigma > 0$, independent of h , such that $\max_{K \in \mathcal{T}_h} \frac{h_K}{\rho_K} \leq \sigma$, ρ_K being the diameter of the largest ball inscribed in K .

Chapter 6. The Raviart-Thomas discretization of the Darcy problem

In the case of triangles and tetrahedra, we consider as reference element \hat{K} is the unit d -simplex, *i.e.*, the triangle of vertices $(0, 0)$, $(1, 0)$, $(0, 1)$ if $d = 2$ and the tetrahedron of vertices $(0, 0, 0)$, $(1, 0, 0)$, $(0, 1, 0)$, $(0, 0, 1)$ when $d = 3$. For quadrilaterals, the reference element \hat{K} is the unit d -cube $[0, 1]^d$.

Let us construct the spaces of polynomials on the reference element. For the triangular meshes (see Section 2.3.1 of [22]),

$$\mathbb{RT}_k(\hat{K}) := \left(\mathbb{P}_k(\hat{K}) \right)^d \oplus \mathbf{x} \tilde{\mathbb{P}}_k(\hat{K}), \quad \mathbb{M}_k(\hat{K}) := \mathbb{P}_k(\hat{K}),$$

while, in the case of quadrilaterals (see [7] and Section 2.4.1 of [22]), it reads as follows

$$\mathbb{RT}_k(\hat{K}) := \begin{cases} \mathbb{Q}_{k+1,k}(\hat{K}) \times \mathbb{Q}_{k,k+1}(\hat{K}), & \text{if } d = 2, \\ \mathbb{Q}_{k+1,k,k}(\hat{K}) \times \mathbb{Q}_{k,k+1,k}(\hat{K}) \times \mathbb{Q}_{k,k,k+1}(\hat{K}), & \text{if } d = 3, \end{cases} \quad \mathbb{M}_k(\hat{K}) := \mathbb{Q}_k(\hat{K}).$$

Remark 6.0.1. For quadrilaterals, $\mathbb{RT}_k(\hat{K})$ can equivalently be defined as

$$\mathbb{RT}_k(\hat{K}) := \mathbb{Q}_k(\hat{K})^d \oplus \mathbf{x} \mathbb{Q}_k(\hat{K}).$$

Let $\mathbf{F}_K : \hat{K} \rightarrow K$ be a diffeomorphism mapping the reference element to a general $K \in \mathcal{T}_h$. For triangles we consider an affine bijection $\mathbf{F}_K(\hat{x}) := B_K \hat{x} + b_K$, where $B_K \in \mathbb{R}^{d \times d}$ is non-singular and invertible, and $b_K \in \mathbb{R}^d$. For quadrilateral meshes, an affine mapping would constrain us to parallelograms, hence we let \mathbf{F}_K being a bilinear bijection for each component, so that we can map the reference element to arbitrary convex quadrilaterals. The diffeomorphism \mathbf{F}_K induces the following pull-back operators.

$$\mathbf{F}_K^p : L^2(K) \rightarrow L^2(\hat{K}), \quad \mathbf{F}_K^p(q) := |\det(D\mathbf{F}_K)| q \circ \mathbf{F}_K, \quad (6.2)$$

$$\mathbf{F}_K^v : \mathbf{H}(\text{div}; K) \rightarrow \mathbf{H}(\text{div}; \hat{K}), \quad \mathbf{F}_K^v(\mathbf{v}) := |\det(D\mathbf{F}_K)| D\mathbf{F}_K^{-1} \mathbf{v} \circ \mathbf{F}_K. \quad (6.3)$$

Let us observe that \mathbf{F}_K^p and \mathbf{F}_K^v are isometric isomorphisms (see, for instance, [118]). For the construction of our discrete spaces, we will use \mathbf{F}_K^p and \mathbf{F}_K^v . The inverse of \mathbf{F}_K^v is commonly known as the *contravariant Piola transform* or, more simply, *Piola transform*, and we denote it as follows

$$\mathcal{P}_K : \mathbf{H}(\text{div}; \hat{K}) \rightarrow \mathbf{H}(\text{div}; K), \quad \mathcal{P}_K(\hat{\mathbf{v}}) := |\det(D\mathbf{F}_K)|^{-1} D\mathbf{F}_K \hat{\mathbf{v}} \circ \mathbf{F}_K^{-1}.$$

We define the following finite-dimensional vector spaces

$$\begin{aligned} V_h &:= \left\{ \mathbf{v}_h \in \mathbf{H}(\text{div}; \Omega) : \mathbf{F}_K^v \left(\mathbf{v}_h \Big|_K \right) \in \mathbb{RT}_k(\hat{K}), \quad \forall K \in \mathcal{T}_h \right\} \\ &= \left\{ \mathbf{v}_h \in \mathbf{H}(\text{div}; \Omega) : \mathbf{v}_h \Big|_K \in \mathbb{RT}_k(K), \quad \forall K \in \mathcal{T}_h \right\}, \\ Q_h &:= \left\{ q_h \in L^2(\Omega) : \mathbf{F}_K^p \left(q_h \Big|_K \right) \in \mathbb{M}_k(\hat{K}), \quad \forall K \in \mathcal{T}_h \right\} \\ &= \left\{ q_h \in L^2(\Omega) : q_h \Big|_K \in \mathbb{M}_k(K), \quad \forall K \in \mathcal{T}_h \right\}, \end{aligned}$$

where $\mathbb{RT}_k(K) := \{\mathcal{P}_K(\hat{\mathbf{w}}_h) : \hat{\mathbf{w}}_h \in \mathbb{RT}_k(\hat{K})\}$ and $\mathbb{M}_k(K) := \{\hat{m}_h \circ (\mathbf{F}_K^p)^{-1} : \hat{m}_h \in \mathbb{M}_k(\hat{K})\}$. Remember that in the pure essential case, *i.e.*, $\Gamma = \Gamma_N$, we have to filter out the constant functions from Q_h by imposing the zero average constraint.

Instead of exhibiting the degrees of freedom associated with the polynomial spaces \mathbb{RT}_k and \mathbb{M}_k , let us construct the interpolants associated with them.

We start with the velocity. For every $\mathbf{v} \in \mathbf{H}^s(\widehat{K})$, $s > \frac{1}{2}$, $r_{\widehat{K}}(\mathbf{v})$ is uniquely defined by:

$$\begin{aligned} \int_{\widehat{f}} r_{\widehat{K}}(\mathbf{v}) \cdot \mathbf{n} \widehat{q}_h &= \int_{\widehat{f}} \widehat{\mathbf{v}} \cdot \mathbf{n} \widehat{q}_h, \quad \forall \widehat{q}_h \in \Psi_k(\widehat{f}), \\ \int_{\widehat{K}} r_{\widehat{K}}(\mathbf{v}) \cdot \widehat{\mathbf{w}}_h &= \int_{\widehat{K}} \widehat{\mathbf{v}} \cdot \widehat{\mathbf{w}}_h, \quad \forall \widehat{\mathbf{w}}_h \in \Psi_k(\widehat{K}), \quad \text{if } k > 0, \end{aligned} \quad (6.4)$$

where, for triangles,

$$\Psi_k(\widehat{K}) := \left(\mathbb{P}_{k-1}(\widehat{K}) \right)^d, \quad \Psi_k(\widehat{f}) := \mathbb{P}_k(\widehat{f}),$$

and, for quadrilaterals,

$$\begin{aligned} \Psi_k(\widehat{K}) &:= \begin{cases} \mathbb{Q}_{k-1,k}(\widehat{K}) \times \mathbb{Q}_{k,k-1}(\widehat{K}), & \text{if } d = 2, \\ \mathbb{Q}_{k-1,k,k}(\widehat{K}) \times \mathbb{Q}_{k,k-1,k}(\widehat{K}) \times \mathbb{Q}_{k,k,k-1}(\widehat{K}), & \text{if } d = 3, \end{cases} \\ \Psi_k(\widehat{f}) &:= \begin{cases} \mathbb{P}_k(\widehat{f}), & \text{if } d = 2, \\ \mathbb{Q}_k(\widehat{f}), & \text{if } d = 3, \end{cases} \end{aligned}$$

for all facets (edges if $d = 2$, faces if $d = 3$) \widehat{f} of \widehat{K} . We define $r_K : \mathbf{H}^s(K) \rightarrow \mathbb{RT}_k(K)$, $s > \frac{1}{2}$, so that the diagram in (6.5) commutes, namely $r_K = (\mathbf{F}_K^v)^{-1} \circ r_{\widehat{K}} \circ \mathbf{F}_K^v = \mathcal{P}_K \circ r_{\widehat{K}} \circ \mathcal{P}_K^{-1}$.

$$\begin{array}{ccc} \mathbf{H}^s(K) & \xrightarrow{r_K} & \mathbb{RT}_k(K) \\ \downarrow \mathbf{F}_K^v & & \downarrow \mathbf{F}_K^v \\ \mathbf{H}^s(\widehat{K}) & \xrightarrow{r_{\widehat{K}}} & \mathbb{RT}_k(\widehat{K}), \end{array} \quad (6.5)$$

The global interpolant $r_h : \mathbf{H}(\text{div}; \Omega) \cap \prod_{K \in \mathcal{T}_h} \mathbf{H}^s(K) \rightarrow V_h$, $s > \frac{1}{2}$, is readily defined by gluing together the local interpolation operators, that is $r_h|_K := r_K$, $K \in \mathcal{T}_h$. Let us move to the pressure case. We start from the reference element \widehat{K} , and define $\Pi_{\widehat{K}} : L^2(\widehat{K}) \rightarrow \mathbb{M}_k(\widehat{K})$ which acts on $\xi \in L^2(\widehat{K})$ as

$$\int_K \Pi_{\widehat{K}} \xi q_h = \int_{\widehat{K}} \xi q_h, \quad \forall q_h \in \mathbb{M}_k(\widehat{K}). \quad (6.6)$$

Then, for a general $K \in \mathcal{T}_h$, we define $\Pi_K : L^2(K) \rightarrow \mathbb{M}_k(K)$ such that the diagram (6.7) commutes, namely $\Pi_K = (\mathbf{F}_K^p)^{-1} \circ \Pi_{\widehat{K}} \circ \mathbf{F}_K^p$.

$$\begin{array}{ccc} L^2(K) & \xrightarrow{\Pi_K} & \mathbb{M}_k(K) \\ \downarrow \mathbf{F}_K^p & & \downarrow \mathbf{F}_K^p \\ L^2(\widehat{K}) & \xrightarrow{\Pi_{\widehat{K}}} & \mathbb{M}_k(\widehat{K}). \end{array} \quad (6.7)$$

Finally, let $\Pi_h : L^2(\Omega) \rightarrow Q_h$ such that for every $K \in \mathcal{T}_h$, $\Pi_h|_K := \Pi_K$.

Remark 6.0.2. Given $\mathbf{v} \in \mathbf{H}(\text{div}; \Omega) \cap \prod_{K \in \mathcal{T}_h} \mathbf{H}^s(K)$, $s > \frac{1}{2}$, the degrees of freedom for $r_{\widehat{K}}(\mathbf{v}|_{\widehat{K}})$ given by (6.4) are invariant under \mathbf{F}_K^v , for every $K \in \mathcal{T}_h$. Similarly, given $q \in L^2(\Omega)$, the degrees of freedom for $\Pi_{\widehat{K}}(q|_{\widehat{K}})$ given by (6.6) are invariant under \mathbf{F}_K^p , for every $K \in \mathcal{T}_h$.

We now state a key property of the Raviart-Thomas element.

Theorem 6.0.3. *The following diagram commutes:*

$$\begin{array}{ccc} \mathbf{H}(\operatorname{div}; \Omega) \cap \prod_{K \in \mathcal{T}_h} \mathbf{H}^s(K) & \xrightarrow{\operatorname{div}} & L^2(\Omega) \\ \downarrow r_h & & \downarrow \Pi_h \\ V_h & \xrightarrow{\operatorname{div}} & Q_h. \end{array}$$

In particular, it holds $\operatorname{div} V_h = Q_h$.

Proof. For the commutative diagram note that, for every $\mathbf{v} \in \mathbf{H}(\operatorname{div}; \Omega) \cap \prod_{K \in \mathcal{T}_h} \mathbf{H}^s(K)$, it holds

$$\begin{aligned} \int_K \Pi_h(\operatorname{div} \mathbf{v}) \varphi_h &= \int_K \operatorname{div} \mathbf{v} \varphi_h = - \int_K \mathbf{v} \cdot \nabla \varphi_h + \int_{\partial K} \varphi_h \mathbf{v} \cdot \mathbf{n} \\ &= - \int_K r_h(\mathbf{v}) \cdot \nabla \varphi_h + \int_{\partial K} \varphi_h r_h(\mathbf{v}) \cdot \mathbf{n} \\ &= \int_K \operatorname{div} r_h(\mathbf{v}) \varphi_h, \quad \forall \varphi_h \in \mathbb{M}_k(K). \end{aligned}$$

A direct calculation readily shows the inclusion $\operatorname{div} V_h \subseteq Q_h$. Let us prove the other one. Let $q_h \in Q_h$, then, by the surjectivity of the divergence operator [22], there exists $\mathbf{v} \in \mathbf{H}^1(\Omega) \subset \mathbf{H}(\operatorname{div}; \Omega) \cap \prod_{K \in \mathcal{T}_h} \mathbf{H}^s(K)$ such that $\operatorname{div} \mathbf{v} = q_h$. Let us define $\mathbf{v}_h := r_h(\mathbf{v})$. Thanks to the commutativity diagram we have $\operatorname{div} \mathbf{v}_h = q_h$. \square

We are now ready to discretize (6.1). To incorporate the boundary conditions, we shall define $V_h^0 := V_h \cap \mathbf{H}_{0, \Gamma_N}(\operatorname{div}; \Omega)$ (assuming that the family of meshes is such that no elements' facet is shared between Γ_D and Γ_N). Moreover, let $\tilde{\mathbf{u}} \in H(\operatorname{div}; \Omega)$ be such that $\tilde{\mathbf{u}} \cdot \mathbf{n} = u_N$ on Γ_N in the sense of traces. We look for (\mathbf{u}_h, p_h) such that $\mathbf{u}_h = \mathbf{u}_h^0 + \tilde{\mathbf{u}}$ and $(\mathbf{u}_h^0, p_h) \in V_h^0 \times Q_h$ solves

$$\begin{aligned} a(\mathbf{u}_h^0, \mathbf{v}_h) + b_0(\mathbf{v}_h, p_h) &= F(\mathbf{v}_h), & \forall \mathbf{v}_h \in V_h^0, \\ b_0(\mathbf{u}_h^0, q_h) &= G(q_h), & \forall q_h \in Q_h, \end{aligned} \tag{6.8}$$

where

$$\begin{aligned} a(\mathbf{w}_h, \mathbf{v}_h) &:= \int_{\Omega} \kappa^{-1} \mathbf{w}_h \cdot \mathbf{v}_h, & \mathbf{w}_h, \mathbf{v}_h \in V_h, \\ b(\mathbf{w}_h, \mathbf{v}_h) &:= \int_{\Omega} q_h \operatorname{div} \mathbf{v}_h, & \mathbf{v}_h \in V_h, \quad q_h \in Q_h, \\ F(\mathbf{v}_h) &:= \int_{\Omega} \mathbf{f} \cdot \mathbf{v}_h + \int_{\Gamma_D} p_D \mathbf{v}_h \cdot \mathbf{n} - a(\tilde{\mathbf{u}}, \mathbf{v}_h), & \mathbf{v}_h \in V_h, \\ G(q_h) &:= \int_{\Omega} g q_h, & q_h \in Q_h. \end{aligned}$$

Formulation (6.8) is a consistent discretization of problem (6.1). It is stable in the sense of Theorem 5.2.5 of [22]. In particular, the inf-sup stability can be proved with the so-called *Fortin's trick* (Proposition 5.4.2 of [22]), thanks to Theorem 6.0.3.

7 Weak imposition of the essential boundary conditions for the Darcy flow: fitted case

This chapter proposes two families of discrete formulations for the weak imposition of the essential boundary conditions for the Darcy flow. The Raviart-Thomas mixed finite element on both triangular and quadrilateral meshes is considered for both methods. One is a consistent discretization depending on a weighting parameter scaling as $\mathcal{O}(h^{-1})$. The other is a penalty-type formulation obtained as the discretization of a perturbation of the original problem and relies on a parameter scaling as $\mathcal{O}(h^{-(k+1)})$, k being the order of the Raviart-Thomas space. We rigorously prove that both methods are stable and result in optimal convergent numerical schemes with respect to appropriate mesh-dependent norms, although the chosen norms do not scale as the usual L^2 -norm. However, we can still recover the optimal a priori L^2 -error estimates for the velocity field for high-order and the lowest-order Raviart-Thomas discretizations, for the first and second numerical schemes, respectively.

Let us briefly sketch the outline of the paper. In Section 7.1 we introduce, respectively, the strong formulation of the Darcy problem and a singularly perturbed formulation of it. In Section 7.2, the Raviart-Thomas finite element is introduced together with our two discrete formulations, both depending on a mesh-dependent weighting parameter. As already mentioned, for the first one, the penalty parameter is $\mathcal{O}(h^{-1})$, while for the other it is $\mathcal{O}(h^{-(k+1)})$. In Section 7.3, we prove the desired stability estimates with respect to different mesh-dependent norms, guaranteeing the well-posedness of the associated problems. Then, in Section 7.4, optimal *a priori error* estimates, in terms of the chosen norms, are demonstrated for the velocity and pressure fields. We recover optimality for the L^2 -error of the velocity field as well. Finally, some numerical examples corroborating the theory are provided.

The content of this chapter has been accepted for publication, see [41].

In the following, C will denote generic positive constants that may change with each occurrence throughout the chapter but are always independent of the mesh size unless otherwise specified. Given $x, y \in \mathbb{R}$, we will write $x \lesssim y$ if there exists $c > 0$, independent on the mesh size, such that $x \leq cy$ and $x \sim y$ if $x \lesssim y$ and $y \lesssim x$.

7.1 The Darcy problem and a perturbed formulation

Let Ω be a Lipschitz-regular domain of \mathbb{R}^d , $d \in \{2, 3\}$. We assume its boundary Γ to be partitioned into $\Gamma = \bar{\Gamma}_N \cup \bar{\Gamma}_D$, where Γ_D , Γ_N are open and disjoint. Let us consider the Darcy problem that has been introduced in Chapter 6.

Chapter 7. Weak imposition of the essential boundary conditions for the Darcy flow: fitted case

Given $\mathbf{f} \in \mathbf{L}^2(\Omega)$, $g \in L^2(\Omega)$, $u_N \in H^{-\frac{1}{2}}(\Gamma_N)$, $p_D \in H^{\frac{1}{2}}(\Gamma_D)$, we look for $\mathbf{u} : \Omega \rightarrow \mathbb{R}^d$ and $p : \Omega \rightarrow \mathbb{R}$ such that

$$\begin{aligned} \kappa^{-1} \mathbf{u} - \nabla p &= \mathbf{f}, & \text{in } \Omega, \\ \operatorname{div} \mathbf{u} &= g, & \text{in } \Omega, \\ \mathbf{u} \cdot \mathbf{n} &= u_N, & \text{on } \Gamma_N, \\ p &= p_D, & \text{on } \Gamma_D. \end{aligned} \tag{7.1}$$

Here, $\kappa \in \mathbb{R}^{d \times d}$ is symmetric positive definite with eigenvalues λ_i such that $0 < \lambda_{\min} \leq \lambda_i \leq \lambda_{\max} < +\infty$, for every $1 \leq i \leq d$.

Remark 7.1.1. We observe that the subscripts N and D (in Γ_D , Γ_N) refer to the Dirichlet and Neumann boundary conditions for the Poisson problem, from which (7.1) can be derived by duality techniques (see Chapter 1 of [22]). Contrary to the case of the Poisson problem, here, the boundary conditions for the pressure on Γ_D are *natural*, in the sense that they can be implicitly enforced in the weak formulation of the problem. In contrast, the boundary conditions for the velocity on Γ_N are *essential*, *i.e.*, they are imposed on the functional space. Moreover, let us observe that in the pure essential case $\Gamma = \Gamma_N$, in order to have well-posedness, we have to “filter out” the constant pressures, *i.e.*, the trial and test functions for the pressures are required to lie in $L_0^2(\Omega)$, and to impose a compatibility condition on the data: $\int_{\Gamma_N} u_N = \int_{\Omega} g$.

Let us consider the following perturbation of problem (7.1).

Find $\mathbf{u}^\varepsilon : \Omega \rightarrow \mathbb{R}^d$ and $p^\varepsilon : \Omega \rightarrow \mathbb{R}$ such that

$$\begin{aligned} \kappa^{-1} \mathbf{u}^\varepsilon - \nabla p^\varepsilon &= \mathbf{f}, & \text{in } \Omega, \\ \operatorname{div} \mathbf{u}^\varepsilon &= g, & \text{in } \Omega, \\ \varepsilon^{-1} \mathbf{u}^\varepsilon \cdot \mathbf{n} &= \varepsilon^{-1} u_N - p^\varepsilon, & \text{on } \Gamma_N, \\ p^\varepsilon &= p_D, & \text{on } \Gamma_D. \end{aligned} \tag{7.2}$$

Note that as $\varepsilon \rightarrow 0^+$ problem (7.2) formally degenerates to (7.1). In this sense (7.2) is a perturbation of problem (7.1).

In the subsequent analysis we are going to consider, for the sake of simplicity, $\kappa = I$ the identity matrix.

Proposition 7.1.2. *Let $(\mathbf{u}^\varepsilon, p^\varepsilon)$, (\mathbf{u}, p) be respectively the solutions to (7.2) and (7.1), and assume that $\mathbf{f} \in \mathbf{H}(\operatorname{div}; \Omega)$. Then there exists $C > 0$ such that*

$$\|\mathbf{u} - \mathbf{u}^\varepsilon\|_{L^2(\Omega)} \leq C\varepsilon \left(\|\operatorname{div} \mathbf{f}\|_{L^2(\Omega)} + \|g\|_{L^2(\Omega)} + \|u_N\|_{H^{-\frac{1}{2}}(\Gamma_N)} + \|p_D\|_{H^{\frac{1}{2}}(\Gamma_D)} \right).$$

Proof. Let us observe that if (\mathbf{u}, p) and $(\mathbf{u}^\varepsilon, p^\varepsilon)$ solve, respectively, the problems (7.1) and (7.2), then p and p^ε are the solutions of

$$\begin{aligned} -\Delta p &= -g + \operatorname{div} \mathbf{f}, & \text{in } \Omega, \\ \frac{\partial p}{\partial n} &= u_N - \mathbf{f} \cdot \mathbf{n}, & \text{on } \Gamma_N, \\ p &= p_D, & \text{on } \Gamma_D, \end{aligned} \tag{7.3}$$

and

$$\begin{aligned} -\Delta p^\varepsilon &= -g + \operatorname{div} \mathbf{f}, & \text{in } \Omega, \\ \frac{\partial p^\varepsilon}{\partial n} + \varepsilon p^\varepsilon &= u_N - \mathbf{f} \cdot \mathbf{n}, & \text{on } \Gamma_N, \\ p^\varepsilon &= p_D, & \text{on } \Gamma_D. \end{aligned} \tag{7.4}$$

7.1. The Darcy problem and a perturbed formulation

Let $\delta := p - p^\varepsilon$, with p and p^ε , respectively, the solutions of (7.3) and (7.4), then δ solves

$$\begin{aligned} -\Delta \delta &= 0, & \text{in } \Omega, \\ \delta + \varepsilon^{-1} \frac{\partial \delta}{\partial n} &= p, & \text{on } \Gamma_N, \\ \delta &= 0, & \text{on } \Gamma_D. \end{aligned} \quad (7.5)$$

We rewrite (7.5) in variational form.

Find $\delta \in H_{0,\Gamma_D}^1(\Omega)$ such that

$$\int_{\Omega} \nabla \delta \cdot \nabla \varphi + \varepsilon \int_{\Gamma_N} \delta \varphi = \varepsilon \int_{\Gamma_N} p \varphi, \quad \forall \varphi \in H_{0,\Gamma_D}^1(\Omega). \quad (7.6)$$

Since δ vanishes on a part of the boundary, a Poincaré-like inequality entails $\|\delta\|_{H^1(\Omega)} \leq C_P \|\nabla \delta\|_{L^2(\Omega)}$, with $C_P > 0$ independent of ε . Now, by testing (7.6) with δ , we get

$$\|\nabla \delta\|_{L^2(\Omega)}^2 + \varepsilon \|\delta\|_{L^2(\Gamma_N)}^2 = \varepsilon \int_{\Gamma_N} p \delta.$$

The Cauchy-Schwarz, a standard trace inequality, and the Poincaré inequality above imply

$$\|\nabla \delta\|_{L^2(\Omega)}^2 \lesssim \varepsilon \|p\|_{H^1(\Omega)} \|\nabla \delta\|_{L^2(\Omega)}.$$

On the other hand, p solves (7.3), hence

$$\|\nabla \delta\|_{L^2(\Omega)}^2 \lesssim \varepsilon \left(\|\operatorname{div} \mathbf{f}\|_{L^2(\Omega)} + \|g\|_{L^2(\Omega)} + \|u_N\|_{H^{-\frac{1}{2}}(\Gamma_N)} + \|p_D\|_{H^{\frac{1}{2}}(\Gamma_D)} \right) \|\nabla \delta\|_{L^2(\Omega)}.$$

Since $\mathbf{u} - \mathbf{u}^\varepsilon = \nabla p + \mathbf{f} - (\nabla p^\varepsilon + \mathbf{f}) = \nabla (p - p^\varepsilon) = \nabla \delta$, then the proof is completed. \square

Remark 7.1.3. With the extra assumption $\mathbf{f} \cdot \mathbf{n} = 0$ on Γ_N , it turns out that problems (7.1) and (7.2) are equivalent to problems (7.3) and (7.4), respectively.

In order to avoid technicalities, let us assume Ω to be a convex domain with a Lipschitz polygonal boundary, $u_N = 0$ and $\mathbf{f} \cdot \mathbf{n} = 0$ on Γ_N .

Proposition 7.1.4. *Let $(\mathbf{u}^\varepsilon, p^\varepsilon)$ be the solution of (7.2) and suppose that Ω is a convex domain with a Lipschitz polygonal boundary Γ , $\mathbf{f} \cdot \mathbf{n} = 0$ on Γ_N and $u_N = 0$. Then there exists $C > 0$, independent of ε , such that*

$$\|\mathbf{u}^\varepsilon\|_{H^1(\Omega)} \leq C \left(\|\mathbf{f}\|_{H^1(\Omega)} + \|g\|_{L^2(\Omega)} + \|p_D\|_{H^{\frac{1}{2}}(\Gamma_D)} \right). \quad (7.7)$$

Proof. For the sake of brevity, we are not giving the details of the proof. As above, observe that if $(\mathbf{u}^\varepsilon, p^\varepsilon)$ solves (7.2), then p_ε is the solution of (7.4). We first assume that Ω is a convex C^2 -domain and, without loss of generality, we put ourselves in the pure essential case $\Gamma = \Gamma_N$. Then the statement follows as a particular case of the *a priori* inequality of Theorem 3.1.2.3 in [66], which itself is based on the special integration by parts identity of Theorem 3.1.1.1 in [66]. Finally, as observed in Remark 3.2.4.6 in [66], the statement can be generalized to a convex domain with Lipschitz polygonal boundary, since it can be approximated with a sequence of convex C^2 -domains. \square

7.2 The finite element discretization

Let $(\mathcal{T}_h)_{h>0}$ denote a family of triangular or quadrilateral meshes of Ω . It will be useful to partition the *facets* (edges if $d = 2$ and faces if $d = 3$) \mathcal{F}_h of \mathcal{T}_h into three collections: the internal ones \mathcal{F}_h^i and the ones lying on Γ_N and on Γ_D , grouped, respectively, in $\mathcal{F}_h^\partial(\Gamma_N)$ and $\mathcal{F}_h^\partial(\Gamma_D)$, $\mathcal{F}_h^\partial = \mathcal{F}_h^\partial(\Gamma_N) \cup \mathcal{F}_h^\partial(\Gamma_D)$. For every $K \in \mathcal{T}_h$, $h > 0$, let $h_K := \text{diam}(K)$ and $h := \max_{K \in \mathcal{T}_h} h_K$. We assume the mesh to be *shape-regular*, *i.e.*, there exists $\sigma > 0$, independent of h , such that $\max_{K \in \mathcal{T}_h} \frac{h_K}{\rho_K} \leq \sigma$, ρ_K being the diameter of the largest ball inscribed in K . Moreover, \mathcal{T}_h is supposed to be *quasi-uniform* in the sense that there exists $\tau > 0$, independent of h , such that $\min_{K \in \mathcal{T}_h} h_K \geq \tau h$. We fix an orientation for the internal faces, given $f \in \mathcal{F}_h^i$ such that $f = \partial K_1 \cap \partial K_2$ we assume that unit normal vector on f points from K_1 toward K_2 . Note that nothing said from here on will depend on this choice. Let $\varphi : \Omega \rightarrow \mathbb{R}$ be smooth enough so that for every $K \in \mathcal{T}_h$ its restriction $\varphi|_K$ can be extended up to the boundary ∂K . Then, for all $f \in \mathcal{F}_h^i$ and every $x \in f$, we define the *jump* of φ as

$$[\varphi]_f(x) := \varphi|_{K_1}(x) - \varphi|_{K_2}(x),$$

where $f = \partial K_1 \cap \partial K_2$. We may remove the subscript f when it is clear from the context to which facet we refer to.

In order to discretize problem (7.1), we choose the Raviart-Thomas finite element, defined in Chapter 6, which reads as

$$\begin{aligned} V_h &:= \{\mathbf{v}_h \in \mathbf{H}(\text{div}; \Omega) : \mathbf{v}_h|_K \in \mathbb{RT}_k(K) \quad \forall K \in \mathcal{T}_h\}, \\ Q_h &:= \{q_h \in L^2(\Omega) : q_h|_K \in \mathbb{M}_k(K) \quad \forall K \in \mathcal{T}_h\}. \end{aligned}$$

We refer to Chapter 6 for the definitions of $\mathbb{RT}_k(K)$ and $\mathbb{M}_k(K)$. Remember that in the case $\Gamma = \Gamma_N$, we have to filter out constant discrete pressures by imposing the zero average constraint to the space Q_h .

By proceeding as in Chapter 6, we can construct the interpolation operators $r_h : \mathbf{H}(\text{div}; \Omega) \cap \prod_{K \in \mathcal{T}_h} \mathbf{H}^s(K) \rightarrow V_h$, where $s > \frac{1}{2}$, and $\Pi_h : L^2(\Omega) \rightarrow Q_h$, satisfying the following commutative diagram:

$$\begin{array}{ccc} \mathbf{H}(\text{div}; \Omega) \cap \prod_{K \in \mathcal{T}_h} \mathbf{H}^s(K) & \xrightarrow{\text{div}} & L^2(\Omega) \\ \downarrow r_h & & \downarrow \Pi_h \\ V_h & \xrightarrow{\text{div}} & Q_h. \end{array} \quad (7.8)$$

Diagram (7.8) implies, in particular, $\text{div } V_h = Q_h$.

We are now ready to introduce the following two discretizations of problem (7.1).

First formulation

Find $(\mathbf{u}_h, p_h) \in V_h \times Q_h$ such that

$$\begin{aligned} a_h(\mathbf{u}_h, \mathbf{v}_h) + b_1(\mathbf{v}_h, p_h) &= \int_{\Omega} \mathbf{f} \cdot \mathbf{v}_h + h^{-1} \int_{\Gamma_N} u_N \mathbf{v}_h \cdot \mathbf{n} + \int_{\Gamma_D} p_D \mathbf{v}_h \cdot \mathbf{n}, \quad \forall \mathbf{v}_h \in V_h, \\ b_m(\mathbf{u}_h, q_h) &= \int_{\Omega} g q_h - m \int_{\Gamma_N} q_h u_N, \quad \forall q_h \in Q_h, \end{aligned} \quad (7.9)$$

where $m \in \{0, 1\}$. Here,

$$\begin{aligned} a_h(\mathbf{w}_h, \mathbf{v}_h) &:= \int_{\Omega} \mathbf{w}_h \cdot \mathbf{v}_h + h^{-1} \int_{\Gamma_N} (\mathbf{w}_h \cdot \mathbf{n})(\mathbf{v}_h \cdot \mathbf{n}), & \mathbf{w}_h, \mathbf{v}_h \in V_h, \\ b_m(\mathbf{w}_h, q_h) &:= \int_{\Omega} q_h \operatorname{div} \mathbf{w}_h - m \int_{\Gamma_N} q_h \mathbf{w}_h \cdot \mathbf{n}, & \mathbf{w}_h \in V_h, q_h \in Q_h. \end{aligned}$$

In what follows just the analysis for the symmetric case $m = 1$ will be presented, however numerical results will be provided for the case $m = 0$ as well.

Second formulation

Find $(\mathbf{u}_h, p_h) \in V_h \times Q_h$ such that

$$\begin{aligned} a_{\varepsilon}(\mathbf{u}_h, \mathbf{v}_h) + b_0(\mathbf{v}_h, p_h) &= \int_{\Omega} \mathbf{f} \cdot \mathbf{v}_h + \varepsilon^{-1} \int_{\Gamma_N} u_N \mathbf{v}_h \cdot \mathbf{n} + \int_{\Gamma_D} p_D \mathbf{v}_h \cdot \mathbf{n}, & \forall \mathbf{v}_h \in V_h, \\ b_0(\mathbf{u}_h, q_h) &= \int_{\Omega} g q_h, & \forall q_h \in Q_h. \end{aligned} \quad (7.10)$$

where

$$a_{\varepsilon}(\mathbf{w}_h, \mathbf{v}_h) := \int_{\Omega} \mathbf{u}_h \cdot \mathbf{v}_h + \varepsilon^{-1} \int_{\Gamma_N} (\mathbf{w}_h \cdot \mathbf{n})(\mathbf{v}_h \cdot \mathbf{n}), \quad \mathbf{w}_h, \mathbf{v}_h \in V_h.$$

Remark 7.2.1. Let us observe that both the non-symmetric version of problem (7.9), *i.e.*, with $m = 0$, and formulation (7.10), thanks to (7.8) allow for a *weakly divergence-free* numerical solution \mathbf{u}_h , namely $\operatorname{div} \mathbf{u}_h = 0$ in the sense of L^2 , provided that the right hand side g vanishes.

Lemma 7.2.2. *Formulations (7.9) and (7.10) are consistent discretizations of (7.1) and (7.2) respectively.*

Proof. It is clear that (7.9) is a consistent discretization of (7.1). Let $(\mathbf{u}^{\varepsilon}, p^{\varepsilon})$ be the solution to (7.2). Of course, we have

$$b_0(\mathbf{u}^{\varepsilon}, q_h) = \int_{\Omega} g q_h, \quad \forall q_h \in Q_h.$$

By integrating by parts the first equation of (7.2), we obtain

$$\int_{\Omega} \mathbf{u}^{\varepsilon} \cdot \mathbf{v}_h + b_0(\mathbf{v}_h, p^{\varepsilon}) - \int_{\Gamma_N} p^{\varepsilon} \mathbf{v}_h \cdot \mathbf{n} = \int_{\Omega} \mathbf{f} \cdot \mathbf{v}_h + \int_{\Gamma_D} p_D \mathbf{v}_h \cdot \mathbf{n}, \quad \forall \mathbf{v}_h \in V_h. \quad (7.11)$$

By performing *static condensation* of the multiplier from the boundary conditions, we obtain

$$p^{\varepsilon} = \varepsilon^{-1} (u_N - \mathbf{u}^{\varepsilon} \cdot \mathbf{n}), \quad \text{on } \Gamma_N. \quad (7.12)$$

Substituting (7.12) back into (7.11), we obtain

$$a_{\varepsilon}(\mathbf{u}^{\varepsilon}, \mathbf{v}_h) + b_0(\mathbf{v}_h, p^{\varepsilon}) = \int_{\Omega} \mathbf{f} \cdot \mathbf{v}_h + \int_{\Gamma_N} \varepsilon^{-1} u_N \mathbf{v}_h \cdot \mathbf{n} + \int_{\Gamma_D} p_D \mathbf{v}_h \cdot \mathbf{n}, \quad \forall \mathbf{v}_h \in V_h.$$

□

For the numerical analysis of (7.9), we endow the discrete spaces with the following mesh-dependent norms

$$\begin{aligned}\|\mathbf{v}_h\|_{0,h}^2 &:= \|\mathbf{v}_h\|_{L^2(\Omega)}^2 + \sum_{f \in \mathcal{F}_h^\partial(\Gamma_N)} h^{-1} \|\mathbf{v}_h \cdot \mathbf{n}\|_{L^2(f)}^2, & \mathbf{v}_h \in V_h \\ \|q_h\|_{1,h}^2 &:= \sum_{K \in \mathcal{T}_h} \|\nabla q_h\|_{L^2(K)}^2 + \sum_{f \in \mathcal{F}_h^i} h^{-1} \|[q_h]\|_{L^2(f)}^2 + \sum_{f \in \mathcal{F}_h^\partial(\Gamma_D)} h^{-1} \|q_h\|_{L^2(f)}^2, & q_h \in Q_h,\end{aligned}$$

while for (7.10) we are going to employ:

$$\begin{aligned}\|\mathbf{v}_h\|_{0,h,\varepsilon}^2 &:= \|\mathbf{v}_h\|_{L^2(\Omega)}^2 + \sum_{f \in \mathcal{F}_h^\partial(\Gamma_N)} \varepsilon^{-1} \|\mathbf{v}_h \cdot \mathbf{n}\|_{L^2(f)}^2, & \mathbf{v}_h \in V_h \\ \|q_h\|_{1,h,\varepsilon}^2 &:= \sum_{K \in \mathcal{T}_h} \|\nabla q_h\|_{L^2(K)}^2 + \sum_{f \in \mathcal{F}_h^i} h^{-1} \|[q_h]\|_{L^2(f)}^2 + \sum_{f \in \mathcal{F}_h^\partial} h^{-1} \|q_h\|_{L^2(f)}^2, & q_h \in Q_h.\end{aligned}$$

Remark 7.2.3. Concerning formulation (7.9), we restrict ourselves to the numerical analysis of the symmetric case, *i.e.*, $m = 1$. The generalization to case $m = 0$ is readily done by considering a norm for the pressure controlling the whole boundary region and not just Γ_D , namely

$$\|q_h\|_{1,h}^2 := \sum_{K \in \mathcal{T}_h} \|\nabla q_h\|_{L^2(K)}^2 + \sum_{f \in \mathcal{F}_h^i} h^{-1} \|[q_h]\|_{L^2(f)}^2 + \sum_{f \in \mathcal{F}_h^\partial} h^{-1} \|q_h\|_{L^2(f)}^2, \quad q_h \in Q_h.$$

In this way, the proofs given in Section 7.3 easily generalize to the non-symmetric case.

Remark 7.2.4. Note that the natural functional setting for the mixed formulation of the Poisson problem is $\mathbf{H}(\text{div}; \Omega) \times L^2(\Omega)$, but here we consider norms that induce the same topology as that of $\mathbf{H}^1(\Omega) \times H^1(\Omega)$. Moreover, we observe that in both formulations (7.9) and (7.10) a superpenalty parameter (h^{-1} in (7.9) and ε^{-1} in (7.10)) is imposed in the flux variable. Indeed, the natural weight, mimicking the $H^{-\frac{1}{2}}$ -scalar product, would be $h \int_{\Gamma_N} (\mathbf{u}_h \cdot \mathbf{n})(\mathbf{v}_h \cdot \mathbf{n})$. However, such weight does not lead to an optimally converging scheme. In addition, this is also what destroys the conditioning (see Section 7.5.2).

7.3 Stability estimates

In this section, we carry on at the same time the proofs of the well-posedness of the two discrete formulations.

Proposition 7.3.1. *There exist $M_a, M_{a_\varepsilon}, M_{b_m} > 0$, $m = 0, 1$, such that, for $\varepsilon \lesssim h$,*

$$\begin{aligned}|a_h(\mathbf{w}_h, \mathbf{v}_h)| &\leq M_a \|\mathbf{w}_h\|_{0,h} \|\mathbf{v}_h\|_{0,h}, & \forall \mathbf{w}_h, \mathbf{v}_h \in V_h, \\ |a_\varepsilon(\mathbf{w}_h, \mathbf{v}_h)| &\leq M_{a_\varepsilon} \|\mathbf{w}_h\|_{0,h,\varepsilon} \|\mathbf{v}_h\|_{0,h,\varepsilon}, & \forall \mathbf{w}_h, \mathbf{v}_h \in V_h, \\ |b_1(\mathbf{v}_h, q_h)| &\leq M_{b_1} \|\mathbf{v}_h\|_{0,h} \|q_h\|_{1,h}, & \forall \mathbf{v}_h \in V_h, q_h \in Q_h, \\ |b_0(\mathbf{v}_h, q_h)| &\leq M_{b_0} \|\mathbf{v}_h\|_{0,h,\varepsilon} \|q_h\|_{1,h,\varepsilon}, & \forall \mathbf{v}_h \in V_h, q_h \in Q_h.\end{aligned}$$

Proof. Let $\mathbf{w}_h, \mathbf{v}_h \in V_h$, $q_h \in Q_h$ be arbitrary. It holds

$$\begin{aligned}|a_h(\mathbf{w}_h, \mathbf{v}_h)| &\leq \|\mathbf{w}_h\|_{L^2(\Omega)} \|\mathbf{v}_h\|_{L^2(\Omega)} + h^{-\frac{1}{2}} \|\mathbf{v}_h \cdot \mathbf{n}\|_{L^2(\Gamma_N)} h^{-\frac{1}{2}} \|\mathbf{w}_h \cdot \mathbf{n}\|_{L^2(\Gamma_N)} \\ &\leq \|\mathbf{w}_h\|_{0,h} \|\mathbf{v}_h\|_{0,h}, \\ |a_\varepsilon(\mathbf{w}_h, \mathbf{v}_h)| &\leq \|\mathbf{w}_h\|_{L^2(\Omega)} \|\mathbf{v}_h\|_{L^2(\Omega)} + \varepsilon^{-\frac{1}{2}} \|\mathbf{v}_h \cdot \mathbf{n}\|_{L^2(\Gamma_N)} \varepsilon^{-\frac{1}{2}} \|\mathbf{w}_h \cdot \mathbf{n}\|_{L^2(\Gamma_N)} \\ &\leq \|\mathbf{w}_h\|_{0,h,\varepsilon} \|\mathbf{v}_h\|_{0,h,\varepsilon}.\end{aligned}$$

By integration by parts, we get

$$\begin{aligned} b_1(\mathbf{v}_h, q_h) &= \int_{\Omega} q_h \operatorname{div} \mathbf{v}_h - \int_{\Gamma_N} q_h \mathbf{v}_h \cdot \mathbf{n} = \sum_{K \in \mathcal{T}_h} \int_K q_h \operatorname{div} \mathbf{v}_h - \sum_{f \in \mathcal{F}_h^{\partial}(\Gamma_N)} \int_f q_h \mathbf{v}_h \cdot \mathbf{n} \\ &= - \sum_{K \in \mathcal{T}_h} \int_K \nabla q_h \cdot \mathbf{v}_h + \sum_{f \in \mathcal{F}_h^i} \int_f [q_h] \mathbf{v}_h \cdot \mathbf{n} + \sum_{f \in \mathcal{F}_h^{\partial}(\Gamma_D)} \int_f q_h \mathbf{v}_h \cdot \mathbf{n}. \end{aligned}$$

Thus,

$$\begin{aligned} |b_1(\mathbf{v}_h, q_h)| &\leq \sum_{K \in \mathcal{T}_h} \|\nabla q_h\|_{L^2(K)} \|\mathbf{v}_h\|_{L^2(K)} + \sum_{f \in \mathcal{F}_h^i} h^{-\frac{1}{2}} \|[q_h]\|_{L^2(f)} h^{\frac{1}{2}} \|\mathbf{v}_h \cdot \mathbf{n}\|_{L^2(f)} \\ &\quad + \sum_{f \in \mathcal{F}_h^{\partial}(\Gamma_D)} h^{-\frac{1}{2}} \|q_h\|_{L^2(f)} h^{\frac{1}{2}} \|\mathbf{v}_h \cdot \mathbf{n}\|_{L^2(f)}. \end{aligned}$$

By combining standard trace and inverse inequalities, we have

$$h^{\frac{1}{2}} \|\mathbf{v}_h \cdot \mathbf{n}\|_{L^2(f)} \lesssim \|\mathbf{v}_h\|_{L^2(K)}, \quad f \in \mathcal{F}_h^{\partial}(\Gamma_D), f \in \mathcal{F}_h^i, f \subset \partial K. \quad (7.13)$$

In this way, we obtain

$$|b_1(\mathbf{v}_h, q_h)| \lesssim \|\mathbf{v}_h\|_{0,h} \|q_h\|_{1,h}.$$

On the other hand,

$$\begin{aligned} b_0(\mathbf{v}_h, q_h) &= - \sum_{K \in \mathcal{T}_h} \int_K \nabla q_h \cdot \mathbf{v}_h + \int_{\partial K} q_h \mathbf{v}_h \cdot \mathbf{n} = - \sum_{K \in \mathcal{T}_h} \int_K \nabla q_h \cdot \mathbf{v}_h + \sum_{f \in \mathcal{F}_h^i} \int_f [q_h] \mathbf{v}_h \cdot \mathbf{n} \\ &\quad + \sum_{f \in \mathcal{F}_h^{\partial}(\Gamma_N)} \int_f q_h \mathbf{v}_h \cdot \mathbf{n} + \sum_{f \in \mathcal{F}_h^{\partial}(\Gamma_D)} \int_f q_h \mathbf{v}_h \cdot \mathbf{n}. \end{aligned}$$

We have

$$\begin{aligned} |b_0(\mathbf{v}_h, q_h)| &\leq \sum_{K \in \mathcal{T}_h} \|\nabla q_h\|_{L^2(K)} \|\mathbf{v}_h\|_{L^2(K)} + \sum_{f \in \mathcal{F}_h^i} h^{-\frac{1}{2}} \|[q_h]\|_{L^2(f)} h^{\frac{1}{2}} \|\mathbf{v}_h \cdot \mathbf{n}\|_{L^2(f)} \\ &\quad + \sum_{f \in \mathcal{F}_h^{\partial}} h^{-\frac{1}{2}} \|q_h\|_{L^2(f)} h^{\frac{1}{2}} \|\mathbf{v}_h \cdot \mathbf{n}\|_{L^2(f)} \lesssim \|\mathbf{v}_h\|_{0,h,\varepsilon} \|q_h\|_{1,h,\varepsilon}, \end{aligned}$$

having used again (7.13) and $h^{-\frac{1}{2}} \lesssim \varepsilon^{-\frac{1}{2}}$ for $\varepsilon \lesssim h$. \square

Proposition 7.3.2. *It holds*

$$\begin{aligned} a_h(\mathbf{v}_h, \mathbf{v}_h) &= \|\mathbf{v}_h\|_{0,h}^2, \quad \forall \mathbf{v}_h \in V_h, \\ a_{\varepsilon}(\mathbf{v}_h, \mathbf{v}_h) &= \|\mathbf{v}_h\|_{0,h,\varepsilon}^2, \quad \forall \mathbf{v}_h \in V_h. \end{aligned}$$

Proof. The proof is trivial, hence we skip it. \square

Proposition 7.3.3. *There exist $\beta_0, \beta_1 > 0$, such that*

$$\begin{aligned} \inf_{q_h \in Q_h} \sup_{\mathbf{v}_h \in V_h} \frac{b_1(\mathbf{v}_h, q_h)}{\|\mathbf{v}_h\|_{0,h} \|q_h\|_{1,h}} &\geq \beta_1, \\ \inf_{q_h \in Q_h} \sup_{\mathbf{v}_h \in V_h} \frac{b_0(\mathbf{v}_h, q_h)}{\|\mathbf{v}_h\|_{0,h,\varepsilon} \|q_h\|_{1,h,\varepsilon}} &\geq \beta_0. \end{aligned}$$

Chapter 7. Weak imposition of the essential boundary conditions for the Darcy flow: fitted case

Proof. We start with the first inequality. Let us fix $q_h \in Q_h$ arbitrary. We construct \mathbf{v}_h by using the degrees of freedom of the Raviart-Thomas space (see Chapter 6).

$$\int_f \mathbf{v}_h \cdot \mathbf{n} \varphi_h = h^{-1} \int_f [q_h] \varphi_h, \quad \forall f \in \mathcal{F}_h^i, \varphi_h \in \Psi_k(f), \quad (7.14)$$

$$\int_f \mathbf{v}_h \cdot \mathbf{n} \varphi_h = 0, \quad \forall f \in \mathcal{F}_h^\partial(\Gamma_N), \varphi_h \in \Psi_k(f), \quad (7.15)$$

$$\int_f \mathbf{v}_h \cdot \mathbf{n} \varphi_h = h^{-1} \int_f q_h \varphi_h, \quad \forall f \in \mathcal{F}_h^\partial(\Gamma_D), \varphi_h \in \Psi_k(f), \quad (7.16)$$

$$\int_K \mathbf{v}_h \cdot \boldsymbol{\psi}_h = - \int_K \nabla q_h \cdot \boldsymbol{\psi}_h, \quad \forall K \in \mathcal{T}_h, \boldsymbol{\psi}_h \in \Psi_k(K), \text{ if } k > 0. \quad (7.17)$$

We refer the reader to Chapter 6 for the definitions of $\Psi_k(f)$ and $\Psi_k(K)$. By using the definition of \mathbf{v}_h ,

$$\begin{aligned} b_1(\mathbf{v}_h, q_h) &= \int_\Omega q_h \operatorname{div} \mathbf{v}_h - \int_{\Gamma_N} q_h \mathbf{v}_h \cdot \mathbf{n} = \sum_{K \in \mathcal{T}_h} \int_K q_h \operatorname{div} \mathbf{v}_h - \sum_{f \in \mathcal{F}_h^\partial(\Gamma_N)} \int_f q_h \mathbf{v}_h \cdot \mathbf{n} \\ &= - \sum_{K \in \mathcal{T}_h} \left(\int_K \nabla q_h \cdot \mathbf{v}_h + \int_{\partial K} q_h \mathbf{v}_h \cdot \mathbf{n} \right) - \sum_{f \in \mathcal{F}_h^\partial(\Gamma_N)} \int_f q_h \mathbf{v}_h \cdot \mathbf{n} \\ &= - \sum_{K \in \mathcal{T}_h} \int_K \nabla q_h \cdot \mathbf{v}_h + \sum_{f \in \mathcal{F}_h^i} \int_f [q_h] \mathbf{v}_h \cdot \mathbf{n} + \sum_{f \in \mathcal{F}_h^\partial(\Gamma_D)} \int_f q_h \mathbf{v}_h \cdot \mathbf{n} \\ &= \sum_{K \in \mathcal{T}_h} \|\nabla q_h\|_{L^2(K)}^2 + \sum_{f \in \mathcal{F}_h^i} h^{-1} \| [q_h] \|_{L^2(f)}^2 + \sum_{f \in \mathcal{F}_h^\partial(\Gamma_D)} h^{-1} \| q_h \|_{L^2(f)}^2 = \| q_h \|_{1,h}^2. \end{aligned}$$

Finally, let us show that $\|\mathbf{v}_h\|_{0,h} \leq C \|q_h\|_{1,h}$. Note that for every $f \in \mathcal{F}_h^\partial(\Gamma_N)$, since $\mathbf{v}_h \cdot \mathbf{n}|_f \in \Psi_k(f)$, (7.15) implies

$$\|\mathbf{v}_h \cdot \mathbf{n}\|_{L^2(f)}^2 = \int_f (\mathbf{v}_h \cdot \mathbf{n})(\mathbf{v}_h \cdot \mathbf{n}) = 0 \quad \Rightarrow \quad \mathbf{v}_h \cdot \mathbf{n} = 0, \quad \text{on } f.$$

Then, let us show $\|\mathbf{v}_h\|_{L^2(\Omega)} \leq C \|q_h\|_{1,h}$. From (7.14), it holds $\mathbf{v}_h \cdot \mathbf{n}|_f = h_K^{-1} \pi_{f,k}([q_h])|_f$ for every $f \in \mathcal{F}_h^i$ and, from (7.17), we have $\pi_{K,k}(\mathbf{v}_h)|_K = -\pi_{K,k}(\nabla q_h)|_K$ for every $K \in \mathcal{T}_h$. Note that here $\pi_{K,k}$ denotes the L^2 -orthogonal projection onto $\Psi_k(K)$. Similarly, $\pi_{f,k}$ is the L^2 -projection onto $\Psi_k(f)$. From finite dimensionality it holds $\|\widehat{\mathbf{v}}_h\|_{L^2(\widehat{K})}^2 \lesssim \|\pi_{\widehat{K},k}(\widehat{\mathbf{v}}_h)\|_{L^2(\widehat{K})}^2 + \|\widehat{\mathbf{v}}_h \cdot \widehat{\mathbf{n}}\|_{L^2(\widehat{f})}^2$. Hence, $\|\mathbf{v}_h\|_{L^2(K)}^2 \lesssim \|\nabla q_h\|_{L^2(K)}^2 + h_K^{-1} \| [q_h] \|_{L^2(f)}^2$, f being a facet of K , which follows by a standard scaling argument (see Proposition 2.1 of [40]) and by construction of \mathbf{v}_h .

We move now to the inequality involving β_0 . Let $q_h \in Q_h$. We define \mathbf{v}_h as follows:

$$\begin{aligned} \int_f \mathbf{v}_h \cdot \mathbf{n} \varphi_h &= h^{-1} \int_f [q_h] \varphi_h, \quad \forall f \in \mathcal{F}_h^i, \varphi_h \in \Psi_k(f), \\ \int_f \mathbf{v}_h \cdot \mathbf{n} \varphi_h &= h^{-1} \int_f q_h \varphi_h, \quad \forall f \in \mathcal{F}_h^\partial(\Gamma_N), \varphi_h \in \Psi_k(f), \\ \int_f \mathbf{v}_h \cdot \mathbf{n} \varphi_h &= h^{-1} \int_f q_h \varphi_h, \quad \forall f \in \mathcal{F}_h^\partial(\Gamma_D), \varphi_h \in \Psi_k(f), \\ \int_K \mathbf{v}_h \cdot \boldsymbol{\psi}_h &= - \int_K \nabla q_h \cdot \boldsymbol{\psi}_h, \quad \forall K \in \mathcal{T}_h, \boldsymbol{\psi}_h \in \Psi_k(K), \text{ if } k > 0. \end{aligned}$$

Hence,

$$\begin{aligned}
 b_0(\mathbf{v}_h, q_h) &= \int_{\Omega} q_h \operatorname{div} \mathbf{v}_h = \sum_{K \in \mathcal{T}_h} \int_K q_h \operatorname{div} \mathbf{v}_h = - \sum_{K \in \mathcal{T}_h} \left(\int_K \nabla q_h \cdot \mathbf{v}_h + \int_{\partial K} q_h \mathbf{v}_h \cdot \mathbf{n} \right) \\
 &= - \sum_{K \in \mathcal{T}_h} \int_K \nabla q_h \cdot \mathbf{v}_h + \sum_{f \in \mathcal{F}_h^i} \int_f [q_h] \mathbf{v}_h \cdot \mathbf{n} + \sum_{f \in \mathcal{F}_h^\partial(\Gamma_N)} \int_f q_h \mathbf{v}_h \cdot \mathbf{n} \\
 &\quad + \sum_{f \in \mathcal{F}_h^\partial(\Gamma_D)} \int_f q_h \mathbf{v}_h \cdot \mathbf{n} \\
 &= \sum_{K \in \mathcal{T}_h} \|\nabla q_h\|_{L^2(K)}^2 + \sum_{f \in \mathcal{F}_h^i} h^{-1} \|[q_h]\|_{L^2(f)}^2 + \sum_{f \in \mathcal{F}_h^\partial} h^{-1} \|q_h\|_{L^2(f)}^2 = \|q_h\|_{1,h,\varepsilon}^2.
 \end{aligned}$$

We refer the reader to [85] for the inequality $\|\mathbf{v}_h\|_{0,h,\varepsilon} \leq C \|q_h\|_{1,h,\varepsilon}$. \square

7.4 *A priori* error estimates

In this section we will prove *a priori* error estimates for the formulations (7.9) and (7.10). We observe that all the constants appearing throughout this section and concerning the error bounds for the formulation (7.10) are independent of the parameter ε . This is due to the orthogonality properties of the interpolants along the boundary.

Lemma 7.4.1. *Let (\mathbf{u}, p) be the solution of the continuous problem (7.1) and $(\mathbf{u}_h, p_h) \in V_h \times Q_h$ the one of the discrete problem (7.9) with $m = 1$. Then*

$$\|\mathbf{u}_h - r_h(\mathbf{u})\|_{0,h} + \|p_h - \Pi_h(p)\|_{1,h} \lesssim \|\mathbf{u} - r_h(\mathbf{u})\|_{L^2(\Omega)} + h^{\frac{1}{2}} \sum_{f \in \mathcal{F}_h^\partial(\Gamma_N)} \|p - \Pi_h(p)\|_{L^2(f)}.$$

Proof. The stability estimates previously shown for $a_h(\cdot, \cdot)$ and $b_1(\cdot, \cdot)$ with respect to $\|\cdot\|_{0,h}$ and $\|\cdot\|_{1,h}$ imply

$$\|\|\boldsymbol{\eta}_h, s_h\|\|_h \lesssim \sup_{(\mathbf{v}_h, q_h) \in V_h \times Q_h} \frac{\mathcal{A}_h((\boldsymbol{\eta}_h, s_h), (\mathbf{v}_h, q_h))}{\|\|\mathbf{v}_h, q_h\|\|_h}, \quad \forall (\boldsymbol{\eta}_h, s_h) \in V_h \times Q_h, \quad (7.18)$$

where

$$\begin{aligned}
 \mathcal{A}_h((\boldsymbol{\eta}_h, s_h), (\mathbf{v}_h, q_h)) &:= a_h(\boldsymbol{\eta}_h, \mathbf{v}_h) + b_1(\mathbf{v}_h, s_h) + b_1(\boldsymbol{\eta}_h, q_h), \\
 \|\|\boldsymbol{\eta}_h, s_h\|\|_h^2 &:= \|\boldsymbol{\eta}_h\|_{0,h}^2 + \|s_h\|_{1,h}^2.
 \end{aligned}$$

Using (7.18), for $(\mathbf{u}_h - r_h(\mathbf{u}), p_h - \Pi_h(p))$ there exists $(\mathbf{v}_h, q_h) \in V_h \times Q_h$ such that

$$\begin{aligned}
 \|\mathbf{u}_h - r_h(\mathbf{u})\|_{0,h} + \|p_h - \Pi_h(p)\|_{1,h} &\leq \sqrt{d} \|\|\mathbf{u}_h - r_h(\mathbf{u}), p_h - \Pi_h(p)\|\|_h \\
 &\lesssim \frac{\mathcal{A}_h((\mathbf{u}_h - r_h(\mathbf{u}), p_h - \Pi_h(p)), (\mathbf{v}_h, q_h))}{\|\|\mathbf{v}_h, q_h\|\|_h}.
 \end{aligned}$$

Hence, we have

$$\begin{aligned}
\mathcal{A}_h((\mathbf{u}_h - r_h(\mathbf{u}), p_h - \Pi_h(p)), (\mathbf{v}_h, q_h)) &= \int_{\Omega} (\mathbf{u}_h - \mathbf{u}) \cdot \mathbf{v}_h + \int_{\Omega} (\mathbf{u} - r_h(\mathbf{u})) \cdot \mathbf{v}_h \\
&\quad + h^{-1} \int_{\Gamma_N} ((\mathbf{u}_h - \mathbf{u}) \cdot \mathbf{n}) (\mathbf{v}_h \cdot \mathbf{n}) \\
&\quad + h^{-1} \int_{\Gamma_N} ((\mathbf{u} - r_h(\mathbf{u})) \cdot \mathbf{n}) (\mathbf{v}_h \cdot \mathbf{n}) + b_0(\mathbf{v}_h, p_h - p) \\
&\quad + b_0(\mathbf{v}_h, p - \Pi_h(p)) \\
&\quad - \int_{\Gamma_N} (p_h - p) \mathbf{v}_h \cdot \mathbf{n} - \int_{\Gamma_N} (p - \Pi_h(p)) \mathbf{v}_h \cdot \mathbf{n} \\
&\quad + b_1(\mathbf{u}_h - \mathbf{u}, q_h) + b_1(\mathbf{u} - r_h(\mathbf{u}), q_h).
\end{aligned} \tag{7.19}$$

By construction of r_h and Π_h we have, respectively,

$$\begin{aligned}
h^{-1} \int_{\Gamma_N} ((\mathbf{u} - r_h(\mathbf{u})) \cdot \mathbf{n}) (\mathbf{v}_h \cdot \mathbf{n}) &= 0, \quad \forall \mathbf{v}_h \in V_h, \\
b_1(\mathbf{u} - r_h(\mathbf{u}), q_h) &= - \sum_{K \in \mathcal{T}_h} \int_K \nabla q_h \cdot (\mathbf{u} - r_h(\mathbf{u})) + \sum_{f \in \mathcal{F}_h^i} \int_f [q_h] (\mathbf{u} - r_h(\mathbf{u})) \cdot \mathbf{n} = 0, \quad \forall q_h \in Q_h, \\
b_0(\mathbf{v}_h, p - \Pi_h(p)) &= 0, \quad \forall \mathbf{v}_h \in V_h.
\end{aligned}$$

By consistency (Lemma 7.2.2), we have

$$\begin{aligned}
\int_{\Omega} (\mathbf{u}_h - \mathbf{u}) \cdot \mathbf{v}_h + h^{-1} \int_{\Gamma_N} ((\mathbf{u}_h - \mathbf{u}) \cdot \mathbf{n}) (\mathbf{v}_h \cdot \mathbf{n}) + b_0(\mathbf{v}_h, p_h - p) \\
+ \int_{\Gamma_N} (p_h - p) \mathbf{v}_h \cdot \mathbf{n} &= 0, \quad \forall \mathbf{v}_h \in V_h, \\
b_1(\mathbf{u}_h - \mathbf{u}, q_h) &= 0, \quad \forall q_h \in Q_h.
\end{aligned}$$

Hence, in (7.19) we are left with

$$\mathcal{A}_h((\mathbf{u}_h - r_h(\mathbf{u}), p_h - \Pi_h(p)), (\mathbf{v}_h, q_h)) = \int_{\Omega} (\mathbf{u} - r_h(\mathbf{u})) \cdot \mathbf{v}_h - \int_{\Gamma_N} (p - \Pi_h(p)) \mathbf{v}_h \cdot \mathbf{n}.$$

We have

$$\begin{aligned}
\int_{\Omega} (\mathbf{u} - r_h(\mathbf{u})) \cdot \mathbf{v}_h - \int_{\Gamma_N} (p - \Pi_h(p)) \mathbf{v}_h \cdot \mathbf{n} &\leq \|\mathbf{u} - r_h(\mathbf{u})\|_{L^2(\Omega)} \|\mathbf{v}_h\|_{L^2(\Omega)} \\
&\quad + \sum_{f \in \mathcal{F}_h^\partial(\Gamma_N)} h^{\frac{1}{2}} \|p - \Pi_h(p)\|_{L^2(f)} h^{-\frac{1}{2}} \|\mathbf{v}_h \cdot \mathbf{n}\|_{L^2(\Gamma_N)},
\end{aligned}$$

and we can write

$$\begin{aligned}
\|\mathbf{u}_h - r_h(\mathbf{u})\|_{0,h} + \|p_h - \Pi_h(p)\|_{1,h} &\lesssim \frac{\left(\|\mathbf{u} - r_h(\mathbf{u})\|_{L^2(\Omega)} + h^{\frac{1}{2}} \sum_{f \in \mathcal{F}_h^\partial(\Gamma_N)} \|p - \Pi_h(p)\|_{L^2(f)} \right) \|\mathbf{v}_h, 0\|_h}{\|\mathbf{v}_h, q_h\|_h} \\
&\lesssim \|\mathbf{u} - r_h(\mathbf{u})\|_{L^2(\Omega)} + h^{\frac{1}{2}} \sum_{f \in \mathcal{F}_h^\partial(\Gamma_N)} \|p - \Pi_h(p)\|_{L^2(f)}.
\end{aligned}$$

□

Lemma 7.4.2. *Let $(\mathbf{u}^\varepsilon, p^\varepsilon)$ be the solution of the perturbed continuous problem (7.2) and $(\mathbf{u}_h, p_h) \in V_h \times Q_h$ the one of the discrete problem (7.10). Then*

$$\|\mathbf{u}_h - r_h(\mathbf{u}^\varepsilon)\|_{0,h,\varepsilon} + \|p_h - \Pi_h(p^\varepsilon)\|_{1,h,\varepsilon} \lesssim \|\mathbf{u}^\varepsilon - r_h(\mathbf{u}^\varepsilon)\|_{L^2(\Omega)}.$$

Proof. The stability estimates previously shown for $a_\varepsilon(\cdot, \cdot)$ and $b_0(\cdot, \cdot)$ with respect to $\|\cdot\|_{0,h,\varepsilon}$ and $\|\cdot\|_{1,h,\varepsilon}$ imply

$$\|\boldsymbol{\eta}_h, s_h\|_{h,\varepsilon} \lesssim \sup_{(\mathbf{v}_h, q_h) \in V_h \times Q_h} \frac{\mathcal{A}_\varepsilon((\boldsymbol{\eta}_h, s_h), (\mathbf{v}_h, q_h))}{\|\mathbf{v}_h, q_h\|_{h,\varepsilon}}, \quad \forall (\boldsymbol{\eta}_h, s_h) \in V_h \times Q_h,$$

where

$$\begin{aligned} \mathcal{A}_\varepsilon((\boldsymbol{\eta}_h, s_h), (\mathbf{v}_h, q_h)) &:= a_\varepsilon(\boldsymbol{\eta}_h, \mathbf{v}_h) + b_0(\mathbf{v}_h, s_h) + b_0(\boldsymbol{\eta}_h, q_h), \\ \|\boldsymbol{\eta}_h, s_h\|^2 &:= \|\boldsymbol{\eta}_h\|_{0,h,\varepsilon}^2 + \|s_h\|_{1,h,\varepsilon}^2. \end{aligned}$$

Hence, for $(\mathbf{u}_h - r_h(\mathbf{u}^\varepsilon), p_h - \Pi_h(p^\varepsilon))$ there exists $(\mathbf{v}_h, q_h) \in V_h \times Q_h$ such that

$$\begin{aligned} \|\mathbf{u}_h - r_h(\mathbf{u}^\varepsilon)\|_{0,h,\varepsilon} + \|p_h - \Pi_h(p^\varepsilon)\|_{1,h,\varepsilon} &\leq \sqrt{d} \|\mathbf{u}_h - r_h(\mathbf{u}^\varepsilon), p_h - \Pi_h(p^\varepsilon)\|_{h,\varepsilon} \\ &\lesssim \frac{\mathcal{A}_\varepsilon((\mathbf{u}_h - r_h(\mathbf{u}^\varepsilon), p_h - \Pi_h(p^\varepsilon)), (\mathbf{v}_h, q_h))}{\|\mathbf{v}_h, q_h\|_{h,\varepsilon}}. \end{aligned}$$

Hence, we have

$$\begin{aligned} \mathcal{A}_\varepsilon((\mathbf{u}_h - r_h(\mathbf{u}^\varepsilon), p_h - \Pi_h(p^\varepsilon)), (\mathbf{v}_h, q_h)) &= \int_\Omega (\mathbf{u}_h - \mathbf{u}^\varepsilon) \cdot \mathbf{v}_h + \int_\Omega (\mathbf{u}^\varepsilon - r_h(\mathbf{u}^\varepsilon)) \cdot \mathbf{v}_h \\ &\quad + \varepsilon^{-1} \int_{\Gamma_N} ((\mathbf{u}_h - \mathbf{u}^\varepsilon) \cdot \mathbf{n}) (\mathbf{v}_h \cdot \mathbf{n}) \\ &\quad + \varepsilon^{-1} \int_{\Gamma_N} ((\mathbf{u}^\varepsilon - r_h(\mathbf{u}^\varepsilon)) \cdot \mathbf{n}) (\mathbf{v}_h \cdot \mathbf{n}) \\ &\quad + b_0(\mathbf{v}_h, p_h - p^\varepsilon) + b_0(\mathbf{v}_h, p^\varepsilon - \Pi_h(p^\varepsilon)) + b_0(\mathbf{u}_h - \mathbf{u}^\varepsilon, q_h) \\ &\quad + b_0(\mathbf{u}^\varepsilon - r_h(\mathbf{u}^\varepsilon), q_h). \end{aligned}$$

The following orthogonality relations hold by definition of r_h and Π_h :

$$\begin{aligned} \varepsilon^{-1} \int_{\Gamma_N} ((\mathbf{u}^\varepsilon - r_h(\mathbf{u}^\varepsilon)) \cdot \mathbf{n}) (\mathbf{v}_h \cdot \mathbf{n}) &= 0, \quad \forall \mathbf{v}_h \in V_h, \\ b_0(\mathbf{v}_h, p^\varepsilon - \Pi_h(p^\varepsilon)) &= 0, \quad \forall \mathbf{v}_h \in V_h, \\ b_0(\mathbf{u}^\varepsilon - r_h(\mathbf{u}^\varepsilon), q_h) &= - \sum_{K \in \mathcal{T}_h} \int_K \nabla q_h \cdot (\mathbf{u}^\varepsilon - r_h(\mathbf{u}^\varepsilon)) \\ &\quad + \sum_{f \in \mathcal{F}_h^i} \int_f [q_h] (\mathbf{u}^\varepsilon - r_h(\mathbf{u}^\varepsilon)) \cdot \mathbf{n} + \sum_{f \in \mathcal{F}_h^\partial(\Gamma_N)} \int_f q_h (\mathbf{u}^\varepsilon - r_h(\mathbf{u}^\varepsilon)) \cdot \mathbf{n} = 0, \quad \forall q_h \in Q_h. \end{aligned}$$

Moreover, by consistency (Lemma 7.2.2), we have

$$\begin{aligned} \int_\Omega (\mathbf{u}_h - \mathbf{u}^\varepsilon) \cdot \mathbf{v}_h + \varepsilon \int_{\Gamma_N} ((\mathbf{u}_h - \mathbf{u}^\varepsilon) \cdot \mathbf{n}) (\mathbf{v}_h \cdot \mathbf{n}) + b_0(\mathbf{v}_h, p_h - p^\varepsilon) &= 0, \quad \forall \mathbf{v}_h \in V_h, \\ b_0(\mathbf{u}_h - \mathbf{u}^\varepsilon, q_h) &= 0, \quad \forall q_h \in Q_h. \end{aligned}$$

Hence,

$$\mathcal{A}_\varepsilon((\mathbf{u}_h - r_h(\mathbf{u}^\varepsilon), p_h - \Pi_h(p^\varepsilon)), (\boldsymbol{\tau}_h, q_h)) = \int_\Omega (\mathbf{u}^\varepsilon - r_h(\mathbf{u}^\varepsilon)) \cdot \mathbf{v}_h,$$

and we can write

$$\|\mathbf{u}_h - r_h(\mathbf{u}^\varepsilon)\|_{0,h,\varepsilon} + \|p_h - \Pi_h(p^\varepsilon)\|_{1,h,\varepsilon} \lesssim \frac{\|\mathbf{u}^\varepsilon - r_h(\mathbf{u}^\varepsilon)\|_{L^2(\Omega)} \|\mathbf{v}_h, 0\|_{h,\varepsilon}}{\|\mathbf{v}_h, q_h\|_{h,\varepsilon}} \lesssim \|\mathbf{u}^\varepsilon - r_h(\mathbf{u}^\varepsilon)\|_{L^2(\Omega)}.$$

□

Proposition 7.4.3. *Let $(\mathbf{u}, p) \in \mathbf{H}^{r+1}(\Omega) \times H^{t+1}(\Omega)$ be the solution of (7.1) and $(\mathbf{u}_h, p_h) \in V_h \times Q_h$ the one of (7.9) with $m = 1$. There exists $C > 0$ such that, for $s = \min\{r, t, k\}$,*

$$\|\mathbf{u}_h - r_h(\mathbf{u})\|_{0,h} + \|p_h - \Pi_h(p)\|_{1,h} \leq Ch^{s+1} \left(\|\mathbf{u}\|_{H^{r+1}(\Omega)} + \|p\|_{H^{t+1}(\Omega)} \right). \quad (7.20)$$

Proof. By Lemma 7.4.1, a multiplicative trace inequality for Sobolev functions, and the standard Deny-Lions argument (Theorem 3.4.1 of [112])

$$\begin{aligned} \|\mathbf{u}_h - r_h(\mathbf{u})\|_{0,h} + \|p_h - \Pi_h(p)\|_{1,h} &\lesssim \|\mathbf{u} - r_h(\mathbf{u})\|_{L^2(\Omega)} + \sum_{f \in \mathcal{F}_h^\partial(\Gamma_N)} h^{\frac{1}{2}} \|p - \Pi_h(p)\|_{L^2(f)} \\ &\lesssim \|\mathbf{u} - r_h(\mathbf{u})\|_{L^2(\Omega)} \\ &\quad + \sum_{K \in \mathcal{T}_h} h^{\frac{1}{2}} \|p - \Pi_h(p)\|_{L^2(K)}^{\frac{1}{2}} \|\nabla(p - \Pi_h(p))\|_{L^2(K)}^{\frac{1}{2}} \\ &\lesssim \|\mathbf{u} - r_h(\mathbf{u})\|_{L^2(\Omega)} + h^{\frac{1}{2}} h^{\frac{t+1}{2}} \|p\|_{H^{t+1}(\Omega)}^{\frac{1}{2}} h^{\frac{t}{2}} \|p\|_{H^{t+1}(\Omega)}^{\frac{1}{2}} \\ &= \|\mathbf{u} - r_h(\mathbf{u})\|_{L^2(\Omega)} + h^{t+1} \|p\|_{H^{t+1}(\Omega)}. \end{aligned}$$

By using Deny-Lions argument (Theorem 3.4.1 of [112]), we get

$$\|\mathbf{u}_h - r_h(\mathbf{u})\|_{0,h} + \|p_h - \Pi_h(p)\|_{1,h} \lesssim h^{r+1} \|\mathbf{u}\|_{H^{r+1}(\Omega)} + h^{t+1} \|p\|_{H^{t+1}(\Omega)},$$

with $0 \leq t \leq k$ and $0 \leq r \leq k$. □

Proposition 7.4.4. *Let $(\mathbf{u}^\varepsilon, p^\varepsilon) \in \mathbf{H}^{r+1}(\Omega) \times H^{t+1}(\Omega)$ be the solution of the perturbed continuous problem (7.2) and $(\mathbf{u}_h, p_h) \in V_h \times Q_h$ the one to (7.10). There exists $C > 0$ such that, for $s = \min\{r, t, k\}$,*

$$\|\mathbf{u}_h - r_h(\mathbf{u}^\varepsilon)\|_{0,h,\varepsilon} + \|p_h - \Pi_h(p^\varepsilon)\|_{1,h,\varepsilon} \leq Ch^{s+1} \|\mathbf{u}^\varepsilon\|_{H^{s+1}(\Omega)}. \quad (7.21)$$

Proof. By Lemma 7.4.2 and the Deny-Lions argument (Theorem 3.4.1 of [112]), we get

$$\|\mathbf{u}_h - r_h(\mathbf{u}^\varepsilon)\|_{0,h,\varepsilon} + \|p_h - \Pi_h(p^\varepsilon)\|_{1,h,\varepsilon} \lesssim h^{s+1} \|\mathbf{u}^\varepsilon\|_{H^{s+1}(\Omega)}.$$

□

Remark 7.4.5. Let us remark that the quantities $\|\mathbf{u}_h - r_h(\mathbf{u}_h)\|_{0,h}$, $\|p_h - \Pi_h(p)\|_{1,h}$ in (7.20) and $\|p_h - \Pi_h(p^\varepsilon)\|_{1,h,\varepsilon}$, $\|\mathbf{u}_h - r_h(\mathbf{u}^\varepsilon)\|_{0,h,\varepsilon}$ in (7.21), respectively, are super convergent.

Theorem 7.4.6. *Let $(\mathbf{u}, p) \in \mathbf{H}^{r+1}(\Omega) \times H^{t+1}(\Omega)$ be the solution to (7.1) and $(\mathbf{u}_h, p_h) \in V_h \times Q_h$ the one to (7.9) with $m = 1$. Then there exists $C > 0$ such that, for $s = \min\{r, t, k\}$,*

$$\|\mathbf{u} - \mathbf{u}_h\|_{L^2(\Omega)} \leq Ch^{s+1} \left(\|\mathbf{u}\|_{H^{r+1}(\Omega)} + \|p\|_{H^{t+1}(\Omega)} \right).$$

Proof. Let us proceed by triangular inequality.

$$\|\mathbf{u} - \mathbf{u}_h\|_{L^2(\Omega)} \leq \|\mathbf{u} - r_h(\mathbf{u})\|_{L^2(\Omega)} + \|r_h(\mathbf{u}) - \mathbf{u}_h\|_{L^2(\Omega)}.$$

The first and the second terms in the rhs scale as $\mathcal{O}(h^{r+1})$ and $\mathcal{O}(h^{s+1})$, respectively, because of Deny-Lions argument (Theorem 3.4.1 of [112]) and Proposition 7.4.3. □

Lemma 7.4.7. *Let $(\mathbf{u}^\varepsilon, p^\varepsilon) \in \mathbf{H}^{r+1}(\Omega) \times H^{t+1}(\Omega)$ be the solution to the perturbed continuous problem (7.2) and $(\mathbf{u}_h, p_h) \in V_h \times Q_h$ the one to (7.10). Then there exists $C > 0$ such that, for $s = \min\{r, k\}$,*

$$\|\mathbf{u}^\varepsilon - \mathbf{u}_h\|_{L^2(\Omega)} \leq Ch^{s+1} \|\mathbf{u}^\varepsilon\|_{H^{s+1}(\Omega)}.$$

Proof. Let us proceed by triangular inequality.

$$\|\mathbf{u}^\varepsilon - \mathbf{u}_h\|_{L^2(\Omega)} \leq \|\mathbf{u}^\varepsilon - r_h(\mathbf{u}^\varepsilon)\|_{L^2(\Omega)} + \|r_h(\mathbf{u}^\varepsilon) - \mathbf{u}_h\|_{L^2(\Omega)}.$$

The first and the second terms in the rhs scale as $\mathcal{O}(h^{s+1})$, respectively, because of Deny-Lions argument (Theorem 3.4.1 of [112]) and Proposition 7.4.4. \square

Theorem 7.4.8. *Let $(\mathbf{u}, p) \in \mathbf{H}^1(\Omega) \times H^2(\Omega)$ be the solution to the continuous (7.1) and $(\mathbf{u}_h, p_h) \in V_h \times Q_h$ the one to (7.10) with $\varepsilon = h$. Assume Ω to be a convex domain with a Lipschitz polygonal boundary Γ , $\mathbf{f} \in \mathbf{H}^1(\Omega)$, $\mathbf{f} \cdot \mathbf{n} = 0$ on Γ_N and $u_N = 0$. Then, there exists $C > 0$ such that*

$$\|\mathbf{u} - \mathbf{u}_h\|_{L^2(\Omega)} \leq Ch \left(\|\mathbf{f}\|_{H^1(\Omega)} + \|g\|_{L^2(\Omega)} + \|p_D\|_{H^{\frac{1}{2}}(\Gamma_D)} \right).$$

Proof. Let us proceed by triangular inequality.

$$\begin{aligned} \|\mathbf{u} - \mathbf{u}_h\|_{L^2(\Omega)} &\leq \|\mathbf{u} - \mathbf{u}^\varepsilon\|_{L^2(\Omega)} + \|\mathbf{u}^\varepsilon - \mathbf{u}_h\|_{L^2(\Omega)} \\ &\lesssim_\varepsilon \left(\|\operatorname{div} \mathbf{f}\|_{L^2(\Omega)} + \|g\|_{L^2(\Omega)} + \|p_D\|_{H^{\frac{1}{2}}(\Gamma_D)} \right) + h \|\mathbf{u}^\varepsilon\|_{H^1(\Omega)} \\ &\lesssim_\varepsilon \left(\|\operatorname{div} \mathbf{f}\|_{L^2(\Omega)} + \|g\|_{L^2(\Omega)} + \|p_D\|_{H^{\frac{1}{2}}(\Gamma_D)} \right) \\ &\quad + h \left(\|\mathbf{f}\|_{H^1(\Omega)} + \|g\|_{L^2(\Omega)} + \|p_D\|_{H^{\frac{1}{2}}(\Gamma_D)} \right). \end{aligned}$$

We used Lemma 7.4.7, Proposition 7.1.2 and Proposition 7.1.4. Finally, let us choose $\varepsilon = h$. \square

Remark 7.4.9. We observe that for both formulations, (7.9) and (7.10), all dimensionless parameters have been set for simplicity to 1, unlike for the standard Nitsche method for the Poisson problem [126], where the dimensionless parameter needs to be taken large enough.

7.5 Numerical examples

7.5.1 Convergence results

In this first set of numerical examples we verify the optimal *a priori* error estimates of Theorems 7.4.6, 7.4.8. We also check that the result of Theorem 7.4.6 holds in the non-symmetric case $m = 0$, as already mentioned in Section 7.2. Moreover, we study the L^2 -error of the pressure field, for which optimal convergence is observed in general and super convergence in the case of the lowest order Raviart-Thomas element and triangular meshes. Although Theorem 7.4.8 guarantees us optimal *a priori* error estimates for the discretization (7.10) only with the lowest order Raviart-Thomas element, numerical results show that we have optimal convergence rates also for higher orders.

Unit square with triangular meshes

We approximate the Darcy problem in the *unit square* $\Omega = (0, 1)^2$ using a family of triangular meshes, with weakly enforced essential boundary conditions on the whole boundary, using as manufactured solutions

$$\mathbf{u}_{ex} = \begin{pmatrix} x \sin(x) \sin(y) \\ \sin(x) \cos(y) + x \cos(x) \cos(y) \end{pmatrix}, \quad p_{ex} = x^3 y - 0.125.$$

Note that \mathbf{u}_{ex} is divergence-free. The numerical results are in Figure 7.1.

Unit circle with triangular meshes

Now, we consider the *unit circle* $\Omega = \{(x, y) \in \mathbb{R}^2 : x^2 + y^2 \leq 1\}$ which is meshed using triangles. We weakly impose the essential boundary conditions on the boundary and consider the following reference solutions:

$$\mathbf{u}_{ex} = \begin{pmatrix} \frac{1}{10} e^x \sin(xy) \\ x^4 + y^2 \end{pmatrix}, \quad p_{ex} = x^3 \cos(x) + y^2 \sin(x).$$

This time $\operatorname{div} \mathbf{u}_{ex} = 2y + \frac{1}{10} (e^x \sin(xy) + y e^x \cos(xy))$. See Figure 7.2.

Unit square with quadrilateral meshes

Let us consider the *unit square* $\Omega = (0, 1)^2$ meshed using quadrilaterals. We impose natural boundary conditions on $\{(x, y) : 0 \leq x \leq 1, y = 0\}$ and essential boundary conditions everywhere else in a weak sense. The reference solutions are:

$$\mathbf{u}_{ex} = \begin{pmatrix} \cos(x) \cosh(y) \\ \sin(x) \cosh(y) \end{pmatrix}, \quad p_{ex} = -\sin(x) \sinh(y) - (\cos(1) - 1) (\cosh(1) - 1).$$

We have $\operatorname{div} \mathbf{u}_{ex} = 0$. For the numerical results we refer to Figure 7.3.

Quarter of annulus with quadrilateral isoparametric elements

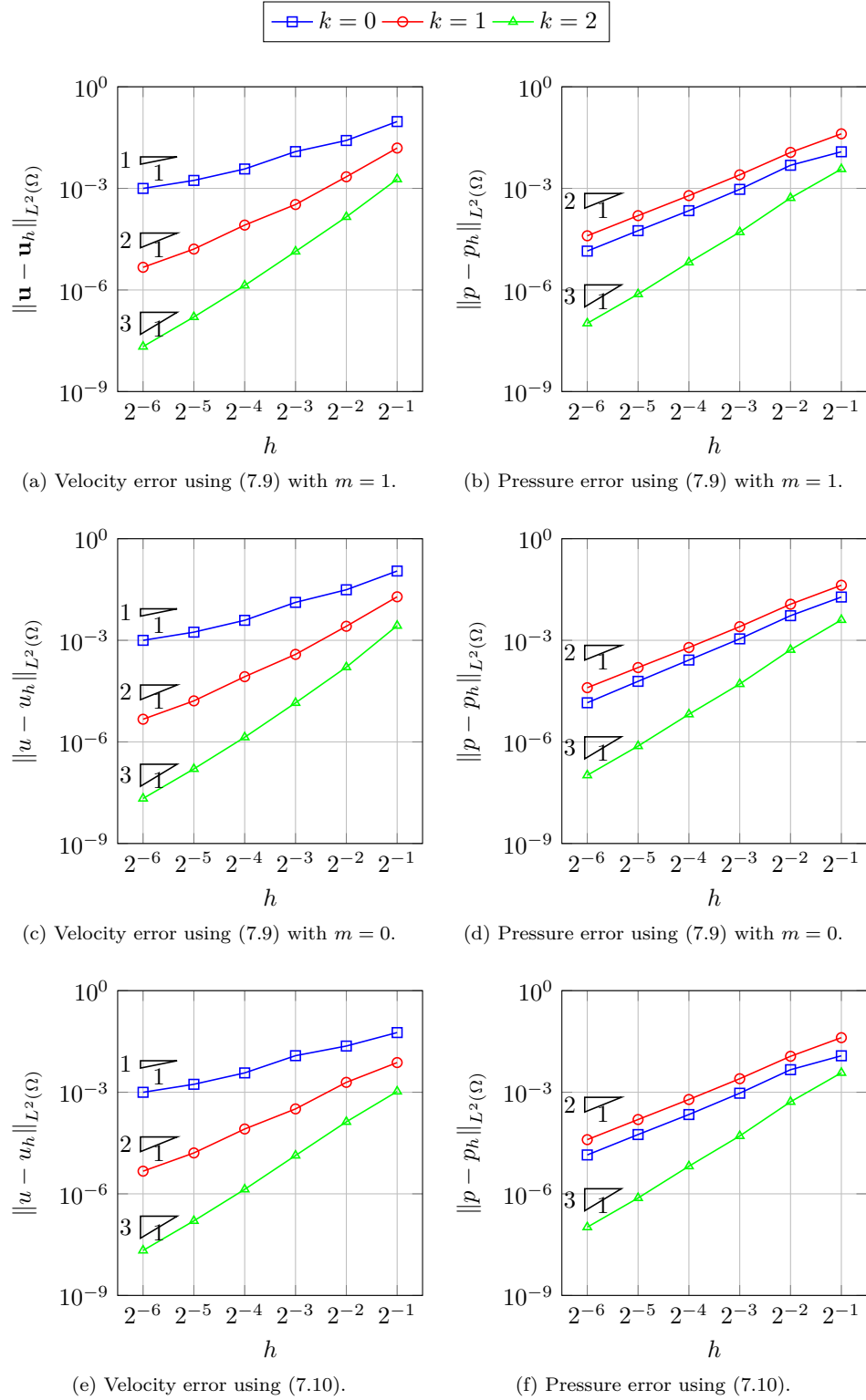
Let us consider the *quarter of annulus* centered in the origin with inner and outer radii, respectively, $r = 1$ and $R = 2$, discretized using quadrilateral isoparametric elements [82]. We impose natural boundary conditions on the straight edges $\{(x, y) : 1 \leq x \leq 2, y = 0\}$ and $\{(x, y) : x = 0, 1 \leq y \leq 2\}$ and weak essential boundary conditions on the curved ones. The manufactured solutions are:

$$\mathbf{u}_{ex} = \begin{pmatrix} -xy^2 \\ -x^2 y - \frac{3}{2} y^2 \end{pmatrix}, \quad p_{ex} = \frac{1}{2} (x^2 y^2 + y^3),$$

with $\operatorname{div} \mathbf{u}_{ex} = -x^2 - y^2 - 3y$. See Figure 7.4.

7.5.2 A remark about the condition numbers

Proceeding as in [55] it would be possible to prove that the ℓ^2 -condition number of the stiffness matrix arising from the discretizations (7.9), for both $m \in \{0, 1\}$, scales as h^{-2} , as Figures 7.5a, 7.5b, 7.6a, 7.6b confirm. The penalty parameter for the weak imposition of the essential boundary conditions is the responsible of the deterioration of the conditioning with respect to


 Figure 7.1 – Convergence rates in the *unit square* with triangular meshes.

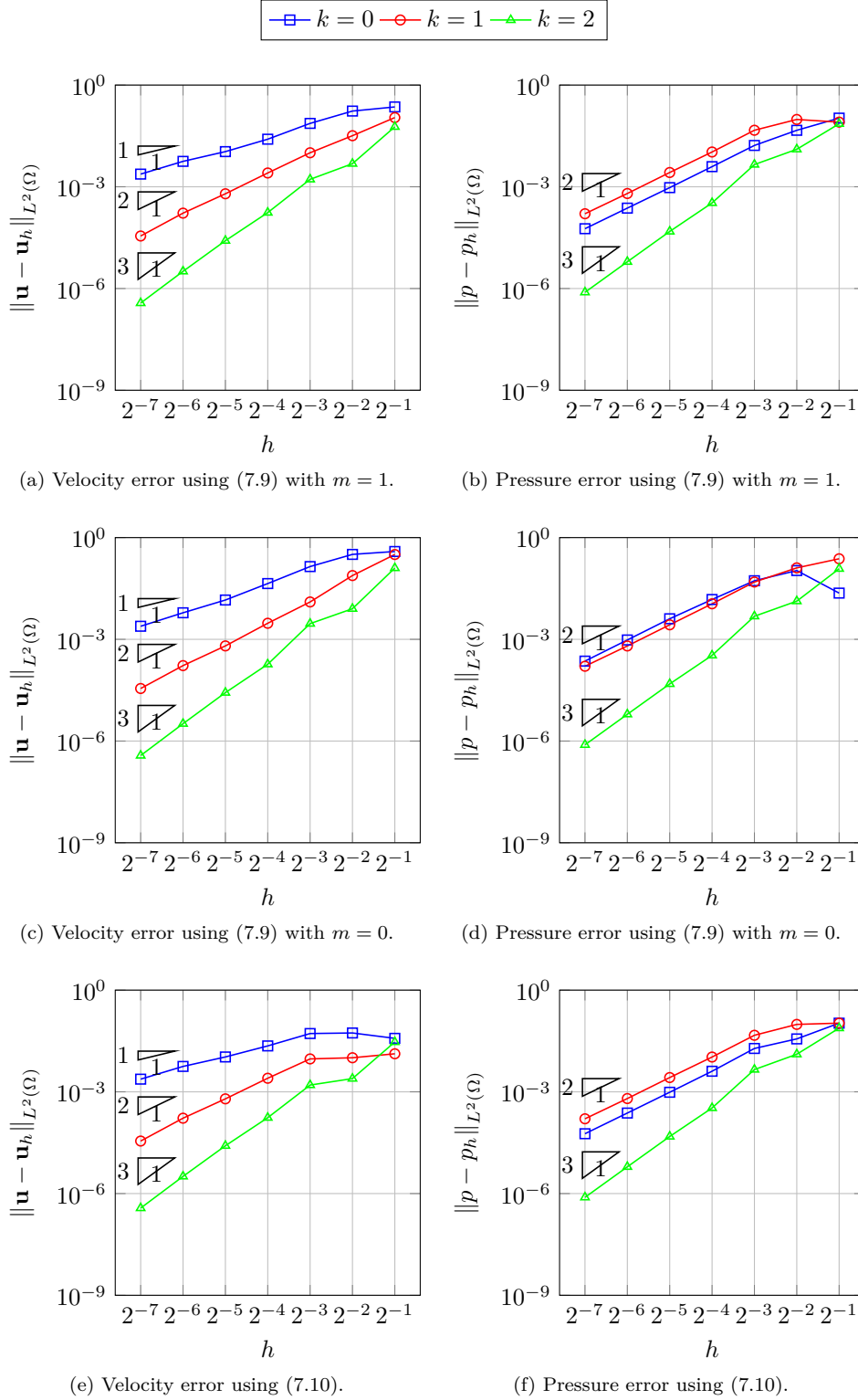
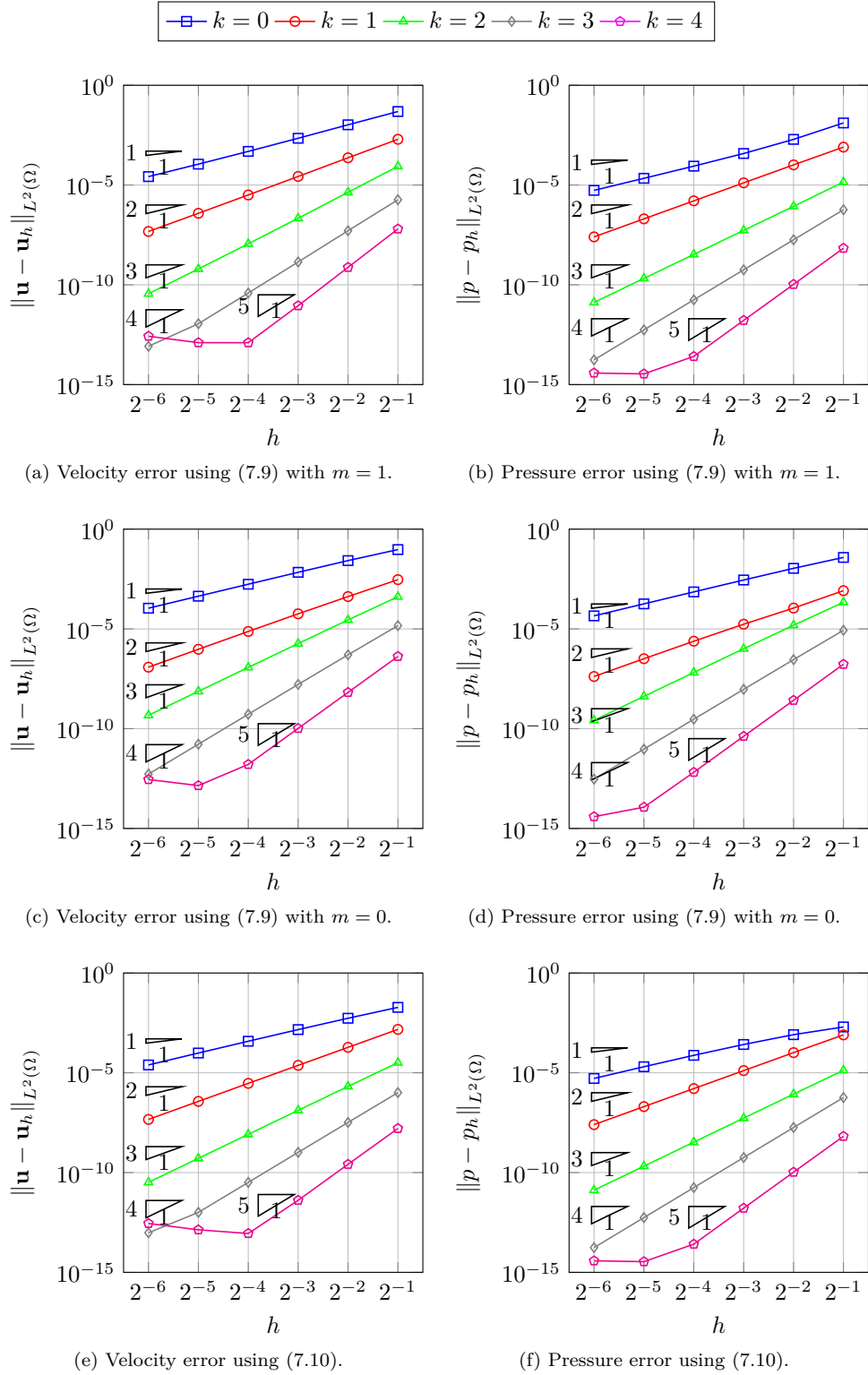


Figure 7.2 – Convergence rates in the *unit circle* with triangular meshes.


 Figure 7.3 – Convergence rates in the *unit square* with quadrilateral meshes.

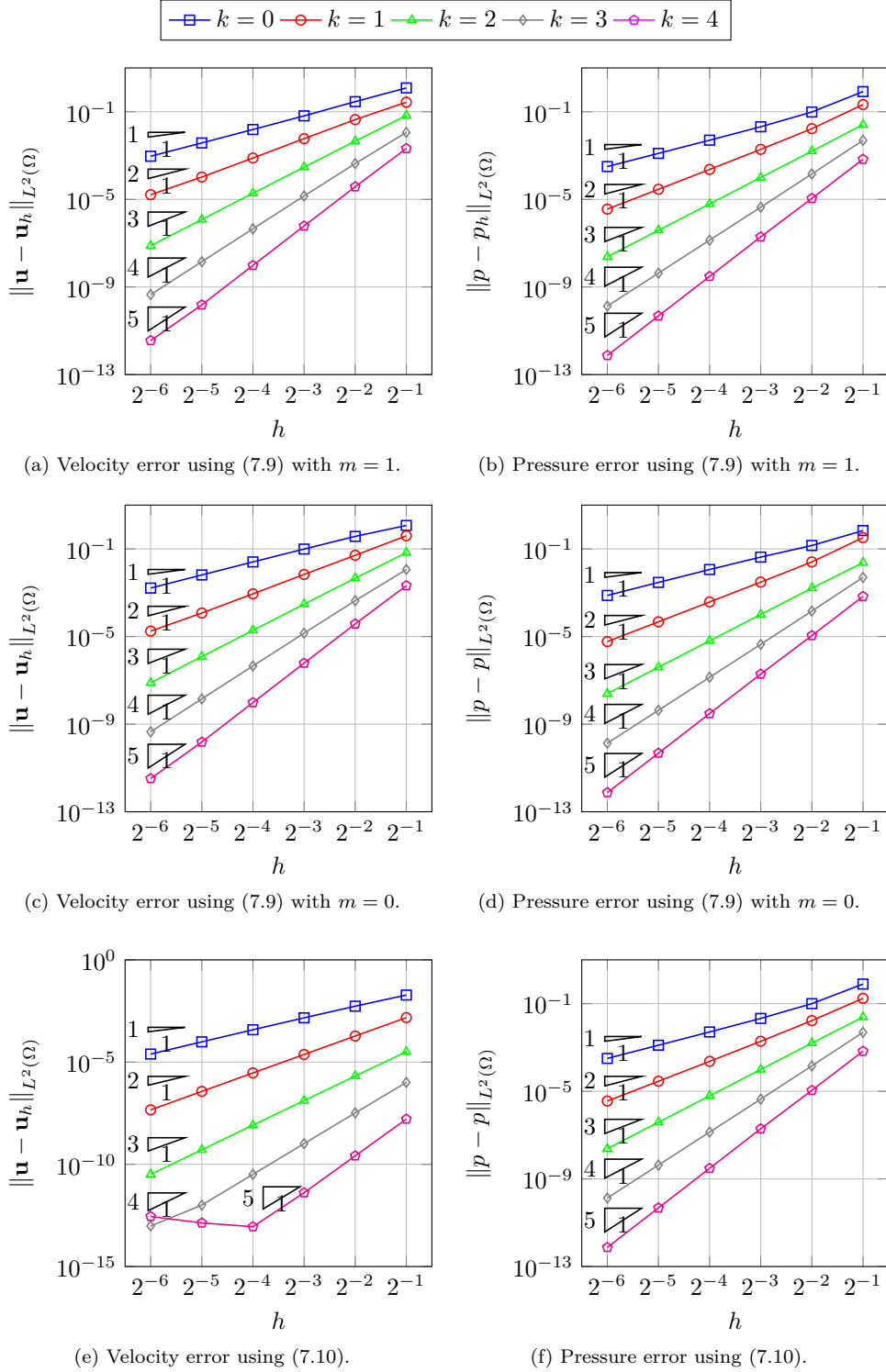
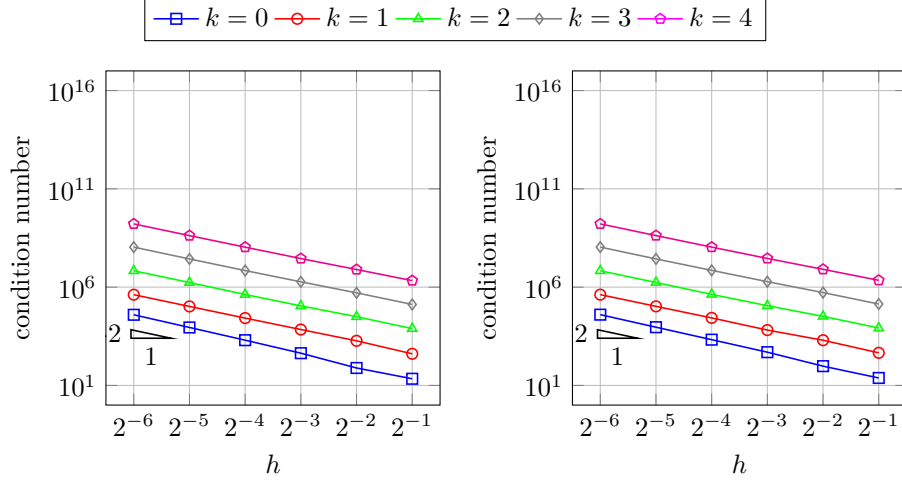


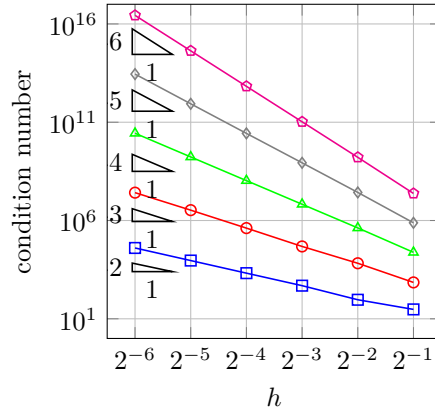
Figure 7.4 – A priori errors in the $quarter$ of annulus with isoparametric quadrilateral meshes.

the standard mixed finite element discretization of the Poisson problem, for which the condition number scales as h^{-1} . An even worse situation occurs when formulation (7.10) is employed. In

this case the condition number scales as $h^{-(s+2)}$, $s = \min\{r, k\}$, r being the Sobolev regularity of the exact solution for the pressure field and k the polynomial degree of the Raviart-Thomas discretization, as confirmed by Figures 7.5c, 7.6c.



(a) Condition number using (7.9) with $m = 1$. (b) Condition number using (7.9) with $m = 0$.



(c) Condition number using (7.10).

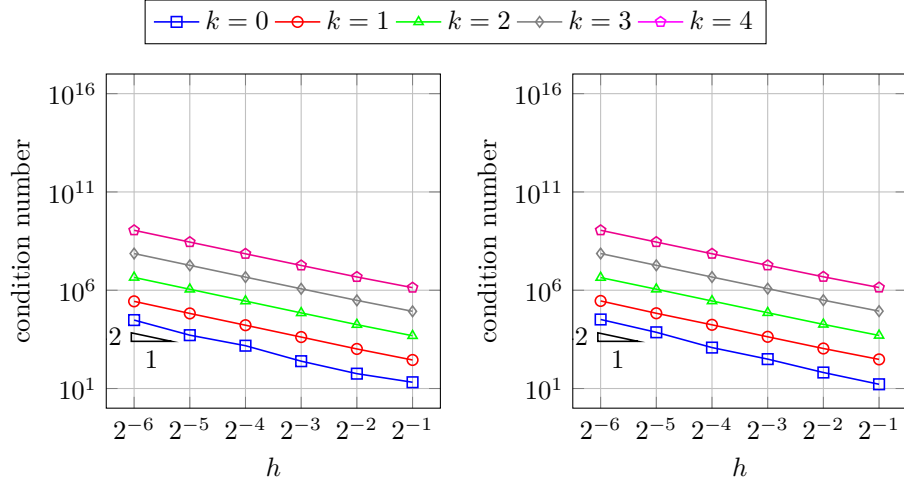
Figure 7.5 – Condition numbers in the *unit square* with quadrilateral meshes.

7.5.3 The optimality of the penalty parameter

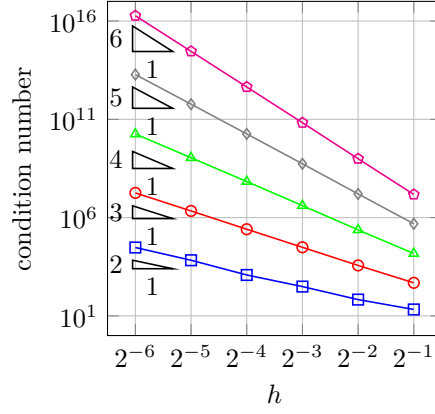
We want to analyze the optimality of the penalty parameter, denoted through this Section as γ , for both numerical schemes. Let us observe indeed that in order for formulations (7.9) and (7.10) to be extended in the unfitted case and provide an optimal convergence scheme, we would expect γ to scale as $\mathcal{O}(h)$ (see also Remark 7.2.4). Let us consider the Raviart-Thomas element of order $k = 1$ and compare the numerical results for the L^2 -error of the velocity field with respect to different powers of the mesh-size as penalty parameter. The first set of numerical experiences is performed using triangular meshes, then we move to quadrilaterals.

Figures 7.7, 7.8, 7.9, 7.10 correspond to the settings introduced in Section 7.5.1.

In all numerical experiments, we do not detect any particular sensitivity of the convergence of the error of the velocities with respect to γ in the case of method (7.9), see for instance Figures 7.8a.



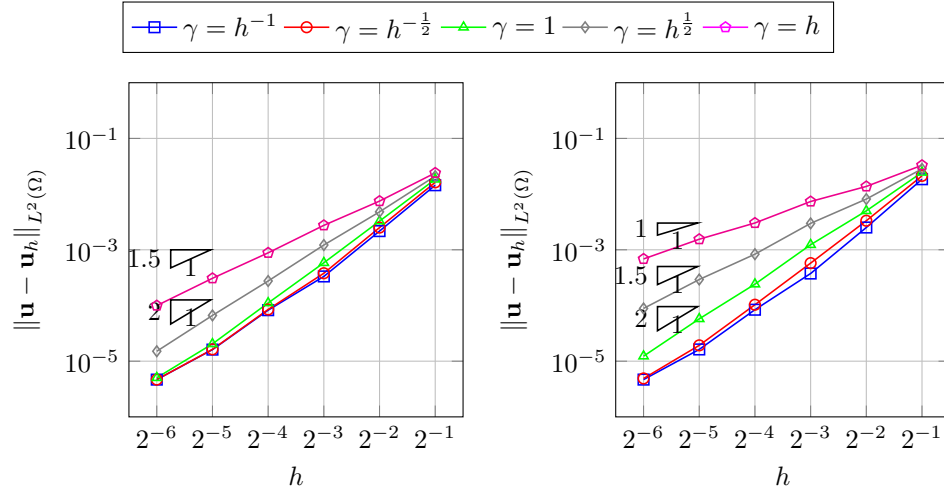
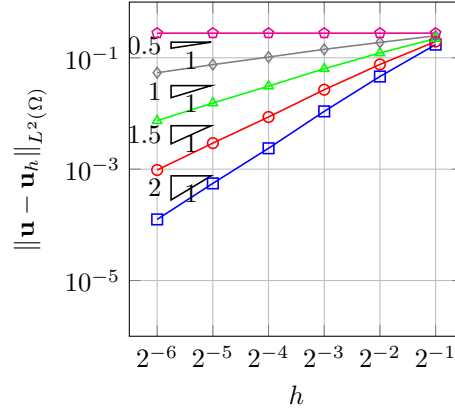
(a) Condition number using (7.9) with $m = 1$. (b) Condition number using (7.9) with $m = 0$.



(c) Condition number using (7.10).

Figure 7.6 – Condition numbers in the *quarter of annulus* with isoparametric quadrilateral elements.

On the other hand, for the formulation (7.10) strong influence of varying γ is clearly seen in Figures 7.7c, 7.8c, 7.9c, 7.10c. Let us observe indeed that for formulations (7.9) and (7.10) to be extended in the unfitted case and provide an optimal convergence scheme, we would expect γ to scale as $\mathcal{O}(h)$. In this sense, the method (7.9) seems a more promising approach.

(a) Velocity error using (7.9) with $m = 1$.(b) Velocity error using (7.9) with $m = 0$.

(c) Velocity error using (7.10).

Figure 7.7 – Compare L^2 -errors for the velocity in the *unit square* with respect to different values of the penalty parameter γ with triangular meshes.

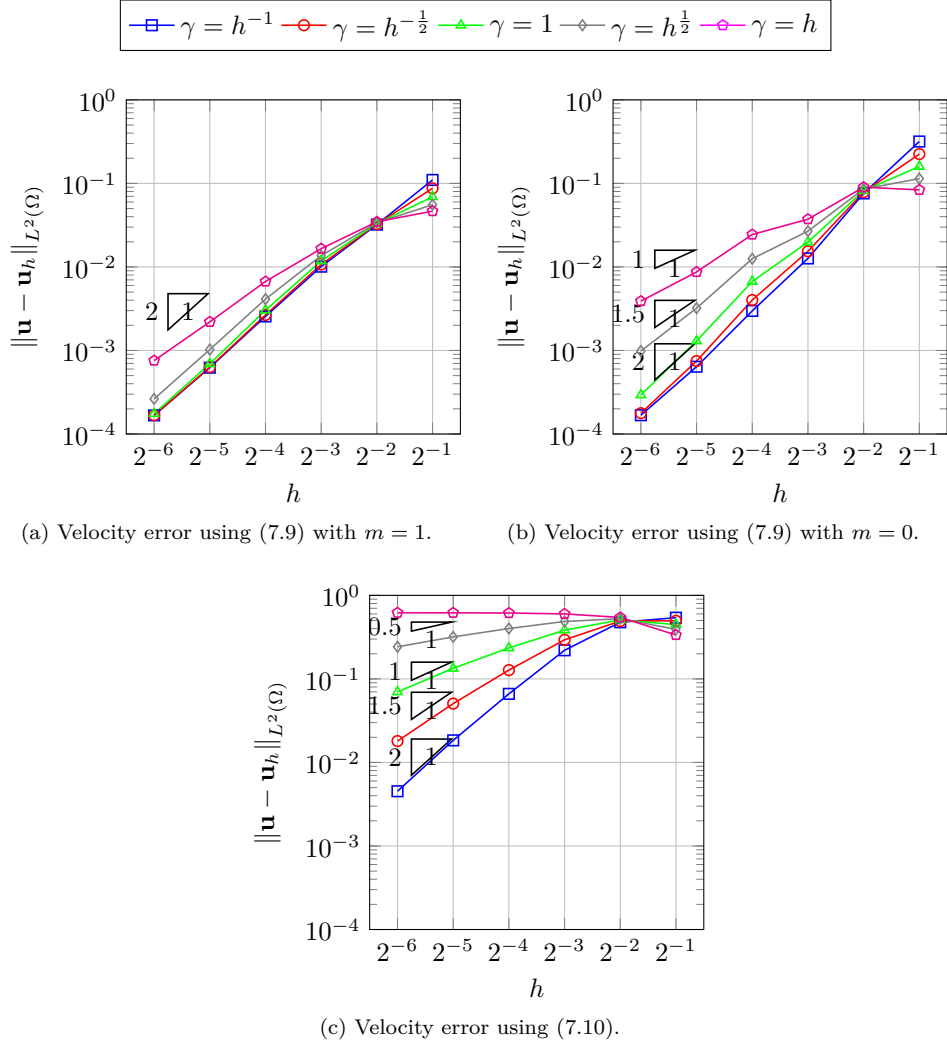
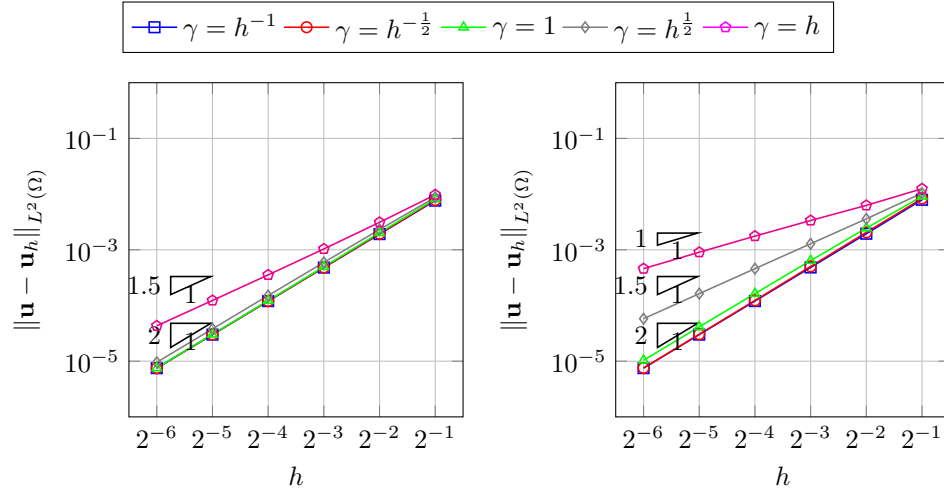
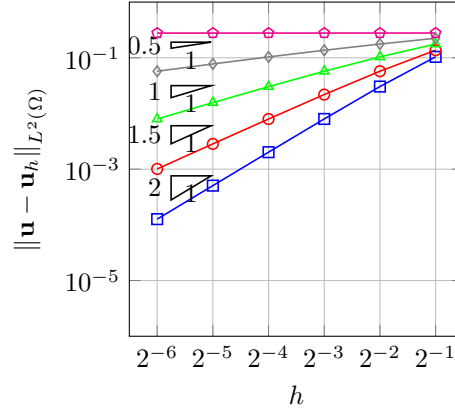


Figure 7.8 – Compare L^2 -errors for the velocity in the *unit circle* with respect to different values of the penalty parameter γ with triangular meshes.

(a) Velocity error using (7.9) with $m = 1$.(b) Velocity error using (7.9) with $m = 0$.

(c) Velocity error using (7.10).

Figure 7.9 – Compare L^2 -errors for the velocity in the *unit square* with respect to different values of the penalty parameter γ with quadrilateral meshes.

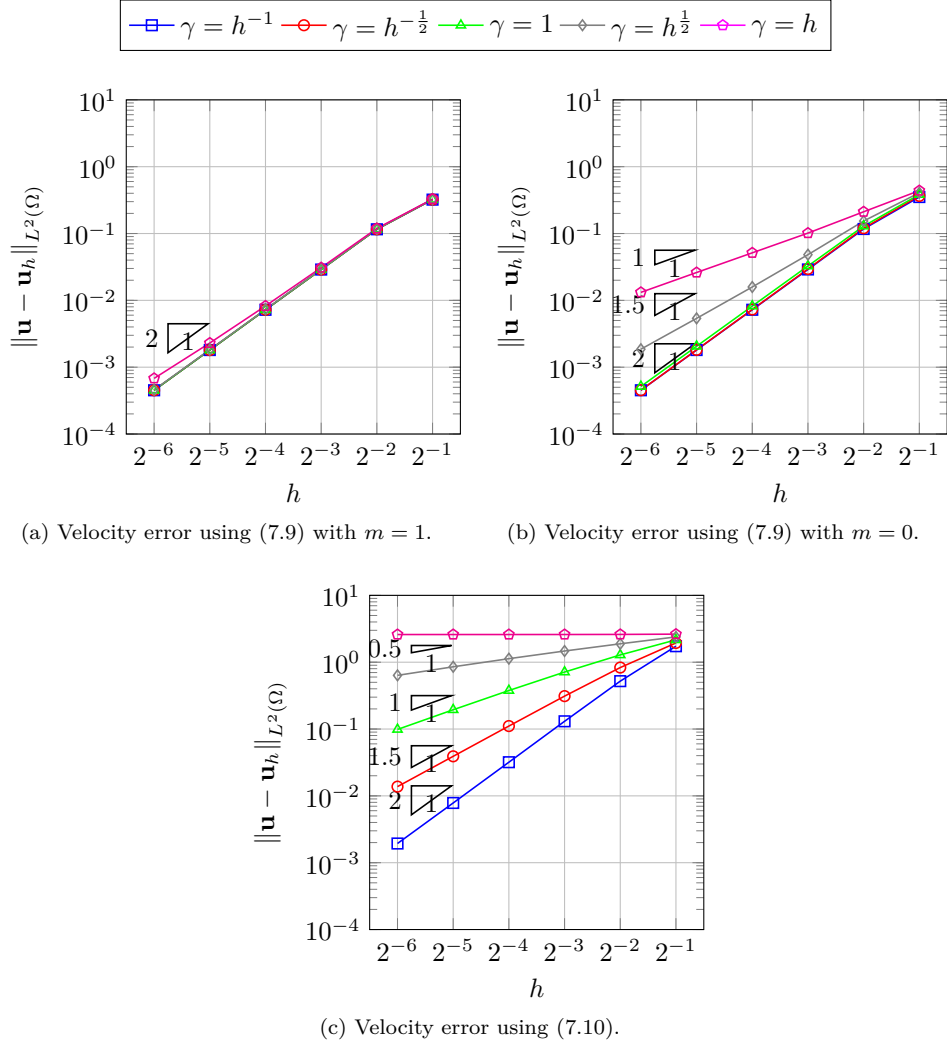


Figure 7.10 – Compare L^2 -errors for the velocity in the *quarter of annulus* with respect to different values of the penalty parameter γ with isoparametric quadrilateral elements.

8 Weak imposition of the essential boundary conditions for the Darcy flow: unfitted case

In this chapter, we study the Nitsche method introduced in Chapter 7 in the case of a mesh that does not fit the boundary of the domain. The discrete formulation is very ill-posed because of the mismatch between the computational mesh and the physical domain where the PDEs live. We show that this affects the accuracy of the approximation scheme and the conditioning of the arising linear system. Our strategy to recover the well-posedness of the discrete formulation is in line with [35, 37, 38]. It adds to the variational formulation at the discrete level two weakly consistent ghost penalty operators acting separately on the velocity and pressure fields. The discrete functional setting is unusual since it is based on mesh-dependent norms scaling as $\mathbf{H}^1 \times H^1$, instead of the standard $\mathbf{H}(\text{div}) \times L^2$. Hence, we derive *a priori* error estimates for the velocity and pressure fields which are optimal for the chosen topology but not for the usual ones. We also prove optimal estimates for the condition number of the stiffness matrix.

An outline of the chapter follows. In Section 8.1, we introduce the model problem and its Raviart-Thomas discretization for both triangular and quadrilateral meshes. In Section 8.2 we explain how we interpolate regular functions when the mesh does not fit the boundary of the physical domain. Section 8.3 contains the discrete stabilized formulation and its numerical analysis: we rigorously derive the estimates guaranteeing the stability of our formulation and prove the *a priori* error estimates. Section 8.4 is devoted to the study of the condition number of the stiffness matrix. We prove that the ghost penalty stabilization restores the usual conditioning of the boundary-fitted case. In Section 8.5 we explain how to treat the case of pure natural boundary conditions. Finally, in Section 8.6 we present some numerical experiments illustrating the theory.

Given $x, y \in \mathbb{R}$, we will write $x \lesssim y$ if there exists $c > 0$, independent of x, y , such that $x \leq cy$ and $x \sim y$ if $x \lesssim y$ and $y \lesssim x$. C will denote generic positive constants that may change with each occurrence throughout the chapter but are always independent of the local mesh size and the mutual position of mesh and domain unless otherwise specified.

8.1 Model problem and notation

Let Ω be a Lipschitz-regular domain of \mathbb{R}^d , $d \in \{2, 3\}$, with boundary Γ such that $\Gamma = \Gamma_N \cup \Gamma_D$, where Γ_N, Γ_D are open and disjoint. We consider the Darcy problem introduced in Chapter 6.

Given $\mathbf{f} \in L^2(\Omega)$, $g \in L^2(\Omega)$, $u_N \in H^{-\frac{1}{2}}(\Gamma_N)$, $p_D \in H^{\frac{1}{2}}(\Gamma_D)$, we look for $\mathbf{u} : \Omega \rightarrow \mathbb{R}^d$ and

$p : \Omega \rightarrow \mathbb{R}$ such that

$$\begin{aligned} \kappa^{-1} \mathbf{u} - \nabla p &= \mathbf{f}, & \text{in } \Omega, \\ \operatorname{div} \mathbf{u} &= g, & \text{in } \Omega, \\ \mathbf{u} \cdot \mathbf{n} &= u_N, & \text{on } \Gamma_N, \\ p &= p_D, & \text{on } \Gamma_D. \end{aligned} \tag{8.1}$$

In the subsequent analysis we are going to consider, for the sake of simplicity, $\kappa = I$ the identity matrix.

Let us introduce $(\mathcal{T}_h)_{h>0}$, a family of triangular or quadrilateral meshes such that, for every $h > 0$, $\overline{\Omega} \subsetneq \Omega_{\mathcal{T}}$, $\Omega_{\mathcal{T}}$ being the *fictitious domain*, i.e., $\overline{\Omega}_{\mathcal{T}} := \cup_{K \in \mathcal{T}_h} K$. Let us denote the collection of all the facets (edges if $d = 2$ and faces if $d = 3$) as \mathcal{F}_h and partition the latter into two disjoint sets: the faces lying on the boundary of $\Omega_{\mathcal{T}}$, denoted as \mathcal{F}_h^{∂} , and \mathcal{F}_h^i , the internal ones. For every cut element $K \in \mathcal{T}_h$, let us denote its intersection with the boundary as Γ_K . It will be clear from the context if with Γ_K we mean the intersection with the whole boundary, i.e., $\Gamma_K := \Gamma \cap K^{\circ}$ or with just one of its disjoint components Γ_N , i.e., $\Gamma_K := \Gamma_N \cap K^{\circ}$, or Γ_D , i.e., $\Gamma_K := \Gamma_D \cap K^{\circ}$. It will also be useful to define the collection of the cut-elements, namely $\mathcal{G}_h := \{K \in \mathcal{T}_h : |\Gamma_K| \neq 0\}$, its two sub-collections $\mathcal{G}_h(\Gamma_N) := \{K \in \mathcal{T}_h : |\Gamma_N \cap K^{\circ}| \neq 0\}$ and $\mathcal{G}_h(\Gamma_D) := \{K \in \mathcal{T}_h : |\Gamma_D \cap K^{\circ}| \neq 0\}$, that we assume to be disjoint, and the interior part $\Omega_{I,h} := \Omega \setminus \cup_{K \in \mathcal{G}_h} K$. Let $\mathcal{T}_h(\Omega_{I,h}) := \{K \in \mathcal{T}_h : K \subset \Omega_{I,h}\}$. The collections of the internal and boundary facets entirely contained in $\Omega_{I,h}$ are respectively denoted as $\mathcal{F}_h^i(\Omega_{I,h})$ and $\mathcal{F}_h^{\partial}(\Omega_{I,h})$. The collection of internal facets in the boundary region are denoted as $\mathcal{F}_h^{\Gamma} := \{f \in \mathcal{F}_h^i : \exists K \in \mathcal{G}_h \text{ such that } f \subset \partial K\}$.

Let us assign to each element $K \in \mathcal{T}_K$ its diameter h_K and denote $h := \max_{K \in \mathcal{T}_h} h_K$. We assume the background mesh to be *shape-regular*, i.e., there exists $\sigma > 0$, independent of h , such that $\max_{K \in \mathcal{T}_h} \frac{h_K}{\rho_K} \leq \sigma$, ρ_K being the diameter of the largest ball inscribed in K . Moreover, \mathcal{T}_h is supposed to be *quasi-uniform* in the sense that there exists $\tau > 0$, independent of h , such that $\min_{K \in \mathcal{T}_h} h_K \geq \tau h$. We fix an orientation for the internal faces, i.e., given $f \in \mathcal{F}_h^i$ such that $f = \partial K_1 \cap \partial K_2$, we assume that the unit normal on f points from K_1 toward K_2 . Let $\varphi : \Omega \rightarrow \mathbb{R}$ be smooth enough. Then, for all $f \in \mathcal{F}_h^i$ and a.e. $x \in f$, we define the *jump* of φ as

$$[\varphi]_f(x) := \varphi|_{K_1}(x) - \varphi|_{K_2}(x),$$

where $f = \partial K_1 \cap \partial K_2$. We may remove the subscript f when it is clear from the context to which facet we refer to.

The following mild assumptions on how the mesh may be intersected by the boundary Γ will be helpful. First, let us require that the number of facets to be crossed to move from a cut element K to an uncut element K' is uniformly bounded with respect to h .

Assumption 8.1.1. There exists $N > 1$ such that, for every $h > 0$ and $K \in \mathcal{G}_h$, there exist $K' \in \mathcal{T}_h(\Omega_{I,h})$ and at most N elements $(K_i)_{i=1}^N \subset \mathcal{T}_h$ such that $K_1 = K$, $K_N = K'$ and $K_i \cap K_{i+1}$ is a cut facet, for every $1 \leq i \leq N - 1$.

Then, we assume that it is possible to subdivide the boundary region into patches, each consisting of a moderate number of elements and with a sufficient overlap with the physical domain.

Assumption 8.1.2. The boundary zone $\cup_{K \in \mathcal{G}_h} K$ can be decomposed into $N_{\mathcal{P}}$ patches $(\mathcal{P}_{\ell})_{\ell=1}^{N_{\mathcal{P}}}$, $\overline{\mathcal{P}}_{\ell} = \cup_{K \in \mathcal{P}_{\ell}} K$, $1 \leq \ell \leq N_{\mathcal{P}}$, satisfying:

- (i) for every $K \in \mathcal{G}_h$ there exists (at least) $1 \leq \ell \leq N_{\mathcal{P}}$ such that $K \in \mathcal{P}_{\ell}$;
- (ii) for every $1 \leq \ell \leq N_{\mathcal{P}}$ there exists $K'_{\ell} \in \mathcal{T}_h(\Omega_{I,h}) \cap \mathcal{P}_{\ell}$;

- (iii) there exists $C > 0$ such that, for every $1 \leq \ell \leq N_{\mathcal{P}}$ and $K \in \mathcal{P}_\ell$, it holds $h_K \geq Ch_{\mathcal{P}_\ell}$, where $h_{\mathcal{P}_\ell} := \text{diam}(P_\ell)$;

For every $1 \leq \ell \leq N_{\mathcal{P}}$, we denote $\mathcal{F}_\ell := \{f \in \mathcal{F}_h^i : f \subseteq P_\ell, f \not\subseteq \partial P_\ell\}$.

Let us construct a suitable couple of subspaces $V_h \subset \mathbf{H}(\text{div}; \Omega_{\mathcal{T}})$ and $Q_h \subset L^2(\Omega_{\mathcal{T}})$ defined in the whole fictitious domain $\Omega_{\mathcal{T}}$. We define

$$\begin{aligned} V_h &:= \{\mathbf{v}_h \in \mathbf{H}(\text{div}; \Omega_{\mathcal{T}}) : \mathbf{v}_h|_K \in \mathbb{RT}_k(K), \quad \forall K \in \mathcal{T}_h\}, \\ Q_h &:= \{q_h \in L^2(\Omega_{\mathcal{T}}) : q_h|_K \in \mathbb{M}_k(K), \quad \forall K \in \mathcal{T}_h\}, \end{aligned}$$

where $\mathbb{RT}_k(K)$ and $\mathbb{M}_k(K)$ have been defined in Chapter 6. Remember that in the pure essential case, *i.e.*, $\Gamma = \Gamma_N$, we have to filter out constant discrete pressures by imposing the zero average constraint on the space Q_h .

8.2 Interpolation strategy

By proceeding as in Chapter 6, we construct the interpolation operators $r_h^{\mathcal{T}} : \mathbf{H}(\text{div}; \Omega_{\mathcal{T}}) \cap \prod_{K \in \mathcal{T}_h} \mathbf{H}^s(K) \rightarrow V_h$, $s > \frac{1}{2}$, and $\Pi_h^{\mathcal{T}} : L^2(\Omega_{\mathcal{T}}) \rightarrow Q_h$ such that the following diagram commutes and, in particular, $\text{div } V_h = Q_h$.

$$\begin{array}{ccc} \mathbf{H}(\text{div}; \Omega_{\mathcal{T}}) \cap \prod_{K \in \mathcal{T}_h} \mathbf{H}^s(K) & \xrightarrow{\text{div}} & L^2(\Omega_{\mathcal{T}}) \\ \downarrow r_h^{\mathcal{T}} & & \downarrow \Pi_h^{\mathcal{T}} \\ V_h & \xrightarrow{\text{div}} & Q_h. \end{array} \quad (8.2)$$

From [75], there exist $\mathbf{E} : \mathbf{H}^t(\Omega) \rightarrow \mathbf{H}^t(\mathbb{R}^d)$, $t \geq 1$, and $E : H^r(\Omega) \rightarrow H^r(\mathbb{R}^d)$, $r \geq 1$, universal (degree-independent) Sobolev-Stein extensions such that $\text{div} \circ \mathbf{E} = E \circ \text{div}$. We define, for $t \geq 1$ and $r \geq 1$,

$$\begin{aligned} r_h : \mathbf{H}^t(\Omega) &\rightarrow V_h, & \mathbf{v} &\mapsto r_h^{\mathcal{T}} \left(\mathbf{E}(\mathbf{v})|_{\Omega_{\mathcal{T}}} \right), \\ \Pi_h : H^r(\Omega) &\rightarrow Q_h, & q &\mapsto \Pi_h^{\mathcal{T}} \left(E(q)|_{\Omega_{\mathcal{T}}} \right). \end{aligned}$$

Remark 8.2.1. By construction, the commutativity of diagram (8.2) is preserved when restricting to the physical domain Ω , namely when employing $V_h|_{\Omega}$, $\mathbf{H}(\text{div}; \Omega)$, r_h , and $Q_h|_{\Omega}$, $L^2(\Omega)$, Π_h instead of V_h , $\mathbf{H}(\text{div}; \Omega_{\mathcal{T}})$, $r_h^{\mathcal{T}}$, and Q_h , $L^2(\Omega_{\mathcal{T}})$, $\Pi_h^{\mathcal{T}}$. See Section 8.6.3.

8.3 The stabilized formulation

Given $k \in \mathbb{N}$, the order of the Raviart-Thomas element employed for the discretization, we introduce two *ghost penalty* jumps-based operators to enhance the stability of our discrete formulation and, in particular, to recover stability estimates independent of the mesh-boundary

intersection (see [35, 38, 68, 96]). We define

$$\begin{aligned} j_h(\mathbf{w}_h, \mathbf{v}_h) &:= \sum_{f \in \mathcal{F}_h^\Gamma} \sum_{j=0}^k h^{2j+1} \int_f [\partial_n^j \mathbf{w}_h] [\partial_n^j \mathbf{v}_h], & \mathbf{w}_h, \mathbf{v}_h \in V_h, \\ j_h(m_h, q_h) &:= \sum_{f \in \mathcal{F}_h^\Gamma} \sum_{j=0}^k h^{2j-1} \int_f [\partial_n^j m_h] [\partial_n^j q_h], & m_h, q_h \in Q_h. \end{aligned} \quad (8.3)$$

Remark 8.3.1. A wide zoo of ghost penalty operators has been proposed in the literature. For instance, it is possible to show that $\hat{j}_h(\cdot, \cdot)$ and $j_h(\cdot, \cdot)$ are equivalent to the following operators.

$$\begin{aligned} s_h(\mathbf{w}_h, \mathbf{v}_h) &:= \sum_{\ell=1}^{N_P} \int_{P_\ell} (\mathbf{w}_h - \pi_\ell(\mathbf{w}_h)) \mathbf{v}_h, & w_h, \mathbf{v}_h \in V_h, \\ g_h(\mathbf{w}_h, \mathbf{v}_h) &:= \sum_{\ell=1}^{N_P} \int_{P_\ell} [\mathbf{w}_h]_{\mathcal{P}_\ell} [\mathbf{v}_h]_{\mathcal{P}_\ell}, & w_h, \mathbf{v}_h \in V_h, \\ s_h(m_h, q_h) &:= \sum_{\ell=1}^{N_P} h^{-2} \int_{P_\ell} (m_h - \pi_\ell(m_h)) q_h, & m_h, q_h \in Q_h, \\ g_h(m_h, q_h) &:= \sum_{\ell=1}^{N_P} h^{-2} \int_{P_\ell} [m_h]_{\mathcal{P}_\ell} [q_h]_{\mathcal{P}_\ell}, & m_h, q_h \in Q_h, \end{aligned}$$

namely it holds, respectively,

$$\begin{aligned} j_h(\mathbf{v}_h, \mathbf{v}_h) &\lesssim s_h(\mathbf{v}_h, \mathbf{v}_h) \lesssim \hat{j}_h(\mathbf{v}_h, \mathbf{v}_h), & j_h(\mathbf{v}_h, \mathbf{v}_h) &\lesssim g_h(\mathbf{v}_h, \mathbf{v}_h) \lesssim \hat{j}_h(\mathbf{v}_h, \mathbf{v}_h), & \forall \mathbf{v}_h \in V_h, \\ j_h(q_h, q_h) &\lesssim s_h(q_h, q_h) \lesssim \hat{j}_h(q_h, q_h), & j_h(q_h, q_h) &\lesssim g_h(q_h, q_h) \lesssim \hat{j}_h(q_h, q_h), & \forall q_h \in Q_h. \end{aligned}$$

Here,

$$\pi_\ell : L^2(\mathcal{P}_\ell) \rightarrow \mathbb{RT}_k(\mathcal{P}_\ell), \quad \pi_\ell : L^2(\mathcal{P}_\ell) \rightarrow \mathbb{M}_k(\mathcal{P}_\ell),$$

denote the L^2 -orthogonal projections onto $\mathbb{RT}_k(\mathcal{P}_\ell) := \{\mathcal{E}_\ell(\varphi_h)|_{P_\ell} : \varphi_h \in \mathbb{RT}_k(K'_\ell)\}$ and $\mathbb{M}_k(\mathcal{P}_\ell) := \{\mathcal{E}_\ell(\psi_h)|_{P_\ell} : \psi_h \in \mathbb{M}_k(K'_\ell)\}$, K'_ℓ is the uncut element of the ℓ -th patch (see Assumption 8.1.2), and \mathcal{E}_ℓ and \mathcal{E}_ℓ are the canonical extension operators of the respective polynomial space. For $\mathbf{v}_h \in V_h$ and $q_h \in Q_h$,

$$\begin{aligned} [\mathbf{v}_h]_{\mathcal{P}_\ell}(x) &:= \mathbf{v}_h(x) - \mathcal{E}_\ell \left(\mathbf{v}_h|_{K'_\ell} \right)(x), & x \in P_\ell, \\ [q_h]_{\mathcal{P}_\ell}(x) &:= q_h(x) - \mathcal{E}_\ell \left(q_h|_{K'_\ell} \right)(x), & x \in P_\ell, \end{aligned}$$

see [88, 110].

From the implementation point of view, the operators $s_h(\cdot, \cdot)$, $s_h(\cdot, \cdot)$ and $g_h(\cdot, \cdot)$, $g_h(\cdot, \cdot)$ turn out to be a more convenient choice of $\hat{j}_h(\cdot, \cdot)$, $j_h(\cdot, \cdot)$, respectively, when a higher-order discretization is employed because of the evaluation of the high order derivatives. In the numerical experiments of Section 8.6 we use the projection-based operators $s_h(\cdot, \cdot)$ and $s_h(\cdot, \cdot)$.

We are now ready to introduce our stabilized discrete formulation. The idea is to employ the Nitsche formulation for the Darcy flow, which has been proposed and analyzed in Chapter 7, stabilizing it with the ghost penalty operators introduced above.

Find $(\mathbf{u}_h, p_h) \in V_h \times Q_h$ such that

$$\begin{aligned} a_h(\mathbf{u}_h, \mathbf{v}_h) + \mathbf{j}_h(\mathbf{u}_h, \mathbf{v}_h) + b_1(\mathbf{v}_h, p_h) &= \int_{\Omega} \mathbf{f} \cdot \mathbf{v}_h + \int_{\Gamma_D} p_D \mathbf{v}_h \cdot \mathbf{n} + h^{-1} \int_{\Gamma_N} u_N \mathbf{v}_h \cdot \mathbf{n}, \quad \forall \mathbf{v}_h \in V_h, \\ b_1(\mathbf{u}_h, q_h) - j_h(p_h, q_h) &= \int_{\Omega} g q_h - \int_{\Gamma_N} u_N q_h, \quad \forall q_h \in Q_h, \end{aligned} \quad (8.4)$$

where

$$\begin{aligned} a_h(\mathbf{w}_h, \mathbf{v}_h) &:= \int_{\Omega} \mathbf{w}_h \cdot \mathbf{v}_h + h^{-1} \int_{\Gamma_N} (\mathbf{w}_h \cdot \mathbf{n}) (\mathbf{v}_h \cdot \mathbf{n}), \quad \mathbf{w}_h, \mathbf{v}_h \in V_h, \\ b_1(\mathbf{v}_h, q_h) &:= \int_{\Omega} q_h \operatorname{div} \mathbf{v}_h - \int_{\Gamma_N} q_h \mathbf{v}_h \cdot \mathbf{n}, \quad \mathbf{v}_h \in V_h, q_h \in Q_h. \end{aligned}$$

It will be convenient to rewrite (8.4) in the following more compact form.

Find $(\mathbf{u}_h, p_h) \in V_h \times Q_h$ such that

$$\mathcal{A}_h((\mathbf{u}_h, p_h); (\mathbf{v}_h, q_h)) = \mathcal{F}_h(\mathbf{v}_h, q_h), \quad \forall (\mathbf{v}_h, q_h) \in V_h \times Q_h, \quad (8.5)$$

where, for $(\mathbf{w}_h, m_h), (\mathbf{v}_h, q_h) \in V_h \times Q_h$,

$$\begin{aligned} \mathcal{A}_h((\mathbf{w}_h, m_h); (\mathbf{v}_h, q_h)) &:= a_h(\mathbf{w}_h, \mathbf{v}_h) + \mathbf{j}_h(\mathbf{w}_h, \mathbf{v}_h) + b_1(\mathbf{v}_h, m_h) + b_1(\mathbf{w}_h, q_h) - j_h(m_h, q_h), \\ \mathcal{F}_h(\mathbf{v}_h, q_h) &:= \int_{\Omega} \mathbf{f} \cdot \mathbf{v}_h + \int_{\Gamma_D} p_D \mathbf{v}_h \cdot \mathbf{n} + h^{-1} \int_{\Gamma_N} u_N \mathbf{v}_h \cdot \mathbf{n} + \int_{\Omega} g q_h - \int_{\Gamma_N} u_N q_h. \end{aligned}$$

Proposition 8.3.2 (Weak Galerkin Orthogonality). *Let $(\mathbf{u}, p) \in \mathbf{H}(\operatorname{div}; \Omega) \times L^2(\Omega)$ be the solution of (8.1) and (\mathbf{u}_h, p_h) the one of (8.5). Then,*

$$\mathcal{A}_h((\mathbf{u} - \mathbf{u}_h, p - p_h); (\mathbf{v}_h, q_h)) = \mathbf{j}_h(\mathbf{u}, \mathbf{v}_h) - j_h(p, q_h), \quad \forall (\mathbf{v}_h, q_h) \in V_h \times Q_h.$$

Proof. The proof is trivial, hence we skip it. \square

Remark 8.3.3. We note that the formulation (8.5) no longer fits into the framework of saddle-point problems. Hence, in order to study its stability, we will need to resort to the more general *Banach-Nečas-Babuška Theorem* [55]. The case of pure natural boundary conditions will be covered separately in Section 8.5. Moreover, note that all the dimensionless parameters have been set for simplicity to 1, unlike for the standard Nitsche method for the Poisson problem [61], where the dimensionless parameter needs to be taken large enough.

We endow V_h and Q_h with the following mesh-dependent norms.

$$\begin{aligned} \|\mathbf{v}_h\|_{0,h,\Omega_T}^2 &:= \|\mathbf{v}_h\|_{L^2(\Omega_T)}^2 + \sum_{K \in \mathcal{G}_h(\Gamma_N)} h^{-1} \|\mathbf{v}_h \cdot \mathbf{n}\|_{L^2(\Gamma_K)}^2, \quad \mathbf{v}_h \in V_h, \\ \|q_h\|_{1,h,\Omega_I}^2 &:= \sum_{K \in \mathcal{T}_h(\Omega_{I,h})} \|\nabla q_h\|_{L^2(K)}^2 + \sum_{f \in \mathcal{F}_h^i(\Omega_{I,h})} h^{-1} \|[q_h]\|_{L^2(f)}^2, \quad q_h \in Q_h, \\ \|q_h\|_{1,h,\Omega_T}^2 &:= \sum_{K \in \mathcal{T}_h} \|\nabla q_h\|_{L^2(K)}^2 + \sum_{f \in \mathcal{F}_h^i} h^{-1} \|[q_h]\|_{L^2(f \cap \Omega)}^2 + \sum_{K \in \mathcal{G}_h(\Gamma_D)} h^{-1} \|q_h\|_{L^2(\Gamma_K)}^2, \quad q_h \in Q_h. \end{aligned}$$

The space $V_h \times Q_h$ is equipped with the product norm

$$\|(\mathbf{v}_h, q_h)\|^2 := \|\mathbf{v}_h\|_{0,h,\Omega_T}^2 + \|q_h\|_{1,h,\Omega_T}^2, \quad (\mathbf{v}_h, q_h) \in V_h \times Q_h. \quad (8.6)$$

Let us illustrate the salient properties of the ghost penalty operators that are needed to study the well-posedness of formulation (8.4).

Lemma 8.3.4. *The bilinear forms $j_h(\cdot, \cdot)$ and $j_h(\cdot, \cdot)$ induce semi-inner products on V_h and Q_h , respectively. In particular,*

$$\begin{aligned} j_h(\mathbf{w}_h, \mathbf{v}_h) &\leq j_h(\mathbf{w}_h, \mathbf{w}_h)^{\frac{1}{2}} j_h(\mathbf{v}_h, \mathbf{v}_h)^{\frac{1}{2}}, & \forall \mathbf{w}_h, \mathbf{v}_h \in V_h, \\ j_h(m_h, q_h) &\leq j_h(m_h, m_h)^{\frac{1}{2}} j_h(q_h, q_h)^{\frac{1}{2}}, & \forall m_h, q_h \in Q_h. \end{aligned}$$

Proof. It suffices to apply the Cauchy-Schwarz inequality, first in the L^2 -setting and then in the ℓ^2 -setting. Let us show, for instance, the bound for $j_h(\cdot, \cdot)$. Given $m_h, q_h \in Q_h$, it holds

$$\begin{aligned} j_h(m_h, q_h) &= \sum_{f \in \mathcal{F}_h^\Gamma} \sum_{j=0}^k h^{2j-1} \int_f [\partial_n^j m_h] [\partial_n^j q_h] \leq \sum_{f \in \mathcal{F}_h^\Gamma} \sum_{j=0}^k h^{\frac{1}{2}(2j-1)} \|\partial_n^j m_h\|_{L^2(f)} h^{\frac{1}{2}(2j-1)} \|\partial_n^j q_h\|_{L^2(f)} \\ &\leq \left(\sum_{f \in \mathcal{F}_h^\Gamma} \sum_{j=0}^k h^{2j-1} \|\partial_n^j m_h\|_{L^2(f)}^2 \right)^{\frac{1}{2}} \left(\sum_{f \in \mathcal{F}_h^\Gamma} \sum_{j=0}^k h^{2j-1} \|\partial_n^j q_h\|_{L^2(f)}^2 \right)^{\frac{1}{2}} \\ &= j_h(m_h, m_h)^{\frac{1}{2}} j_h(q_h, q_h)^{\frac{1}{2}}. \end{aligned}$$

The inequality for $j_h(\cdot, \cdot)$ follows in a similar fashion. \square

Lemma 8.3.5. *Let $K_1, K_2 \in \mathcal{T}_h$ with a facet $f = \partial K_1 \cap \partial K_2$. Let φ_h be a piecewise polynomial such that $\varphi_1 := \varphi_h|_{K_1} \in \mathbb{M}_{k_1}(K_1)$ and $\varphi_2 := \varphi_h|_{K_2} \in \mathbb{M}_{k_2}(K_2)$, and let $k := \max\{k_1, k_2\}$. There exist $C_1, C_2 > 0$, independent of $h > 0$, but dependent on the shape-regularity constant and on k , such that*

$$\begin{aligned} \|\varphi_1\|_{L^2(K_1)}^2 &\leq C_1 \left(\|\varphi_2\|_{L^2(K_2)}^2 + \sum_{j=0}^k h^{2j+1} \|\partial_n^j \varphi_h\|_{L^2(f)}^2 \right), \\ \left\| \frac{\partial \varphi_1}{\partial x_j} \right\|_{L^2(K_1)}^2 &\leq C_2 \left(\left\| \frac{\partial \varphi_2}{\partial x_j} \right\|_{L^2(K_2)}^2 + \sum_{j=0}^k h^{2j-1} \|\partial_n^j \varphi_h\|_{L^2(f)}^2 \right), \quad \forall 1 \leq j \leq d. \end{aligned} \tag{8.7}$$

Proof. The first inequality in (8.7) has been proven in Lemma 5.1 in [96]. For the second inequality, see Lemma 5.2 of [88]. \square

The following results enable us to control the norms in the whole $\Omega_{\mathcal{T}}$ in terms of the norms in the domain $\Omega_{I,h}$ through the ghost penalty operators.

Theorem 8.3.6. *The following inequalities hold.*

$$\|\mathbf{v}_h\|_{L^2(\Omega_{\mathcal{T}})}^2 \lesssim \|\mathbf{v}_h\|_{L^2(\Omega_{I,h})}^2 + j_h(\mathbf{v}_h, \mathbf{v}_h), \quad \forall \mathbf{v}_h \in V_h, \tag{8.8}$$

$$\sum_{K \in \mathcal{T}_h} \|\nabla q_h\|_{L^2(K)}^2 \lesssim \sum_{K \in \mathcal{T}_h(\Omega_{I,h})} \|\nabla q_h\|_{L^2(K)}^2 + j_h(q_h, q_h), \quad \forall q_h \in Q_h, \tag{8.9}$$

$$\sum_{f \in \mathcal{F}_h^i} h^{-1} \|[q_h]\|_{L^2(f)}^2 \lesssim \sum_{f \in \mathcal{F}_h^i(\Omega_{I,h})} h^{-1} \|[q_h]\|_{L^2(f)}^2 + j_h(q_h, q_h), \quad \forall q_h \in Q_h. \tag{8.10}$$

Proof. Let us start with the proof of (8.8). Since we can decompose $\Omega_{\mathcal{T}} = \Omega_{I,h} \cup \bigcup_{K \in \mathcal{G}_h} K$, it is sufficient to show

$$\sum_{K \in \mathcal{G}_h} \|\mathbf{v}_h\|_{L^2(K)}^2 \lesssim \|\mathbf{v}_h\|_{L^2(\Omega_{I,h})}^2 + j_h(\mathbf{v}_h, \mathbf{v}_h), \quad \forall \mathbf{v}_h \in V_h,$$

which holds by Assumption 8.1.1, the shape-regularity of \mathcal{T}_h , and Lemma 8.3.5. See also Lemma 2 of [68] and Proposition 5.1 of [96]. Inequality (8.9) for the pressures follows in a similar fashion.

Let us move to (8.10). Note that in view of Remark 8.3.1, we may replace $j_h(\cdot, \cdot)$ with $s_h(\cdot, \cdot)$. Without loss of generality, let $f \in \mathcal{F}_h^i \setminus \mathcal{F}_h^i(\Omega_{I,h})$. Assumption 8.1.2 guarantees the existence of a patch \mathcal{P}_ℓ such that $f \in \mathcal{F}_\ell$ and of an internal face $f' \in \mathcal{F}_\ell \cap \mathcal{F}_h^i(\Omega_{I,h})$. We proceed by a scaling argument. Let us take $q_h \in Q_h$ and map P_ℓ to the reference patch \hat{P} . \hat{P} can be defined as $\hat{P} := \{\mathbf{F}_{K'_\ell}^{-1}(x) : x \in P_\ell\}$, where $K'_\ell \in \mathcal{P}_\ell \cap \mathcal{T}_h(\Omega_{I,h})$ (whose existence follows from Assumption 8.1.2), see Section 2.4.1 of [90]. Note that $\text{diam}(\hat{P}) = \mathcal{O}(1)$ and \hat{P} depends on the shape of P_ℓ . We denote $\hat{f} := \mathbf{F}_{K'_\ell}^{-1}(f)$, $\hat{f}' := \mathbf{F}_{K'_\ell}^{-1}(f')$, $\hat{q}_h := q_h \circ \mathbf{F}_{K'_\ell}$, and $\hat{\pi} : L^2(\hat{P}) \rightarrow \mathbb{M}_k(\hat{P})$ the L^2 -orthogonal projection. Moreover, let $\hat{\mathcal{F}} := \{\hat{f} : \hat{f} = \mathbf{F}_{K'_\ell}^{-1}(f), f \in \mathcal{F}_h^i, f \subseteq P_\ell, f \not\subseteq \partial P_\ell\}$. We also write

$$\hat{s}(\hat{q}_h, \hat{q}_h) := \int_{\hat{P}} (\hat{q}_h - \hat{\pi}(\hat{q}_h)) \hat{q}_h.$$

It is sufficient to show that

$$\|[\hat{q}_h]\|_{L^2(\hat{f})}^2 \leq C(\hat{P}) \|[\hat{q}_h]\|_{L^2(\hat{f}')}^2 + \hat{s}(\hat{q}_h, \hat{q}_h). \quad (8.11)$$

We decompose $\hat{q}_h = \hat{q}_1 + \hat{q}_2$, where $\hat{q}_1 \in \ker(\hat{s})$ and $\hat{q}_2 \in (\ker(\hat{s}))^\perp$, where the orthogonal complement is taken with respect to the L^2 -scalar product on \hat{P} . Note that $\ker(\hat{s}) = \mathbb{M}_k(\hat{P}) = \text{Im}(\hat{\pi})$. We have, of course,

$$\|[\hat{q}_1 + \hat{q}_2]\|_{L^2(\hat{f})}^2 \leq \|[\hat{q}_1 + \hat{q}_2]\|_{L^2(\hat{f}')}^2 + \|[\hat{q}_2]\|_{L^2(\hat{f}')}^2. \quad (8.12)$$

From norms equivalence on discrete spaces, it holds

$$\sum_{f \in \hat{\mathcal{F}}} \|[\hat{q}_2]\|_{L^2(\hat{f})}^2 \lesssim \|\hat{q}_2\|_{L^2(\hat{P})}^2. \quad (8.13)$$

Indeed, it is easy to check that both terms in (8.13) are norms on $(\ker(\hat{s}))^\perp$. In particular, (8.13) entails

$$\|[\hat{q}_2]\|_{L^2(\hat{f})}^2 \lesssim \|\hat{q}_2\|_{L^2(\hat{P})}^2, \quad \forall \hat{f} \in \hat{\mathcal{F}}. \quad (8.14)$$

By combining (8.12) and (8.14), we have $\|[\hat{q}_1 + \hat{q}_2]\|_{L^2(\hat{f})}^2 \leq \|[\hat{q}_1 + \hat{q}_2]\|_{L^2(\hat{f}')}^2 + \|\hat{q}_2\|_{L^2(\hat{P})}^2$. The reader can easily check $\hat{s}(\hat{q}_1 + \hat{q}_2, \hat{q}_1 + \hat{q}_2) = \|\hat{q}_2\|_{L^2(\hat{P})}^2$. Hence,

$$\|[\hat{q}_1 + \hat{q}_2]\|_{L^2(\hat{f})}^2 \leq \|[\hat{q}_1 + \hat{q}_2]\|_{L^2(\hat{f}')}^2 + \hat{s}(\hat{q}_1 + \hat{q}_2, \hat{q}_1 + \hat{q}_2).$$

By compactness, it holds $\sup_{\hat{P}} C(\hat{P}) \leq C$, see Section 2.2.7 of [22]. The claim follows by scaling back to the physical patch P_ℓ , summing over all the patches, using Assumption 8.1.2, and the shape-regularity of the mesh. \square

8.3.1 Stability estimates

Let us prove the main ingredients that allow us to show the well-posedness of formulation (8.5).

Proposition 8.3.7. *The bilinear forms appearing in the weak formulation (8.5) are continuous, namely, there exist $M_a, M_{b_1}, M_j, M_j > 0$, such that*

$$\begin{aligned} |a_h(\mathbf{w}_h, \mathbf{v}_h)| &\leq M_a \|\mathbf{w}_h\|_{0,h,\Omega_\mathcal{T}} \|\mathbf{v}_h\|_{0,h,\Omega_\mathcal{T}}, & \forall \mathbf{w}_h, \mathbf{v}_h \in V_h, \\ |b_1(\mathbf{v}_h, q_h)| &\leq M_{b_1} \|\mathbf{v}_h\|_{0,h,\Omega_\mathcal{T}} \|q_h\|_{1,h,\Omega_\mathcal{T}}, & \forall \mathbf{v}_h \in V_h, \forall q_h \in Q_h, \\ |j_h(\mathbf{w}_h, \mathbf{v}_h)| &\leq M_j \|\mathbf{w}_h\|_{0,h,\Omega_\mathcal{T}} \|\mathbf{v}_h\|_{0,h,\Omega_\mathcal{T}}, & \forall \mathbf{w}_h, \mathbf{v}_h \in V_h, \\ |j_h(m_h, q_h)| &\leq M_j \|m_h\|_{1,h,\Omega_\mathcal{T}} \|q_h\|_{1,h,\Omega_\mathcal{T}}, & \forall m_h, q_h \in Q_h. \end{aligned}$$

Proof. Let us fix any $\mathbf{w}_h, \mathbf{v}_h \in V_h$ and $m_h, q_h \in Q_h$. By Cauchy-Schwartz's inequality

$$\begin{aligned} |a_h(\mathbf{w}_h, \mathbf{v}_h)| &\leq \|\mathbf{w}_h\|_{L^2(\Omega)} \|\mathbf{v}_h\|_{L^2(\Omega)} + h^{-\frac{1}{2}} \|\mathbf{w}_h \cdot \mathbf{n}\|_{L^2(\Gamma_N)} h^{-\frac{1}{2}} \|\mathbf{v}_h \cdot \mathbf{n}\|_{L^2(\Gamma_N)} \\ &\leq \|\mathbf{w}_h\|_{0,h,\Omega_\mathcal{T}} \|\mathbf{v}_h\|_{0,h,\Omega_\mathcal{T}}, \end{aligned}$$

hence $M_a = 1$. By integration by parts, we get

$$\begin{aligned} b_1(\mathbf{v}_h, q_h) &= \int_\Omega q_h \operatorname{div} \mathbf{v}_h - \int_{\Gamma_N} q_h \mathbf{v}_h \cdot \mathbf{n} = \sum_{K \in \mathcal{T}_h} \int_{K \cap \Omega} q_h \operatorname{div} \mathbf{v}_h - \sum_{K \in \mathcal{G}_h(\Gamma_N)} \int_{\Gamma_K} q_h \mathbf{v}_h \cdot \mathbf{n} \\ &= - \sum_{K \in \mathcal{T}_h} \int_{K \cap \Omega} \nabla q_h \cdot \mathbf{v}_h + \sum_{f \in \mathcal{F}_h^i} \int_{f \cap \Omega} [q_h] \mathbf{v}_h \cdot \mathbf{n} + \sum_{K \in \mathcal{G}_h(\Gamma_D)} \int_{\Gamma_K} q_h \mathbf{v}_h \cdot \mathbf{n}. \end{aligned}$$

From Cauchy-Schwarz's inequality, Lemma A.1.2, and a standard inverse estimate (Proposition 6.3.2 of [112]), we obtain

$$\begin{aligned} \sum_{f \in \mathcal{F}_h^i} \int_{f \cap \Omega} [q_h] \mathbf{v}_h \cdot \mathbf{n} &\leq \sum_{f \in \mathcal{F}_h^i} h^{-\frac{1}{2}} \|[q_h]\|_{L^2(f \cap \Omega)} h^{\frac{1}{2}} \|\mathbf{v}_h \cdot \mathbf{n}\|_{L^2(f \cap \Omega)} \\ &\leq C \left(\sum_{f \in \mathcal{F}_h^i} h^{-1} \|[q_h]\|_{L^2(f \cap \Omega)}^2 \right)^{\frac{1}{2}} \left(\sum_{K \in \mathcal{T}_h} \|\mathbf{v}_h\|_{L^2(K)}^2 \right)^{\frac{1}{2}} \\ &\leq C \|q_h\|_{1,h,\Omega_\mathcal{T}} \|\mathbf{v}_h\|_{0,h,\Omega_\mathcal{T}}, \end{aligned}$$

and, analogously,

$$\begin{aligned} \sum_{K \in \mathcal{G}_h(\Gamma_D)} \int_{\Gamma_K} q_h \mathbf{v}_h \cdot \mathbf{n} &\leq \sum_{K \in \mathcal{G}_h(\Gamma_D)} h^{-\frac{1}{2}} \|q_h\|_{L^2(\Gamma_K)} h^{\frac{1}{2}} \|\mathbf{v}_h \cdot \mathbf{n}\|_{L^2(\Gamma_K)} \\ &\leq C \left(\sum_{K \in \mathcal{G}_h(\Gamma_D)} h^{-1} \|q_h\|_{L^2(\Gamma_K)}^2 \right)^{\frac{1}{2}} \left(\sum_{K \in \mathcal{T}_h} \|\mathbf{v}_h\|_{L^2(K)}^2 \right)^{\frac{1}{2}} \\ &\leq C \|q_h\|_{1,h,\Omega_\mathcal{T}} \|\mathbf{v}_h\|_{0,h,\Omega_\mathcal{T}}. \end{aligned}$$

Thus,

$$\begin{aligned} |b_1(\mathbf{v}_h, q_h)| &\leq \sum_{K \in \mathcal{T}_h} \|\nabla q_h\|_{L^2(K \cap \Omega)} \|\mathbf{v}_h\|_{L^2(K \cap \Omega)} + C \|q_h\|_{1,h,\Omega_\mathcal{T}} \|\mathbf{v}_h\|_{0,h,\Omega_\mathcal{T}} \\ &\leq C \|q_h\|_{1,h,\Omega_\mathcal{T}} \|\mathbf{v}_h\|_{0,h,\Omega_\mathcal{T}}. \end{aligned}$$

The bounds for $j_h(\cdot, \cdot)$ and $j_h(\cdot, \cdot)$ follow as well straightforward. \square

Proposition 8.3.8. *There exists $\alpha > 0$, such that,*

$$a_h(\mathbf{v}_h, \mathbf{v}_h) + j_h(\mathbf{v}_h, \mathbf{v}_h) \geq \alpha \|\mathbf{v}_h\|_{0,h,\Omega_\mathcal{T}}^2, \quad \forall \mathbf{v}_h \in V_h.$$

Proof. This is just a consequence of Theorem 8.3.6. \square

Proposition 8.3.9. *There exists $\beta_1 > 0$ such that*

$$\inf_{q_h \in Q_h} \sup_{\mathbf{v}_h \in V_h} \frac{b_1(\mathbf{v}_h, q_h)}{\|\mathbf{v}_h\|_{0,h,\Omega_T}} \geq \beta_1 \|q_h\|_{1,h,\Omega_{I,h}}.$$

Proof. Let us fix $q_h \in Q_h$ and construct $\mathbf{v}_h \in V_h$ using just the internal degrees of freedom of V_h , namely

$$\begin{aligned} \int_f \mathbf{v}_h \cdot \mathbf{n} \varphi_h &= h^{-1} \int_f [q_h] \varphi_h, & \forall f \in \mathcal{F}_h^i(\Omega_{I,h}), \forall \varphi_h \in \Psi_k(f), \\ \int_f \mathbf{v}_h \cdot \mathbf{n} \varphi_h &= 0, & \forall f \in \mathcal{F}_h^\partial(\Omega_{I,h}), \forall \varphi_h \in \Psi_k(f), \\ \int_K \mathbf{v}_h \cdot \boldsymbol{\psi}_h &= - \int_K \nabla q_h \cdot \boldsymbol{\psi}_h, & \forall K \in \mathcal{T}_h(\Omega_{I,h}), \forall \boldsymbol{\psi}_h \in \Psi_k(K), \quad \text{if } k > 0. \end{aligned}$$

We refer the reader to Chapter 6 for the definitions of $\Psi_k(K)$ and $\Psi_k(f)$. Let us extend \mathbf{v}_h to zero outside $\Omega_{I,h}$. It holds

$$\begin{aligned} b_1(\mathbf{v}_h, q_h) &= - \sum_{K \in \mathcal{T}_h(\Omega_{I,h})} \int_K \nabla q_h \cdot \mathbf{v}_h + \sum_{f \in \mathcal{F}_h^i(\Omega_{I,h})} \int_f [q_h] \mathbf{v}_h \cdot \mathbf{n} \\ &= \sum_{K \in \mathcal{T}_h(\Omega_{I,h})} \|\nabla q_h\|_{L^2(K)}^2 + \sum_{f \in \mathcal{F}_h^i(\Omega_{I,h})} h^{-1} \|[q_h]\|_{L^2(f)}^2 = \|q_h\|_{1,h,\Omega_{I,h}}^2. \end{aligned}$$

Now, we prove that $\|\mathbf{v}_h\|_{0,h,\Omega_T} \lesssim \|q_h\|_{1,h,\Omega_{I,h}}$. By construction of \mathbf{v}_h , it is sufficient to show

$$\sum_{K \in \mathcal{T}_h(\Omega_{I,h})} \|\mathbf{v}_h\|_{L^2(K)}^2 \lesssim \sum_{K \in \mathcal{T}_h(\Omega_{I,h})} \|\nabla q_h\|_{L^2(K)}^2 + \sum_{f \in \mathcal{F}_h^i(\Omega_{I,h})} h^{-1} \|[q_h]\|_{L^2(f)}^2.$$

We mimic the proof of Proposition 2.1 in [40]. Let $K \in \mathcal{T}_h(\Omega_{I,h})$ and \widehat{K} be the reference element. Let f be a face of K and \widehat{f} be its preimage through \mathbf{F}_K (see Chapter 6 for the definitions of \widehat{K} and \mathbf{F}_K). Finite dimensionality implies

$$\|\widehat{\mathbf{v}}_h\|_{L^2(\widehat{K})}^2 \lesssim \left\| \pi_{\widehat{K},k-1}(\widehat{\mathbf{v}}_h) \right\|_{L^2(\widehat{K})}^2 + \|\widehat{\mathbf{v}}_h \cdot \mathbf{n}\|_{L^2(\widehat{f})}^2,$$

where $\pi_{\widehat{K},k-1}$ is the L^2 -projection onto $\Psi_k(\widehat{K})$. By pushing forward to the element K , a scaling argument implies

$$\|\mathbf{v}_h\|_{L^2(K)}^2 \lesssim \|\pi_{K,k-1}(\mathbf{v}_h)\|_{L^2(K)}^2 + h \|\mathbf{v}_h \cdot \mathbf{n}\|_{L^2(f)}^2.$$

This time $\pi_{K,k-1}$ is the L^2 -projection onto $\Psi_k(K)$ By construction of \mathbf{v}_h ,

$$\|\mathbf{v}_h\|_{L^2(K)}^2 \lesssim \|\pi_{K,k-1}(\nabla q_h)\|_{L^2(K)}^2 + h^{-1} \|\pi_{f,k}([q_h])\|_{L^2(f)}^2 = \|\nabla q_h\|_{L^2(K)}^2 + h^{-1} \|[q_h]\|_{L^2(f)}^2,$$

where $\pi_{f,k}$ denotes the L^2 -projection onto $\Psi_k(f)$. \square

We are left with the proof of the well-posedness of formulation (8.5). In order to do that, we verify that the bilinear form $\mathcal{A}_h(\cdot; \cdot)$ satisfies the hypotheses of the Banach-Nečas-Babuška Theorem.

Theorem 8.3.10. *There exists $\eta > 0$ such that*

$$\inf_{(\mathbf{v}_h, q_h) \in V_h \times Q_h} \sup_{(\mathbf{w}_h, m_h) \in V_h \times Q_h} \frac{\mathcal{A}_h((\mathbf{v}_h, q_h); (\mathbf{w}_h, m_h))}{\|(\mathbf{v}_h, q_h)\| \|(\mathbf{w}_h, m_h)\|} \geq \eta.$$

Proof. Let $(\mathbf{v}_h, q_h) \in V_h \times Q_h$ be arbitrary and $-\mathbf{w}_h$ be the element attaining the supremum in Proposition 8.3.9, namely

$$-b_1(\mathbf{w}_h, q_h) = \|q_h\|_{1,h,\Omega_{I,h}}^2, \quad \|\mathbf{w}_h\|_{0,h,\Omega_\mathcal{T}} \lesssim \|q_h\|_{1,h,\Omega_{I,h}}. \quad (8.15)$$

From Proposition 8.3.7, we have

$$\begin{aligned} \mathcal{A}_h((\mathbf{v}_h, q_h); (-\mathbf{w}_h, 0)) &= -a_h(\mathbf{v}_h, \mathbf{w}_h) - \mathbf{j}_h(\mathbf{v}_h, \mathbf{w}_h) - b_1(\mathbf{w}_h, q_h) + b_1(\mathbf{v}_h, 0) - j_h(q_h, 0) \\ &\geq -2 \|\mathbf{v}_h\|_{0,h,\Omega_\mathcal{T}} \|\mathbf{w}_h\|_{0,h,\Omega_\mathcal{T}} + \|q_h\|_{1,h,\Omega_{I,h}}^2 \\ &\gtrsim -2 \|\mathbf{v}_h\|_{0,h,\Omega_\mathcal{T}} \|q_h\|_{1,h,\Omega_{I,h}} + \|q_h\|_{1,h,\Omega_{I,h}}^2 \\ &\gtrsim -\frac{1}{\varepsilon} \|\mathbf{v}_h\|_{0,h,\Omega_\mathcal{T}}^2 + (1 - \varepsilon) \|q_h\|_{1,h,\Omega_{I,h}}^2, \end{aligned}$$

where $\varepsilon > 0$ arises from the Young inequality. On the other hand, it holds

$$\begin{aligned} \mathcal{A}_h((\mathbf{v}_h, q_h); (\mathbf{v}_h, -q_h)) &= a_h(\mathbf{v}_h, \mathbf{v}_h) + \mathbf{j}_h(\mathbf{v}_h, \mathbf{v}_h) + b_1(\mathbf{v}_h, q_h) - b_1(\mathbf{v}_h, q_h) + j_h(q_h, q_h) \\ &\gtrsim \|\mathbf{v}_h\|_{0,h,\Omega_\mathcal{T}}^2 + j_h(q_h, q_h). \end{aligned}$$

By choosing $(\mathbf{v}_h - \delta \mathbf{w}_h, -q_h) \in V_h \times Q_h$, for $\delta > 0$ to be set later on, we get

$$\mathcal{A}_h((\mathbf{v}_h, q_h); (\mathbf{v}_h - \delta \mathbf{w}_h, -q_h)) \gtrsim \left(1 - \frac{\delta}{\varepsilon}\right) \|\mathbf{v}_h\|_{0,h,\Omega_\mathcal{T}}^2 + \delta(1 - \varepsilon) \|q_h\|_{1,h,\Omega_{I,h}}^2 + j_h(q_h, q_h).$$

Let us take, for instance, $\varepsilon = \frac{1}{2}$ and any $0 < \delta < \frac{1}{2}$, so that

$$\begin{aligned} \mathcal{A}_h((\mathbf{v}_h, q_h); (\mathbf{v}_h - \delta \mathbf{w}_h, -q_h)) &\gtrsim \|\mathbf{v}_h\|_{0,h,\Omega_\mathcal{T}}^2 + \|q_h\|_{1,h,\Omega_{I,h}}^2 + j_h(q_h, q_h) \\ &\gtrsim \|\mathbf{v}_h\|_{0,h,\Omega_\mathcal{T}}^2 + \|q_h\|_{1,h,\Omega_\mathcal{T}}^2, \end{aligned}$$

where in the last inequality we used $\|q_h\|_{1,h,\Omega_\mathcal{T}}^2 \lesssim \|q_h\|_{1,h,\Omega_{I,h}}^2 + j_h(q_h, q_h)$, which follows from Theorem 8.3.6. We are left with proving that $\|(\mathbf{v}_h - \delta \mathbf{w}_h, q_h)\| \lesssim \|(\mathbf{v}_h, q_h)\|$, which is a consequence of (8.15). \square

8.3.2 *A priori* error estimates

Theorem 8.3.11. *There exists $C > 0$ such that, for every $(\mathbf{v}, q) \in \mathbf{H}^t(\Omega) \times H^r(\Omega)$, $t \geq 1$, $r \geq 1$, it holds*

$$\|\mathbf{E}(\mathbf{v}) - r_h(\mathbf{v})\|_{0,h,\Omega_\mathcal{T}} + \|E(q) - \Pi_h(q)\|_{1,h,\Omega_\mathcal{T}} \leq Ch^s \left(\|\mathbf{v}\|_{H^t(\Omega)} + \|q\|_{H^r(\Omega)} \right),$$

where $s := \min\{t - 1, r - 1, k\}$, \mathbf{E} and E have been introduced in Section 8.2.

Proof. Let us start with the velocity. We have

$$\|\mathbf{E}(\mathbf{v}) - r_h(\mathbf{v})\|_{0,h,\Omega_\mathcal{T}}^2 = \|\mathbf{E}(\mathbf{v}) - r_h(\mathbf{v})\|_{L^2(\Omega_\mathcal{T})}^2 + h^{-1} \sum_{K \in \mathcal{G}_h(\Gamma_N)} \|(\mathbf{E}(\mathbf{v}) - r_h(\mathbf{v})) \cdot \mathbf{n}\|_{L^2(\Gamma_K)}^2.$$

For the volumetric term, let us apply the standard Deny-Lions argument (Chapter 3 of [112]) to the interpolant r_h and get

$$\|\mathbf{E}(\mathbf{v}) - r_h(\mathbf{v})\|_{L^2(\Omega_T)}^2 = \sum_{K \in \mathcal{T}_h} \|\mathbf{E}(\mathbf{v}) - r_h(\mathbf{v})\|_{L^2(K)}^2 \leq C \sum_{K \in \mathcal{T}_h} h^{2t} \|\mathbf{E}(\mathbf{v})\|_{H^t(K)}^2 \leq Ch^{2t} \|\mathbf{v}\|_{H^t(\Omega)}^2.$$

For the boundary part, let us first use the multiplicative trace inequality of Lemma A.1.2 (componentwise) and then, again, the Deny-Lions argument:

$$\begin{aligned} h^{-1} \sum_{K \in \mathcal{G}_h(\Gamma_N)} \|(\mathbf{E}(\mathbf{v}) - r_h(\mathbf{v})) \cdot \mathbf{n}\|_{L^2(\Gamma_K)}^2 &\leq h^{-1} \sum_{K \in \mathcal{G}_h(\Gamma_N)} \|\mathbf{E}(\mathbf{v}) - r_h(\mathbf{v})\|_{L^2(\Gamma_K)}^2 \\ &\leq Ch^{-1} \sum_{K \in \mathcal{G}_h(\Gamma_N)} \|\mathbf{E}(\mathbf{v}) - r_h(\mathbf{v})\|_{H^1(K)} \|\mathbf{E}(\mathbf{v}) - r_h(\mathbf{v})\|_{L^2(K)} \\ &\leq Ch^{-1} \sum_{K \in \mathcal{T}_h} h^{t-1} \|\mathbf{E}(\mathbf{v})\|_{H^t(K)} h^t \|\mathbf{E}(\mathbf{v})\|_{H^t(K)} \\ &\leq Ch^{2(t-1)} \|\mathbf{v}\|_{H^t(\Omega)}^2. \end{aligned}$$

We move to the pressure case.

$$\begin{aligned} \|E(q) - \Pi_h(q)\|_{1,h,\Omega_T}^2 &= \sum_{K \in \mathcal{T}_h} \|\nabla(E(q) - \Pi_h(q))\|_{L^2(K)}^2 + \sum_{f \in \mathcal{F}_h^i} h^{-1} \| [E(q) - \Pi_h(q)] \|_{L^2(f \cap \Omega)}^2 \\ &\quad + \sum_{K \in \mathcal{G}_h(\Gamma_D)} h^{-1} \|E(q) - \Pi_h(q)\|_{L^2(\Gamma_K)}^2. \end{aligned} \tag{8.16}$$

For the volumetric term we may proceed as in the case of the velocity to easily obtain

$$\sum_{K \in \mathcal{T}_h} \|\nabla(E(q) - \Pi_h(q))\|_{L^2(K)}^2 \leq Ch^{2(r-1)} \|q\|_{H^r(\Omega)}^2.$$

Let us focus on the jump part of (8.16) and take $f \in \mathcal{F}_h^i$ such that $f = K_1 \cap K_2$. Then, by Lemma A.1.2 and the Deny-Lions Lemma, we have

$$\begin{aligned} h^{-1} \| [E(q) - \Pi_h(q)] \|_{L^2(f \cap \Omega)}^2 &= h^{-1} \left\| (E(q) - \Pi_h(q)) \Big|_{K_1} - (E(q) - \Pi_h(q)) \Big|_{K_2} \right\|_{L^2(f)}^2 \\ &\leq Ch^{-1} \|E(q) - \Pi_h(q)\|_{L^2(K_1)} \|E(q) - \Pi_h(q)\|_{H^1(K_1)} \\ &\quad + Ch^{-1} \|E(q) - \Pi_h(q)\|_{L^2(K_2)} \|E(q) - \Pi_h(q)\|_{H^1(K_2)} \\ &\leq Ch^{2(r-1)} \left(\|E(q)\|_{H^r(K_1)}^2 + \|E(q)\|_{H^r(K_2)}^2 \right). \end{aligned}$$

Hence,

$$\sum_{f \in \mathcal{F}_h^i} h^{-1} \| [E(q) - \Pi_h(q)] \|_{L^2(f \cap \Omega)}^2 \leq Ch^{2(r-1)} \|q\|_{H^r(\Omega)}^2.$$

The bound for the boundary part of (8.16) follows in a similar fashion. \square

Lemma 8.3.12. *For every $\mathbf{v} \in \mathbf{H}^t(\Omega)$ and $q \in H^r(\Omega)$, $t \geq 1$, $r \geq 1$,*

$$\begin{aligned} j_h(r_h(\mathbf{v}), r_h(\mathbf{v}))^{\frac{1}{2}} &\lesssim h^m \|\mathbf{v}\|_{H^t(\Omega)}, \\ j_h(\Pi_h(q), \Pi_h(q))^{\frac{1}{2}} &\lesssim h^\ell \|q\|_{H^r(\Omega)}, \end{aligned}$$

where $m := \min\{k+1, t\}$ and $\ell := \min\{k, r-1\}$.

Proof. Note that

$$j_h(\Pi_h(q) - E(q), \Pi_h(q) - E(q)) = j_h(\Pi_h(q), \Pi_h(q)) - j_h(\Pi_h(q), E(q)) - j_h(E(q), \Pi_h(q)) + j_h(E(q), E(q)). \quad (8.17)$$

Given $0 \leq k \leq r-1$, for every $0 \leq j \leq k$, and α multi-index such that $|\alpha| = j$, then $D^\alpha E(q) \in H^{r-j}(\Omega_\mathcal{T}) \subset H^1(\Omega_\mathcal{T})$, hence $[\partial_n^j E(q)]_f$ vanishes across every $f \in \mathcal{F}_h^i$. Thus, (8.17) implies that

$$j_h(\Pi_h(q), \Pi_h(q)) = j_h(\Pi_h(q) - E(q), \Pi_h(q) - E(q)).$$

Now, by using Corollary A.1.3 and a standard approximation argument, we obtain

$$\begin{aligned} j_h(\Pi_h(q) - E(q), \Pi_h(q) - E(q)) &= \sum_{f \in \mathcal{F}_h^\Gamma} \sum_{i=0}^k h^{2i-1} \|\partial_n^i(\Pi_h(q) - E(q))\|_{L^2(f)}^2 \\ &\leq C \sum_{K \in \mathcal{G}_h} \sum_{i=0}^k h^{2i-1} \|D^i(\Pi_h(q) - E(q))\|_{L^2(K)} \|D^{i+1}(\Pi_h(q) - E(q))\|_{L^2(K)} \\ &\leq Ch^{2\ell} \|E(q)\|_{H^r(\Omega_\mathcal{T})}^2 \leq Ch^{2\ell} \|q\|_{H^r(\Omega)}^2, \end{aligned}$$

where $\ell := \min\{k, r-1\}$ and the last inequality follows from the boundedness of E . The bound for $j_h(\cdot, \cdot)$ follows in a completely similar fashion. \square

Theorem 8.3.13. *Let $(\mathbf{u}, p) \in \mathbf{H}^t(\Omega) \times H^r(\Omega)$, $t \geq 1$, $r \geq 1$, be the solution of problem (8.1). Then, the finite element solution $(\mathbf{u}_h, p_h) \in V_h \times Q_h$ of (8.4) satisfies*

$$\|\mathbf{u} - \mathbf{u}_h\|_{L^2(\Omega)} + \left(\sum_{K \in \mathcal{T}_h} \|\nabla(p - p_h)\|_{L^2(K \cap \Omega)}^2 \right)^{\frac{1}{2}} \leq Ch^s \left(\|\mathbf{u}\|_{H^t(\Omega)} + \|p\|_{H^r(\Omega)} \right),$$

where $s := \min\{t-1, r-1, k\}$.

Proof. Firstly, we observe that

$$\begin{aligned} \|\mathbf{u} - \mathbf{u}_h\|_{L^2(\Omega)} + \left(\sum_{K \in \mathcal{T}_h} \|\nabla(p - p_h)\|_{L^2(K \cap \Omega)}^2 \right)^{\frac{1}{2}} &\leq \|\mathbf{E}(\mathbf{u}) - \mathbf{u}_h\|_{0,h,\Omega_\mathcal{T}} + \|E(p) - p_h\|_{1,h,\Omega_\mathcal{T}} \\ &\leq \sqrt{d} \|\mathbf{E}(\mathbf{u}) - \mathbf{u}_h, E(p) - p_h\|, \end{aligned}$$

it suffices to bound $\|\mathbf{E}(\mathbf{u}) - \mathbf{u}_h, E(p) - p_h\|$. Let us proceed by triangular inequality:

$$\|\mathbf{E}(\mathbf{u}) - \mathbf{u}_h, E(p) - p_h\| \leq \underbrace{\|\mathbf{E}(\mathbf{u}) - r_h(\mathbf{u}), E(p) - \Pi_h(p)\|}_I + \underbrace{\|r_h(\mathbf{u}) - \mathbf{u}_h, \Pi_h(p) - p_h\|}_{II}. \quad (8.18)$$

Theorem 8.3.11 implies, for $s = \min\{t-1, r-1, k\}$,

$$I \leq Ch^s \left(\|\mathbf{u}\|_{H^t(\Omega)} + \|p\|_{H^r(\Omega)} \right). \quad (8.19)$$

By Theorem 8.3.10, for $(\mathbf{u}_h - r_h(\mathbf{u}), p_h - \Pi_h(p))$ there exists $(\mathbf{v}_h, q_h) \in V_h \times Q_h$ such that

$$II = \|\mathbf{u}_h - r_h(\mathbf{u}), p_h - \Pi_h(p)\| \lesssim \frac{\mathcal{A}_h((\mathbf{u}_h - r_h(\mathbf{u}), p_h - \Pi_h(p)); (\mathbf{v}_h, q_h))}{\|(\mathbf{v}_h, q_h)\|}. \quad (8.20)$$

From Propositions 8.3.2, 8.3.7, and the definition of $\|\cdot\|$, it holds

$$\begin{aligned} \mathcal{A}_h((\mathbf{u}_h - r_h(\mathbf{u}), p_h - \Pi_h(p)); (\mathbf{v}_h, q_h)) &= \mathcal{A}_h((\mathbf{u}_h - \mathbf{u}, p_h - p); (\mathbf{v}_h, q_h)) \\ &+ \mathcal{A}_h((\mathbf{u} - r_h(\mathbf{u}), p - \Pi_h(p)); (\mathbf{v}_h, q_h)) = -\mathbf{j}_h(\mathbf{u}, \mathbf{v}_h) + j_h(p, q_h) + a_h(\mathbf{u} - r_h(\mathbf{u}), \mathbf{v}_h) \\ &+ b_1(\mathbf{v}_h, p - \Pi_h(p)) + b_1(\mathbf{u} - r_h(\mathbf{u}), q_h) + \mathbf{j}_h(\mathbf{u} - r_h(\mathbf{u}), \mathbf{v}_h) + j_h(p - \Pi_h(p), q_h) \\ &\lesssim |\mathbf{j}_h(r_h(\mathbf{u}), \mathbf{v}_h)| + |j_h(\Pi_h(p), q_h)| + \|(\mathbf{u} - r_h(\mathbf{u}), p - \Pi_h(p))\| \|(\mathbf{v}_h, q_h)\|. \end{aligned} \quad (8.21)$$

Lemmas 8.3.4, 8.3.12 entail, for $s := \min\{t - 1, r - 1, k\}$,

$$\begin{aligned} |\mathbf{j}_h(r_h(\mathbf{u}), \mathbf{v}_h)| + |j_h(\Pi_h(p), q_h)| &\leq \mathbf{j}_h(r_h(\mathbf{u}), r_h(\mathbf{u}))^{\frac{1}{2}} \mathbf{j}_h(\mathbf{v}_h, \mathbf{v}_h)^{\frac{1}{2}} + j_h(\Pi_h(p), \Pi_h(p))^{\frac{1}{2}} j_h(q_h, q_h)^{\frac{1}{2}} \\ &\lesssim h^s \|\mathbf{u}\|_{H^t(\Omega)} \|\mathbf{v}_h\|_{0,h,\Omega_T} + h^s \|p\|_{H^r(\Omega)} \|q_h\|_{1,h,\Omega_T} \\ &\lesssim h^s \left(\|\mathbf{u}\|_{H^t(\Omega)} + \|p\|_{H^r(\Omega)} \right) \|(\mathbf{v}_h, q_h)\|, \end{aligned} \quad (8.22)$$

where $s := \min\{t - 1, r - 1, k\}$. By plugging (8.22) back into (8.21) and using Theorem 8.3.11, we obtain

$$\mathcal{A}_h((\mathbf{u}_h - r_h(\mathbf{u}), p_h - \Pi_h(p)); (\mathbf{v}_h, q_h)) \lesssim h^s \left(\|\mathbf{u}\|_{H^t(\Omega)} + \|p\|_{H^r(\Omega)} \right) \|(\mathbf{v}_h, q_h)\|. \quad (8.23)$$

We combine (8.18), (8.19), (8.20) and (8.23), getting

$$\|(\mathbf{E}(\mathbf{u}) - \mathbf{u}_h, E(p) - p_h)\| \lesssim h^s \left(\|\mathbf{u}\|_{H^t(\Omega)} + \|p\|_{H^r(\Omega)} \right),$$

where $s := \min\{t - 1, r - 1, k\}$. \square

Remark 8.3.14. The convergence rates given by Theorem 8.3.11 are optimal for the chosen discrete norms. On the other hand, the scaling of the energy norm $\|\cdot\|_{0,h,\Omega_T}$ does not allow us to obtain optimal convergence rates for the velocities with respect to the L^2 -norm by simply applying Theorem 8.3.11. This is due to the term $h^{-1} \int_{\Gamma_N} (\mathbf{u}_h \cdot \mathbf{n})(\mathbf{v}_h \cdot \mathbf{n})$: the natural weight, mimicking the $H^{-\frac{1}{2}}$ -scalar product, would be h instead of h^{-1} . However, as already discussed in Chapter 7 such weight does not lead to an optimally converging scheme.

8.4 The condition number

Following [54] and [96], we want to show that the Euclidean condition number of the matrix arising from the discretization (8.5) is uniformly bounded by Ch^{-2} , where $C > 0$ is independent of how the underlying mesh cuts the boundary. Let us observe that the usual scaling of the condition number for a finite element discretization of the Darcy problem is $\mathcal{O}(h^{-1})$. We pay with a factor h^{-1} because of the choice of the discrete norms.

Denoting $N = \dim V_h \times Q_h$, we can expand an arbitrary element $(\mathbf{v}_h, q_h) \in V_h \times Q_h$ as $(\mathbf{v}_h, q_h) = \sum_{i=1}^N \mathcal{V}_i \varphi_i$, where $(\varphi)_{i=1}^N$ is the finite element basis for the product space $V_h \times Q_h$ and $\mathcal{V} \in \mathbb{R}^N$ is its coordinate vector. The previous expansion of the elements of $V_h \times Q_h$ uniquely defines a canonical isometric isomorphism between $V_h \times Q_h$ and \mathbb{R}^N , namely

$$\mathcal{C} : V_h \times Q_h \rightarrow \mathbb{R}^N, \quad (\mathbf{v}_h, q_h) \mapsto \mathcal{V}.$$

Here, \mathbb{R}^N is equipped with the standard Euclidean scalar product, denoted as $(\cdot, \cdot)_{\ell^2}$, and the induced norm $|\cdot|_{\ell^2}$. Given $M \in \mathbb{R}^{N \times N}$, we denote as $\|M\|_2$ the matrix norm of M induced by $|\cdot|_{\ell^2}$. Let $A \in \mathbb{R}^{N \times N}$ denote the matrix associated to the discrete formulation (8.5), namely

$$(A\mathcal{V}, \mathcal{W})_{\ell^2} = \mathcal{A}_h((\mathbf{v}_h, q_h); (\mathbf{w}_h, m_h)), \quad \forall \mathcal{V}, \mathcal{W} \in \mathbb{R}^N,$$

where $\mathcal{V} = \mathcal{C}(\mathbf{v}_h, q_h)$, $\mathcal{W} = \mathcal{C}(\mathbf{w}_h, m_h)$ and $(\mathbf{v}_h, q_h), (\mathbf{w}_h, m_h) \in V_h \times Q_h$.

Remark 8.4.1. In the pure essential case $\Gamma = \Gamma_N$ the solution to (8.5) for the pressure is determined up to a constant, hence A is singular and $\ker A = \text{span}\{\mathcal{C}(\mathbf{0}, 1)\}$. We shall consider, instead of A , its bijective restriction $A|_{\widehat{\mathbb{R}}^N} : \widehat{\mathbb{R}}^N \rightarrow \widetilde{\mathbb{R}}^N$, where $\widehat{\mathbb{R}}^N := \mathbb{R}^N / \ker A$ and $\widetilde{\mathbb{R}}^N := \text{Im}(A)$.

As already said, the goal is to analyze the Euclidean condition number $\kappa_2(A) := \|A\|_2 \|A^{-1}\|_2$. From [112], we know that the main ingredients for the conditioning analysis are the following:

1. the stability of the discrete formulation with respect to a given norm $\|\cdot\|_a$;
2. the ℓ^2 -stability of the basis with respect to a given norm $\|\cdot\|_b$;
3. the equivalence between the norms $\|\cdot\|_a$ and $\|\cdot\|_b$.

In the subsequent exposition, the product norm (8.6) plays the role of $\|\cdot\|_b$, while $\|\cdot\|_{L^2(\Omega_T)}$, defined as $\|(\mathbf{v}_h, q_h)\|_{L^2(\Omega_T)}^2 := \|\mathbf{v}_h\|_{L^2(\Omega_T)}^2 + \|q_h\|_{L^2(\Omega_T)}^2$, corresponds to $\|\cdot\|_a$.

Lemma 8.4.2. *There exist $C_1, C_2 > 0$ such that, for every $(\mathbf{v}_h, q_h) \in V_h \times Q_h$,*

$$C_1 h^{\frac{d}{2}} |\mathcal{V}|_{\ell^2} \leq \|(\mathbf{v}_h, q_h)\|_{L^2(\Omega_T)} \leq C_2 h^{\frac{d}{2}} |\mathcal{V}|_{\ell^2},$$

where $\mathcal{V} = \mathcal{C}(\mathbf{v}_h, q_h)$.

Proof. The result holds because the background mesh is shape-regular and quasi-uniform. We refer the interested reader to Lemma A.1 in [55]. \square

Lemma 8.4.3. *There exist $C_1, C_2 > 0$ such that, for every $(\mathbf{v}_h, q_h) \in V_h \times Q_h$,*

$$C_1 \|(\mathbf{v}_h, q_h)\|_{L^2(\Omega_T)} \leq \|(\mathbf{v}_h, q_h)\| \leq C_2 h^{-1} \|(\mathbf{v}_h, q_h)\|_{L^2(\Omega_T)}.$$

Proof. The first bound follows because of a Poincaré-Friedrichs inequality for piecewise H^1 -functions (Section 10.6 of [25] and [52]). For the second inequality it is sufficient to apply standard inverse estimates for boundary-fitted finite elements. \square

Theorem 8.4.4. *There exists $C > 0$ such that*

$$\kappa_2(A) \leq Ch^{-2}.$$

Proof. Let us start by bounding $\|A\|_{\ell^2}$. Given $(\mathbf{v}_h, q_h), (\mathbf{w}_h, m_h) \in V_h \times Q_h$ such that $\mathcal{C}(\mathbf{v}_h, q_h) = \mathcal{V}$, $\mathcal{C}(\mathbf{w}_h, m_h) = \mathcal{W}$, we have

$$\begin{aligned} (A\mathcal{V}, \mathcal{W})_{\ell^2} &= \mathcal{A}_h((\mathbf{v}_h, q_h); (\mathbf{w}_h, m_h)) \lesssim \|(\mathbf{v}_h, q_h)\| \|(\mathbf{w}_h, m_h)\| \\ &\lesssim h^{-2} \|(\mathbf{v}_h, q_h)\|_{L^2(\Omega_T)} \|(\mathbf{w}_h, m_h)\|_{L^2(\Omega_T)} \lesssim h^{d-2} |\mathcal{V}|_{\ell^2} |\mathcal{W}|_{\ell^2}. \end{aligned}$$

In the previous inequalities we used, respectively, the continuity of $\mathcal{A}_h(\cdot; \cdot)$, Lemma 8.4.3 and Lemma 8.4.2. Hence, $\|A\|_2 \lesssim h^{d-2}$. We need to bound $\|A^{-1}\|_2$. Since (the restriction of) A^{-1} is invertible, we can write

$$\|A^{-1}\|_2 = \sup_{\mathcal{V} \in \widehat{\mathbb{R}}^N \setminus \{0\}} \frac{|A^{-1}\mathcal{V}|_{\ell^2}}{|\mathcal{V}|_{\ell^2}} = \sup_{\substack{A\mathcal{V} \in \widetilde{\mathbb{R}}^N \\ \mathcal{V} \in \widehat{\mathbb{R}}^N \setminus \{0\}}} \frac{|\mathcal{V}|}{|A\mathcal{V}|} = \sup_{\substack{A\mathcal{V} \in \widetilde{\mathbb{R}}^N \\ \mathcal{V} \in \widehat{\mathbb{R}}^N \setminus \{0\}}} \sup_{\mathcal{W} \in \widetilde{\mathbb{R}}^N \setminus \{0\}} \frac{|\mathcal{V}|_{\ell^2} |\mathcal{W}|_{\ell^2}}{(A\mathcal{V}, \mathcal{W})_{\ell^2}}. \quad (8.24)$$

From Theorem 8.3.10, we know that, for every $\mathcal{V} \in \widehat{\mathbb{R}}^N \setminus \{\mathbf{0}\}$, there exists \mathcal{W} such that

$$\begin{aligned} (A\mathcal{V}, \mathcal{W})_{\ell^2} &= \mathcal{A}_h((\mathbf{v}_h, q_h); (\mathbf{w}_h, q_h)) \gtrsim |||(\mathbf{v}_h, q_h)||| |||(\mathbf{w}_h, m_h)||| \gtrsim |||(\mathbf{v}_h, q_h)|||_{L^2(\Omega_T)} |||(\mathbf{w}_h, m_h)|||_{L^2(\Omega_T)} \\ &\gtrsim h^d |\mathcal{V}|_{\ell^2} |\mathcal{W}|_{\ell^2}, \end{aligned} \quad (8.25)$$

where in the last two inequalities we used, respectively, Lemma 8.4.3 and Lemma 8.4.2. By combining (8.24) and (8.25) we get $\|A^{-1}\|_2 \lesssim h^{-d}$. Hence, we are done. \square

8.5 The pure natural case

The goal of this section is to sketch the main steps required to analyze formulation (8.4) in the pure natural case. If $\Gamma = \Gamma_D$, then we consider the following Raviart-Thomas finite element discretization of problem (8.1).

Find $(\mathbf{u}_h, p_h) \in V_h \times Q_h$ such that

$$\begin{aligned} \int_{\Omega} \mathbf{u}_h \cdot \mathbf{v}_h + b_0(\mathbf{v}_h, p_h) &= \int_{\Omega} \mathbf{f} \cdot \mathbf{v}_h + \int_{\Gamma} p_D \mathbf{v}_h \cdot \mathbf{n}, \quad \forall \mathbf{v}_h \in V_h, \\ b_0(\mathbf{u}_h, q_h) &= \int_{\Omega} g q_h, \quad \forall q_h \in Q_h. \end{aligned} \quad (8.26)$$

It is natural to equip the discrete spaces V_h and Q_h with $\|\cdot\|_{H(\text{div}; \Omega)}$ and $\|\cdot\|_{L^2(\Omega)}$, respectively. It is readily seen that formulation (8.26) satisfies the standard stability estimates for saddle point problems (see the hypotheses of Theorem 5.2.5 of [22]). Hence *a priori* error estimates can be obtained by standard techniques (again, we refer the reader to Section 5.2 of [22]). This time, the convergence rates are optimal because of the choice of the norms. However, the conditioning of the arising linear system will still strongly depend on the way the boundary cuts the mesh. As for the general case with mixed boundary conditions, we propose to cure this issue with a ghost penalty-based stabilization.

$$\begin{aligned} \tilde{j}_h(\mathbf{w}_h, \mathbf{v}_h) &:= \sum_{f \in \mathcal{F}_h^\Gamma} \sum_{j=0}^k h^{2j+1} \int_f [\partial_n^j \mathbf{w}_h] [\partial_n^j \mathbf{v}_h], \quad \mathbf{w}_h, \mathbf{v}_h \in V_h, \\ \tilde{j}_h(m_h, q_h) &:= \sum_{f \in \mathcal{F}_h^\Gamma} \sum_{j=0}^k h^{2j+1} \int_f [\partial_n^j m_h] [\partial_n^j q_h], \quad m_h, q_h \in Q_h. \end{aligned}$$

Let us observe that the ghost penalty operators scale differently than in (8.3) because of the different choices of the norms to the mixed case. The stabilized formulation reads as follows.

Find $(\mathbf{u}_h, p_h) \in V_h \times Q_h$ such that

$$\begin{aligned} \int_{\Omega} \mathbf{u}_h \cdot \mathbf{v}_h + \tilde{j}_h(\mathbf{u}_h, \mathbf{v}_h) + b_0(\mathbf{v}_h, p_h) &= \int_{\Omega} \mathbf{f} \cdot \mathbf{v}_h + \int_{\Gamma} p_D \mathbf{v}_h \cdot \mathbf{n}, \quad \forall \mathbf{v}_h \in V_h, \\ b_0(\mathbf{u}_h, q_h) + \tilde{j}_h(p_h, q_h) &= \int_{\Omega} g q_h, \quad \forall q_h \in Q_h, \end{aligned} \quad (8.27)$$

By mimicking the same lines of Section 8.4, it is possible to show that the condition number of (8.27) goes as $\mathcal{O}(h^{-1})$.

8.6 Numerical examples

In the following, we use the ghost penalty projection-based operators $\mathbf{s}_h(\cdot, \cdot)$ and $s_h(\cdot, \cdot)$ defined in Remark 8.3.1. As already observed, this choice is convenient from the implementation point of view since it spares us to calculate the jumps of possibly high-order normal derivatives through the facets in the vicinity of the cut boundary. We limit the scope of our numerical investigations to the case of Cartesian quadrilateral meshes in 2D. To integrate in the cut elements, we employ the strategy depicted in [4]: the cut elements are reparametrized using polynomials with the same approximation order of the Raviart-Thomas space employed for the space discretization.

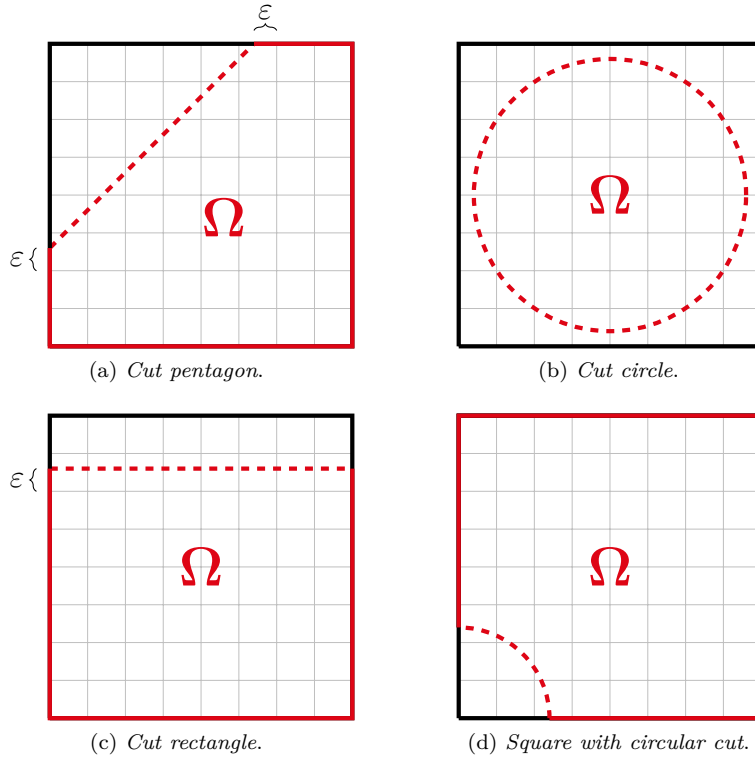


Figure 8.1 – Unfitted domains employed for the numerical experiments.

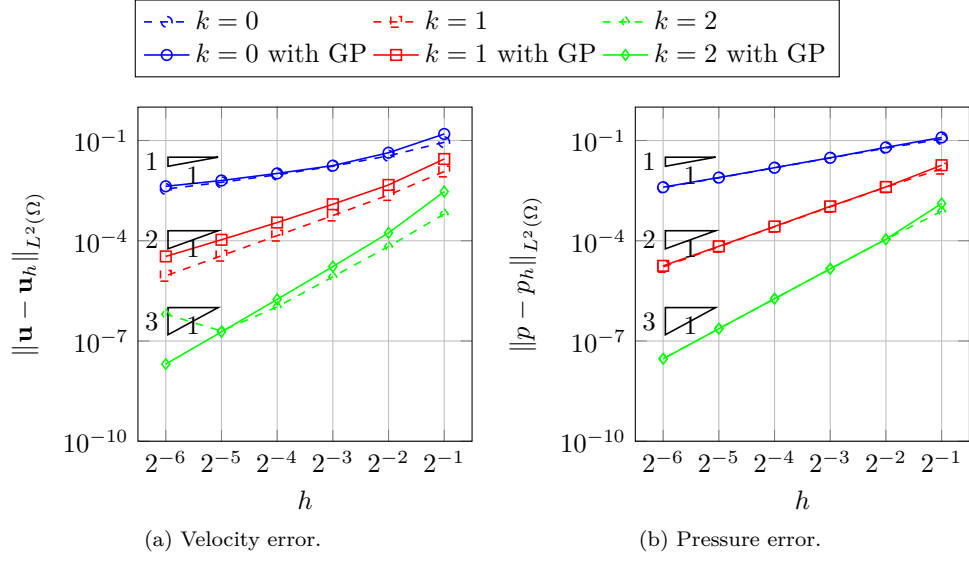
8.6.1 Convergence rates

Cut pentagon

Let $\Omega_0 = (0, 1)^2$, Ω_1 be the triangle with vertices $(0, 0.25 + \varepsilon) - (0, 1) - (0.75 - \varepsilon, 1)$ and $\Omega = \Omega_0 \setminus \overline{\Omega}_1$, with $\varepsilon = 10^{-9}$, see Figure 8.1(a). The reference solutions are

$$\mathbf{u}_{ex} = \begin{pmatrix} y \sin(x) \cos(y) \\ -x \sin(y) \cos(x) \end{pmatrix}, \quad p_{ex} = x^3 y.$$

Essential boundary conditions are imposed on the whole boundary, weakly just on the sides that do not fit the underlying mesh. We compute the approximation errors of the velocity and pressure fields for different degrees $k \in \{0, 1, 2\}$, see Figure 8.2. We have optimal convergence, despite the sub-optimal result of Theorem 8.3.13.

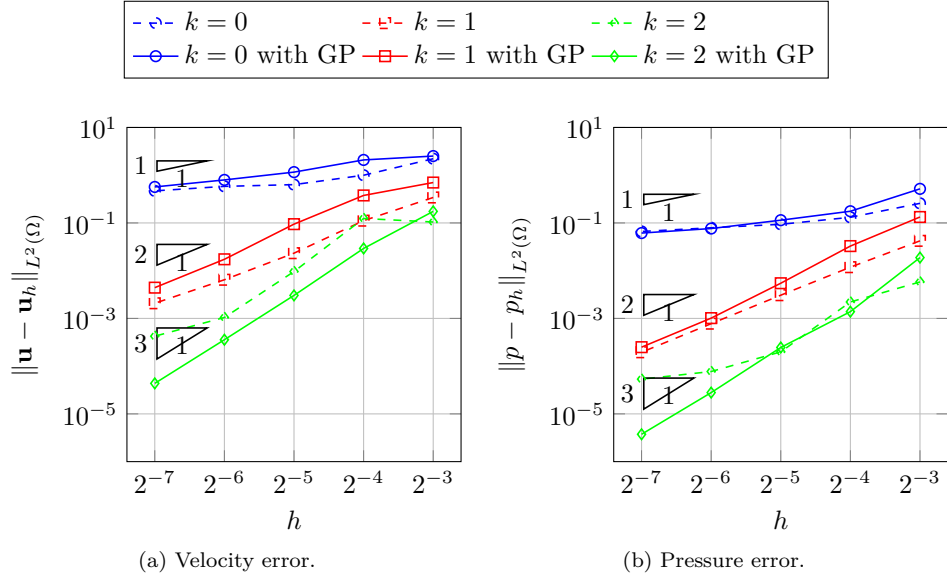
Figure 8.2 – Convergence rates of the errors in the *cut pentagon*.

Cut circle

Let us consider $\Omega = B_r(x_0)$, with $x_0 = (0.5, 0.5)$ and $r = 0.45$, see Figure 8.1(b). The manufactured solution for the pressure is

$$p_{ex} = \sin(2\pi x) \cos(2\pi y),$$

and the velocity field is computed from Darcy's law (8.1) when \mathbf{f} is taken to be zero. We weakly prescribe essential boundary conditions on the whole boundary, which does not fit the underlying mesh. The L^2 -errors for the velocity and pressure fields are plotted in Figure 8.3. We can see optimal orders of convergence and better accuracy in the stabilized case for $k = 2$.

Figure 8.3 – Convergence rates of the errors in the *cut circle*.

8.6.2 Condition number

Cut rectangle

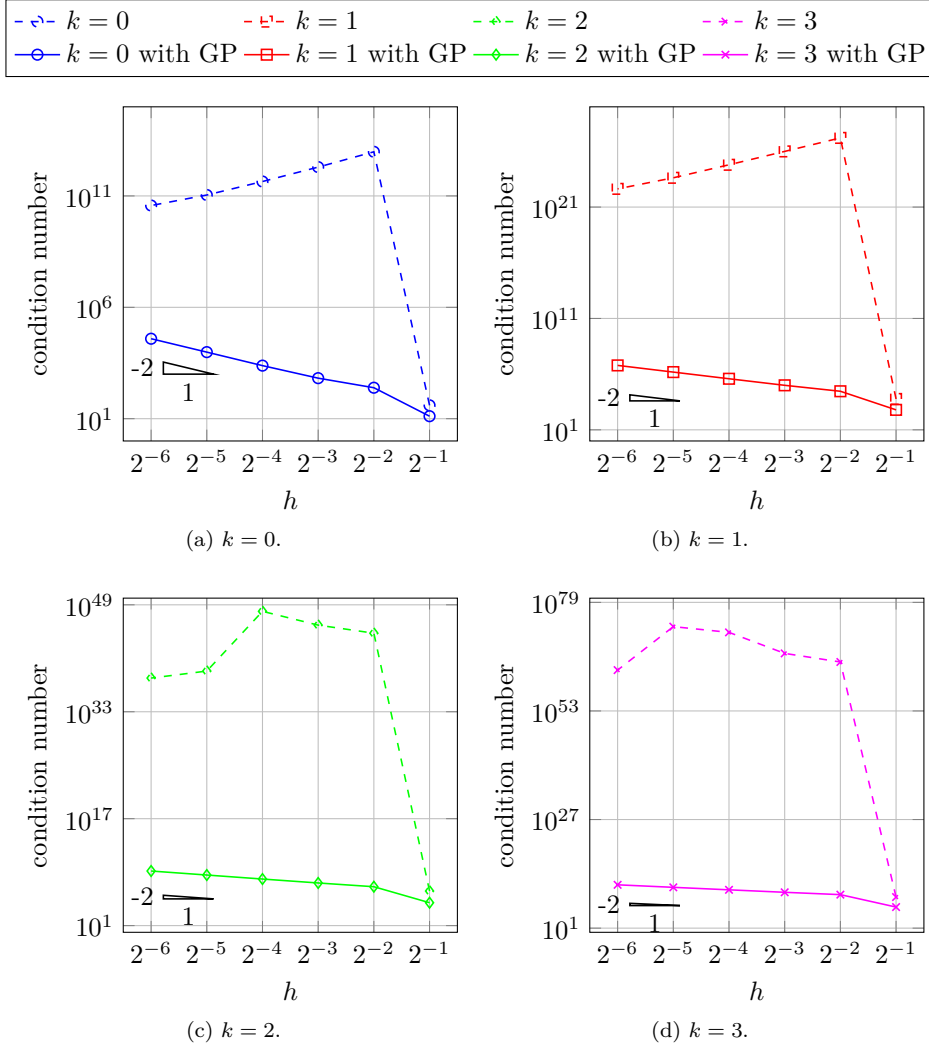
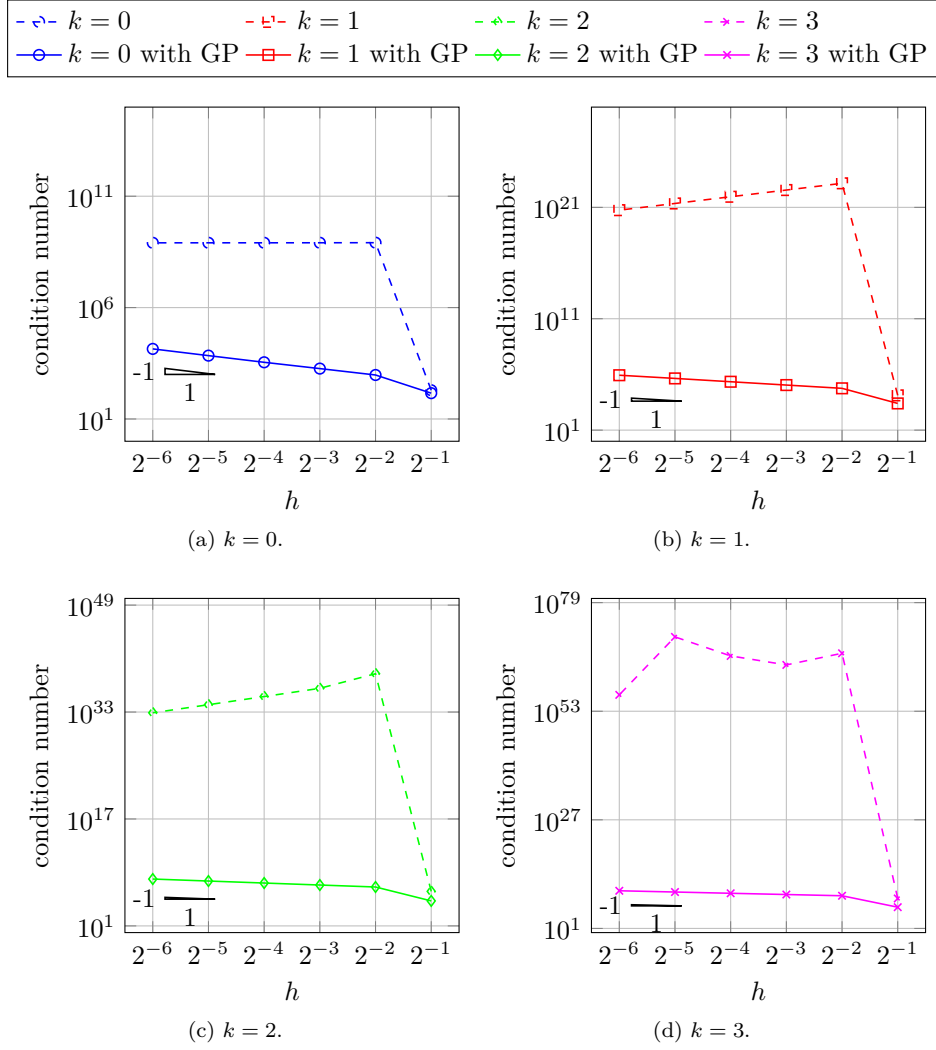


Figure 8.4 – Condition number for the *cut rectangle* with essential boundary conditions.

Let us consider as physical domain the *cut rectangle* $\Omega = (0, 1) \times (0, 0.75 + \varepsilon)$ where $\varepsilon = 10^{-7}$, see Figure 8.1c. We impose essential boundary conditions weakly on the whole boundary. In Figure 8.4 we compare the conditioning of the stabilized and non-stabilized formulations. Similarly, in Figure 8.5 we compare the conditioning of the stabilized and non-stabilized formulations when natural boundary conditions are imposed. The results are in agreement with the theory developed in Sections 8.4, 8.5. In particular, we observe that without stabilization, the condition number is negatively affected by the presence of cut elements and seems to grow without control, while in the stabilized case, the expected scaling of the conditioning is restored: $\mathcal{O}(h^{-2})$ for the essential case and $\mathcal{O}(h^{-1})$ for the pure natural case.

Figure 8.5 – Condition number for the *cut rectangle* with natural boundary conditions.

8.6.3 On mass conservation

Mass conservation is an important feature for finite element discretizations of incompressible flows, whose violation is not tolerable in many applications [81]. As observed in Remark 8.2.1, the Raviart-Thomas finite element satisfies $\operatorname{div} V_h = Q_h$ in the unfitted configuration as well. The formulation (8.4) as it stands is bound to fail to satisfy the incompressibility constraint in a weak sense, which is why, to exploit this property when the right-hand side g vanishes, we consider the following non-symmetric variant of formulation (8.4).

Find $(\mathbf{u}_h, p_h) \in V_h \times Q_h$ such that

$$\begin{aligned}
 a_h(\mathbf{u}_h, \mathbf{v}_h) + b_1(\mathbf{v}_h, p_h) + \mathbf{j}_h(\mathbf{u}_h, \mathbf{v}_h) &= \int_{\Omega} \mathbf{f} \cdot \mathbf{v}_h + \int_{\Gamma_D} p_D \mathbf{v}_h \cdot \mathbf{n} + h^{-1} \int_{\Gamma_N} u_N \mathbf{v}_h \cdot \mathbf{n}, \quad \forall \mathbf{v}_h \in V_h, \\
 b_0(\mathbf{u}_h, q_h) + \mathbf{j}_h(p_h, q_h) &= 0, \quad \forall q_h \in Q_h,
 \end{aligned}
 \tag{8.28}$$

where

$$b_0(\mathbf{w}_h, q_h) := \int_{\Omega} q_h \operatorname{div} \mathbf{w}_h, \quad \mathbf{w}_h \in V_h, q_h \in Q_h.$$

Let us test formulation (8.28) in the stabilized and non-stabilized cases. We take as reference solutions

$$\mathbf{u}_{ex} = \begin{pmatrix} \cos(x) \sinh(y) \\ \sin(x) \cosh(y) \end{pmatrix}, \quad p_{ex} = -\sin(x) \sinh(y) - (\cos(1) - 1)(\cosh(1) - 1).$$

Note that $\operatorname{div} \mathbf{u}_{ex} = 0$. We impose natural boundary conditions on $\{(x, y) : x = 2, 0 \leq y \leq 2\}$ and on $\{(x, y) : 0 \leq x \leq 2, y = 2\}$, and weak essential boundary conditions on the rest of the boundary. The computed divergence of the discrete solution for the velocity is shown in Figure 8.6 for $k = 1$ and $h = 2^{-4}$. We observe that the ghost penalty stabilization pollutes the divergence of the velocity, hence also the non-symmetric formulation (8.28) fails to the mass conservation at the discrete level.

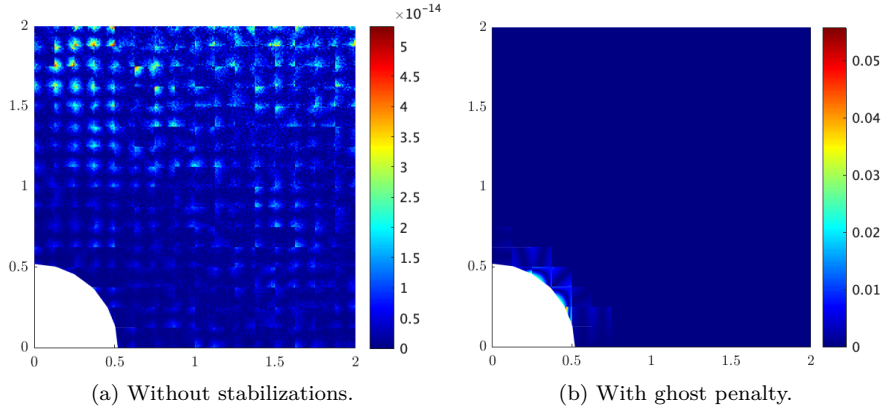


Figure 8.6 – $|\operatorname{div} \mathbf{u}_h|$ in the square with circular cut obtained with (8.28).

Summary of Part II

In the second part of the dissertation, we considered the Raviart-Thomas finite element discretization of the Darcy problem. We proposed and analyzed a Nitsche and a penalty method for the weak imposition of the essential boundary conditions in the boundary fitted case. We provided a theoretical framework for the numerical analysis of the two schemes and delivered optimal *a priori* error estimates for the L^2 -error of the velocity. From our analysis, the Nitsche method must be preferred to the penalty method. Indeed, the latter relies on a mesh-dependent parameter growing at a much higher rate compared to the other terms in the stiffness matrix. This leads to the rapid deterioration of the conditioning of the final linear system.

We moved to the much more complicated situation of a mesh unfitted with the domain. To perform integration in the cut elements, we relied on the same polynomial reparametrization discussed in the first part of the thesis. The Nitsche method previously introduced cannot be directly used as it is, since it is severely ill-posed. The presence of cut elements destroys the conditioning of the linear system, and the stability estimates shown in the boundary-fitted case cannot be retrieved. Indeed, the main techniques previously used for the theoretical proofs break down. We showed that by adding some weakly consistent ghost penalty operators acting separately on the velocity and the pressure in the spirit of [35] we restore the expected behavior of the condition number and prove *a priori* convergence estimates.

However, the content of Chapter 8 should be considered a preliminary step towards the design of a satisfactory method in the unfitted case. The current analysis did not recover the optimal convergence of the velocity in the L^2 -norm, even though numerical experiments show that it should hold. The major limitation remains that our stabilization procedure pollutes the divergence of the discrete velocity and does not allow for a conservative numerical scheme at the discrete level. A natural direction of research will be to try to overcome these drawbacks.

A Appendix

A.1 Useful inequalities

In this section, we collect some technical results repeatedly employed in different chapters of this thesis. We rely on the notation introduced in Section 2.1.1. The constants that will appear in the inequalities below, unless otherwise specified, are intended to be robust with respect to the mesh size and mutual position between trimming curve and active physical Bézier mesh.

Lemma A.1.1. *There exists $C > 0$ such that, for every $K \in \mathcal{G}_h$, it holds $|\Gamma_K| \leq Ch_K^{d-1}$.*

Proof. The result holds since Γ is assumed to be Lipschitz-regular, hence not too oscillating. See [62]. \square

Lemma A.1.2. *There exists $C > 0$, depending on Γ , such that, for every $K \in \mathcal{G}_h$,*

$$\|v\|_{L^2(\Gamma_K)}^2 \leq C \|v\|_{L^2(K)} \|v\|_{H^1(K)}, \quad \forall v \in H^1(K).$$

Proof. See, for instance, Lemma 3 in [69], Lemma 3 in [70], or Lemma 4.1 of [116]. \square

Corollary A.1.3. *There exists $C > 0$, depending on Γ , such that, for every $K \in \mathcal{G}_h$,*

$$\left\| \frac{\partial v}{\partial n} \right\|_{L^2(\Gamma_K)}^2 \leq C \|\nabla v\|_{L^2(K)} \|\nabla v\|_{H^1(K)}, \quad \forall v \in H^2(K).$$

Proof. It immediately follows from Lemma A.1.2. \square

Lemma A.1.4. *Let $Q, Q' \in \widehat{\mathcal{M}}_h$ be neighbor elements in the sense of Definition 2.3.1. There exists $C > 0$ such that*

$$\|\varphi\|_{L^\infty(Q)} \leq C \|\varphi\|_{L^\infty(Q')}, \quad \forall \varphi \in \mathbb{Q}_p(\mathbb{R}^d),$$

where C depends on p , on the shape regularity of the mesh, and on the distance between Q and Q' .

Proof. Let $N := (p+1)^d = \dim \mathbb{Q}_k(\mathbb{R}^d)$ and define

$$\Psi : \mathbb{R}^N \setminus \{0\} \rightarrow \mathbb{R}, \quad \Psi(\boldsymbol{\eta}) = \frac{\|\varphi\|_{L^\infty(Q)}}{\|\varphi\|_{L^\infty(Q')}} = \frac{\max_{x \in Q} \left| \sum_{i=1}^N \eta_i \mathbf{b}_i(x) \right|}{\max_{x \in Q'} \left| \sum_{i=1}^N \eta_i \mathbf{b}_i(x) \right|},$$

Appendix A. Appendix

where $\boldsymbol{\eta} = (\eta)_{i=1}^N$ are the coordinates of φ with respect to the Bernstein basis $(\mathbf{b}_i)_{i=1}^N$. Note that Ψ is continuous and homogeneous of degree 0, i.e., $\Psi(t\boldsymbol{\eta}) = \Psi(\boldsymbol{\eta})$, $\forall t > 0$. In particular, by homogeneity

$$\Psi(\boldsymbol{\eta}) = \psi\left(|\boldsymbol{\eta}|_{\mathbb{R}^N} \frac{\boldsymbol{\eta}}{|\boldsymbol{\eta}|_{\mathbb{R}^N}}\right) = \Psi\left(\frac{\boldsymbol{\eta}}{|\boldsymbol{\eta}|_{\mathbb{R}^N}}\right),$$

that is Ψ is determined by its values on the unit sphere $S = \{\boldsymbol{\eta} \in \mathbb{R}^N : |\boldsymbol{\eta}|_{\mathbb{R}^N} = 1\}$, which is compact. By Weierstrass theorem Ψ attains its maximum on S , i.e., there exists $C > 0$ such that $|\Psi(\boldsymbol{\eta})| \leq C$. Note that C depends on the dimension N (i.e., on the degree p), on the shape regularity of the mesh and on the distance between Q and Q' (we are evaluating the same basis functions $(\mathbf{b}_i)_{i=1}^N$ at points which are far from each other). \square

The next result says that the L^2 -norm on the cut portion of an element Q controls the L^∞ -norm (and hence any other) on the whole element with an equivalence constant depending on the relative measure of the cut portion.

Lemma A.1.5. *Let $\theta \in (0, 1]$. There exists $C > 0$ such that, for every $Q \in \widehat{\mathcal{M}}_h$ and every $S \subset Q$ measurable such that $|S| \geq \theta |Q|$, we have*

$$\|\varphi\|_{L^\infty(Q)} \leq Ch^{-\frac{d}{2}} \|\varphi\|_{L^2(S)}, \quad \forall \varphi \in \mathbb{Q}_p(\mathbb{R}^d),$$

where C depends only on θ , p , and the mesh regularity.

Proof. See Proposition 1 in [62]. \square

Let us recall a more standard inverse inequality with an explicit dependence on the polynomial degree p .

Lemma A.1.6. *There exists $C > 0$, depending on the shape regularity of the mesh, such that, for every $Q \in \widehat{\mathcal{M}}_h$,*

$$\|\varphi\|_{L^\infty(Q)} \leq Cp^d h_Q^{-\frac{d}{2}} \|\varphi\|_{L^2(Q)}, \quad \forall \varphi \in \mathbb{Q}_p(Q).$$

Proof. Since it is not easy to find a proof of this result in the literature, let us enclose one based on the Legendre polynomials. Let us consider the reference element $\widehat{Q} := (-1, 1)^d$ and $\varphi \in \mathbb{Q}_p(\widehat{Q})$. We can expand $\varphi(x) = \sum_{i_1=0}^p \dots \sum_{i_d=0}^p c_{i_1, \dots, i_d} \widetilde{L}_{i_1}(x_1) \dots \widetilde{L}_{i_d}(x_d)$, where

$$\widetilde{L}_k(t) := \left(\frac{2k+1}{2}\right)^{\frac{1}{2}} L_k(t), \quad t \in [-1, 1],$$

and $(L_k)_{k=0}^p$ are the univariate Legendre polynomials (see [122]). Let us recall that

$$\int_{-1}^1 L_i(t) L_j(t) dt = \frac{2}{2i+1} \delta_{ij}, \quad \|L_i\|_{L^2(-1,1)} = \left(\frac{2}{2i+1}\right)^{\frac{1}{2}}, \quad \|L_i\|_{L^\infty(-1,1)} = 1,$$

so that

$$\|\widetilde{L}_i\|_{L^2(-1,1)} = 1, \quad \|\varphi\|_{L^2(\widehat{Q})}^2 = \sum_{i_1=0}^p \dots \sum_{i_d=0}^p |c_{i_1, \dots, i_d}|^2, \quad \|\widetilde{L}_i\|_{L^\infty(-1,1)} = \left(\frac{2i+1}{2}\right)^{\frac{1}{2}}. \quad (\text{A.1})$$

By the triangle inequality, we have

$$\begin{aligned} \|\varphi\|_{L^\infty(\widehat{K})} &\leq \sum_{i_1=0}^p \cdots \sum_{i_d=0}^p |c_{i_1, \dots, i_d}| \|\tilde{L}_{i_1}\|_{L^\infty(-1,1)} \cdots \|\tilde{L}_{i_d}\|_{L^\infty(-1,1)} \\ &\leq \|\tilde{L}_p\|_{L^\infty(-1,1)}^d \sum_{i_1=0}^p \cdots \sum_{i_d=0}^p |c_{i_1, \dots, i_d}|. \end{aligned}$$

Using (A.1) and $\sum_{i=1}^d |x_i| \leq d^{\frac{1}{2}} \left(\sum_{i=1}^d |x_i|^2 \right)^{\frac{1}{2}}$, we have

$$\begin{aligned} \|\varphi\|_{L^\infty(\widehat{Q})} &\leq \left(\frac{2p+1}{2} \right)^{\frac{d}{2}} (p+1)^{\frac{d}{2}} \left(\sum_{i_1=0}^p \cdots \sum_{i_d=0}^p |c_{i_1, \dots, i_d}|^2 \right)^{\frac{1}{2}} \\ &= \left(\frac{2p+1}{2} \right)^{\frac{d}{2}} (p+1)^{\frac{d}{2}} \|\varphi\|_{L^2(\widehat{Q})}. \end{aligned}$$

For every $Q \in \mathcal{M}_h$, there exists $T_Q : \widehat{Q} \rightarrow Q$ affine bijection such that $Q = T_Q(\widehat{Q})$ and $|\det(DT_Q)| = \frac{|Q|}{|\widehat{Q}|} = \left(\frac{h_Q}{2} \right)^d$. Hence, a simple change of variable leads, for $\varphi \in \mathbb{Q}_p(Q)$ and $\widehat{\varphi} := \varphi \circ T_Q \in \mathbb{Q}_p(\widehat{Q})$,

$$\begin{aligned} \|\varphi\|_{L^\infty(Q)} &= \|\widehat{\varphi}\|_{L^\infty(\widehat{Q})} \leq \left(\frac{2p+1}{2} \right)^{\frac{d}{2}} (p+1)^{\frac{d}{2}} \|\widehat{\varphi}\|_{L^2(\widehat{Q})} \\ &\leq \left(\frac{2p+1}{2} \right)^{\frac{d}{2}} (p+1)^{\frac{d}{2}} \left| \det(DT_Q^{-1}) \right|^{\frac{1}{2}} \|\varphi\|_{L^2(Q)} \\ &= (2p+1)^{\frac{d}{2}} (p+1)^{\frac{d}{2}} h_Q^{-\frac{d}{2}} \|\varphi\|_{L^2(Q)}. \end{aligned}$$

□

For the next two results, let us define, for every $x \in \Omega$, $d(x) := \text{dist}(x, \Gamma) = \inf_{y \in \Gamma} |x - y|$.

Lemma A.1.7 (Hardy's inequality). *There exists $C > 0$ such that*

$$\left\| \frac{u}{d} \right\|_{L^2(\Omega)} \leq C \|\nabla u\|_{L^2(\Omega)}, \quad \forall u \in H_0^1(\Omega). \quad (\text{A.2})$$

Proof. See [27].

□

Lemma A.1.8. *Let $C \geq 1$ and define the boundary strip $S_h := \{x \in \Omega : d(x) \leq Ch\}$. It holds that*

$$\|v\|_{L^2(S_h)} \leq Ch^s \|v\|_{H_i^s(\Omega)}, \quad \forall v \in H_i^s(\Omega),$$

where the interpolation space $H_i^s(\Omega)$ or $(H_0^1(\Omega), L^2(\Omega))_{s,2}$ is isomorphic to $H^s(\Omega)$ for $0 \leq s < \frac{1}{2}$, to $H_{00}^{\frac{1}{2}}(\Omega)$ for $s = \frac{1}{2}$, and to $H_0^s(\Omega)$ for $\frac{1}{2} < s \leq 1$ (see [130]).

Proof. We prove the following (like in [89]):

$$\|v\|_{L^2(S_h)} \leq Ch \|\nabla v\|_{L^2(\Omega)}, \quad \forall v \in H_0^1(\Omega). \quad (\text{A.3})$$

Appendix A. Appendix

Recall that, for $x \in S_h$, it holds $1 \leq \frac{Ch^2}{|d(x)|^2}$, so that, by Lemma A.1.7,

$$\int_{S_h} |v|^2 \leq Ch^2 \int_{S_h} \frac{|v|^2}{|d|^2} \leq Ch^2 \int_{\Omega} \frac{|v|^2}{|d|^2} \leq Ch^2 \int_{\Omega} |\nabla v|^2.$$

On the other hand, it is clear that

$$\|v\|_{L^2(S_h)} \leq \|v\|_{L^2(\Omega)}, \quad \forall v \in L^2(\Omega). \quad (\text{A.4})$$

It suffices to interpolate the estimates (A.3) and (A.4), getting

$$\|v\|_{L^2(\Omega \setminus \bar{\Omega}_1)} \leq Ch^s \|v\|_{H_i^s(\Omega)}, \quad \forall v \in H_i^s(\Omega).$$

□

A.2 Technical proofs

Proof of Theorem 5.2.17. In order to prove (5.14), let us show that there exist $c_1, c_2 > 0$ such that, for every $(\mathbf{v}_h, q_h, \boldsymbol{\mu}_h) \in V_h \times \bar{Q}_h \times \Lambda_h$, there exists $(\mathbf{w}_h, r_h, \boldsymbol{\eta}_h) \in V_h \times \bar{Q}_h \times \Lambda_h$ such that $\bar{\mathcal{A}}_h((\mathbf{w}_h, r_h, \boldsymbol{\eta}_h); (\mathbf{v}_h, q_h, \boldsymbol{\mu}_h)) \geq c_1 \|(\mathbf{v}_h, q_h, \boldsymbol{\mu}_h)\|^2$ and $\|(\mathbf{w}_h, r_h, \boldsymbol{\eta}_h)\| \leq c_2 \|(\mathbf{v}_h, q_h, \boldsymbol{\mu}_h)\|$. Let us take $(\mathbf{v}_h, q_h, \boldsymbol{\mu}_h) \in V_h \times \bar{Q}_h \times \Lambda_h$. It holds

$$\begin{aligned} \bar{\mathcal{A}}_h((\mathbf{v}_h, -q_h, -\boldsymbol{\mu}_h); (\mathbf{v}_h, q_h, \boldsymbol{\mu}_h)) &= \sum_{i=0}^N \|D\mathbf{v}_i\|_{L^2(\Omega_i)}^2 \\ &+ \sum_{i=1}^N \sum_{j=0}^{i-1} \gamma^{-1} \left(\left\| \mathbf{h}^{\frac{1}{2}} \boldsymbol{\mu}_h \right\|_{L^2(\Gamma_{ij})}^2 - 2 \int_{\Gamma_{ij}} \mathbf{h} \boldsymbol{\mu}_h \langle q_h \mathbf{n} \rangle_t - \left\| \mathbf{h}^{\frac{1}{2}} \langle DR_{ij}^v(\mathbf{v}_h) \mathbf{n} \rangle_t \right\|_{L^2(\Gamma_{ij})}^2 + \left\| \mathbf{h}^{\frac{1}{2}} \langle q_h \mathbf{n} \rangle_t \right\|_{L^2(\Gamma_{ij})}^2 \right). \end{aligned}$$

Notice that

$$\gamma^{-1} \left\| \mathbf{h}^{\frac{1}{2}} (-\boldsymbol{\mu}_h + \langle q_h \mathbf{n} \rangle_t) \right\|_{L^2(\Gamma_{ij})}^2 = \gamma^{-1} \left(\left\| \mathbf{h}^{\frac{1}{2}} \boldsymbol{\mu}_h \right\|_{L^2(\Gamma_{ij})}^2 - 2 \int_{\Gamma_{ij}} \mathbf{h} \boldsymbol{\mu}_h \langle q_h \mathbf{n} \rangle_t + \left\| \mathbf{h}^{\frac{1}{2}} \langle q_h \mathbf{n} \rangle_t \right\|_{L^2(\Gamma_{ij})}^2 \right).$$

Hence, by using Proposition 5.2.7 and choosing $\gamma > 0$ large enough,

$$\begin{aligned} \bar{\mathcal{A}}_h((\mathbf{v}_h, -q_h, -\boldsymbol{\mu}_h); (\mathbf{v}_h, q_h, \boldsymbol{\mu}_h)) &\geq (1 - C\gamma^{-1}) \sum_{i=0}^N \|D\mathbf{v}_i\|_{L^2(\Omega_i)}^2 + \gamma^{-1} \sum_{i=1}^N \sum_{j=0}^{i-1} \left\| \mathbf{h}^{\frac{1}{2}} (-\boldsymbol{\mu}_h + \langle q_h \mathbf{n} \rangle_t) \right\|_{L^2(\Gamma_{ij})}^2 \\ &\geq \frac{1}{2} \sum_{i=0}^N \|D\mathbf{v}_i\|_{L^2(\Omega_i)}^2 + \gamma^{-1} \sum_{i=1}^N \sum_{j=0}^{i-1} \left\| \mathbf{h}^{\frac{1}{2}} (-\boldsymbol{\mu}_h + \langle q_h \mathbf{n} \rangle_t) \right\|_{L^2(\Gamma_{ij})}^2. \end{aligned} \quad (\text{A.5})$$

Now, let $\mathbf{w}_h^q \in V_h$ be the supremizer of Lemma 5.2.16. Since $b_0(\mathbf{w}_h^q, q_h) \geq C \|q_h\|_{0,h}^2$, we have

$$\begin{aligned} \bar{\mathcal{A}}_h((\mathbf{w}_h^q, 0, \mathbf{0}); (\mathbf{v}_h, q_h, \boldsymbol{\mu}_h)) &\geq \sum_{i=0}^N \int_{\Omega_i} D\mathbf{v}_i : D\mathbf{w}_i^q + C \|q_h\|_{0,h}^2 + \sum_{i=1}^N \sum_{j=0}^{i-1} \int_{\Gamma_{ij}} \boldsymbol{\mu}_h [\mathbf{w}_h^q] \\ &- \sum_{i=1}^N \sum_{j=0}^{i-1} \gamma^{-1} \int_{\Gamma_{ij}} \mathbf{h} \langle DR_{ij}^v(\mathbf{v}_h) \mathbf{n} \rangle_t \langle DR_{ij}^v(\mathbf{w}_h^q) \mathbf{n} \rangle_t \\ &+ \sum_{i=1}^N \sum_{j=0}^{i-1} \gamma^{-1} \int_{\Gamma_{ij}} \mathbf{h} (-\boldsymbol{\mu}_h + \langle q_h \mathbf{n} \rangle_t) \langle DR_{ij}^v(\mathbf{w}_h^q) \mathbf{n} \rangle_t. \end{aligned} \quad (\text{A.6})$$

By the Cauchy-Schwarz inequality

$$\begin{aligned}
 & \sum_{i=1}^N \sum_{j=0}^{i-1} \int_{\Gamma_{ij}} \mathbf{h} \langle DR_{ij}^v(\mathbf{v}_h) \mathbf{n} \rangle_t \langle DR_{ij}^v(\mathbf{w}_h^q) \mathbf{n} \rangle_t \\
 & \leq \sum_{i=1}^N \sum_{j=0}^{i-1} \left\| \mathbf{h}^{\frac{1}{2}} \langle DR_{ij}^v(\mathbf{v}_h) \mathbf{n} \rangle_t \right\|_{L^2(\Gamma_{ij})} \left\| \mathbf{h}^{\frac{1}{2}} \langle DR_{ij}^v(\mathbf{w}_h^q) \mathbf{n} \rangle_t \right\|_{L^2(\Gamma_{ij})}, \\
 & \sum_{i=1}^N \sum_{j=0}^{i-1} \left| \int_{\Gamma_{ij}} \mathbf{h} (-\boldsymbol{\mu}_h + \langle q_h \mathbf{n} \rangle_t) \langle DR_{ij}^v(\mathbf{w}_h^q) \mathbf{n} \rangle_t \right| \\
 & \leq \sum_{i=1}^N \sum_{j=0}^{i-1} \left\| \mathbf{h}^{\frac{1}{2}} (-\boldsymbol{\mu}_h + \langle q_h \mathbf{n} \rangle_t) \right\|_{L^2(\Gamma_{ij})} \left\| \mathbf{h}^{\frac{1}{2}} \langle DR_{ij}^v(\mathbf{w}_h^q) \mathbf{n} \rangle_t \right\|_{L^2(\Gamma_{ij})}.
 \end{aligned}$$

By using Young's inequality, for $s, \delta > 0$, Proposition 5.2.7 and the construction of \mathbf{w}_h^q in the proof of Lemma 5.2.16, there exists $C_1 > 0$ such that

$$\begin{aligned}
 & \sum_{i=1}^N \sum_{j=0}^{i-1} \gamma^{-1} \int_{\Gamma_{ij}} \mathbf{h} \langle DR_{ij}^v(\mathbf{v}_h) \mathbf{n} \rangle_t \langle DR_{ij}^v(\mathbf{w}_h^q) \mathbf{n} \rangle_t \geq -\frac{C_1}{2\gamma s} \sum_{i=0}^N \|D\mathbf{v}_i\|_{L^2(\Omega_i)}^2 - \frac{sC_1}{2\gamma} \|q_h\|_{0,h}^2, \\
 & \sum_{i=1}^N \sum_{j=0}^{i-1} \gamma^{-1} \int_{\Gamma_{ij}} \mathbf{h} (-\boldsymbol{\mu}_h + \langle q_h \mathbf{n} \rangle_t) \langle DR_{ij}^v(\mathbf{w}_h^q) \mathbf{n} \rangle_t \geq -\frac{C_1}{2\gamma\delta} \sum_{i=1}^N \sum_{j=0}^{i-1} \left\| \mathbf{h}^{\frac{1}{2}} (-\boldsymbol{\mu}_h + \langle q_h \mathbf{n} \rangle_t) \right\|_{L^2(\Gamma_{ij})}^2 \\
 & \quad - \frac{\delta C_1}{2\gamma} \|q_h\|_{0,h}^2.
 \end{aligned}$$

From the Cauchy-Schwarz inequality, the construction of \mathbf{w}_h^q , and Young's inequality, there exists $C_2 > 0$ such that, for $\varepsilon > 0$,

$$\sum_{i=0}^N \int_{\Omega_i} D\mathbf{v}_i : D\mathbf{w}_i^p \geq -\frac{C_2}{2\varepsilon} \sum_{i=0}^N \|D\mathbf{v}_i\|_{L^2(\Omega_i)}^2 - \frac{\varepsilon C_2}{2} \|q_h\|_{0,h}^2.$$

In an analogous fashion, there exists $C_3 > 0$ such that, for $r > 0$,

$$\sum_{i=1}^N \sum_{j=0}^{i-1} \int_{\Gamma_{ij}} \boldsymbol{\mu}_h [\mathbf{w}_h^q] \geq -\frac{C_3}{2r} \sum_{i=1}^N \sum_{j=0}^{i-1} \left\| \mathbf{h}^{\frac{1}{2}} \boldsymbol{\mu}_h \right\|_{L^2(\Gamma_{ij})}^2 - \frac{rC_3}{2} \|q_h\|_{0,h}^2.$$

Let us go back to (A.6). We have

$$\begin{aligned}
 \overline{\mathcal{A}}_h((\mathbf{w}_h^q, 0, 0); (\mathbf{v}_h, q_h, \boldsymbol{\mu}_h)) & \geq -\frac{C_2}{2\varepsilon} \sum_{i=0}^N \|D\mathbf{v}_i\|_{L^2(\Omega_i)}^2 - \frac{\varepsilon C_2}{2} \|q_h\|_{0,h}^2 + C \|q_h\|_{0,h}^2 \\
 & \quad - \frac{C_3}{2r} \sum_{i=1}^N \sum_{j=0}^{i-1} \left\| \mathbf{h}^{\frac{1}{2}} \boldsymbol{\mu}_h \right\|_{L^2(\Gamma_{ij})}^2 - \frac{rC_3}{2} \|q_h\|_{0,h}^2 - \frac{C_1}{2\gamma s} \sum_{i=0}^N \|D\mathbf{v}_i\|_{L^2(\Omega_i)}^2 \\
 & \quad - \frac{sC_1}{2\gamma} \|q_h\|_{0,h}^2 - \frac{C_1}{2\gamma\delta} \sum_{i=1}^N \sum_{j=0}^{i-1} \left\| \mathbf{h}^{\frac{1}{2}} (-\boldsymbol{\mu}_h + \langle q_h \mathbf{n} \rangle_t) \right\|_{L^2(\Gamma_{ij})}^2 - \frac{\delta C_1}{2\gamma} \|q_h\|_{0,h}^2 \\
 & = \left(C - \frac{\varepsilon C_2}{2} - \frac{rC_3}{2} - \frac{sC_1}{2\gamma} - \frac{\delta C_1}{2\gamma} \right) \|q_h\|_{0,h}^2 + \left(-\frac{C_2}{2\varepsilon} - \frac{C_1}{2\gamma s} \right) \sum_{i=0}^N \|D\mathbf{v}_i\|_{L^2(\Omega_i)}^2 \\
 & \quad - \frac{C_1}{2\gamma\delta} \sum_{i=1}^N \sum_{j=0}^{i-1} \left\| \mathbf{h}^{\frac{1}{2}} (-\boldsymbol{\mu}_h + \langle q_h \mathbf{n} \rangle_t) \right\|_{L^2(\Gamma_{ij})}^2 - \frac{C_3}{2r} \sum_{i=1}^N \sum_{j=0}^{i-1} \left\| \mathbf{h}^{\frac{1}{2}} \boldsymbol{\mu}_h \right\|_{L^2(\Gamma_{ij})}^2.
 \end{aligned}$$

Appendix A. Appendix

Let $\varepsilon, r, s, \delta > 0$ be small enough such that $C - \frac{\varepsilon C_2}{2} - \frac{r C_3}{2} - \frac{s C_1}{2\gamma} - \frac{\delta C_1}{2\gamma} \geq \frac{C}{2}$. Hence, there exist $C_4, C_5, C_6 > 0$ such that

$$\begin{aligned} \overline{\mathcal{A}}_h((\mathbf{w}_h^q, 0, \mathbf{0}); (\mathbf{v}_h, q_h, \boldsymbol{\mu}_h)) &\geq \frac{C}{2} \|q_h\|_{0,h}^2 - C_4 \sum_{i=0}^N \|D\mathbf{v}_i\|_{L^2(\Omega_i)}^2 \\ &\quad - C_5 \sum_{i=1}^N \sum_{j=0}^{i-1} \left\| \mathbf{h}^{\frac{1}{2}} (-\boldsymbol{\mu}_h + \langle q_h \mathbf{n} \rangle_t) \right\|_{L^2(\Gamma_{ij})}^2 - C_6 \sum_{i=1}^N \sum_{j=0}^{i-1} \left\| \mathbf{h}^{\frac{1}{2}} \boldsymbol{\mu}_h \right\|_{L^2(\Gamma_{ij})}^2. \end{aligned} \quad (\text{A.7})$$

Let $P_h : \bigoplus_{0 \leq j < i \leq N} L^2(\Gamma_{ij}) \rightarrow \Lambda_h$ be the L^2 -orthogonal projection. From condition (5.6), we have $\mathbf{h}^{-1}[\mathbf{v}_h] \Big|_{\Gamma_{ij}} = P_h \mathbf{h}^{-1}[\mathbf{v}_h] \Big|_{\Gamma_{ij}}$, for every $0 \leq j < i \leq N$. Therefore, from the Cauchy-Schwartz inequality, we have

$$\begin{aligned} \overline{\mathcal{A}}_h((\mathbf{0}, 0, P_h \mathbf{h}^{-1}[\mathbf{v}_h]); (\mathbf{v}_h, q_h, \boldsymbol{\mu}_h)) &\geq \sum_{i=1}^N \sum_{j=0}^{i-1} \left\| \mathbf{h}^{-\frac{1}{2}}[\mathbf{v}_h] \right\|_{L^2(\Gamma_{ij})}^2 \\ &\quad - \gamma^{-1} \left(\sum_{i=1}^N \sum_{j=0}^{i-1} \left\| \mathbf{h}^{\frac{1}{2}} \langle DR_{ij}^v(\mathbf{v}_h) \mathbf{n} \rangle_t \right\|_{L^2(\Gamma_{ij})} \left\| \mathbf{h}^{-\frac{1}{2}}[\mathbf{v}_h] \right\|_{L^2(\Gamma_{ij})} \right. \\ &\quad \left. + \sum_{i=1}^N \sum_{j=0}^{i-1} \left\| \mathbf{h}^{\frac{1}{2}} (-\boldsymbol{\mu}_h + \langle q_h \mathbf{n} \rangle_t) \right\|_{L^2(\Gamma_{ij})} \left\| \mathbf{h}^{-\frac{1}{2}}[\mathbf{v}_h] \right\|_{L^2(\Gamma_{ij})} \right). \end{aligned}$$

By Proposition 5.2.7 and Young's inequality, there exists $C_7 > 0$ such that, for $a, b > 0$,

$$\begin{aligned} - \sum_{i=1}^N \sum_{j=0}^{i-1} \left\| \mathbf{h}^{\frac{1}{2}} \langle DR_{ij}^v(\mathbf{v}_h) \mathbf{n} \rangle_t \right\|_{L^2(\Gamma_{ij})} \left\| \mathbf{h}^{-\frac{1}{2}}[\mathbf{v}_h] \right\|_{L^2(\Gamma_{ij})} &\geq - \frac{C_7}{2a} \sum_{i=0}^N \|D\mathbf{v}_i\|_{L^2(\Omega_i)}^2 \\ &\quad - \frac{aC_7}{2} \sum_{i=1}^N \sum_{j=0}^{i-1} \left\| \mathbf{h}^{-\frac{1}{2}}[\mathbf{v}_h] \right\|_{L^2(\Gamma_{ij})}^2, \\ - \sum_{i=1}^N \sum_{j=0}^{i-1} \left\| \mathbf{h}^{\frac{1}{2}} (-\boldsymbol{\mu}_h + \langle q_h \mathbf{n} \rangle_t) \right\|_{L^2(\Gamma_{ij})} \left\| \mathbf{h}^{-\frac{1}{2}}[\mathbf{v}_h] \right\|_{L^2(\Gamma_{ij})} &\geq - \frac{1}{2b} \sum_{i=1}^N \sum_{j=0}^{i-1} \left\| \mathbf{h}^{\frac{1}{2}} (-\boldsymbol{\mu}_h + \langle q_h \mathbf{n} \rangle_t) \right\|_{L^2(\Gamma_{ij})}^2 \\ &\quad - \frac{b}{2} \sum_{i=1}^N \sum_{j=0}^{i-1} \left\| \mathbf{h}^{-\frac{1}{2}}[\mathbf{v}_h] \right\|_{L^2(\Gamma_{ij})}^2. \end{aligned}$$

Thus,

$$\begin{aligned} \overline{\mathcal{A}}_h((\mathbf{0}, 0, P_h \mathbf{h}^{-1}[\mathbf{v}_h]); (\mathbf{v}_h, q_h, \boldsymbol{\mu}_h)) &\geq \left(1 - \frac{aC_7}{2\gamma} - \frac{b}{2\gamma}\right) \sum_{i=1}^N \sum_{j=0}^{i-1} \left\| \mathbf{h}^{-\frac{1}{2}}[\mathbf{v}_h] \right\|_{L^2(\Gamma_{ij})}^2 \\ &\quad - \frac{C_7}{2a\gamma} \sum_{i=0}^N \|D\mathbf{v}_i\|_{L^2(\Omega_i)}^2 - \frac{1}{2b\gamma} \sum_{i=1}^N \sum_{j=0}^{i-1} \left\| \mathbf{h}^{\frac{1}{2}} (-\boldsymbol{\mu}_h + \langle q_h \mathbf{n} \rangle_t) \right\|_{L^2(\Gamma_{ij})}^2. \end{aligned}$$

Let us choose $a, b > 0$ small enough such that $1 - \frac{aC_7}{2\gamma} - \frac{b}{2\gamma} \geq \frac{1}{2}$. Hence, there exist $C_8, C_9 > 0$ such that

$$\begin{aligned} \overline{\mathcal{A}}_h((\mathbf{0}, 0, P_h \mathbf{h}^{-1}[\mathbf{v}_h]); (\mathbf{v}_h, q_h, \boldsymbol{\mu}_h)) &\geq \frac{1}{2} \sum_{i=1}^N \sum_{j=0}^{i-1} \left\| \mathbf{h}^{-\frac{1}{2}}[\mathbf{v}_h] \right\|_{L^2(\Gamma_{ij})}^2 - C_8 \sum_{i=0}^N \|D\mathbf{v}_i\|_{L^2(\Omega_i)}^2 \\ &\quad - C_9 \sum_{i=1}^N \sum_{j=0}^{i-1} \left\| \mathbf{h}^{\frac{1}{2}} (-\boldsymbol{\mu}_h + \langle q_h \mathbf{n} \rangle_t) \right\|_{L^2(\Gamma_{ij})}^2. \end{aligned} \quad (\text{A.8})$$

Let us put together (A.5), (A.7), (A.8). For $k, \eta > 0$, we have

$$\begin{aligned} \overline{\mathcal{A}}_h((\mathbf{v}_h + k\mathbf{w}_h^q, -q_h, -\boldsymbol{\mu}_h + \eta P_h \mathbf{h}^{-1}[\mathbf{v}_h]); (\mathbf{v}_h, q_h, \boldsymbol{\mu}_h)) &\geq \left(\frac{1}{2} - kC_4 - \eta C_8\right) \sum_{i=0}^N \|D\mathbf{v}_i\|_{L^2(\Omega_i)}^2 \\ &+ \left(\frac{1}{\gamma} - kC_5 - \eta C_9\right) \sum_{i=1}^N \sum_{j=0}^{i-1} \left\| \mathbf{h}^{\frac{1}{2}} (-\boldsymbol{\mu}_h + \langle q_h \mathbf{n} \rangle_t) \right\|_{L^2(\Gamma_{ij})}^2 + \frac{kC}{2} \|q_h\|_{0,h}^2 \\ &- kC_6 \sum_{i=1}^N \sum_{j=0}^{i-1} \left\| \mathbf{h}^{\frac{1}{2}} \boldsymbol{\mu}_h \right\|_{L^2(\Gamma_{ij})}^2 + \frac{\eta}{2} \sum_{i=1}^N \sum_{j=0}^{i-1} \left\| \mathbf{h}^{-\frac{1}{2}} [\mathbf{v}_h] \right\|_{L^2(\Gamma_{ij})}^2. \end{aligned}$$

From Proposition 5.2.5, there exists $C_{10} > 0$ such that

$$\begin{aligned} \overline{\mathcal{A}}_h((\mathbf{v}_h + k\mathbf{w}_h^q, -q_h, -\boldsymbol{\mu}_h + \eta P_h \mathbf{h}^{-1}[\mathbf{v}_h]); (\mathbf{v}_h, q_h, \boldsymbol{\mu}_h)) &\geq \left(\frac{1}{2} - kC_4 - \eta C_8\right) \sum_{i=0}^N \|D\mathbf{v}_i\|_{L^2(\Omega_i)}^2 \\ &+ \left(\frac{1}{\gamma} - kC_5 - \eta C_9\right) \sum_{i=1}^N \sum_{j=0}^{i-1} \left\| \mathbf{h}^{\frac{1}{2}} (-\boldsymbol{\mu}_h + \langle q_h \mathbf{n} \rangle_t) \right\|_{L^2(\Gamma_{ij})}^2 + \frac{k}{4C_{10}} \sum_{i=1}^N \sum_{j=0}^{i-1} \left\| \mathbf{h}^{\frac{1}{2}} \langle q_h \rangle_t \right\|_{L^2(\Gamma_{ij})}^2 \\ &+ \frac{kC}{4} \|q_h\|_{0,h}^2 - kC_6 \sum_{i=1}^N \sum_{j=0}^{i-1} \left\| \mathbf{h}^{\frac{1}{2}} \boldsymbol{\mu}_h \right\|_{L^2(\Gamma_{ij})}^2 + \frac{\eta}{2} \sum_{i=1}^N \sum_{j=0}^{i-1} \left\| \mathbf{h}^{-\frac{1}{2}} [\mathbf{v}_h] \right\|_{L^2(\Gamma_{ij})}^2. \end{aligned} \quad (\text{A.9})$$

Let $C_{11} := \frac{4}{kC_{10}}$ and $C_{12} := \frac{1}{\gamma} - kC_5 - \eta C_9$, so that we can write

$$\begin{aligned} &C_{11} \sum_{i=1}^N \sum_{j=0}^{i-1} \left\| \mathbf{h}^{\frac{1}{2}} \langle q_h \rangle_t \right\|_{L^2(\Gamma_{ij})}^2 + C_{12} \sum_{i=1}^N \sum_{j=0}^{i-1} \left\| \mathbf{h}^{\frac{1}{2}} (-\boldsymbol{\mu}_h + \langle q_h \mathbf{n} \rangle_t) \right\|_{L^2(\Gamma_{ij})}^2 \\ &= C_{12} \sum_{i=1}^N \sum_{j=0}^{i-1} \left(\left(\frac{C_{11}}{C_{12}} + 1 \right) \left\| \mathbf{h}^{\frac{1}{2}} \langle q_h \mathbf{n} \rangle_t \right\|_{L^2(\Gamma_{ij})}^2 + \left\| \mathbf{h}^{\frac{1}{2}} \boldsymbol{\mu}_h \right\|_{L^2(\Gamma_{ij})}^2 - 2 \int_{\Gamma_{ij}} \mathbf{h}^{\frac{1}{2}} \boldsymbol{\mu}_h \mathbf{h}^{\frac{1}{2}} \langle q_h \mathbf{n} \rangle_t \right). \end{aligned}$$

From the Cauchy-Schwartz and the Young inequalities, for $\ell > 0$, it holds

$$-2 \int_{\Gamma_{ij}} \mathbf{h}^{\frac{1}{2}} \boldsymbol{\mu}_h \mathbf{h}^{\frac{1}{2}} \langle q_h \mathbf{n} \rangle_t \geq -\ell \left\| \mathbf{h}^{\frac{1}{2}} \langle q_h \mathbf{n} \rangle_t \right\|_{L^2(\Gamma_{ij})}^2 - \frac{1}{\ell} \left\| \mathbf{h}^{\frac{1}{2}} \boldsymbol{\mu}_h \right\|_{L^2(\Gamma_{ij})}^2.$$

By observing $\left\| \mathbf{h}^{\frac{1}{2}} \langle q_h \mathbf{n} \rangle_t \right\|_{L^2(\Gamma_{ij})}^2 = \left\| \mathbf{h}^{\frac{1}{2}} \langle q_h \rangle_t \right\|_{L^2(\Gamma_{ij})}^2$, we have

$$\begin{aligned} &C_{11} \sum_{i=1}^N \sum_{j=0}^{i-1} \left\| \mathbf{h}^{\frac{1}{2}} \langle q_h \rangle_t \right\|_{L^2(\Gamma_{ij})}^2 + C_{12} \sum_{i=1}^N \sum_{j=0}^{i-1} \left\| \mathbf{h}^{\frac{1}{2}} (-\boldsymbol{\mu}_h + \langle q_h \mathbf{n} \rangle_t) \right\|_{L^2(\Gamma_{ij})}^2 \\ &\geq C_{12} \sum_{i=1}^N \sum_{j=0}^{i-1} \left(\left(\frac{C_{11}}{C_{12}} + 1 - \ell \right) \left\| \mathbf{h}^{\frac{1}{2}} \langle q_h \rangle_t \right\|_{L^2(\Gamma_{ij})}^2 + \left(1 - \frac{1}{\ell} \right) \left\| \mathbf{h}^{\frac{1}{2}} \boldsymbol{\mu}_h \right\|_{L^2(\Gamma_{ij})}^2 \right). \end{aligned} \quad (\text{A.10})$$

By plugging (A.10) back into (A.9), we have

$$\begin{aligned} \overline{\mathcal{A}}_h((\mathbf{v}_h + k\mathbf{w}_h^q, -q_h, -\boldsymbol{\mu}_h + \eta P_h \mathbf{h}^{-1}[\mathbf{v}_h]); (\mathbf{v}_h, q_h, \boldsymbol{\mu}_h)) &\geq \left(\frac{1}{2} - kC_4 - \eta C_8\right) \sum_{i=0}^N \|D\mathbf{v}_i\|_{L^2(\Omega_i)}^2 \\ &+ C_{12} \left(\frac{C_{11}}{C_{12}} + 1 - \ell \right) \sum_{i=1}^N \sum_{j=0}^{i-1} \left\| \mathbf{h}^{\frac{1}{2}} \langle q_h \rangle_t \right\|_{L^2(\Gamma_{ij})}^2 + \left(C_{12} \left(1 - \frac{1}{\ell} \right) - kC_6 \right) \sum_{i=1}^N \sum_{j=0}^{i-1} \left\| \mathbf{h}^{\frac{1}{2}} \boldsymbol{\mu}_h \right\|_{L^2(\Gamma_{ij})}^2 \\ &+ \frac{kC}{4} \|q_h\|_{0,h}^2 + \frac{\eta}{2} \sum_{i=1}^N \sum_{j=0}^{i-1} \left\| \mathbf{h}^{-\frac{1}{2}} [\mathbf{v}_h] \right\|_{L^2(\Gamma_{ij})}^2. \end{aligned}$$

Appendix A. Appendix

We require $1 < \ell < \frac{C_{11}}{C_{12}} + 1$ and k, η to be small enough so that $\frac{1}{2} - kC_4 - \eta C_8 \geq \frac{1}{4}$, $C_{12} \left(\frac{C_{11}}{C_{12}} + 1 - \ell \right) \geq C_{13}$, $C_{12} \left(1 - \frac{1}{\ell} \right) - kC_6 \geq C_{14}$, for some $C_{13}, C_{14} > 0$. Note that the choice of ℓ depends on k and η . On the other hand, there exist $C_{15}, C_{16} > 0$ such that $\frac{kC}{4} \geq C_{15}$ and $\frac{\eta}{2} \geq C_{16}$. Hence,

$$\begin{aligned} \overline{\mathcal{A}}_h \left((\mathbf{v}_h + k\mathbf{w}_h^q, -q_h, -\boldsymbol{\mu}_h + \eta P_h \mathbf{h}^{-1}[\mathbf{v}_h]) ; (\mathbf{v}_h, q_h, \boldsymbol{\mu}_h) \right) &\geq \frac{1}{4} \sum_{i=0}^N \|D\mathbf{v}_i\|_{L^2(\Omega_i)}^2 \\ &+ C_{13} \sum_{i=1}^N \sum_{j=0}^{i-1} \left\| \mathbf{h}^{\frac{1}{2}} \langle q_h \rangle_t \right\|_{L^2(\Gamma_{ij})}^2 + C_{14} \sum_{i=1}^N \sum_{j=0}^{i-1} \left\| \mathbf{h}^{\frac{1}{2}} \boldsymbol{\mu}_h \right\|_{L^2(\Gamma_{ij})}^2 \\ &+ C_{15} \|q_h\|_{0,h}^2 + C_{16} \sum_{i=1}^N \sum_{j=0}^{i-1} \left\| \mathbf{h}^{-\frac{1}{2}} [\mathbf{v}_h] \right\|_{L^2(\Gamma_{ij})}^2. \end{aligned}$$

Finally, the stability property of \mathbf{w}_h^q , namely $\|\mathbf{w}_h^q\|_{1,h} \leq C \|q_h\|_{0,h}$, entails

$$\left\| (\mathbf{v}_h + k\mathbf{w}_h^q, -q_h, -\boldsymbol{\mu}_h + \eta P_h \mathbf{h}^{-1}[\mathbf{v}_h]) \right\| \leq C \left\| (\mathbf{v}_h, q_h, \boldsymbol{\mu}_h) \right\|.$$

□

Bibliography

- [1] *Isogeometric analysis: progress and challenges [preface]*, Comput. Methods Appl. Mech. Engrg., 316 (2017), p. 1.
- [2] *Open CASCADE SAS. Open CASCADE technology (version 7.3.0)*. <https://www.opencascade.com>, 2018.
- [3] R. A. ADAMS AND J. J. F. FOURNIER, *Sobolev spaces*, vol. 140 of Pure and Applied Mathematics (Amsterdam), Elsevier/Academic Press, Amsterdam, second ed., 2003.
- [4] P. ANTOLIN, A. BUFFA, AND M. MARTINELLI, *Isogeometric analysis on V-reps: first results*, Comput. Methods Appl. Mech. Engrg., 355 (2019), pp. 976–1002.
- [5] P. ANTOLIN, A. BUFFA, R. PUPPI, AND X. WEI, *Overlapping multipatch isogeometric method with minimal stabilization*, SIAM J. Sci. Comput., 43 (2021), pp. A330–A354.
- [6] P. ANTOLÍN, PABLO, X. WEI, AND A. BUFFA, *Robust numerical integration on curved polyhedra based on folded decompositions*. arXiv, 2021.
- [7] D. N. ARNOLD, D. BOFFI, AND R. S. FALK, *Quadrilateral $H(\text{div})$ finite elements*, SIAM J. Numer. Anal., 42 (2005), pp. 2429–2451.
- [8] I. BABUŠKA, *The finite element method with Lagrangian multipliers*, Numer. Math., 20 (1972/73), pp. 179–192.
- [9] —, *The finite element method with penalty*, Math. Comp., 27 (1973), pp. 221–228.
- [10] I. BABUŠKA, U. BANERJEE, AND J. E. OSBORN, *Meshless and generalized finite element methods: a survey of some major results*, in Meshfree methods for partial differential equations (Bonn, 2001), vol. 26 of Lect. Notes Comput. Sci. Eng., Springer, Berlin, 2003, pp. 1–20.
- [11] I. BABUŠKA, U. BANERJEE, AND J. E. OSBORN, *Survey of meshless and generalized finite element methods: a unified approach*, Acta Numer., 12 (2003), pp. 1–125.
- [12] J. W. BARRETT AND C. M. ELLIOTT, *A finite-element method for solving elliptic equations with Neumann data on a curved boundary using unfitted meshes*, IMA J. Numer. Anal., 4 (1984), pp. 309–325.
- [13] —, *Finite element approximation of the Dirichlet problem using the boundary penalty method*, Numer. Math., 49 (1986), pp. 343–366.
- [14] —, *Finite-element approximation of elliptic equations with a Neumann or Robin condition on a curved boundary*, IMA J. Numer. Anal., 8 (1988), pp. 321–342.
- [15] K.-J. BATHE, *The inf-sup condition and its evaluation for mixed finite element methods*, Comput. & Structures, 79 (2001), pp. 243–252.

Bibliography

- [16] E. BAYRAKTAR, O. MIERKA, AND S. TUREK, *Benchmark computations of 3d laminar flow around a cylinder with cfx*, International Journal of Computational Science and Engineering, (2012), pp. 10–1504.
- [17] Y. BAZILEVS, L. BEIRÃO DA VEIGA, J. A. COTTRELL, T. J. R. HUGHES, AND G. SANGALLI, *Isogeometric analysis: approximation, stability and error estimates for h-refined meshes*, Math. Models Methods Appl. Sci., 16 (2006), pp. 1031–1090.
- [18] R. BECKER, P. HANSBO, AND R. STENBERG, *A finite element method for domain decomposition with non-matching grids*, M2AN Math. Model. Numer. Anal., 37 (2003), pp. 209–225.
- [19] L. BEIRÃO DA VEIGA, A. BUFFA, G. SANGALLI, AND R. VÁZQUEZ, *Mathematical analysis of variational isogeometric methods*, Acta Numer., 23 (2014), pp. 157–287.
- [20] L. BEIRÃO DA VEIGA, D. CHO, AND G. SANGALLI, *Anisotropic NURBS approximation in isogeometric analysis*, Comput. Methods Appl. Mech. Engrg., 209/212 (2012), pp. 1–11.
- [21] C. BERNARDI, C. CANUTO, AND Y. MADAY, *Generalized inf-sup conditions for Chebyshev spectral approximation of the Stokes problem*, SIAM J. Numer. Anal., 25 (1988), pp. 1237–1271.
- [22] D. BOFFI, F. BREZZI, AND M. FORTIN, *Mixed finite element methods and applications*, vol. 44 of Springer Series in Computational Mathematics, Springer, Heidelberg, 2013.
- [23] C. BRACCO, A. BUFFA, C. GIANNELLI, AND R. VÁZQUEZ, *Adaptive isogeometric methods with hierarchical splines: an overview*, Discrete Contin. Dyn. Syst., 39 (2019), pp. 241–261.
- [24] J. H. BRAMBLE, J. E. PASCIAK, AND O. STEINBACH, *On the stability of the L^2 projection in $H^1(\Omega)$* , Math. Comp., 71 (2002), pp. 147–156.
- [25] S. C. BRENNER AND L. R. SCOTT, *The mathematical theory of finite element methods*, vol. 15 of Texts in Applied Mathematics, Springer, New York, third ed., 2008.
- [26] A. BRESSAN AND E. SANDE, *Approximation in FEM, DG and IGA: a theoretical comparison*, Numer. Math., 143 (2019), pp. 923–942.
- [27] H. BREZIS, *Functional analysis, Sobolev spaces and partial differential equations*, Universitext, Springer, New York, 2011.
- [28] A. BUFFA, C. DE FALCO, AND G. SANGALLI, *IsoGeometric Analysis: stable elements for the 2D Stokes equation*, Internat. J. Numer. Methods Fluids, 65 (2011), pp. 1407–1422.
- [29] A. BUFFA, G. GANTNER, C. GIANNELLI, D. PRAETORIUS, AND R. VÁZQUEZ, *Mathematical foundations of adaptive isogeometric analysis*, 2021.
- [30] A. BUFFA, E. M. GARAU, C. GIANNELLI, AND G. SANGALLI, *On quasi-interpolation operators in spline spaces*, in Building bridges: connections and challenges in modern approaches to numerical partial differential equations, vol. 114 of Lect. Notes Comput. Sci. Eng., Springer, [Cham], 2016, pp. 73–91.
- [31] A. BUFFA, H. HARBRECHT, A. KUNOTH, AND G. SANGALLI, *BPX-preconditioning for isogeometric analysis*, Comput. Methods Appl. Mech. Engrg., 265 (2013), pp. 63–70.
- [32] A. BUFFA, R. HERNANDEZ VÁZQUEZ, G. SANGALLI, AND L. BEIRÃO DA VEIGA, *Approximation estimates for isogeometric spaces in multipatch geometries*, Numer. Methods Partial Differential Equations, 31 (2015), pp. 422–438.

-
- [33] A. BUFFA, R. PUPPI, AND R. VÁZQUEZ, *A minimal stabilization procedure for isogeometric methods on trimmed geometries*, SIAM J. Numer. Anal., 58 (2020), pp. 2711–2735.
 - [34] A. BUFFA, J. RIVAS, G. SANGALLI, AND R. VÁZQUEZ, *Isogeometric discrete differential forms in three dimensions*, SIAM J. Numer. Anal., 49 (2011), pp. 818–844.
 - [35] E. BURMAN, *Ghost penalty*, C. R. Math. Acad. Sci. Paris, 348 (2010), pp. 1217–1220.
 - [36] E. BURMAN, S. CLAUS, P. HANSBO, M. G. LARSON, AND A. MASSING, *CutFEM: discretizing geometry and partial differential equations*, Internat. J. Numer. Methods Engrg., 104 (2015), pp. 472–501.
 - [37] E. BURMAN AND P. HANSBO, *Fictitious domain finite element methods using cut elements: II. A stabilized Nitsche method*, Appl. Numer. Math., 62 (2012), pp. 328–341.
 - [38] ———, *Fictitious domain methods using cut elements: III. A stabilized Nitsche method for Stokes’ problem*, ESAIM Math. Model. Numer. Anal., 48 (2014), pp. 859–874.
 - [39] E. BURMAN, P. HANSBO, M. G. LARSON, AND S. ZAHEDI, *Cut finite element methods for coupled bulk-surface problems*, Numer. Math., 133 (2016), pp. 203–231.
 - [40] E. BURMAN, M. G. LARSON, AND L. OKSANEN, *Primal-dual mixed finite element methods for the elliptic Cauchy problem*, SIAM J. Numer. Anal., 56 (2018), pp. 3480–3509.
 - [41] E. BURMAN AND R. PUPPI, *Two mixed finite element formulations for the weak imposition of the neumann boundary conditions for the darcy flow*, Journal of Numerical Mathematics, (2021), p. 000010151520210042.
 - [42] P. G. CIARLET, *The finite element method for elliptic problems*, vol. 40 of Classics in Applied Mathematics, Society for Industrial and Applied Mathematics (SIAM), Philadelphia, PA, 2002. Reprint of the 1978 original [North-Holland, Amsterdam; MR0520174 (58 #25001)].
 - [43] E. COHEN, T. MARTIN, R. M. KIRBY, T. LYCHE, AND R. F. RIESENFELD, *Analysis-aware modeling: understanding quality considerations in modeling for isogeometric analysis*, Comput. Methods Appl. Mech. Engrg., 199 (2010), pp. 334–356.
 - [44] A. COLLIN, G. SANGALLI, AND T. TAKACS, *Analysis-suitable G^1 multi-patch parametrizations for C^1 isogeometric spaces*, Comput. Aided Geom. Design, 47 (2016), pp. 93–113.
 - [45] J. A. COTTRELL, T. J. R. HUGHES, AND Y. BAZILEVS, *Isogeometric analysis*, John Wiley & Sons, Ltd., Chichester, 2009. Toward integration of CAD and FEA.
 - [46] W. DAHMEN, R. DEVORE, AND K. SCHERER, *Multidimensional spline approximation*, SIAM J. Numer. Anal., 17 (1980), pp. 380–402.
 - [47] M. DAUGE, A. DÜSTER, AND E. RANK, *Theoretical and numerical investigation of the finite cell method*, J. Sci. Comput., 65 (2015), pp. 1039–1064.
 - [48] C. DAUX, N. MOËS, J. DOLBOW, N. SUKUMAR, AND T. BELYTSCHKO, *Arbitrary branched and intersecting cracks with the extended finite element method*, International Journal for Numerical Methods in Engineering, 48 (2000), pp. 1741–1760.
 - [49] F. DE PRENTER, C. V. VERHOOSSEL, AND E. H. VAN BRUMMELEN, *Preconditioning immersed isogeometric finite element methods with application to flow problems*, Comput. Methods Appl. Mech. Engrg., 348 (2019), pp. 604–631.
 - [50] F. DE PRENTER, C. V. VERHOOSSEL, E. H. VAN BRUMMELEN, J. A. EVANS, C. MESSE, J. BENZAKEN, AND K. MAUTE, *Multigrid solvers for immersed finite element methods and immersed isogeometric analysis*, Comput. Mech., 65 (2020), pp. 807–838.

Bibliography

- [51] F. DE PRENTER, C. V. VERHOOSSEL, G. J. VAN ZWIETEN, AND E. H. VAN BRUMMELEN, *Condition number analysis and preconditioning of the finite cell method*, Comput. Methods Appl. Mech. Engrg., 316 (2017), pp. 297–327.
- [52] D. A. DI PIETRO AND A. ERN, *Discrete functional analysis tools for discontinuous Galerkin methods with application to the incompressible Navier-Stokes equations*, Math. Comp., 79 (2010), pp. 1303–1330.
- [53] A. EMBAR, J. DOLBOW, AND I. HARARI, *Imposing Dirichlet boundary conditions with Nitsche’s method and spline-based finite elements*, Internat. J. Numer. Methods Engrg., 83 (2010), pp. 877–898.
- [54] A. ERN AND J.-L. GUERMOND, *Theory and practice of finite elements*, vol. 159 of Applied Mathematical Sciences, Springer-Verlag, New York, 2004.
- [55] ———, *Evaluation of the condition number in linear systems arising in finite element approximations*, M2AN Math. Model. Numer. Anal., 40 (2006), pp. 29–48.
- [56] J. A. EVANS, Y. BAZILEVS, I. BABUŠKA, AND T. J. R. HUGHES, *n-widths, sup-infs, and optimality ratios for the k-version of the isogeometric finite element method*, Comput. Methods Appl. Mech. Engrg., 198 (2009), pp. 1726–1741.
- [57] J. A. EVANS AND T. J. R. HUGHES, *Explicit trace inequalities for isogeometric analysis and parametric hexahedral finite elements*, Numer. Math., 123 (2013), pp. 259–290.
- [58] ———, *Isogeometric divergence-conforming B-splines for the Darcy-Stokes-Brinkman equations*, Math. Models Methods Appl. Sci., 23 (2013), pp. 671–741.
- [59] ———, *Isogeometric divergence-conforming B-splines for the steady Navier-Stokes equations*, Math. Models Methods Appl. Sci., 23 (2013), pp. 1421–1478.
- [60] R. T. FAROUKI, *Closing the gap between CAD model and downstream application*, SIAM news, 32 (1999), p. 303.
- [61] S. FERNÁNDEZ-MÉNDEZ AND A. HUERTA, *Imposing essential boundary conditions in mesh-free methods*, Comput. Methods Appl. Mech. Engrg., 193 (2004), pp. 1257–1275.
- [62] M. FOURNIÉ AND A. LOZINSKI, *Stability and optimal convergence of unfitted extended finite element methods with Lagrange multipliers for the Stokes equations*, in Geometrically unfitted finite element methods and applications, vol. 121 of Lect. Notes Comput. Sci. Eng., Springer, Cham, 2017, pp. 143–182.
- [63] J. FREUND AND R. STENBERG, *On weakly imposed boundary conditions in the finite element method*, in The ninth conference on Finite Elements in Fluids, Venezia, 16.-20.10.1995, M. Cecchi, ed., 1995, pp. 327–336.
- [64] V. GIRAULT AND R. GLOWINSKI, *Error analysis of a fictitious domain method applied to a Dirichlet problem*, Japan J. Indust. Appl. Math., 12 (1995), pp. 487–514.
- [65] R. GLOWINSKI, T.-W. PAN, AND J. PÉRIAUX, *A fictitious domain method for Dirichlet problem and applications*, Comput. Methods Appl. Mech. Engrg., 111 (1994), pp. 283–303.
- [66] P. GRISVARD, *Elliptic problems in nonsmooth domains*, vol. 24 of Monographs and Studies in Mathematics, Pitman (Advanced Publishing Program), Boston, MA, 1985.
- [67] F. GÜRCAN, *Streamline topologies in stokes flow within lid-driven cavities*, Theoretical and Computational Fluid Dynamics, 17 (2003), pp. 19–30.

-
- [68] J. GUZMÁN AND M. OLSHANSKII, *Inf-sup stability of geometrically unfitted Stokes finite elements*, Math. Comp., 87 (2018), pp. 2091–2112.
- [69] A. HANSBO AND P. HANSBO, *An unfitted finite element method, based on Nitsche’s method, for elliptic interface problems*, Comput. Methods Appl. Mech. Engrg., 191 (2002), pp. 5537–5552.
- [70] ———, *A finite element method for the simulation of strong and weak discontinuities in solid mechanics*, Comput. Methods Appl. Mech. Engrg., 193 (2004), pp. 3523–3540.
- [71] A. HANSBO, P. HANSBO, AND M. G. LARSON, *A finite element method on composite grids based on Nitsche’s method*, M2AN Math. Model. Numer. Anal., 37 (2003), pp. 495–514.
- [72] P. HANSBO, M. G. LARSON, AND S. ZAHEDI, *A cut finite element method for a Stokes interface problem*, Appl. Numer. Math., 85 (2014), pp. 90–114.
- [73] J. HASLINGER AND Y. RENARD, *A new fictitious domain approach inspired by the extended finite element method*, SIAM J. Numer. Anal., 47 (2009), pp. 1474–1499.
- [74] F. HECHT, *New development in freefem++*, J. Numer. Math., 20 (2012), pp. 251–265.
- [75] R. HIPTMAIR, J. LI, AND J. ZOU, *Universal extension for Sobolev spaces of differential forms and applications*, J. Funct. Anal., 263 (2012), pp. 364–382.
- [76] T. HOANG, *Isogeometric and immersogeometric analysis of incompressible flow problems*, PhD thesis, TU Eindhoven, 2018.
- [77] K. HÖLLIG, U. REIF, AND J. WIPPER, *Weighted extended B-spline approximation of Dirichlet problems*, SIAM J. Numer. Anal., 39 (2001), pp. 442–462.
- [78] T. J. R. HUGHES, J. A. COTTRELL, AND Y. BAZILEVS, *Isogeometric analysis: CAD, finite elements, NURBS, exact geometry and mesh refinement*, Comput. Methods Appl. Mech. Engrg., 194 (2005), pp. 4135–4195.
- [79] A. JOHANSSON, B. KEHLET, M. G. LARSON, AND A. LOGG, *Multimesh finite element methods: solving PDEs on multiple intersecting meshes*, Comput. Methods Appl. Mech. Engrg., 343 (2019), pp. 672–689.
- [80] A. JOHANSSON, M. G. LARSON, AND A. LOGG, *Multimesh finite elements with flexible mesh sizes*, Comput. Methods Appl. Mech. Engrg., 372 (2020), pp. 113420, 27.
- [81] V. JOHN, *Finite element methods for incompressible flow problems*, vol. 51 of Springer Series in Computational Mathematics, Springer, Cham, 2016.
- [82] C. JOHNSON, *Numerical solution of partial differential equations by the finite element method*, Dover Publications, Inc., Mineola, NY, 2009. Reprint of the 1987 edition.
- [83] B. JÜTTLER, A. MANTZAFLARIS, R. PERL, AND M. RUMPF, *On numerical integration in isogeometric subdivision methods for PDEs on surfaces*, Comput. Methods Appl. Mech. Engrg., 302 (2016), pp. 131–146.
- [84] H. KIM, Y. SEO, AND S. YOUN, *Isogeometric analysis for trimmed CAD surfaces*, Comput. Methods Appl. Mech. Engrg., 198 (2009), pp. 2982–2995.
- [85] J. KÖNNÖ, D. SCHÖTZAU, AND R. STENBERG, *Mixed finite element methods for problems with Robin boundary conditions*, SIAM J. Numer. Anal., 49 (2011), pp. 285–308.
- [86] L. KUDELA, N. ZANDER, S. KOLLMANNSSBERGER, AND E. RANK, *Smart octrees: accurately integrating discontinuous functions in 3D*, Comput. Methods Appl. Mech. Engrg., 306 (2016), pp. 406–426.

Bibliography

- [87] B.-G. LEE, T. LYCHE, AND K. MØRKEN, *Some examples of quasi-interpolants constructed from local spline projectors*, in Mathematical methods for curves and surfaces (Oslo, 2000), Innov. Appl. Math., Vanderbilt Univ. Press, Nashville, TN, 2001, pp. 243–252.
- [88] C. LEHRENFELD AND M. OLSHANSKII, *An Eulerian finite element method for PDEs in time-dependent domains*, ESAIM Math. Model. Numer. Anal., 53 (2019), pp. 585–614.
- [89] A. J. LEW AND M. NEGRI, *Optimal convergence of a discontinuous-Galerkin-based immersed boundary method*, ESAIM Math. Model. Numer. Anal., 45 (2011), pp. 651–674.
- [90] T. LUDESCHER, *Multilevel preconditioning of stabilized unfitted finite element discretizations*, PhD thesis, RWTH Aachen University, 2020.
- [91] T. LYCHE AND K. MØRKEN, *Spline methods draft*. 2008.
- [92] B. MARUSSIG, R. HIEMSTRA, AND T. J. R. HUGHES, *Improved conditioning of isogeometric analysis matrices for trimmed geometries*, Comput. Methods Appl. Mech. Engrg., 334 (2018), pp. 79–110.
- [93] B. MARUSSIG AND T. J. R. HUGHES, *A review of trimming in isogeometric analysis: challenges, data exchange and simulation aspects*, Arch. Comput. Methods Eng., 25 (2018), pp. 1059–1127.
- [94] B. MARUSSIG, J. ZECHNER, G. BEER, AND T.-P. FRIES, *Stable isogeometric analysis of trimmed geometries*, Comput. Methods Appl. Mech. Engrg., 316 (2017), pp. 497–521.
- [95] F. MASSARWI AND G. ELBER, *A B-spline based framework for volumetric object modeling*, Comput.-Aided Des., 78 (2016), pp. 36–47.
- [96] A. MASSING, M. G. LARSON, A. LOGG, AND M. E. ROGNES, *A stabilized Nitsche fictitious domain method for the Stokes problem*, J. Sci. Comput., 61 (2014), pp. 604–628.
- [97] ———, *A Nitsche-based cut finite element method for a fluid-structure interaction problem*, Commun. Appl. Math. Comput. Sci., 10 (2015), pp. 97–120.
- [98] N. MOËS, J. DOLBOW, AND T. BELYTSCHKO, *A finite element method for crack growth without remeshing*, Internat. J. Numer. Methods Engrg., 46 (1999), pp. 131–150.
- [99] P. MONK, *Finite element methods for Maxwell’s equations*, Numerical Mathematics and Scientific Computation, Oxford University Press, New York, 2003.
- [100] B. MÖSSNER AND U. REIF, *Stability of tensor product B-splines on domains*, J. Approx. Theory, 154 (2008), pp. 1–19.
- [101] A. P. NAGY AND D. J. BENSON, *On the numerical integration of trimmed isogeometric elements*, Comput. Methods Appl. Mech. Engrg., 284 (2015), pp. 165–185.
- [102] R. A. NICOLAIDES, *Existence, uniqueness and approximation for generalized saddle point problems*, SIAM J. Numer. Anal., 19 (1982), pp. 349–357.
- [103] J. NITSCHKE, *Über ein Variationsprinzip zur Lösung von Dirichlet-Problemen bei Verwendung von Teilräumen, die keinen Randbedingungen unterworfen sind*, Abh. Math. Sem. Univ. Hamburg, 36 (1971), pp. 9–15.
- [104] P. OSWALD, *Multilevel finite element approximation*, Teubner Skripten zur Numerik. [Teubner Scripts on Numerical Mathematics], B. G. Teubner, Stuttgart, 1994. Theory and applications.

-
- [105] J. PARVIZIAN, A. DÜSTER, AND E. RANK, *Finite cell method: h- and p-extension for embedded domain problems in solid mechanics*, Comput. Mech., 41 (2007), pp. 121–133.
 - [106] M. S. PAULETTI, M. MARTINELLI, N. CAVALLINI, AND P. ANTOLIN, *Igatools: an isogeometric analysis library*, SIAM J. Sci. Comput., 37 (2015), pp. C465–C496.
 - [107] C. S. PESKIN, *Flow patterns around heart valves: A numerical method*, Journal of Computational Physics, 10 (1972), pp. 252–271.
 - [108] L. PIEGL AND W. TILLER, *The NURBS Book (2Nd Ed.)*, Springer-Verlag, 1997.
 - [109] L. A. PIEGL, *Ten challenges in computer-aided design*, Comput.-Aided Des., 37 (2005), pp. 461–470.
 - [110] J. PREUSS, *Higher order unfitted isoparametric space-time FEM on moving domains*, PhD thesis, 2018. Master’s thesis.
 - [111] R. PUPPI, *Isogeometric discretizations of the Stokes problem on trimmed geometries*. arXiv, 2020.
 - [112] A. QUARTERONI AND A. VALLI, *Numerical approximation of partial differential equations*, vol. 23 of Springer Series in Computational Mathematics, Springer-Verlag, Berlin, 1994.
 - [113] ———, *Domain decomposition methods for partial differential equations*, Numerical Mathematics and Scientific Computation, The Clarendon Press, Oxford University Press, New York, 1999. Oxford Science Publications.
 - [114] E. RANK, M. RUESS, S. KOLLMANNSSBERGER, D. SCHILLINGER, AND A. DÜSTER, *Geometric modeling, isogeometric analysis and the finite cell method*, Computer Methods in Applied Mechanics and Engineering, 249-252 (2012), pp. 104–115.
 - [115] P.-A. RAVIART AND J. M. THOMAS, *A mixed finite element method for 2nd order elliptic problems*, in Mathematical aspects of finite element methods (Proc. Conf., Consiglio Naz. delle Ricerche (C.N.R.), Rome, 1975), 1977, pp. 292–315. Lecture Notes in Math., Vol. 606.
 - [116] A. REUSKEN, *Analysis of trace finite element methods for surface partial differential equations*, IMA J. Numer. Anal., 35 (2015), pp. 1568–1590.
 - [117] R. F. RIESENFELD, R. HAIMES, AND E. COHEN, *Initiating a CAD renaissance: multidisciplinary analysis driven design: framework for a new generation of advanced computational design, engineering and manufacturing environments*, Comput. Methods Appl. Mech. Engrg., 284 (2015), pp. 1054–1072.
 - [118] M. E. ROGNES, R. C. KIRBY, AND A. LOGG, *Efficient assembly of $H(\text{div})$ and $H(\text{curl})$ conforming finite elements*, SIAM J. Sci. Comput., 31 (2009/10), pp. 4130–4151.
 - [119] M. RUESS, D. SCHILLINGER, A. I. ÖZCAN, AND E. RANK, *Weak coupling for isogeometric analysis of non-matching and trimmed multi-patch geometries*, Comput. Methods Appl. Mech. Engrg., 269 (2014), pp. 46–71.
 - [120] G. SANGALLI AND M. TANI, *Matrix-free weighted quadrature for a computationally efficient isogeometric k-method*, Comput. Methods Appl. Mech. Engrg., 338 (2018), pp. 117–133.
 - [121] F.-J. SAYAS, T. S. BROWN, AND M. E. HASSELL, *Variational techniques for elliptic partial differential equations*, CRC Press, Boca Raton, FL, 2019. Theoretical tools and advanced applications.

Bibliography

- [122] C. SCHWAB, *p- and hp-finite element methods*, Numerical Mathematics and Scientific Computation, The Clarendon Press, Oxford University Press, New York, 1998. Theory and applications in solid and fluid mechanics.
- [123] T. SEDERBERG, G. T. FINNIGAN, X. LI, H. LIN, AND H. IPSON, *Watertight trimmed nurbs*, ACM SIGGRAPH 2008 papers, (2008).
- [124] T. W. SEDERBERG, J. ZHENG, A. BAKENOV, AND A. NASRI, *T-splines and T-NURCCs*, ACM Trans. Graph., 22 (2003), pp. 477–484.
- [125] J. SHEN, J. KOSINKA, M. SABIN, AND N. DODGSON, *Converting a CAD model into a non-uniform subdivision surface*, Comput. Aided Geom. Design, 48 (2016), pp. 17–35.
- [126] R. STENBERG, *On some techniques for approximating boundary conditions in the finite element method*, vol. 63, 1995, pp. 139–148. International Symposium on Mathematical Modelling and Computational Methods Modelling 94 (Prague, 1994).
- [127] ———, *Mortaring by a method of J. A. Nitsche*, in Computational mechanics (Buenos Aires, 1998), Centro Internac. Métodos Numér. Ing., Barcelona, 1998, pp. CD-ROM file.
- [128] I. STROUD, *Boundary Representation Modelling Techniques*, Springer, New York, 2006.
- [129] L. D. STURGES, *Stokes flow in a two-dimensional cavity with moving end walls*, Physics of Fluids, 29 (1986), pp. 1731–1734.
- [130] L. TARTAR, *An introduction to Sobolev spaces and interpolation spaces*, vol. 3 of Lecture Notes of the Unione Matematica Italiana, Springer, Berlin; UMI, Bologna, 2007.
- [131] R. VÁZQUEZ, *A new design for the implementation of isogeometric analysis in Octave and Matlab: GeoPDEs 3.0*, Comput. Math. Appl., 72 (2016), pp. 523–554.
- [132] Q. ZHANG, M. SABIN, AND F. CIRAK, *Subdivision surfaces with isogeometric analysis adapted refinement weights*, Comput.-Aided Des., 102 (2018), pp. 104–114.

Curriculum vitae

PERSONAL DATA

NAME: Riccardo Puppi
PLACE AND DATE OF BIRTH: Mirano (VE), Italy — 7 August 1991
NATIONALITY: Italian
ADDRESS: Avenue de l'Université 20, 1005 Lausanne, Switzerland
EMAIL: riccardo.puppi@gmail.com

EDUCATION

École polytechnique fédérale de Lausanne Lausanne, Switzerland
PH.D. IN MATHEMATICS Dec 2016 – present
Thesis: *Stabilized isogeometric discretizations on trimmed and union geometries, and weak imposition of the boundary conditions for the Darcy flow*
Advisor: Prof. Annalisa Buffa, Co-advisor: Dr. Rafael Vázquez

University of Trento Trento, Italy
M.SC. IN MATHEMATICS Sept 2013 – Jul 2016
Thesis: *Finite element approximation of eddy current problems based on the magnetic scalar potential*
Advisor: Prof. Alberto Valli
Grade: 110/110 *cum laude*

University of Helsinki Helsinki, Finland
ERASMUS PROGRAMME Sept 2014 – Jun 2015
GPA: 5/5

University of Verona Verona, Italy
B.SC. IN APPLIED MATHEMATICS Sept 2010 – Oct 2013
Thesis: *Foundations of nonstandard analysis*
Advisor: Prof. Ruggero Ferro
Grade: 108/110

Liceo scientifico Majorana-Corner Mirano (VE), Italy
HIGH SCHOOL DIPLOMA Sept 2006 – Jul 2010
Grade: 100/100 *cum laude*

LANGUAGES

English Advanced **French** Fluent **Italian** Native

PUBLICATIONS AND PREPRINTS

- [1] P. ANTOLÍN, A. BUFFA, R. PUPPI, X. WEI, *Isogeometric discretizations of the Stokes problem on overlapped multipatch geometries*, in preparation
- [2] R. PUPPI, *A cut finite element method for the Darcy problem*, arXiv preprint 2111.09922 (2021)
- [3] E. BURMAN, R. PUPPI, *Two mixed finite element formulations for the weak imposition of the Neumann boundary conditions for the Darcy flow*, to appear in *Journal of Numerical Mathematics*

- [4] R. PUPPI, *Isogeometric discretizations of the Stokes problem on trimmed geometries*, arXiv preprint 2012.15582 , submitted to Comput. Math. Appl.(2021)
- [5] P. ANTOLÍN, A. BUFFA, R. PUPPI, X. WEI, *Overlapping multipatch isogeometric method with minimal stabilization*, SIAM J. Sci. Comput. 43 (2021), no. 1, A330–A354
- [6] A. BUFFA, R. PUPPI, R. VÁZQUEZ, *A minimal stabilization procedure for Isogeometric methods on trimmed geometries*, SIAM J. Numer. Anal. 58 (2020), no. 5, 2711–2735

TALKS AT CONFERENCES AND WORKSHOPS

- *Isogeometric formulations on trimmed geometries*, 2nd ERC Change workshop, Sestri Levante (IT), November 2019
- *Isogeometric formulations on trimmed geometries*, VII International Conference on Isogeometric Analysis, München (DE), September 2019
- *Multi-Mesh Isogeometric Analysis with Minimal Stabilization*, Workshop in Mathematical Foundations of Isogeometric Analysis, Mathematisches Forschungsinstitut Oberwolfach (DE), July 2019
- *Stabilized isogeometric methods on trimmed geometries*, MATHICSE retreat, Champéry (CH), June 2019
- *Isogeometric methods on trimmed geometries*, The 13th World Congress in Computational Mechanics, New York (US), July 2018
- *Isogeometric methods on trimmed geometries*, MATHICSE retreat, Sainte-Croix (CH), June 2018
- *Ghost penalty in IGA*, MATHICSE retreat, Leysin (CH), June 2017